A Xenograft Model of High Risk Leukemia Reveals an Oligoclonal Composition of Leukemia Initiating Cells

---

Dissertation

zur

Erlangung der naturwissenschaftlichen Doktorwürde

(Dr. sc. nat.)

vorgelegt der

Mathematisch-naturwissenschaftlichen Fakultät

der

Universität Zürich

von

Maike Schmitz

aus

Deutschland

Promotionskomitee

Prof. Dr. Lukas Sommer (Vorsitz)

PD Dr. Jean-Pierre Bourquin (Leitung der Dissertation)

Prof. Dr. Adriano Aguzzi

Dr. Beat C. Bornhauser

Zürich, 2011

The experimental work presented in this thesis was performed at the Division of Pediatric Oncology at the Children's University Hospital Zurich. This thesis was performed under the supervision of PD Dr. Jean-Pierre Bourquin (University Children's Hospital Zürich), Dr. Beat Bornhauser (University Children's Hospital Zürich), Prof. Dr. Lukas Sommer (Institute of Anatomy, University of Zürich) and Prof. Dr. Adriano Aguzzi (Institute of Neuropathology, University Hospital Zürich).

Zürich, May 2011

Maike Schmitz

Table of contents

Summary

Acute lymphoblastic leukemia (ALL) is the most common cancer in childhood and occurs in the bone marrow and blood. Patients can be effectively cured with combinatorial chemotherapy in 80% of cases, but the high toxicity of the treatment and the frequency of relapses still are major obstacles and lead to high mortality. Based on current treatment protocols of one of the biggest study groups on childhood ALL, the BFM study group (named after Berlin-Frankfurt-Münster, to credit the founding members), a group of patients can be identified with particular bad outcome. The prognosis is given based on the measurement of minimal residual disease (MRD). This group of very high risk patients (VHR-ALL) is in need of novel treatment approaches. Due to the scarcity of primary material and the lack of *in vitro* models to study ALL biology we have established a xenograft model of VHR-ALL with the aim to model high-risk disease. Therefore, it is necessary to understand the effects of the selective pressures that are inherent to the xenograft model. Clonal evolution of the leukemogenic compartment could contribute to alter the response to chemotherapy in ALL. Thus, we have investigated the phenotypic and genetic composition of VHR-ALL cases before and after xenotransplantation.

We found that the phenotypic properties remained unchanged, with concordant immunophenotypes after up to 5 passages in NOD/scidIL2Rγnull (NSG) mice and stable in vitro drug response profiles. Analysis of copy number alterations (CNA) showed that the xenografted leukemia, even when reconstituted from hundred ALL cells, remained highly related to the diagnostic sample, with minor changes in CNAs, emerging in most cases in the first passage into mice and occurring in recurrently detected loci in ALL. At the single cell level, the pattern of mono-and bi-allelic deletions of the *CDKN2A* locus revealed distinct leukemia subpopulations, which were reproducibly tracked in xenografts. Only in one case, the major clone of xenografts was different to diagnosis but could be backtracked. In most VHR-ALL cases, the predominant diagnostic clones were reconstituted in xenografts, as shown by multiplex PCR analysis of Ig/TCR loci. In other cases, the pattern in CNAs and Ig/TCR rearrangement was less concordant in xenografts, suggesting the outgrowth of subclones.

In four of six VHR-ALL cases, the relative low number of 100 unsorted cells was enough to propagate leukemia in NSG mice and the resulting leukemias resembled in phenotype, genotype and clonal composition the diagnostic sample in the same way as leukemias generated from more cells. Thus, we have demonstrated the multi-clonal composition of leukemia-propagating cells in VHR-ALL samples, making it likely that if here is a hierarchy in VHR-ALL it is a flat one

Our xenograft model was successfully used as a preclinical model to evaluate new treatment rationales for chemosensitization for VHR-ALL patients. We proved that the small molecule obatoclax could effectively re-sensitize to chemotherapy in the xenograft model. This approach will be translated into a Phase-1 clinical trial. We also exploited the xenograft system as a renewable source of relevant patient material and thereby could contribute to the understanding of the importance of CRLF2 in the context of Down-Syndrome ALL. Taken together, we have established a xenograft model of VHR-ALL that enables to perform functional studies with relevant samples. It is likely that a larger proportion of ALL cells are leukemogenic and the nature of ALL cells is oligo- or even polyclonal, providing the basis for clonal selection and escape of treatment. Consequentially, future treatment approaches

need to consider the full diversity of ALL and targeting of all subpopulations must be reached.

Zusammenfassung

Die häufigste Krebsart bei Kindern ist die akute lymphatische Leukämie (ALL), eine Erkrankung des Blutes und Knochenmarkes. 80% der Patienten können durch eine Kombinationstherapie geheilt werden. Dabei führen die hohe Toxizität der Behandlung und die häufigen Rezidive jedoch zu einer hohen Mortalitätsrate. Aufgrund von den derzeitigen Protokollen einer der grössten Studiengruppen der pädiatrischen ALL, der BFM-Studiengruppe (benannt nach den Gründungszentren in Berlin-Frankfurt-Münster), können Patienten mit einer ausgesprochen schlechten Prognose identifiziert werden. Die Prognose wird anhand der Messung der minimalen Resterkrankung (MRD) erstellt. Diese Patienten mit Hochrisiko-ALL (VHR-ALL) brauchen neue Therapieansätze.
Eine präklinische experimentelle Plattform ist wünschenswert, da diagnostisches Material sehr rar ist und es an *in vitro* Methoden zur Erforschung der ALL mangelt. Wir haben daher ein Xenograft-Modell der VHR-ALL etabliert. Um das Modell zur präklinischen Forschung zu nutzen, ist es notwendig den selektiven Druck genau zu charakterisieren, der durch das Xenograft auf die ALL Zellen wirkt. Die klonale Evolution der Leukämie erzeugenden Subpopulationen könnte das Ansprechen auf die Chemotherapie verändern. Daher haben wir die phänotypische und genetische Zusammensetzung der ALL vor und nach der Xenotransplantation in NOD/scidIL2Rγnull (NSG) Mäusen untersucht. Wir konnten zeigen, dass die phänotypischen Eigenschaften unverändert blieben. Im Einzelnen waren die Immunphänotypen und die *in vitro* Toxizitätsprofile bis zu fünf Passagen lang stabil. Die Analyse von Copy Number Abweichungen (CNA) der DNS zeigte, dass Xenograft-Proben den diagnostischen Proben sehr ähnlich waren, sogar wenn nur 100 Zellen zur Transplantation des Xenografts benutzt wurden. Kleinere Veränderungen traten meistens schon in der ersten Passage auf. Und zwar in solchen Genen, die in der Leukämie schon zuvor als veränderlich bekannt waren. Auf Einzelzellebene wurden mono- und bi-allelische Deletionen des Gens *CDKN2A* angeschaut. Dabei zeigte sich, dass es verschiedene leukämische Subpopulationen gibt. Diese wurden reproduzierbar in mehreren Xenograft Proben detektiert. Nur in einem Fall war der vorherrschende Klon zwischen Diagnose und Xenograft unterschiedlich, konnte jedoch zurückverfolgt werden. In den meisten VHR-ALL Fällen wurden die in der Probe der Diagnose vorherrschenden Klone auch in den Xenograft-Proben nachvollzogen, wie wir mittels PCR Analyse der Ig/TCR-Loci feststellen konnten. In seltenen Fällen war das Muster der CNAs und Ig/TCR Rearrangements weniger konserviert, was auf eine Selektion von Subpopulationen schliessen lässt.
In vier von sechs VHR-ALL Fällen waren 100 unsortierte Zellen ausreichend, um eine Leukämie in den NSG Mäusen zu erzeugen. Die daraus resultierenden Leukämien ähnelten in Phänotyp und Genotyp den diagnostischen Proben genauso stark wie Leukämien, die mit mehr Zellen erzeugt wurden. So konnten wir zeigen, dass die Leukämie erzeugenden Zellen von Hochrisiko Patienten eine multiklonale Zusammensetzung haben und dass diese Zusammensetzung während der Xenotransplantation in NSG Mäuse stabil erhalten bleibt.
Unser Xenograft Modell wurde als präklinisches Modell zur Evaluierung neuer Behandlungsprinzipien zur Chemosensibilisierung von resistenten Patienten erfolgreich angewandt. Wir konnten im Xenograft Modell zeigen, dass das kleine

Molekül Obatoclax zur effektiven Resensibilisierung gegenüber der Chemotherapie geführt hat. Dieser Ansatz wird demnächst in einer klinischen Phase 1 Studie umgesetzt werden. Ausserdem nutzten wir das Xenograft Modell als erneuerbare Quelle für das seltene diagnostische Material und konnten so zu einer Studie über die Bedeutung von CRLF2 im Zusammenhang mit Leukämien von Down-Syndrom Patienten beitragen.
Zusammengefasst haben wir ein Xenograft Modell der VHR-ALL etabliert, welches funktionale Studien mit relevanten Fällen ermöglicht. Da es wahrscheinlich ist, dass ein Grossteil der ALL-Zellen Leukämien induzieren kann und sie oligo- oder sogar polyklonal sind, ist anzunehmen, dass dies der Grund ist, weshalb es zur klonalen Selektion kommt und ein Entrinnen von der Therapie möglich ist. Neue Therapieansätze müssen daher konsequenterweise die Vielfalt der gesamten Leukämischen Population umfassen.

Introduction

Childhood Acute Lymphoblastic Leukemia

Leukemias are the most frequent cancers in childhood. Due to specific risk-directed treatment of patients, progress in the therapy has led to high cure rates (five-year survival) of 80% in acute lymphoblastic leukemia (ALL) and 60% in acute myeloid leukemia (AML). Nevertheless, the high toxicity of the treatment and occurrence of relapses are a major problem. Relapses are ranking under the top four most common diagnoses in pediatric oncology in the US and top five in Switzerland demonstrating the need for novel therapies (Stanulla 2009; Pui 2007; 2011; Bailey 2008; Einsiedel. 2005). ALL is the most frequent type of leukemia in childhood (nearly 80%) in children. ALL derives from B- or T- lymphocyte progenitors, which are blocked in their maturation. The massive proliferation of these cells can overpower the normal hematopoietic differentiation and leads to accumulation of leukemic blasts in primary and secondary hematopoietic sites such as liver, spleen, lymph nodes and thymus (Pui 2007). Leukemic blasts show antigen expression profiles similar to the maturation stages of normal B- and T-cells (Figure 1). These maturation stages can be identified with cell-surface markers and leukemic blasts typically have aberrant patterns of immunoglobulin expression. Immunophenotyping performed at diagnosis allows to sub-classify cases according to the maturation stage at which they are blocked. Clinically important is the distinction of B-cell precursors and of mature B-cells (Pui 2007). Also, different reports have shown that some markers do not remain stable under the early phases of treatment and observed down-modulation of CD10 and CD34 and up-modulation of CD19 and CD20 in residual blasts (Gaipa 2008; Dworzak 2008; Szczepański 2006). These differences can be helpful to create specific antibody-directed therapies. Moreover, the use of immunophenotyping is an important tool for monitoring minimal residual disease (Ratei 2009).

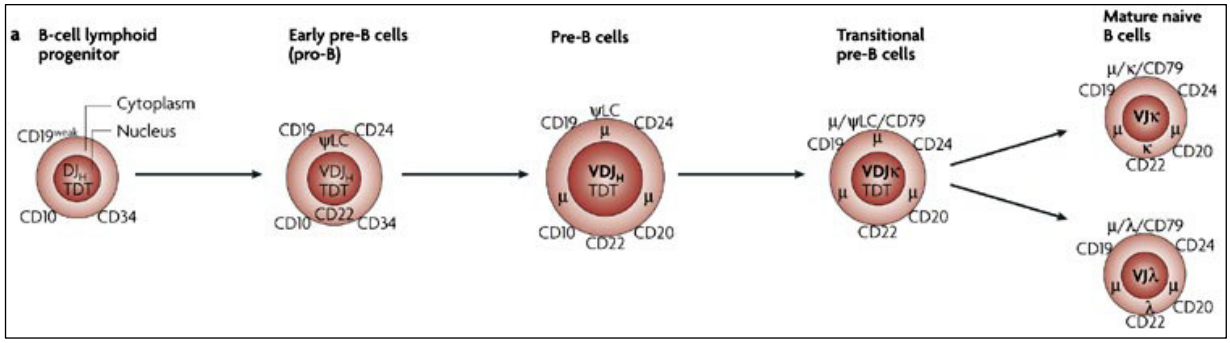

Figure 1. Maturation stages of normal B cells and respective surface marker expression. Adapted from (Pui 2007).

Treatment Response is the Most Important Prognostic Factor

In childhood ALL a limited number of significant risk factors have been described with different clinical and biological characteristics that are used for prognosis and adaptation of the treatment. These include leukocyte count at diagnosis,

immunophenotype, age, chromosomal abnormalities and response to initial therapy (Bailey 2008) (Table 1). These factors are used to stratify patients into different treatment groups and optimize their individual treatment. Thereby patients with unfavorable factors receive more intense chemotherapy, whereas those with "good prognosis" receive less or modified versions of the intensive treatment elements.

Factors commonly used for risk stratification		
Factor	**Favorable**	**Adverse**
Age (years)	1-9	<1 or ≥10
Leukocyte count ($\times 10^9$/L)	<50	>50
Immunophenotype	B-cell precursor	T-cell
Genotype	Hyperdiploidy>50 chromosomes, TEL-AML1 (ETV6-RUNX1)	Hypodiploidy<44 chromosomes, BCR-ABL1, MLL-AF4
MRD after induction	<0.01%	≥1%

Table 1. Risk factors in childhood ALL. Adapted from (Pui 2010).

Currently, the most powerful risk stratification criterion is the initial response to therapy. The European BFM study group (named after the founding centers in Berlin-Frankfurt-München) has developed a powerful method to follow the disease regression over treatment time by measuring the minimal residual disease (MRD). This is a quantification of residual leukemic blasts in the bone marrow and peripheral blood of patients measured either by quantitative PCR of clone specific Immunoglobulin (Ig) and T-cell receptor (TCR) rearrangements and/or by flow cytometry of surface markers (van Dongen 1998; Schrappe 2004; Flohr 2008; Ratei 2009). Multi-parameter flow cytometry uses the atypical expression of leukemia-associated surface proteins to distinguish between normal and malignant cells. For example, CD10 is often expressed at a higher level in precursor B-ALL than in normal B precursor cells. For detection of MRD, proteins that are aberrantly co-expressed on ALL cells, such as CD58 or CD9 for precursor-B ALL will be very useful to clearly distinguish a small population of blasts over the background of normal regenerating lymphoid cells. Other aberrantly expressed markers are cross-lineage expression of T-cell and myeloid cell markers including CD7, CD13 and CD33 (Szczepański 2006).

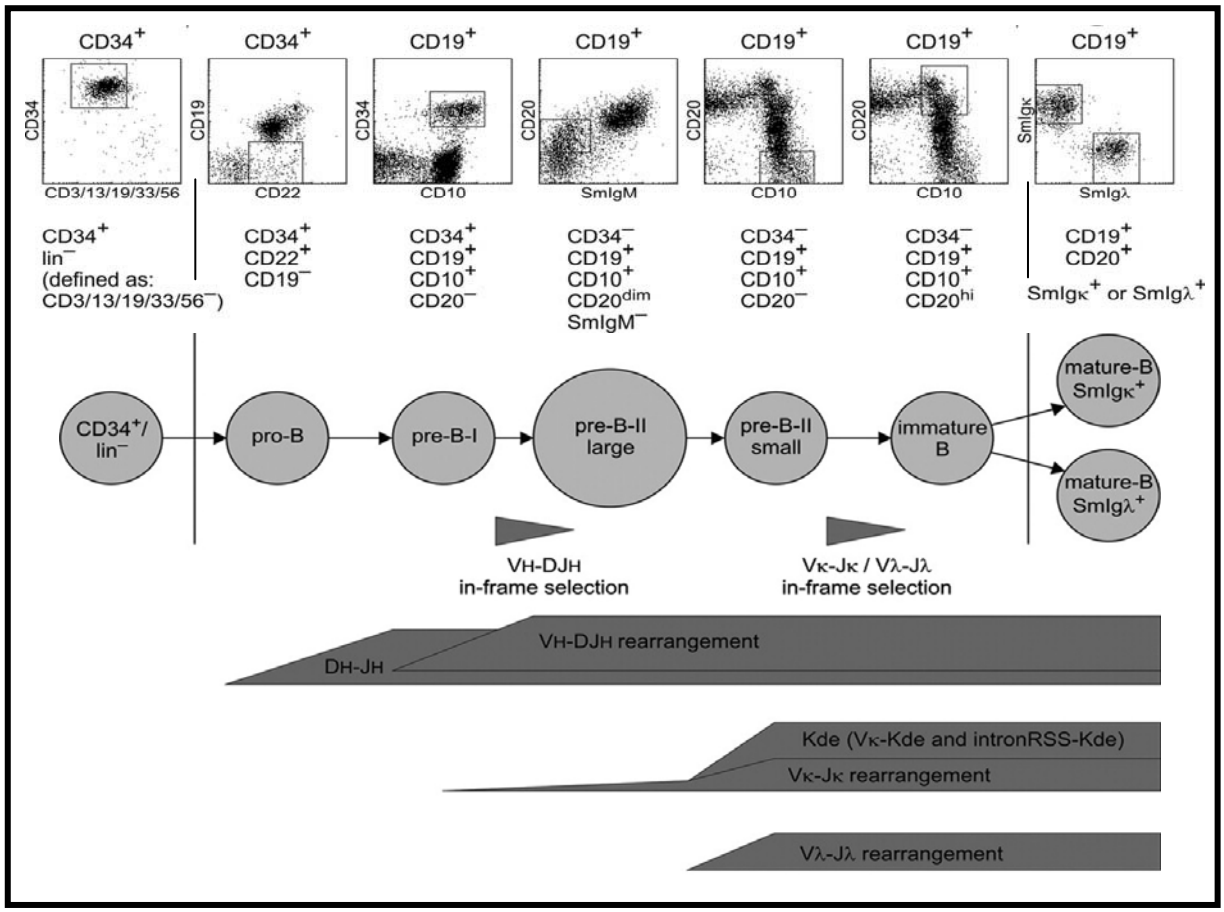

Figure 2. Expression of surface markers and antigen receptor rearrangement in correlation to B-cell development. Adapted from (van Zelm et al. 2005)

The junctional regions of Ig and TCR gene rearrangements are suitable PCR targets as they represent unique sequences, which are created through deletions and random insertions of nucleotides during the rearrangement process of B- and T-cell receptors (Figure 2). Leukemic blasts, stalled in their maturation process have undergone the rearrangement process as normal lymphocytes, but often not until the complete V-D-J rearrangement. Unlike in healthy blood, where one detects multi-clonal rearrangements, reflecting the diversity of B- and T-cells, leukemic blasts are more homogeneous and allow detecting strong signals of monoclonal rearrangements. Extensive studies have established the time points and cut offs for MRD levels that are most suitable to distinguish between patients with a high risk or low risk to relapse with their disease. Patients with persisting MRD levels above the determined cut off (10^{-3} leukemic cells per one normal cell) after 12 weeks of chemotherapy have a high risk of relapse (MRD-HR, Figure 3 left panel). These patients, as well as few additional cases identified based on cytogenetic risk criteria (cases with the translocations t(9;22) or t(4;11), see below and Table1) will qualify for more intensive treatment after this time point. An additional MRD time point at week 22 during consolidation therapy further discriminates a subgroup of patients with very high risk of relapse (VHR-MRD) (Figure 3 right panel). About 50% of these patients also have no response to the steroid treatment, which is given in the first week of ALL treatment.

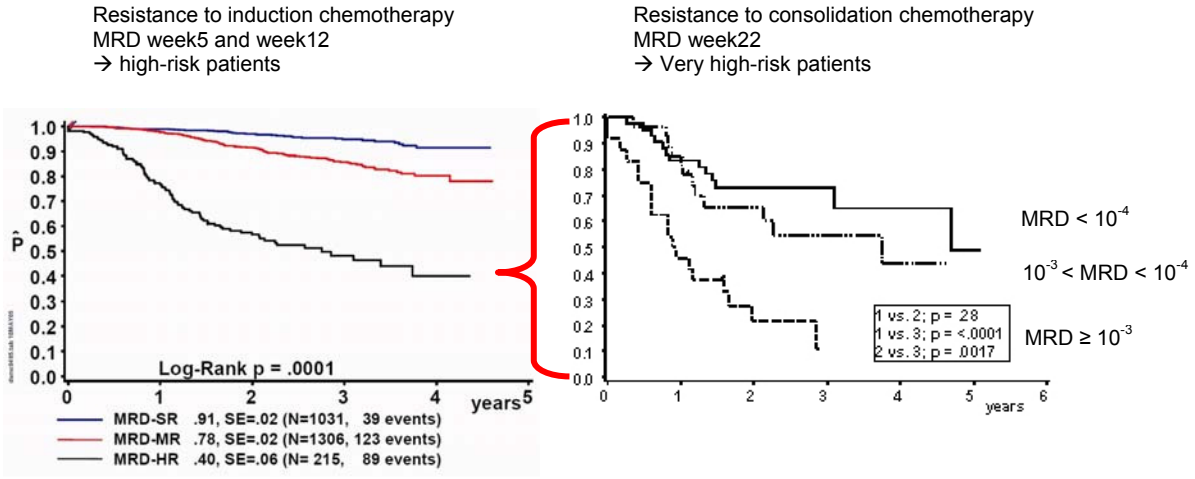

Figure 3. Value of MRD analysis for prognosis. Survival curves of the different MRD subgroups identified by qPCR of Ig/TCR rearrangements at measurements after 12 weeks (left) and 22 weeks (right). Adapted from (Schrauder 2007).

Genetic Subtypes in ALL

Cytogenetic characterization of ALL patients is commonly performed at diagnosis and several subtypes of leukemia can be distinguished based on cytogenetic analysis (Figure 4). Many abnormalities are known but most of them are not commonly used for clinical risk evaluation (Table 1).

Cytogenetic Subtypes with Favorable Outcome

The most common translocation found in childhood B-precursor ALL is the translocation t(12;21)(p13;q22) leading to the TEL-AML1 fusion product (also known as ETV6-RUNX1). It is found in around 25% of patients and is a robust prognostic factor for favorable outcome (McLean 1996). This group of patients represents a distinct biological subset as was shown by gene expression studies (Yeoh 2002). Moreover, it is likely that TEL-AML1 is the initiating event in this subtype as the presence of the translocation on neonatal blood spots demonstrated that the translocation is already present in blood years before the disease is overt (Greaves 2003). Nevertheless, the mechanism of leukemogenesis of TEL-AML1 leukemias is not unraveled yet.
The next common aberration is hyperdiploidy (more than 50 chromosomes), which also confers a favorable prognosis. It was also shown to be a distinct subset of ALL by microarray studies (Yeoh 2002). Around 5% of patients carry the t(1;19) rearrangement, leading to the fusion of the transactivation domain of the transcription factor *E2A* with the homeobox (*HOX*) gene *PBX* (Armstrong 2005). E2A transcription factors plays a role in lymphocyte development and as the translocation impairs one copy it is likely to contribute to leukemogenesis. *HOX* family genes are known for their role in leukemogenesis, and as PBX1 can alter the HOX regulated programs, it may contribute to leukemogenesis (Armstrong 2005).

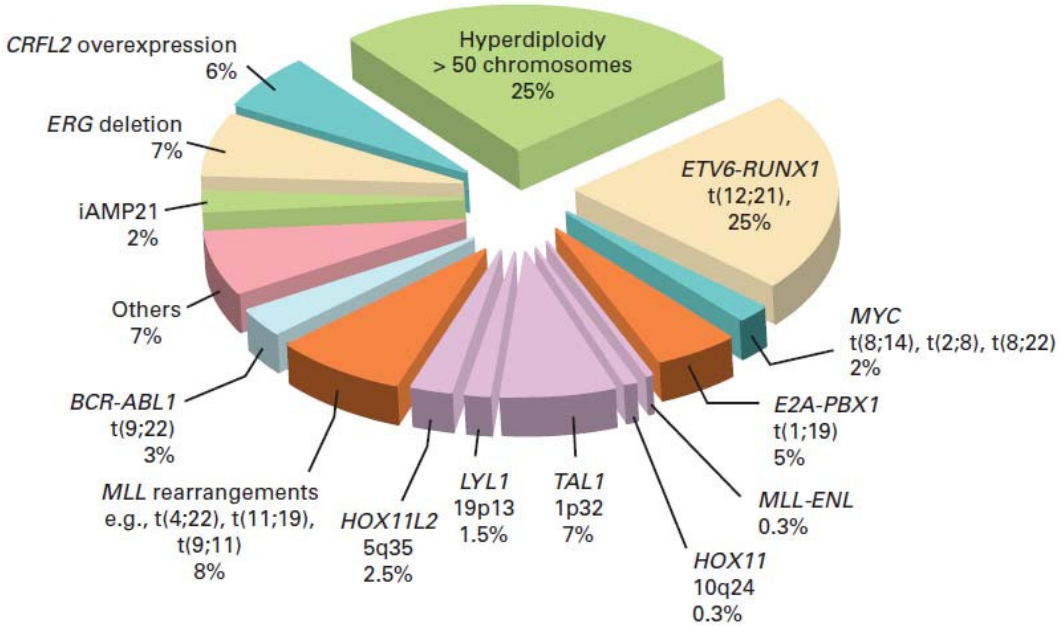

Figure 4. Common genetic abnormalities in B-ALL and T-ALL. Aberrations only found in T-ALL are shown in purple. Adapted from (Pui 2011).

Cytogenetic Subtypes with High-Risk for Relapse

In infant leukemias (age below 1 year), translocations involving *MLL* rearrangements on chromosome 11q23 are common. This risk factor defines a group of children that are expected to have a high risk of relapse (Biondi 2000). These rearrangements can occur in AML and ALL and some cases show both lymphocytic and monocytic involvement, which triggered the naming of *mixed-lineage-leukemia (MLL)* for the gene on 11q23. MLL is a DNA binding protein that is involved in hematopoiesis through the regulation of *HOX*-family genes and was shown to be a leukemia-initiating event (Owens 2002). *MLL* has a variety of fusion partners, MLL-AF4 (t(4;11)) was the first to be identified and is most common in ALL. Now more than 40 partners are identified and as particular translocations are associated with particular immunophenotypes, the fusion partner might play a role (Krivtsov 2007; Armstrong 2002).

A poor prognosis is attributed to translocation t(17;19) (*E2A-HLF*) which occurs in around 1% of ALL patients. Like the t(1;19) rearrangement, t(17;19) contains the E2A transcription factor which plays a crucial role in lymphocyte development (Armstrong 2005). The fusion protein has been shown to be sufficient to immortalize lymphocyte precursors (de Boer 2010) and to up-regulate the anti-apoptotic protein Survivin (Okuya 2010). Both mechanisms could explain the resistance to treatment.

The translocation t(9;22), also called Philadelphia chromosome, is also associated with high risk. It results in the fusion of the BCR signaling protein to the tyrosine kinase ABL1 causing constitutive active kinase activity and interactions with other transforming elements such as RAS, which renders the kinase an interesting target for small molecule targeted therapy (Pui 2007). The BCR-ABL1 inhibitor imatinib is successfully used for the therapy of chronic myeloid leukemia (CML) where the majority of patients carry this translocation (Ren 2005).

Down-Syndrome and ALL

Interestingly, children with Down-Syndrome (DS) have a higher risk of developing leukemias, both AMLs and ALLs, while they generally have a lower risk for developing solid tumors. In case of ALL, DS is associated with higher risk than non-DS, and DS-ALL is a clinical and biological distinct subset from non-DS ALL patients (Hertzberg 2010; Zwaan 2010). Several groups have reported the presence of somatic activating mutations in the Janus kinase *JAK2* in approximately 20% of DS-ALLs (Bercovich 2008; Kearney. 2009; Mullighan 2009c). Similar mutations can also be found in approximately 10% of high-risk ALLs in non-DS children, corresponding to approximately 3% of unselected childhood ALLs (Mullighan 2009c). The mutations involve highly conserved residues of the kinase and pseudo-kinase domains and lead to constitutive-active JAK/STAT signaling and thus to immortalization of hematopoietic progenitors and cytokine-independent growth, as was shown *in-vitro* (Bercovich 2008; Mullighan 2009c).
An additional molecular abnormality was found by gene expression profiling, which revealed that 60% of DS-ALLs overexpress the cytokine receptor CRLF2. This was associated with activating mutations in *JAK2* or the receptor itself (manuscript 4) (Hertzberg 2010). In normal lymphoid development, CRLF2 plays a role in TSLP receptor (thymic stromal-derived lymphopoietin receptor) formation by dimerization with IL7RA (Fujio 2011; Pandey 2000). As IL7RA is expressed on leukemic blasts, CRLF2 could interact to form TSLPR on the leukemic cells in a similar fashion. On the other hand it was also demonstrated that CRLF2 cooperates with JAK2, in the absence of IL7RA, suggesting an independent activation through homodimerization. CRLF2 and mutated JAK2 led to a robust cytokine-independent growth, demonstrating that these two proteins cooperate in providing growth and survival advantage (Figure 5) (Hertzberg 2010). Finally, these data imply that therapeutically targeting of JAK/STAT signaling may be of potential benefit to the majority of DS-ALL patients, not limited only to those with mutated JAK2.

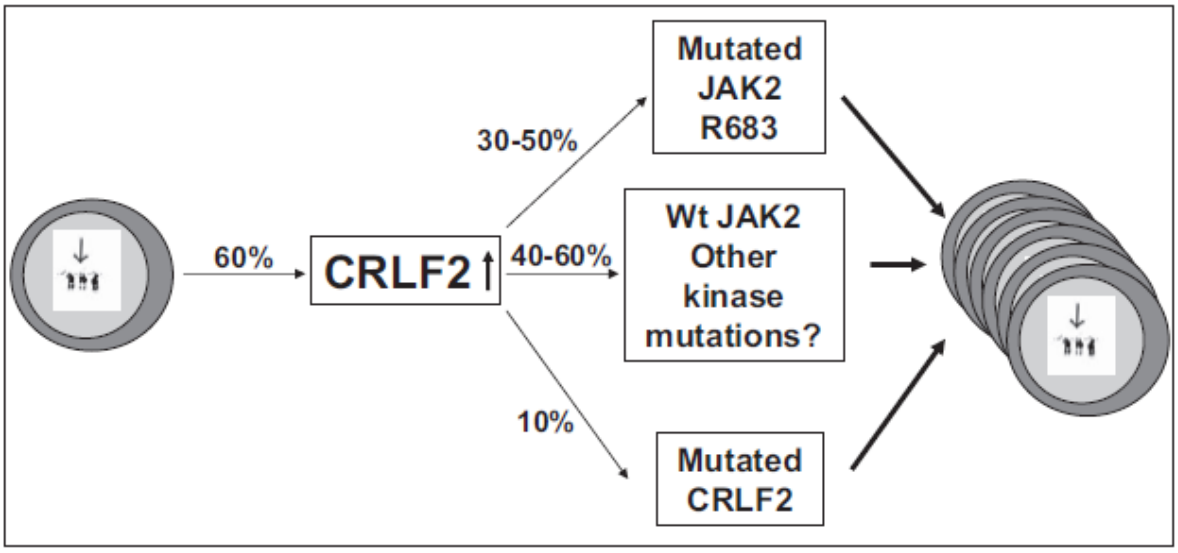

Figure 5. A model of CRLF2 and JAK2 in Down-Syndrome ALL. High levels of CRLF2 as a cause of genomic aberrations are followed by activating mutations in *CRLF2*, *JAK2* or other yet unidentified kinases, which contribute to the growth advantage of DS-ALL blasts. Adapted from (Hertzberg 2010) (manuscript 4).

The cooperation of mutated *JAK2* and high levels of CRLF2 was also observed in 7% of non-DS ALL pre-B leukemias (Mullighan 2009a; Harvey 2010; Russell 2009). Overall, high-levels of CRLF2 were associated with poor event-free survival, but some studies showed that only the rearrangement of CRLF2 with P2RY8, but not the overexpression of CRLF2 alone was an independent predictor for high-risk of relapse for patients otherwise classified as standard risk (Cario 2010; Harvey 2010). Therefore, through the detection of CRLF2 rearrangements a group of patients can be identified in future which are in need of intensified treatment and are not recognized by MRD measurements. Additionally, the use of JAK/STAT inhibitors, also for non-DS ALL patients, needs to be evaluated.

High-Resolution Genomic Profiling

In the last years, a rapid progress has been made in high-throughput genomic technologies, not limiting the genetic analysis to cytogenetics but allowing more in-depth studies. This has led to a very complex and heterogeneous picture of ALL genetics. Several groups have used high-resolution single nucleotide polymorphism (SNP) arrays of diagnostic ALL samples and detected recurrent genetic aberrations. Often these were small genetic lesions, mostly deletions but also chromosomal translocations were detected. With increasing numbers of studies performed, it becomes clearer which cellular pathways are the targets of DNA copy number aberrations (CNA). Most often aberrations were observed in master regulators of lymphoid development, such as PAX5, EBF and IKZF1. Other targets include regulators of the cell cycle (CDKN2A/B), tumor suppressor genes (PTEN, BF1, RB1) and regulators of apoptosis (BTG1) (Mullighan 2009; Mullighan 2009b; Mullighan 2008a; Mullighan 2008; Mullighan 2007; Harvey 2010). In 60% of pre-B ALL cases a loss of genes that regulate B-lymphoid development is observed and it was shown in experimental models that this leads to an acceleration of leukemogenesis (Mullighan 2008; Hu 2004; Ross 2003) and thus these aberrations could also contribute in human leukemogenesis.
Overall, the average number of aberrations is limited to around six per case at diagnosis, demonstrating that there is no general chromosomal instability in ALL. On the other hand, the number of aberrations differs significantly between different subgroups of ALL (Mullighan 2008). MLL-rearranged leukemias carried up to one CNA, indicating that only a limited number of lesions are necessary for leukemia initiation. In BCR-ABL and TEL-AML1 rearranged leukemias more than 6 CNAs were found, suggesting that disruption of multiple pathways is required for leukemia initiation and progression. The most frequent deletion in this group was found in the *IKFZ1* gene. It encodes the transcription factor Ikaros and was deleted in 76.2% of childhood BCR-ABL ALL and in 90.9% of adult BCR-ABL ALL cases. Further, *PAX5*, located on chromosome 9p, was frequently deleted (in 51% of samples), mostly occurring in cases also carrying the *IKZF1* deletion (Mullighan 2008a). Also located on chromosome 9p are the cell cycle regulators *CDKN2A* and *B*, which were frequently deleted and the whole 9p chromosome arm was lost in many cases (Figure 6).

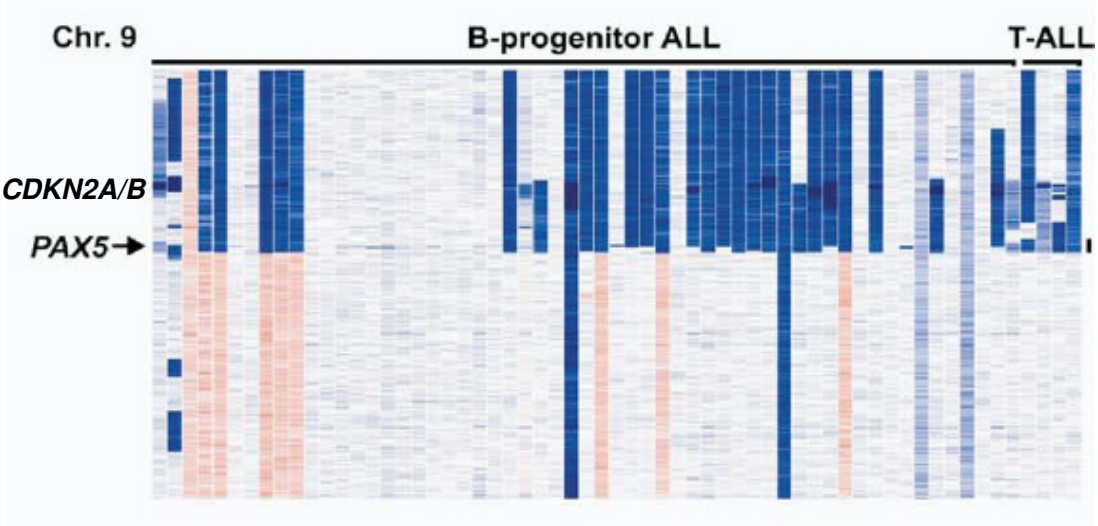

Figure 6. Frequent chromosome 9p aberrations. A heatmap of the full chromosome 9 of several B-ALL and T-ALL cases is depicted and the loci for PAX5 and CDKN2A/B are highlighted. Blue strips indicate lower copy numbers and red strips higher copy numbers. Adapted from (Mullighan 2009).

More recently, a candidate gene sequencing approach has identified mutations in diagnostic and relapsed ALL. Some of them in genes known to be recurrent DNA CNA targets in ALL (e.g. *PAX5, ETV6, JAK1, FBXW7*) and many in novel ALL target genes, such as the transcription coactivators CREBBP and NCOR1 and the transcription factors ERG, SPI1, TCF4 and TCF7L2 (Mullighan 2011). In 18.3% of relapses CREBBP was mutated, which is a histone acetyltransferase binding protein acting as transcription coactivator. The mutation impaired the histone acetylation and transcription of target genes, which included glucocorticoid responsive genes. In 3 of 4 cases the mutation of the relapse could be backtracked to minor clones at diagnosis and thus the mutation might confer treatment resistance to these cases (Mullighan 2011).
In future, the combination of high-throughput genomic techniques, deep-sequencing of the leukemia genome and epigenetic profiling (for example methylation arrays for the detection of promoter and enhancer regions of candidate genes) will lead to the new identification of core lesions in ALL. It will be most important to link these data with biologic functions and clinical significance and it will require experimental platforms for functional investigation of the different lesions (Bonapace 2010).

Cancer Stem Cells, Leukemia Initiating Cells and Clonal Evolution

The concept of cancer stem cells (CSC) predicts that cancer cells are phenotypically and/or genetically heterogeneous and that only a subpopulation has the ability to propagate and maintain the disease. This subset of cells shares characteristics with their counterparts from normal tissue as the abilities to self-renew, to differentiate, to proliferate extensively and to resist to chemotherapeutics (Figure 7b) (Lobo 2007). This concept suggests that cells within a given cancer are hierarchically organized. The CSC concept puts the CSCs in the center for novel targeted therapies, as they are the main responsible elements for occurrence of relapses. In this concept, a pre-cancerous cell or cell-of-origin is created through an oncogenic event. Transformation and tumor formation then occurs through additional supporting

genetic or epigenetic events. The CSC is the cell maintaining and propagating the tumor once it is established, but not necessary the cell-of-origin, which is the cell that is transformed in the “first hit” and might later evolve to be also the CSC (thus the CSC can also be termed tumor-propagating cell, or in case of leukemias, leukemia-initiating cell). Treatment of tumors that follow the CSC model might eradicate most of the cells, but any CSC that is evading can differentiate again and cause a relapse (Bomken 2010). On the other hand, a treatment that targets tumor-propagating cells specifically and not the bulk of the tumor mass could disable the tumor to generate new cells and lead to tumor regression (Huntly 2005).
Tumor-propagating cells are thought to share features with normal stem cells, which render them more resistant to chemotherapy. For example, both hematopoietic stem cells and tumor cells have increased levels of telomerase, which prevents them from replicative senescence and cell death (Morrison 1996; Gal 2006; Campbell 2006). In addition, although they have the potential to self-renew, they usually rest in the G_0 phase of the cell cycle. This means that conventional chemotherapeutic drugs, such as 5-fluorouracil, which act on cycling cells eradicate effectively the normal tumor mass but not the tumor-propagating cells, as was shown in AML (Ravandi 2006). The quiescent state of LICs could contribute to their resistance to treatment. Moreover, the multi-drug resistance of tumors is often associated with higher expression ABC-transporters on tumor-propagating cells, which leads to increased drug efflux from the cells, and thus the drugs are ineffective (de Jonge-Peeters 2007). Therefore, the identification of targeted therapies to tumor-propagating cells could lead to improved outcomes for patients with drug-resistant disease.

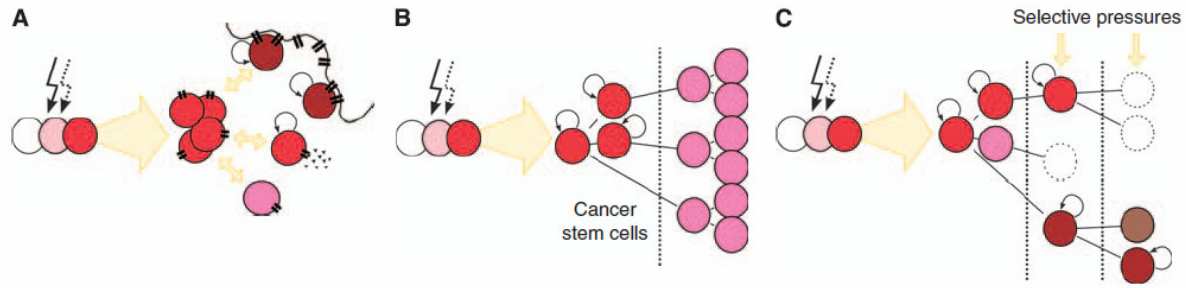

Figure 7. Concepts of tumor heterogeneity. (A) Variations result from intrinsic and extrinsic factors, right combinations thereof could trigger self-renewal. (B) A tumor shows a hierarchy similar to normal tissues with self-renewing cells at the top. (C) Ongoing clonal evolution with sequential genetic and epigenetic changes that result in a polyclonal population. Adapted from (Bomken 2010).

To describe the first CSC it was necessary to sort the different subpopulations based on immunophenotype and to use immuno-compromised mice for evaluation of tumor initiating ability. The methodology of sorting cell subsets and then transplanting them at limiting numbers into immuno-compromised mice has set the gold-standard for the identification of self-renewing and tumor-propagating cells, after its first use for the identification of hematopoietic stem cells by Irving Weissman and colleagues (Clarke 2006; McCune 1988). John Dick’s laboratory was the first to show for myeloid leukemia that a restricted subpopulation was able to propagate the entire original leukemia into NOD/scid mice over serial transplantations. Only the immature CD34+/CD38- cells but not more mature CD34+/CD38+ cells were able to self-renew and recapitulate the tumor using very low numbers of cells (Lapidot 1994; Bonnet 1997). After that, CSCs were identified in solid tumors of the breast (Al-Hajj 2003), brain (Hemmati. 2003; Singh. 2004), and colon (O'Brien 2007; Ricci-Vitiani 2007). Obstacles still are the identification of suitable surface markers to enable sorting of

subpopulations, the scarcity of primary material and the different experimental set-ups used by different groups.

Another concept for heterogeneity of tumor cells within a tumor provides the stochastic model. According to that model, all tumor cells could be biologically equivalent and the heterogeneity derives from extrinsic or intrinsic influences, including niche interactions and intercellular signaling that result in random or stochastic responses (Figure 7a) (Dick 2008; Bomken 2010). The right combinations of these events could enable any cell of the tumor to self-renew and propagate disease. This is not necessarily contradicting to the CSC model, if one accepts that tumor-propagating cells need not be rare and that tumor cells either can evolve or be selected for to re-activate their stem-cell programs. Gupta et al (Gupta 2009) introduced the term bi-directional interconvertability to describe the plasticity of non-CSCs to become CSCs.

In childhood B-ALL, it is quite unclear at the moment if the traditional concept of CSCs is applicable. BCR-ABL positive ALL was described, similar to AML, to harbor the leukemia initiating cells (LICs) in immature CD34+/CD38- compartments, (Cox 2005; Cobaleda 2000). Then two reports showed that the LICs reside in the more mature CD19+/CD34+/CD38dim populations in good-risk ALL (Castor 2005; Hong 2008). And more recently a very immature phenotype, CD133+/CD19-, similar to the hematopoietic stem cell was described to exclusively harbor LIC activity (Cox 2009). These data propose that those leukemia subtypes associated with high-risk and resistance to treatment have more immature LICs resembling normal stem cells. Whereas in leukemias with favorable prognosis, the LICs reside in a more mature compartment.
These studies were however contradicted by others, which showed that LICs could be found in both immature and mature compartments (le Viseur 2008; Kong 2008). In particular, both studies demonstrated that CD34+/CD19- , CD34+/CD19+ and CD34-/CD19+ sorted populations initiated leukemias in NOD/scid-IL2Rγnull (NSG) mice. Importantly these leukemias reflected the complete original immunophenotype and were retransplantable in NSG mice, demonstrating that these populations had the ability to move forth and back between the different populations (le Viseur 2008). In addition, the groups of Andreas Strasser and Scott Armstrong demonstrated in syngeneic mouse models that the frequency of cells with repopulating ability was as high as 1:10 and 1:4, respectively and therefore LICs need not be rare (Kelly 2007; Krivtsov 2006). This was further underlined by work of three groups, including ours, that were able to show that the number of unsorted leukemic blasts needed for initiation of leukemia in the NSG mouse model was between 10-100 cells (see manuscript 1) (Morisot 2010; Rehe 2009; Schmitz 2009). These findings suggest that in B-ALL the LIC organization follows rather the stochastic than the hierarchic CSC model.

Leukemic Clone Evolution and the Origin of Relapse

The conclusion that LICs in B-ALL are not fixed populations, but evolve genetically, phenotypically and functionally must be drawn from the before-mentioned studies. Recently more support for the clonal evolution model was given. By using multiplexed fluorescence *in-situ* hybridization (FISH) analysis a complex, branched, not linear, clonal architecture with successive acquisition of CNAs was detected in TEL-

AML1 positive ALL cases. Moreover, changes in the genetic composition at relapse or after xenograft transplantation could be backtracked to diagnosis (Anderson 2010). These data illustrated that different clones constitute the leukemogenic compartment and that leukemias undergo changes in their composition with different dominant subclones at different points of disease (Figures 7c and 8). Similarly, it was shown in adult BCR-ABL positive ALL using SNP arrays that the leukemic compartment evolves during disease (Notta 2011). A correlation of patient survival with concordance of CNAs before and after xenograft was shown. Less survival was associated with stably detectable CNAs and better survival with discordant CNAs (Notta 2011). This could indicate that more aggressive types of clones had been selected in patients with worse outcome. Therefore, clonal evolution could contribute to disease progression and treatment resistance.

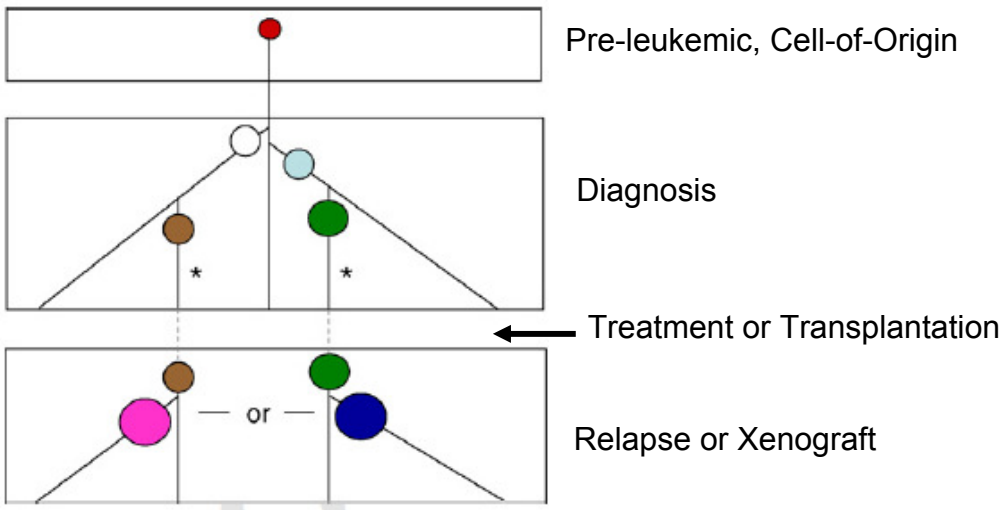

Figure 8. Altered clonal composition at different time points of disease. Different clones (phenotypical and genetical) with altered propagating abilities are observed as the major clone throughout disease. Adapted from (Greaves 2010).

Further evidence underlining the evolution of clones from disease initiation to disease maintenance was presented in twin studies. The pre-leukemic populations of identical twins with TEL-AML1 positive B-ALL were compared; less putative LICs were found in the twin with pre-leukemia compared to the twin with overt ALL. The phenotype and genotype of the pre-leukemic cells was distinct from the B-ALL cells (Hotfilder 2005). It is hypothesized that fusion transcripts (MLL-AF4, TEL-AML1, BCR-ABL) are established prenatally, already in-utero in the cell-of-origin (Vormoor 2009). For TEL-AML1 it was shown in five pairs of monozygotic twins that the fusion gene formation occurred prenatally and was postnatally followed by acquisition of more genetic lesions (Bateman 2010; Hong 2008). Additionally, a mechanism was described that confers TEL-AML1 positive cells with a growth advantage. Transduction of normal cord blood precursor cells with TEL-AML1 increased a subset of cells with a “pre-B leukemia-phenotype”, CD34+/CD38-/CD19+, and these cells had higher self-renewal capacity and survival rates (Hong 2008; Ford 2009). This indicates that the fusion gene formation is the primary leukemogenic event and subsequently further clonal evolution and selection is ongoing until and after overt leukemia is established.

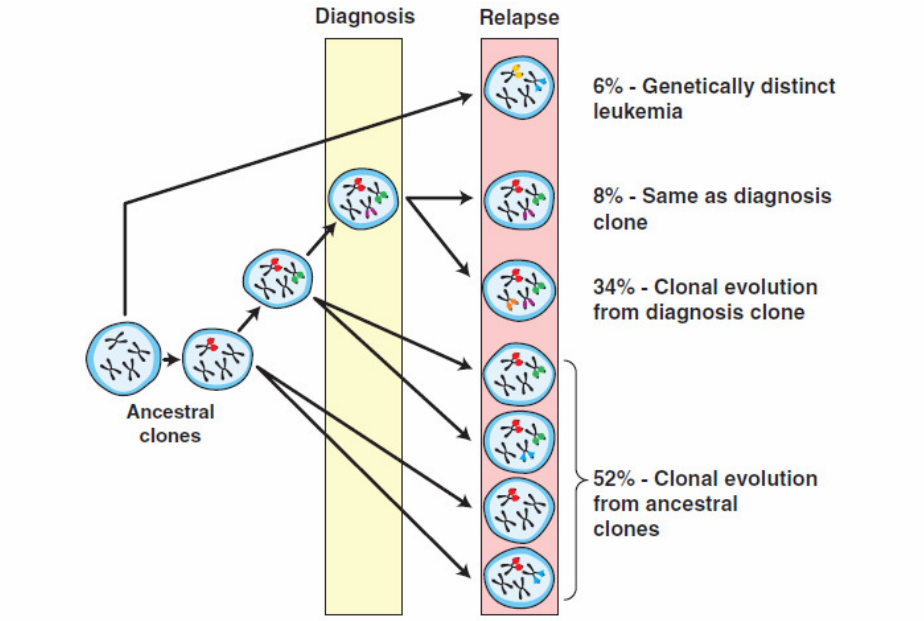

Figure 9. Genetic clonal evolution. Most of the cases at relapse show a clear relation to the diagnosis or to a common ancestral clone as suggested by CNA patterns. Adapted from (Mullighan 2008).

Not only the relation between pre-leukemic clones and diagnosis but also the connection of clones at relapse and at diagnosis was shown. With genome-wide studies large cohorts of matched diagnostic and relapsed cases were analyzed (Mullighan 2008; van Delft 2011; Kuster 2011; Davidsson 2010). Relapse cases showed higher numbers of CNAs than diagnosis cases (mean 12.5 vs. 7.5 CNAs per case in TEL-AML1) (Kuster 2011), and interestingly the obtained CNAs often targeted known oncogenic loci, such as *CDKN2A/B, IKZF1, RAG, PAX5* and *NR3C1*, speaking for a role in treatment resistance and selective advantage for these genes. Overall, in 90% of cases, there were different CNAs detected in diagnosis and relapse nevertheless most of the cases were highly related. Cells from the major subclones at relapse could most often be backtracked to minor subclones at diagnosis, suggesting that clonal selection occurred during treatment (Mullighan 2011; Kuster 2011; van Delft 2011; Davidsson 2010). As most relapses lacked some of the CNAs from diagnosis, it is suggested that a common ancestral clone exists (Figure 9) (Mullighan 2008).
The clonal variability at diagnosis might be the basis of treatment escape and origin of relapse. Thus, it will be crucial to identify the key lesions, which need to be targeted to prevent relapses.

Xenografts and Genetic Mouse Models to Study High-Risk Leukemias

Increasing data are available that characterize leukemia cells on genetic and phenotypic level. This provides the basis for the development of targeted therapies. To evaluate new treatment approaches preclinical models are needed. No cell lines are available that represent high-risk leukemias. And genetic mouse models have not been developed to a large extent as compared to the genetic complexity of ALL which was described above.

Genetic engineered mouse models mimic known genetic aberrations and allow investigating their importance for the biology of the tumor. In the field of leukemia, only a few models could be established. There is a model for BCR-ABL ALL, where the transduction of *arf*-null bone marrow progenitors with BCR-ABL was enough to induce lymphoblastic leukemia. These leukemias were highly tumorigenic in serial transplantations and resistant to imatinib in presence of cytokines (Williams 2007). There are also models for MLL-AF9 leukemias, which result in myeloid, but not lymphoid leukemias in mice (Krivtsov 2006; Somervaille 2006). Other models cover T-cell lymphomas, B-lymphomas, CML and AML (Kelly 2007; Adams 2008; Huntly 2004; Deshpande 2006; Neering 2007), illustrating the variety of tumors that can be modeled but also showing the lack of a representative model for high-risk B-ALL. A general disadvantage of genetic models is that they investigate single genetic aberrations and not the full genetic complexity. Therefore, they represent only a minor fraction of patients. In future, it will be a challenge as it is time consuming, but necessary to generate more genetic mouse models for the characterization of relevant genetic aberrations and their role in tumorigenesis and drug resistance.
For preclinical drug testing, xenografts have been more widely used. In that approach, primary patient material is transplanted into immunodeficient mice and is then recapitulating the original leukemia. The advantages of xenografts are – that the starting material is usually from advanced cancers, - that the tumors represent the original tumor in the patient, including the genetic complexity – and that you can test multiple drugs in different settings against the same set of cells or against different tumors from different patients (Politi 2011). Therefore, by using xenograft models all relevant patient groups can be modeled.

Subject of Investigation

Functional investigations of human ALL are limited by the difficulty to establish representative cell culture systems in vitro. Xenotransplantation of human leukemia cells in immunodeficient mice provides a new and powerful tool to model disease, provided the consequences of the selective pressures that are inherent to this model are better understood. The composition of the leukemia-propagating (or initiating) compartment in ALL appears to be more complex than previously proposed. This has important implications for our understanding of disease progression and treatment resistance mechanisms. The major aim of my PhD Thesis was to:

- Establish a representative xenograft model of childhood precursor B-ALL (manuscript 1 and 2)
- Functionally investigate the clonal composition of the LIC compartment in ALL and understand the consequences of the murine microenvironment for the xenograft model (manuscript 1).

Having established this system, I also contributed significantly to:

- Evaluate new treatment rationales for chemosensitization of de novo highly resistant cases using the xenograft model for in vitro and in vivo drug testing (manuscript 3)
- Use the xenograft system as a renewable source of leukemic cells for the investigation of new ALL subtypes (manuscript 3 and 4)

Manuscript 1: Xenografts of highly resistant leukemia recapitulate the clonal composition of the leukemogenic compartment (first author).
Manuscript 2: Alternative technique for intrafemoral injection and bone marrow sampling in mouse transplantation models (first author).
Manuscript 3: Induction of autophagy-dependent necroptosis is required for childhood acute lymphoblastic leukemia cells to overcome glucocorticoid resistance (co-author).
Manuscript 4: Down syndrome acute lymphoblastic leukemia, a highly heterogeneous disease in which aberrant expression of CRLF2 is associated with mutated JAK2: a report from the International BFM Study Group (co-author).

Manuscript one constitutes the main part of my work and thus will be the essential part in the discussion section.

Results

Xenografts of Highly Resistant Leukemia Recapitulate the Clonal Composition of the Leukemogenic Compartment

Maike Schmitz, Petra Breithaupt, Nastassja Scheidegger, Gunnar Cario, Laura Bonapace, Barbara Meissner, Paulina Mirkowska, Joelle Tchinda, Felix K. Niggli, Martin Stanulla, Martin Schrappe, Andre Schrauder, Beat C. Bornhauser* and Jean-Pierre Bourquin*
* These authors contributed equally

Blood (2011) doi: 10.1182/blood-2010-11-320309

Abstract:
Clonal evolution of the leukemogenic compartment may contribute to alter the therapeutic response in acute lymphoblastic leukemia (ALL). Using xenotransplantation of primary leukemia cells we evaluated the phenotypic and genetic composition of de novo resistant very high risk (VHR) precursor B-cell ALL, a subgroup defined by the persistence of minimal residual disease (MRD) despite intensive chemotherapy. Analysis of copy number alterations (CNA) showed that the xenografted leukemia, even when reconstituted from hundred cells, remained highly related to the diagnostic sample, with minor changes in CNAs, mostly deletions, emerging in most cases in the first passage into mice. At the single cell level, the pattern of mono-and bi-allelic deletions of the *CDKN2A* locus revealed distinct leukemia subpopulations, which were reproducibly tracked in xenografts. In most VHR-ALL cases, the predominant diagnostic clones were reconstituted in xenografts, as shown by multiplex PCR analysis of Ig/TCR loci. In other cases, the pattern in CNAs and Ig/TCR rearrangement was less concordant in xenografts, suggesting the outgrowth of subclones. These results unequivocally demonstrate the existence of clonally closely related but distinct subsets of leukemia initiating cells in ALL, which has important implications for drug development and preclinical disease modeling.

For detailed information, see attached manuscript 1

Alternative Technique for Intrafemoral Injection and Bone Marrow Sampling in Mouse Transplantation Models

Maike Schmitz, Jean-Pierre Bourquin, and Beat C. Bornhauser

Leukemia & Lymphoma (2011) doi: 10.3109/10428194.2011.580023

Letter to the editor:
Bone marrow punctures are often required when modeling hematologic malignancies in mice. Orthotopic intrabone injection resulted in superior engraftment of human hematopoietic stem cells or of human leukemia cells in immunodeficient mice. Similarly, between 10-100 cells from patients with acute lymphoblastic leukemia were sufficient to reconstitute leukemia in immunodeficient NOD/scidIL2Rγnull (NSG) mice after intrafemoral injections. Current protocols for bone marrow procedures in mice involve a two-step process that requires to perforate the cortical bone with a first needle and to retrieve the orifice subsequently with a needle with smaller gauge for injection or aspiration of cells. As alternative, we used a small needle with a stylet in analogy to bone marrow aspiration needles that are used in the clinic. Here we show that a pediatric spinal tap needle (also called atraucan needle) can be used efficiently and conveniently for bone marrow transplantation and sampling procedures in mice. This one step injection procedure (Figure 1) resulted in highly reproducible engraftment with primary human ALL cells (Table-1). 44 out of 45 xenograft ALL samples repopulated secondary recipients. This technique was used to establish an in vivo model of highly resistant leukemia. Furthermore, in serial dilution experiments 100 ALL cells were sufficient for engraftment in 4 different ALL cases, demonstrating that the injections can be performed with minimal losses due to dead volume with this needle. Bone marrow aspiration through the atraucan needle did not damage the bone marrow cells, as shown with 7-AAD stainings for cell viability by flow cytometry (Figure 1b). A homogeneous, viable population of CD19 and CD10 double positive human leukemia cells was detected in the bone marrow at 8 weeks after transplantation. The analysis of engraftment in the peripheral blood showed lower, although detectable, presence of human leukemia cells. By aspirating the femur contralateral to the injection site we collected up to 15’000 lymphocytes in 10 µl bone marrow aspirate without requirement for subsequent erythrolysis. By tail vein bleeding, we collected 50 µl of blood that was enough to detect at least the same number of lymphocytes.
Taken together, the use of the pediatric atraucan needle very effectively eliminates the need to perform two punctures of the cortical bone in order to inject into or sample cells from the bone marrow cavity. We are convinced that this simple modification will be of great interest for many investigators as xenograft models with human normal or malignant hematopoietic cells are increasingly applied.

For detailed information, see attached manuscript 2

Induction of Autophagy-Dependent Necroptosis is Required for Childhood Acute Lymphoblastic Leukemia Cells to Overcome Glucocorticoid Resistance

Laura Bonapace*, Beat C. Bornhauser*, Maike Schmitz, Gunnar Cario, Urs Ziegler, Felix K. Niggli, Beat W. Schäfer, Martin Schrappe, Martin Stanulla, and Jean-Pierre Bourquin
* These authors contributed equally

J Clin Invest. 2010;120(4):1310–1323.

Abstract:
In vivo resistance to first-line chemotherapy, including to glucocorticoids, is a strong predictor of poor out- come in children with acute lymphoblastic leukemia (ALL). Modulation of cell death regulators represents an attractive strategy for subverting such drug resistance. Here we report complete resensitization of multi- drug-resistant childhood ALL cells to glucocorticoids and other cytotoxic agents with subcytotoxic concentrations of obatoclax, a putative antagonist of BCL-2 family members. The reversal of glucocorticoid resistance occurred through rapid activation of autophagy-dependent necroptosis, which bypassed the block in mitochondrial apoptosis. This effect was associated with dissociation of the autophagy inducer beclin-1 from the antiapoptotic BCL-2 family member myeloid cell leukemia sequence 1 (MCL-1) and with a marked decrease in mammalian target of rapamycin (mTOR) activity. Consistent with a protective role for mTOR in glucocorticoid resistance in childhood ALL, combination of rapamycin with the glucocorticoid dexamethasone triggered autophagy-dependent cell death, with characteristic features of necroptosis. Execution of cell death, but not induction of autophagy, was strictly dependent on expression of receptor-interacting protein (RIP-1) kinase and cylindromatosis (turban tumor syndrome) (CYLD), two key regulators of necroptosis. Accordingly, both inhibition of RIP-1 and interference with CYLD restored glucocorticoid resistance completely. Together with evidence for a chemosensitizing activity of obatoclax in vivo, our data provide a compelling rationale for clinical translation of this pharmacological approach into treatments for patients with refractory ALL.

For detailed information, see attached manuscript 3

Down Syndrome Acute Lymphoblastic Leukemia, a Highly Heterogeneous Disease in which Aberrant Expression of CRLF2 is Associated With Mutated JAK2: a Report from the International BFM Study Group

*Libi Hertzberg, *Elena Vendramini, *Ithamar Ganmore, Gianni Cazzaniga, Maike Schmitz, Jane Chalker, Ruth Shiloh, Ilaria Iacobucci, Chen Shochat, Sharon Zeligson, Gunnar Cario, Martin Stanulla, Sabine Strehl, Lisa J. Russell, Christine J. Harrison, Beat Bornhauser, Akinori Yoda, Gideon Rechavi, Dani Bercovich, Arndt Borkhardt, Helena Kempski, †Geertruy te Kronnie, †Jean-Pierre Bourquin, †Eytan Domany, and †Shai Izraeli
*† these authors contributed equally

Blood. 2010;115:1006-1017

Abstract:
We report gene expression and other analyses to elucidate the molecular characteristics of acute lymphoblastic leukemia (ALL) in children with Down syndrome (DS). We find that by gene expression DS-ALL is a highly heterogeneous disease not definable as a unique entity. Nevertheless, 62% (33/53) of the DS-ALL samples analyzed were characterized by high expression of the type I cytokine receptor CRLF2 caused by either immunoglobulin heavy locus (IgH@) translocations or by interstitial deletions creating chimeric transcripts P2RY8-CRLF2. In 3 of these 33 patients, a novel activating somatic mutation, F232C in CRLF2, was identified. Consistent with our previous research, mutations in R683 of JAK2 were identified in 10 specimens (19% of the patients) and, interestingly, all 10 had high CRLF2 expression. Cytokine receptor-like factor 2 (CRLF2) and mutated Janus kinase 2 (Jak2) cooperated in conferring cytokine-independent growth to BaF3 pro-B cells. Intriguingly, the gene expression signature of DS-ALL is enriched with DNA damage and BCL6 responsive genes, suggesting the possibility of B-cell lymphocytic genomic instability. Thus, DS confers increased risk for genetically highly diverse ALLs with frequent overexpression of CRLF2, associated with activating mutations in the receptor itself or in JAK2. Our data also suggest that the majority of DS children with ALL may benefit from therapy blocking the CRLF2/JAK2 pathways.

For detailed information, see attached manuscript 4

Discussion

In this thesis, I describe the establishment of a xenograft model for the study of highly resistant childhood acute lymphoblastic leukemia (ALL) with primary material, the validation as preclinical model of high risk disease and the application to investigate the nature of the leukemia propagating cell compartment.

The functional investigation of the biology of acute leukemias has been hampered by the facts - that diagnostic material is scarce, - that cell lines can only be established for a minority of cases and not necessarily represent the original leukemias, - that in vitro culturing of primary leukemic cells is difficult – and that due to the genetic complexity transgenic mouse models for high-risk subtypes of B-ALL are missing. Therefore, xenografting primary patient material in immunodeficient mice provides an interesting alternative to model disease. Scarce primary material can hereby be repeatedly amplified (on average around 500x of initial cell numbers) creating a bank of primary material for in vitro and in vivo experiments.
However, the consequences of the selective pressure that the xenogenic environment imposes on the leukemic cells must be understood. We therefore established a xenograft model of high risk ALL and evaluated the consequences of xenotransplantation on the genotype and phenotype of leukemia cells.
The leukemia initiating cell (LIC) compartment has been set in the focus for the development of novel treatment approaches and it is crucial to know its composition to be able to understand progression of leukemia and treatment resistance. For that reason, we investigated the clonal composition of LICs in the context of the xenograft model.

Set-Up of the Xenograft Model

The European BFM study group (named after the founding centers in Berlin-Frankfurt-München) has pioneered risk stratification protocols based on measuring minimal residual disease (MRD). This is a quantification of residual leukemic blasts in the bone marrow and peripheral blood of patients (Schrappe 2004; Flohr 2008; Conter 2010). The BFM study group has large banks of primary diagnostic material with clearly defined clinical and genetic characterization. Each year around 1000 de-novo resistant cases and around 300 relapse cases are included. As an integrated part of the BFM we have established the preclinical xenograft model. We picked samples from patients with very poor prognosis (VHR-ALL) and from those with very good prognosis (SR-ALL), according to the BFM MRD classification. For the studies described in this work in total 17 VHR-ALL, 15 SR-ALL, 4 HR-ALL and 8 samples from patients with Down-Syndrome ALL were used. As illustrated in Figure 10, the xenograft model represents the basis of several preclinical research projects.

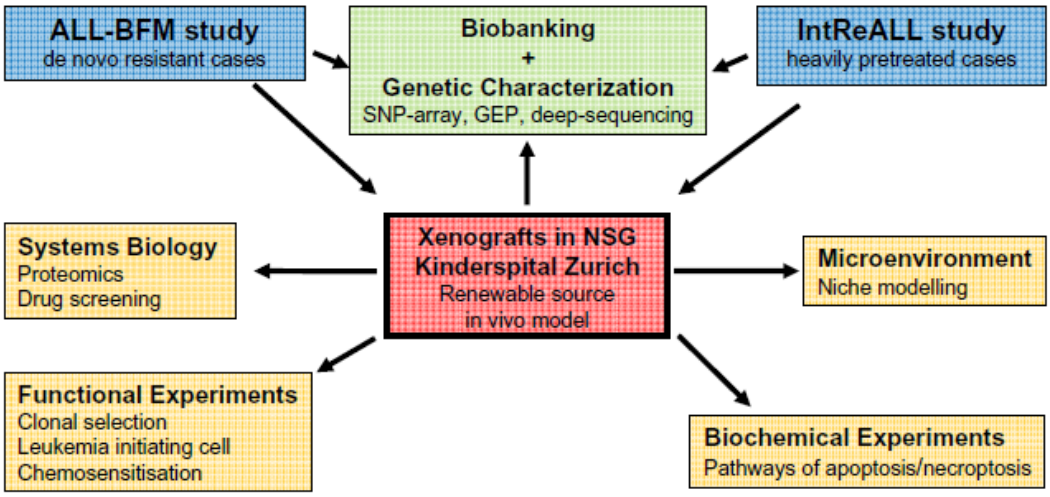

Figure 10. Overview of the BFM xenograft consortium and the current research projects.

For the xenograft model we used the highly immunocompromised mouse strain NOD/scidIL2Rγnull (NSG), that was demonstrated to have superior engrafting potential compared to the NOD/scid mouse strain (McDermott 2010; Agliano 2008). The additional deletion of the γ-chain of the IL2 receptor renders the natural-killer cells of the mouse dysfunctional and thus prevents an immune response towards the transplanted human leukemic cells. And indeed we found that more than 75% of all our patient samples engrafted in NSG mice. If multiple mice were transplanted of one patient with known engraftment potential, the efficiency was close to 100%. Therefore, non-engrafting cells potentially have intrinsic differences rendering them incompatible to engraft in mice (personal communication, D. Bonnet). More refinement of the transplantation efficiency was achieved by using intra-femoral (IF) rather than intra-venous (IV) transplantation. The superiority of IF over IV was demonstrated by limiting dilution experiments, where we saw engraftment at the limiting dose of 100 cells only in the group of mice transplanted via IF route and never if IV route was applied (Schmitz 2009), and was also reported by others for leukemic and normal hematopoietic samples (le Viseur 2008; Mazurier 2003). The reason for that may be a faster and more efficient homing to the bone marrow after transplantation. To facilitate the IF transplantation technique we used an atraucan spinal tap needle usually applied in the clinics for bone marrow aspirations in children. This needle has a stylet, which allows performing the transplantation in one step, and therefore facilitates the procedure also adding to the high engraftment rates (manuscript 2).

Xenografts Mirror the Phenotype of Original Human ALL Cells

To answer the question if xenotransplantation is selecting for certain subpopulations of leukemic cells, for example favoring engraftment of immature subpopulations over differentiated ones, we have investigated the immunophenotype and the functional drug response of cells before and after transplantation. We looked at a panel of eleven different cell-surface markers, which is also used for diagnosis, covering the whole diversity of markers from immature to differentiation to cross-expression, in 16 patients and xenografts thereof and found the phenotypes to be very similar. In five cases we could perform measurements from matched diagnosis and xenograft samples ourselves on the same instrument and had concordant results in 46 of 51

measurements. For the eleven other cases we could not perform analysis of diagnostic material ourselves and therefore compared our data to the data from the BFM reference lab. There we observed changes in 15 of 99 measurements, and changes occurred in different surface markers (CD34, CD20, CD13, CD33, and CD7). Therefore, the changes we observed might reflect a minor selection in NSG mice in the context of the xenogenic environment.
We further investigated whether serial xenotransplantation changed the drug responses to four common chemotherapeutic compounds (namely, Dexamethasone, Vincristine, Cytarabine and Daunorubicine) *in vitro*. As expected, xenograft cells from the VHR samples were highly resistant and xenograft cells from SR patients were sensitive to these compounds. Moreover, the drug response profiles did not change with higher serial passages used. These data suggest that it is rather an adaptation to the mouse environment and not a selection of ALL cells that are intrinsically more resistant to chemotherapeutic agents, which is responsible for the acceleration of engraftment in secondary transplantation of SR-ALL cells.
This conservation of drug response features upon xenografting enabled us to investigate the mechanisms of treatment resistance in VHR-ALL patients (manuscript 3). We evaluated the new compound obatoclax, a pan-BCL-2 inhibitor to act as a chemosensitizer. Using the xenograft model, we demonstrated that obatoclax has a strong chemosensitization effect in VHR-ALL samples *in vivo* (Bonapace 2010). Indeed, mice that were engrafted with leukemia and then treated for two weeks with a combination of obatoclax and dexamethasone had significant better survival than the control groups. With *in vitro* experiments using xenograft material we then found that unexpectedly, resensitization to glucocorticoids resulted from activation of autophagy-dependent necroptosis, an alternative cell death pathway, which bypasses the apoptotic blockade in glucocorticoid resistant cells.
Based on these observations it seems to be justified to go on using xenotransplantation as a way to expand the limited number of cells present at diagnosis and to use this assay as a tool to filter out relevant mechanisms of high risk leukemia biology.

Can Engraftment Kinetics Predict Patient Outcome?

A question often raised in the field is whether the engraftment in mice can reflect the course of disease in patients. In our work we found that the VHR-ALL group of patients had significant faster engraftment times (median 8 weeks) than the SR-ALL patients (median 13 weeks). Concordant with this, it was shown in NOD/scid mice that samples, which engrafted rapidly, were from patients with early relapses (Meyer 2011). One can carefully propose that VHR-ALL samples with very unfavorable leukemia biology have been selected with genetic or epigenetic features that favor proliferation and engraftment in the xenograft model. On the one hand, extrinsic factors like the mouse environment, homing and different cytokines accessible, could force the selection. On the other hand, intrinsic factors to the patients' more aggressive leukemia could be responsible for the faster engraftment. Interestingly, we observed an acceleration of the engraftment kinetics in the SR-ALL group of patients upon secondary transplantation. Secondary engraftment of these cases occurred with similar kinetics than for VHR-ALL samples (median 7 weeks), as VHR-ALL secondary engraftments were not further accelerated. Remarkably, in three of five cases this acceleration correlated with the emergence of readily detectable new Ig/TCR gene rearrangements in the xenografts. It is possible that in VHR-ALL

dominant clones with higher proliferating abilities have already been selected and stably propagate in the mice whereas in SR-ALL higher degrees of clonal selection occur upon xenografting due to the absence of a dominant clone. Similar observations were made in BCR-ABL ALL xenografts where it was shown that the pattern of CNAs was more concordant in cases from fast engrafting patients and that these patients had a trend to shorter survival times (Notta 2011).

Are Leukemia-Initiating Cells Rare?

There is an ongoing debate whether ALL is following a hierarchic cancer stem cell model or rather a stochastic model. Our data (manuscript 1) and that of others (Rehe. 2009; Morisot 2010; Anderson 2010) challenge the hierarchic model which proposes that the leukemia is maintained from a subset of immature stem cells (Cox 2009; Cobaleda 2000). We found that in four of six cases hundred VHR-ALL cells were sufficient to reconstitute leukemia in the NSG mouse strain, which suggests that the LIC compartment is not limited to a rare subpopulation of cells. However, in two cases of SR-ALL 100 cells were never sufficient. Similar LIC frequencies have been demonstrated by other groups for different subtypes of ALL (Morisot 2010; Rehe 2009; Chiu 2010). Likewise, ALL cells from different maturation stages were shown to reconstitute the full leukemic phenotype in NSG mice. Thus, LIC activity is not limited to one certain subset of cells (le Viseur 2008). In addition, Strasser et al demonstrated in syngeneic mouse models that the frequency of leukemia cells with repopulating ability was as high as 1:10 and therefore LICs need not be rare (Kelly. 2007). However, contradicting data comes from other groups who could show in different high-risk subtypes of ALL that LICs reside only in defined rare and immature subpopulations, like the hematopoietic stem cell-like CD133+ compartment or the CD34+/CD38- compartment (Cox 2009; Cox 2005; Cobaleda 2000). And for SR-ALL more mature CD19-positive compartments were proposed to contain the LIC activity (Castor 2005; Hong 2008). In future it will be interesting to see whether leukemias with a favorable outcome are associated with lower frequencies of LICs coming from more mature compartments.
Some of these contradicting results might be attributed to the technical limitations of the xenografts system as was described above. More examples for differing results as a consequence of different experimental set-up come from melanoma, T-ALL and AML. The melanoma stem cell was at first described as a very rare cell, with a frequency of 1 in 10^6 using NOD/scid mice (Fang 2005; Dou 2007), but later Quintana et al showed that the frequency dropped to 1 in 4 using the more immunocompromised NSG mice (Quintana 2008). Also for T-ALL the influence of the model system was shown, as only T-ALL xenograft cells that were negative for the thymic maturation marker CD1a engrafted NOD/scid mice. Repeating this experiment in NSG mice, T-ALL engraftment was more efficient, with evidence also for engraftment of sorted CD1a positive T-ALL cells (Chiu 2010). And in AML the initially non-LIC population CD34+/CD38+ was indeed also able to initiate leukemia (Taussig 2008). In the initial study the use of a certain anti-CD38 antibody led to clearance of the labeled cells in the mice and therefore led to the different interpretation of the results (Taussig 2008). These effects of residual immunologic functions and the xenogenic environment highlight the importance of the many factors contributing to successful transplantation assays. And it raises awareness for the fact that with xenotransplantation assays we are only looking at the reconstitution capacity in the

model chosen, but the situation for cancer stem cells *in situ* might be much more complex than that (e.g. interactions with microenvironment, trafficking to niche).
We performed serial dilution analysis with unsorted samples as in most ALL cases, even extensive multicolor FACS strategies often do not result in the visualization of distinct subpopulations based on lineage maturation or stem cell markers, which limits the identification of an underlying hematopoietic hierarchy based on surface markers. Similarly, difficulties in finding markers that can discriminate subpopulations were observed in a study about melanoma propagating cells (Quintana 2008). Moreover, antibodies used for cell sorting experiments can increase clearance of sorted cells even in immunodeficient mice (Taussig 2008). An alternative could be the use functional markers of stemness, such as Aldehyde dehydrogenase (ALDH) activity. In our set of samples, we did not identify a consistent ALDH positive compartment and positivity did not correlate with a high frequency of LICs in the xenograft system. Also, we did not detect differences in NSG repopulation capacity when sorting cells based on ALDH activity (data not shown). In AML high ALDH activity has been proposed to be a stem cells marker in the CD34+CD38- compartment (Pearce 2005), but for normal mouse hematopoietic stem cell function ALDH activity was shown to be dispensable (Levi 2009). Taken together, we think that in VHR-ALL propagating cells are relatively frequent from the manifestation of the disease on and therefore VHR-ALL is intrinsically difficult to eradicate.

Do Xenografts Filter for Resistant Subpopulations?

To explore whether high-risk leukemias are intrinsically resistant or acquire resistance through mechanisms of clonal evolution or selection we investigated the genetic composition of VHR- and SR-ALL cases before and after xenografting. Overall, we observed a pattern reflecting the propagation of highly related clones.
We performed SNP array analysis of six matched diagnostic, remission and xenograft samples. Only few, up to 8, copy number alterations (CNAs) were observed per sample, as is typical for ALL and was reported before in other datasets (Mullighan 2008a; Mullighan 2007; Mullighan 2008b), with the exception of one high-hyperdiploid case which had more than 30 whole chromosome amplifications. Most of the aberrations were reported before in larger studies and only up to 4 changes were observed per matched diagnosis and xenograft sample (max. 2 new deletions, 3 lost deletions, 2 new amplifications, 1 lost amplifications). These CNA changes occurred at loci recurrently detected in ALL and usually appeared already in the first amplification in the mice (Mullighan 2008a; 2007; Mullighan 2009). This demonstrates that changes in CNAs are most likely neither due to increased genetic instability in the xenograft system nor due to selective pressure from the xenogenic environment.
Among the CNA changes occurring in xenografts, the p-arm of chromosome 9 was a recurrent target. In five of the six samples analyzed aberrations did occur. Deletions occurring on 9p are frequently detected in childhood ALL (Mullighan 2007; Novara 2009; Heerema 2004; Mullighan 2008a). The genes involved are the B-cell development and cell-cycle regulators *CDKN2A* and *CDKN2B*, which seem to play a role in ALL pathogenesis, but their association to relapse is inconsistently described (Heerema 2004; Novara 2009). A study in adult BCR-ABL ALL showed that appearance of *CDKN2A* CNAs in xenografts was associated with a trend towards shorter survival times of the corresponding patients (Notta 2011). On the other hand,

in our cohort and other studies (Sherborne 2010; Sulong 2009) *CDKN2A* aberrations were found in samples from both high-risk and standard-risk subtypes of ALL.
As the number of cases in xenograft studies is understandingly small and as there is a high heterogeneity in ALL subgroups with respect to their genetic features we cannot make a final conclusion of the importance of this finding for pathogenesis. Moreover, a change in CNA after xenografting could simply reflect a growth advantage in the xenogenic environment rather than the relevant mechanism to escape chemotherapy treatment. Nevertheless, with higher numbers and comparative studies including relapse samples the xenograft system could be used in future to filter out the driving events that lead to chemotherapy resistance and disease progression and to evaluate the effect of recurrent mutations especially with respect to clonal selection and drug resistance.

Clonal Stability or Selection in Treatment Resistance?

With further analysis of *CDKN2A* copy numbers on the single-cell level by fluorescence in-situ hybridization (FISH) we observed that the leukemogenic compartment is composed of several distinct clones rather than just one clone. We found nearly half of all patients with aberrations and most patients had various types of aberrations in distinct cells, speaking for clonal diversity within each patient. Sometimes we detected changes in the frequency of clones between diagnosis and xenografts (i.e. a different major clone at diagnosis and xenograft), indicating minor selection of subpopulations. And the analysis of clonal Ig/TCR rearrangements revealed loss of less prominent markers suggesting that most changes involve the loss of minor ALL subclones. Markedly, replica and serial xenografts and also xenografts from limiting dilution appeared almost the same regarding their genetic clonal composition, signifying that selection occurred during the first passage into mice and subsequent stability of the xenograft model.
Other studies further underline our observation that the LIC compartment is oligoclonal. An in-depth study of the clonal composition in TEL-AML1 ALL by multicolor FISH with analysis of up to five genetic loci per cell found a complex genetic architecture with up to 14 distinct clones per leukemia (Anderson 2010). In addition, SNP analysis demonstrated the clonal diversity of adult BCR-ABL ALL (Notta 2011). Together, this data suggests that clonal selection may occur to a certain degree in the xenograft model, usually at the first passage in mice already, and that the overall similarity of the xenografted samples to the original diagnosis samples is high. The multi-clonal appearance of ALL may constitute the ground for clonal selection or evolution and treatment escape. In future, it will be interesting to investigate the clonal complexity during disease course to detect those clones that escape the chemotherapy treatment.

Summary

Collectively, the work performed in this thesis contributes to the understanding of the leukemogenic compartment of high risk ALL. We have established a leukemia xenograft model that enables to perform functional studies with samples that are relevant for translational research. Our findings and those of others demonstrated that LICs are relatively frequent and consist of a heterogeneous population. It appears unlikely to identify one unique subpopulation with repopulating potential and

thus we believe that ALL has, if at all, a flat hierarchy and the LIC compartment is oligoclonal. In the xenograft model, ALL samples were propagated as a dynamic multi-clonal population with highly conserved features after xenotransplantation. The limitations of the xenograft model are the reflections of multiple factors that influence engraftment, for example the homing capability, the self-renewal capacity and the interactions with the murine microenvironment.

The multi-clonal appearance of ALL may constitute the ground for clonal selection or evolution and treatment escape. In future, it will be interesting to investigate the clonal complexity during disease course. Two approaches could be applied, the modeling of the MRD phase in the NSG mice by mild, non-curative treatment of transplanted animals or the engraftment of patient bone marrow samples from MRD measurements. To understand if the outgrowth of minor clones leads to relapses and if this can be modeled in the xenograft system we will need to study matched relapse and diagnostic material from patients that were initially classified in the standard risk group.

The mouse xenograft system will enable to investigate the consequences of different types of interventions on the clonal composition of the disease. With the xenograft system we were able to show the effectiveness of a novel compound, obatoclax, to overcome the apoptotic blockade in glucocorticoid resistant ALL.

Clearly, development of new therapeutic approaches will have to take into account that the whole leukemia population has to be eradicated to prevent the escape of single clones that might generate a relapse. These considerations also reinforce the importance of combination therapy, which is supported by decades of clinical research in oncology. The development of xenograft models of distinct clinical and genetic entities will greatly improve our capability to evaluate new treatment rationales. Based on the availability of the renewable source of relevant patient material that we generated, combinatorial treatment studies that take the clonal complexity of the disease in consideration can be conducted in future.

Bibliography

Adams, J. M., and Strasser, A. (2008). Is tumor growth sustained by rare cancer stem cells or dominant clones? Cancer research 68, 4018-4021.

Agliano, A., Martin-Padura, I., Mancuso, P., Marighetti, P., Rabascio, C., Pruneri, G., Shultz, Leonard D, and Bertolini, F. (2008). Human acute leukemia cells injected in NOD/LtSz-scid/IL-2Rgamma null mice generate a faster and more efficient disease compared to other NOD/scid-related strains. International journal of cancer. 123, 2222-7.

Al-Hajj, M., Wicha, M. S., Benito-Hernandez, A., Morrison, Sean J, and Clarke, Michael F (2003). Prospective identification of tumorigenic breast cancer cells. Proceedings of the National Academy of Sciences of the United States of America 100, 3983-8.

Anderson, Kristina et al. (2010). Genetic variegation of clonal architecture and propagating cells in leukaemia. Nature 469, 356-61.

Armstrong, F. et al. (2002). MLL translocations specify a distinct gene expression profile that distinguishes a unique leukemia. Nature genetics 30, 41-47.

Armstrong, S.A., and Look, A. T. (2005). Molecular genetics of acute lymphoblastic leukemia. Journal of Clinical Oncology 23, 6306-6315.

Bailey, L. C., Lange, B. J., Rheingold, S. R., and Bunin, N. J. (2008). Bone-marrow relapse in paediatric acute lymphoblastic leukaemia. The lancet oncology 9, 873-83.

Bateman, Caroline M et al. (2010). Acquisition of genome-wide copy number alterations in monozygotic twins with acute lymphoblastic leukemia. Blood 115, 3553-8.

Bercovich, D. et al. (2008). Mutations of JAK2 in acute lymphoblastic leukaemias associated with Down□s syndrome. Lancet 372, 1484-92.

Biondi, A, Cimino, G., Pieters, R, and Pui, C.-H. (2000). Biological and therapeutic aspects of infant leukemia. Blood 96, 24.

Boer, J. de, Yeung, J., Ellu, J., Ramanujachar, R., Bornhauser, B, Solarska, O., Hubank, M., Williams, O., and Brady, H. J. M. (2011). The E2A-HLF oncogenic fusion protein acts through Lmo2 and Bcl-2 to immortalize hematopoietic progenitors. Leukemia : official journal of the Leukemia Society of America 25, 321-30.

Bomken, S., Fiser, K., Heidenreich, O, and Vormoor, J (2010). Understanding the cancer stem cell. British journal of cancer 103, 439-45.

Bonapace, L. (2010). New Approaches for Chemosensitization of Refractory Leukemia by Modulation of Programmed Cell Death. University of Zürich.

Bonapace, L. et al. (2010). Induction of autophagy-dependent necroptosis is required for childhood acute lymphoblastic leukemia cells to overcome glucocorticoid resistance. The Journal of clinical investigation 120, 1310-23.

Bonnet, D., and Dick, J. E. (1997). Human acute myeloid leukemia is organized as a hierarchy that originates from a primitive hematopoietic cell. Nature medicine 3, 730-7.

Campbell, L. J., Fidler, C., Eagleton, H., Peniket, a, Kusec, R., Gal, S., Littlewood, T. J., Wainscoat, J. S., and Boultwood, J. (2006). hTERT, the catalytic component of telomerase, is downregulated in the haematopoietic stem cells of patients with chronic myeloid leukaemia. Leukemia : official journal of the Leukemia Society of America, Leukemia Research Fund, U.K 20, 671-9.

Cario, G. et al. (2010). Presence of the P2RY8-CRLF2 rearrangement is associated with a poor prognosis in non-high-risk precursor B-cell acute lymphoblastic leukemia in children treated according to the ALL-BFM 2000 protocol. Blood 115, 5393-5397.

Castor, A. et al. (2005). Distinct patterns of hematopoietic stem cell involvement in acute lymphoblastic leukemia. Nature medicine 11, 630-7.

Chiu, P. P. L., Jiang, H., and Dick, J. E. (2010). Leukemia-initiating cells in human T-lymphoblastic leukemia exhibit glucocorticoid resistance. Blood 116, 5268-79.

Clarke, Michael F, Dick, J. E., Dirks, P. B., Eaves, C. J., Jamieson, C. H. M., Jones, D. L., Visvader, J., Weissman, Irving L, and Wahl, G. M. (2006). Cancer stem cells--perspectives on current status and future directions: AACR Workshop on cancer stem cells. Cancer research 66, 9339-44.

Cobaleda, C., Gutierrez-Cianca, N., Perez-Losada, J., Flores, T., Garcia-Sanz, R., Gonzalez, M., and Sanchez-Garcia, I. (2000). A primitive hematopoietic cell is the target for the leukemic transformation in human philadelphia-positive acute lymphoblastic leukemia. Blood 95, 1007-1013.

Conter, V. et al. (2010). Molecular response to treatment redefines all prognostic factors in children and adolescents with B-cell precursor acute lymphoblastic leukemia : results in 3184 patients of the AIEOP-BFM ALL 2000 study. Blood 115, 3206-3214.

Cox, C V, and Blair, A. (2005). A primitive cell origin for B-cell precursor all? Stem Cell Reviews and Reports, 189-196.

Cox, Charlotte V, Diamanti, P., Evely, R. S., Kearns, P. R., and Blair, A. (2009). Expression of CD133 on leukemia-initiating cells in childhood ALL. Blood 113, 3287-96.

Davidsson, J. et al. (2010). Relapsed childhood high hyperdiploid acute lymphoblastic leukemia: presence of preleukemic ancestral clones and the secondary nature of microdeletions and RTK-RAS mutations. Leukemia 24, 924-31.

Delft, F. W. van et al. (2011). Clonal origins of relapse in ETV6-RUNX1 acute lymphoblastic leukemia. Blood 117, 6247-54.

Deshpande, A. J. et al. (2006). Acute myeloid leukemia is propagated by a leukemic stem cell with lymphoid characteristics in a mouse model of CALM/AF10-positive leukemia. Cancer cell 10, 363-74.

Dick, J. E. (2008). Stem cell concepts renew cancer research. Blood 112, 4793-807.

Dongen, J. J. van et al. (1998). Prognostic value of minimal residual disease in acute lymphoblastic leukaemia in childhood. Lancet 352, 1731-1738.

Dou, J. et al. (2007). Isolation and identification of cancer stem-like cells from murine melanoma cell lines. Cellular & molecular immunology 4, 467-72.

Dworzak, Michael N et al. (2008). CD20 up-regulation in pediatric B-cell precursor acute lymphoblastic leukemia during induction treatment: setting the stage for anti-CD20 directed immunotherapy. Blood 112, 3982-8.

Einsiedel, H. G. et al. (2005). Long-term outcome in children with relapsed ALL by risk-stratified salvage therapy: results of trial acute lymphoblastic leukemia-relapse study of the Berlin-Frankfurt-Munster Group 87. Journal of Clinical Oncology 23, 7942-7950.

Fang, D. et al. (2005). A tumorigenic subpopulation with stem cell properties in melanomas. Cancer research 65, 9328-37.

Flohr, T. et al. (2008). Minimal residual disease-directed risk stratification using real-time quantitative PCR analysis of immunoglobulin and T-cell receptor gene rearrangements in the international multicenter trial AIEOP-BFM ALL 2000 for childhood acute lymphoblastic leukemia. Leukemia : official journal of the Leukemia Society of America, Leukemia Research Fund, U.K 22, 771-82.

Ford, Anthony M, Palmi, C., Bueno, C., Hong, D., Cardus, P., Knight, D., Cazzaniga, Giovanni, Enver, T., and Greaves, M. (2009). The TEL-AML1 leukemia fusion gene dysregulates the TGF-beta pathway in early B lineage progenitor cells. The Journal of clinical investigation 119, 826-36.

Gaipa, G. et al. (2008). Prednisone induces immunophenotypic modulation of CD10 and CD34 in nonapoptotic B-cell precursor acute lymphoblastic leukemia cells. Cytometry. Part B, Clinical cytometry 74, 150-5.

Gal, H. et al. (2006). Gene expression profiles of AML derived stem cells; similarity to hematopoietic stem cells. Leukemia : official journal of the Leukemia Society of America, Leukemia Research Fund, U.K 20, 2147-54.

Greaves, M. (2010). Cancer stem cells: back to Darwin? Seminars in cancer biology 20, 65-70.

Greaves, M. F., and Wiemels, J. (2003). Origins of chromosome translocations in childhood leukaemia. Nature reviews. Cancer 3, 639-49.

Gupta, P. B., Chaffer, C. L., and Weinberg, R. a (2009). Cancer stem cells: mirage or reality? Nature medicine 15, 1010-2.

Harvey, R. C. et al. (2010). Rearrangement of CRLF2 is associated with mutation of JAK kinases, alteration of IKZF1, Hispanic/Latino ethnicity, and a poor outcome in pediatric B-progenitor acute lymphoblastic leukemia. Blood 115, 5312-21.

Harvey, R. C. et al. (2010). Identification of novel cluster groups in pediatric high-risk B-precursor acute lymphoblastic leukemia with gene expression profiling: correlation with genome-wide DNA copy number alterations, clinical characteristics, and outcome. Blood 116, 4874-84.

Heerema, N. A. et al. (2004). Secondary cytogenetic aberrations in childhood Philadelphia chromosome positive acute lymphoblastic leukemia are nonrandom and may be associated with outcome. Leukemia : official journal of the Leukemia Society of America 18, 693-702.

Hemmati, H. D., Nakano, I., Lazareff, J. A., Masterman-Smith, M., Geschwind, D. H., Bronner-Fraser, M., and Kornblum, H. I. (2003). Cancerous stem cells can arise from pediatric brain tumors. Proceedings of the National Academy of Sciences of the United States of America 100, 15178-83.

Hertzberg, L. et al. (2010). Down syndrome acute lymphoblastic leukemia, a highly heterogeneous disease in which aberrant expression of CRLF2 is associated with mutated JAK2: a report from the International BFM Study Group. Blood 115, 1006-17.

Hong, D. et al. (2008). Initiating and cancer-propagating cells in TEL-AML1-associated childhood leukemia. Science (New York, N.Y.) 319, 336-9.

Hotfilder, M., Rottgers, S., Rosemann, A, Schrauder, Andre, Schrappe, M, Pieters, R, Jurgens, H., Harbott, Jochen, and Vormoor, J (2005). Leukemic stem cells in childhood high-risk ALL/t(9;22) and t(4;11) are present in primitive lymphoid-restricted CD34+CD19- cells. Cancer research 65, 1442-1449.

Hu, Y., Liu, Y., Pelletier, S., Buchdunger, E., Warmuth, M., Fabbro, D., Hallek, M., Van Etten, R. A., and Li, S. (2004). Requirement of Src kinases Lyn, Hck and Fgr for BCR-ABL1-induced B-lymphoblastic leukemia but not chronic myeloid leukemia. Nature genetics 36, 453–461.

Huntly, B. J., and Gilliland, D G (2005). Leukaemia stem cells and the evolution of cancer-stem-cell research. Nature Reviews Cancer 5, 311–321.

Jonge-Peeters, S. D. P. W. M. de, Kuipers, F., Vries, E. G. E. de, and Vellenga, E. (2007). ABC transporter expression in hematopoietic stem cells and the role in AML drug resistance. Critical reviews in oncology/hematology 62, 214-26.

Kearney, L. et al. (2009). Specific JAK2 mutation (JAK2R683) and multiple gene deletions in Down syndrome acute lymphoblastic leukemia. Blood 113, 646-648.

Kelly, P. N., Dakic, A., Adams, J. M., Nutt, S. L., and Strasser, A. (2007). Tumor growth need not be driven by rare cancer stem cells. Science 317, 337.

Kelly, P. N., Dakic, A., Adams, J., Nutt, S., and Strasser, A. (2007). Tumor growth need not be driven by rare cancer stem cells. Science 317, 337.

Kong, Y. et al. (2008). CD34+CD38+CD19+ as well as CD34+CD38-CD19+ cells are leukemia-initiating cells with self-renewal capacity in human B-precursor ALL. Leukemia 22, 1207-13.

Krivtsov, A V, and Armstrong, F. (2007). MLL translocations, histone modifications and leukaemia stem-cell development. Nature Reviews Cancer 7, 823-833.

Krivtsov, Andrei V et al. (2006). Transformation from committed progenitor to leukaemia stem cell initiated by MLL-AF9. Nature 442, 818-22.

Kuster, L. et al. (2011). ETV6/RUNX1-positive relapses evolve from an ancestral clone and frequently acquire deletions of genes implicated in glucocorticoid signaling. Blood 117, 2658-67.

Lapidot, T. et al. (1994). A cell initiating human acute myeloid leukaemia after transplantation into SCID mice. Nature 367, 645-648.

Levi, B. P., Yilmaz, O. H., Duester, G., and Morrison, S J (2009). Aldehyde dehydrogenase 1a1 is dispensable for stem cell function in the mouse hematopoietic and nervous systems. Blood 113, 1670-1680.

Lobo, N. A., Shimono, Y., Qian, D., and Clarke, M F (2007). The biology of cancer stem cells. Rev. Cell Dev. Biol. 23, 675-699.

Mazurier, F., Doedens, M., Gan, O. I., and Dick, J. E. (2003). Rapid myeloerythroid repopulation after intrafemoral transplantation of NOD-SCID mice reveals a new class of human stem cells. Nature medicine 9, 959-63.

McCune, J. M., Namikawa, R., Kaneshima, H., Shultz, L D, Lieberman, M., and Weissman, I L (1988). The SCID-hu mouse: murine model for the analysis of human hematolymphoid differentiation and function. Science (New York, N.Y.) 241, 1632-9.

McDermott, S. P., Eppert, K., Lechman, E., Doedens, M., and Dick, J. E. (2010). Comparison of human cord blood engraftment between immunocompromised mouse strains. Blood 116, 1-3.

McLean, T. W. et al. (1996). TEL/AML-1 dimerizes and is associated with a favorable outcome in childhood acute lymphoblastic leukemia. Blood 88, 4252-8.

Meyer, L. H. et al. (2011). Early relapse in all is identified by time to leukemia in NOD/SCID mice and is characterized by a gene signature involving survival pathways. Cancer cell 19, 206-17.

Morisot, S. et al. (2010). High frequencies of leukemia stem cells in poor-outcome childhood precursor-B acute lymphoblastic leukemias. Leukemia 24, 1859-1866.

Morisot, S. et al. (2010). High frequencies of leukemia stem cells in poor-outcome childhood precursor-B acute lymphoblastic leukemias. Leukemia : official journal of the Leukemia Society of America, Leukemia Research Fund, U.K, 1-8.

Morrison, S J, Prowse, K. R., Ho, P., and Weissman, I L (1996). Telomerase activity in hematopoietic cells is associated with self-renewal potential. Immunity 5, 207-16.

Mullighan, C. G. et al. (2009a). Rearrangement of CRLF2 in B-progenitor- and Down syndrome-associated acute lymphoblastic leukemia. Nature genetics 41, 1243-6.

Mullighan, C. G., and Downing, J. R. (2009). Global genomic characterization of acute lymphoblastic leukemia. Seminars in hematology 46, 3-15.

Mullighan, C. G. et al. (2007). Genome-wide analysis of genetic alterations in acute lymphoblastic leukaemia. Nature 446, 758-64.

Mullighan, C. G. et al. (2008). BCR-ABL1 lymphoblastic leukaemia is characterized by the deletion of Ikaros. Nature 453, 110-114.

Mullighan, C. G., Phillips, L. a, Su, X., Ma, J., Miller, Christopher B, Shurtleff, S. a, and Downing, J. R. (2008). Genomic analysis of the clonal origins of relapsed acute lymphoblastic leukemia. Science (New York, N.Y.) 322, 1377-80.

Mullighan, C. G. et al. (2009b). Deletion of IKZF1 and prognosis in acute lymphoblastic leukemia. The New England journal of medicine 360, 470-80.

Mullighan, C. G. et al. (2011). CREBBP mutations in relapsed acute lymphoblastic leukaemia. Nature 471, 235-239.

Mullighan, C. G. et al. (2009c). JAK mutations in high-risk childhood acute lymphoblastic leukemia. Proceedings of the National Academy of Sciences of the United States of America 106, 9414-8.

Neering, S. J. et al. (2007). Leukemia stem cells in a genetically defined murine model of blast-crisis CML. Blood 110, 2578-85.

Notta, F. et al. (2011). Evolution of human BCR–ABL1 lymphoblastic leukaemia-initiating cells. Nature 469, 362-367.

Novara, F. et al. (2009). Different molecular mechanisms causing 9p21 deletions in acute lymphoblastic leukemia of childhood. Human genetics 126, 511-20.

Okuya, M. et al. (2010). Up-regulation of survivin by the E2A-HLF chimera is indispensable for the survival of t(17;19)-positive leukemia cells. The Journal of biological chemistry 285, 1850-60.

others (2000). Molecular cloning of a novel type 1 cytokine receptor similar to the common gamma chain. Blood 95, 2204.

others (2004). MOZ-TIF2, but not BCR-ABL, confers properties of leukemic stem cells to committed murine hematopoietic progenitors. Cancer Cell 6, 587–596.

Owens, B. M., and Hawley, R. G. (2002). HOX and Non-HOX Homeobox Genes in Leukemic Hematopoiesis. Stem Cells 20, 364–379.

O□Brien, C. a, Pollett, A., Gallinger, S., and Dick, J. E. (2007). A human colon cancer cell capable of initiating tumour growth in immunodeficient mice. Nature 445, 106-10.

Pandey, A., Ozaki, K., Baumann, H., Levin, S. D., Puel, A., Farr, A. G., Ziegler, S. F., Leonard, W. J., and Lodish, H. F. (2000). Cloning of a receptor subunit required for signaling by thymic stromal lymphopoietin. Nature immunology 1, 59–64.

Pearce, D.J., Taussig, D., Simpson, C., Allen, K., Rohatiner, A. Z., Lister, T.A., and Bonnet, D. (2005). Characterization of cells with a high aldehyde dehydrogenase activity from cord blood and acute myeloid leukemia samples. Stem Cells 23, 752.

Politi, K., and Pao, W. (2011). How Genetically Engineered Mouse Tumor Models Provide Insights Into Human Cancers. Journal of clinical oncology : official journal of the American Society of Clinical Oncology 28, 1-9.

Pui, C.-H. (2010). Recent Research Advances in Childhood Acute Lymphoblastic Leukemia. Journal of the Formosan Medical Association 109, 777-787.

Pui, C.-H., Carroll, W. L., Meshinchi, S., and Arceci, R. J. (2011). Biology, risk stratification, and therapy of pediatric acute leukemias: an update. Journal of clinical oncology : official journal of the American Society of Clinical Oncology 29, 551-65.

Pui, C.-H., and Jeha, S. (2007). New therapeutic strategies for the treatment of acute lymphoblastic leukaemia. Nature Reviews Drug Discovery 6, 149–165.

Quintana, E., Shackleton, M., Sabel, M. S., Fullen, D. R., Johnson, T. M., and Morrison, S.J. (2008). Efficient tumor formation by single human melanoma cells. Nature 456, 593.

Ratei, R et al. (2009). Monitoring treatment response of childhood precursor B-cell acute lymphoblastic leukemia in the AIEOP-BFM-ALL 2000 protocol with multiparameter flow cytometry: predictive impact of early blast reduction on the remission status after induction. Leukemia 23, 528-534.

Ravandi, F., and Estrov, Z. (2006). Eradication of leukemia stem cells as a new goal of therapy in leukemia. Clinical cancer research : an official journal of the American Association for Cancer Research 12, 340-4.

Rehe, K., Wilson, K., McNeill, H., Schrappe, Martin, Irving, J., and Vormoor, Josef (2009). Disease Propagating Blasts in Standard and High Risk Acute Lymphoblastic Leukemia Are Frequent and of Diverse Immunophenotype. ASH Annual Meeting Abstracts 114, 1421-.

Ren, R. (2005). Mechanisms of BCR-ABL in the pathogenesis of chronic myelogenous leukaemia. Nature reviews. Cancer 5, 172-83.

Ricci-Vitiani, L., Lombardi, D. G., Pilozzi, E., Biffoni, M., Todaro, M., Peschle, C., and De Maria, R. (2007). Identification and expansion of human colon-cancer-initiating cells. Nature 445, 111-5.

Ross, M. E. et al. (2003). Classification of pediatric acute lymphoblastic leukemia by gene expression profiling. Blood 102, 2951-9.

Russell, L. J. et al. (2009). Deregulated expression of cytokine receptor gene, CRLF2, is involved in lymphoid transformation in B-cell precursor acute lymphoblastic leukemia. Blood 114, 2688-98.

Schmitz, M. et al. (2009). Leukemia-Initiating Cells Are Frequent in Very High Risk Childhood Acute Lymphoblastic Leukemia and Give Rise to Relatively Stable Phenotypes in Immunodeficient Mice. In ASH Annual Meeting Abstracts, p. 86-.

Schrappe, M (2004). Evolution of BFM trials for childhood ALL. Annals of hematology 83 Suppl 1, S121-3.

Schrauder, Andre et al. (2007). Prospective Evaluation of MRD-Kinetics in 274 Children with High-Risk ALL Treated in Trial ALL-BFM 2000: Insights into Development of Resistance and Impact on Further Refinement of Treatment Stratification Strategies. Blood 110, 585.

Sherborne, A. L. et al. (2010). Variation in CDKN2A at 9p21.3 influences childhood acute lymphoblastic leukemia risk. Nature genetics 42, 492-4.

Singh, S. K., Hawkins, C., Clarke, I. D., Squire, J. A., Bayani, J., Hide, T., Henkelman, R. M., Cusimano, M. D., and Dirks, P. B. (2004). Identification of human brain tumour initiating cells. Nature 432, 396-401.

Somervaille, T. C. P., and Cleary, M. L. (2006). Identification and characterization of leukemia stem cells in murine MLL-AF9 acute myeloid leukemia. Cancer cell 10, 257-68.

Stanulla, Martin, and Schrappe, Martin (2009). Treatment of childhood acute lymphoblastic leukemia. Seminars in hematology 46, 52-63.

Sulong, S. et al. (2009). A comprehensive analysis of the CDKN2A gene in childhood acute lymphoblastic leukemia reveals genomic deletion, copy number neutral loss of heterozygosity, and association with specific cytogenetic subgroups. Blood 113, 100-107.

Szczepański, T., Velden, V. H. J. van der, and Dongen, Jacques J M van (2006). Flow-cytometric immunophenotyping of normal and malignant lymphocytes. Clinical chemistry and laboratory medicine : CCLM / FESCC 44, 775-96.

Taussig, D. C. et al. (2008). Anti-CD38 antibody-mediated clearance of human repopulating cells masks the heterogeneity of leukemia-initiating cells. Blood 112, 568-75.

Viseur, C. le et al. (2008). In childhood acute lymphoblastic leukemia, blasts at different stages of immunophenotypic maturation have stem cell properties. Cancer cell 14, 47-58.

Vormoor, H. (2009). Malignant stem cells in childhood acute lymphoblastic leukemia: The stem cell concept revisited. Cell Cycle 8, 996-999.

Williams, R. T., Besten, W. den, and Sherr, C. J. (2007). Cytokine-dependent imatinib resistance in mouse BCR-ABL+, Arf-null lymphoblastic leukemia. Genes & development 21, 2283-7.

Yeoh, E.-J. et al. (2002). Classification, subtype discovery, and prediction of outcome in pediatric acute lymphoblastic leukemia by gene expression profiling. Cancer cell 1, 133-43.

Zelm, M. C. van et al. (2005). Ig gene rearrangement steps are initiated in early human precursor B cell subsets and correlate with specific transcription factor expression. Journal of immunology 175, 5912-22.

Zwaan, C. M., Reinhardt, D., Hitzler, J., and Vyas, P. (2010). Acute leukemias in children with Down syndrome. Hematology/oncology clinics of North America 24, 19-34.

Curriculum Vitae

Maike Schmitz

PERSONAL DETAILS

Address:
Breitenlooweg 4
8047 Zurich
Switzerland

Born: 16.02.1982 in Dinkelsbühl, Germany

OCCUPATION

Since October 2007	**PhD Student in the lab of J.-P. Bourquin** University Children's Hospital Zürich, Department of Oncology "A Xenograft Model of High Risk Leukemia Reveals the Oligoclonal Composition of Leukemia Initiating Cells" Member of the Cancer Network Zurich Graduate School

UNIVERSITY STUDIES

October 2001 to September 2003	**Basic studies in biology at the University of Karlsruhe (TH)** Degree: Vordiplom
September 2003 to March 2004	**Erasmus–Semester** at the University College Cork, Ireland
March 2004 to July 2006	**Advanced studies in biology at the University of Konstanz** Degree: Diplom
October 2006 to June 2007	**Diploma thesis** in the group of molecular toxicology, supervised by Prof. A. Bürkle "Flow cytometric analysis of poly(ADP-ribosyl)ation"

WORK EXPERIENCE

May to September 2005	**Internship** **Roche Diagnostics GmbH,** Penzberg Department for cell biology and immunology

CONFERENCES

April 2011	**ESH-EHA scientific workshop**: Leukemic and cancer stem cells, Oral presentation
December 2010	**American Society of Hematology Annual Meeting** Oral presentation, selected for "Best of ASH"
June 2009	**European Hematology Association Annual Meeting** Oral presentation
April 2009	**ESH-EHA scientific workshop**: Leukemic and cancer stem cells, Oral presentation

July 2007 Participant at the 57th **Meeting of Nobel Laureates** in Lindau

PUBLICATIONS

Schmitz M, Breithaupt P, Scheidegger N, et al. Xenografts of highly resistant leukemia recapitulate the clonal composition of the leukemogenic compartment. Blood 2011, 10.1182/blood-2010-11-320309

Schmitz M, Bourquin J-P and Bornhauser B. Alternative technique for intrafemoral injection and bone marrow sampling in mouse transplantation models. Leukemia & Lymphoma. 2011, 10.3109/10428194.2011.580023.

Hertzberg L, Vendramini E, Ganmore I, Schmitz M et al. Down syndrome acute lymphoblastic leukemia, a highly heterogeneous disease in which aberrant expression of CRLF2 is associated with mutated JAK2: a report from the international BFM study group. Blood. 2010;115:1006-17.

Bonapace L, Bornhauser BC, Schmitz M, et al. Induction of autophagy-dependent necroptosis is required for childhood acute lymphoblastic leukemia cells to overcome glucocorticoid resistance. The Journal of clinical investigation. 2010;120:1310-23.

Schmitz M, Mirkowska P, Breithaupt P, et al. Leukemia-initiating cells are frequent in very high risk childhood acute lymphoblastic leukemia and give rise to relatively stable phenotypes in immunodeficient mice. ASH Annual Meeting Abstracts. 2009;114:86.

Weidele K, Kunzmann A, Schmitz M, Beneke S, Bürkle A. Ex-vivo supplementation with nicotinic acid enhances cellular poly (ADP-ribosyl) ation and improves cell viability in human peripheral blood mononuclear cells. Biochemical pharmacology. 2010;80:1103-12.

Acknowledgements

I would like to acknowledge all the people that contributed to or supported this work:

First of all, I am grateful to Jean-Pierre Bourquin and Beat Bornhauser who gave me the opportunity to work in their group, for the supervision of this research work, and for their valuable ideas and suggestions throughout my PhD-project. I greatly appreciated their support which allowed me to visit several conferences all across Europe and in the USA, and to work together with many collaborators and leading scientists.

A warm thank you goes to Lukas Sommer and Adriano Aguzzi for participating in my committee, for their valuable help and inputs for the project, and for their interest in my work and my career.

Thanks also go to Jean Soulier who accepted to review my thesis. I'm sure that with his broad knowledge he will give me important suggestions.

I cannot express how thankful I am to all the members of the leukemia group: Paulina, Jeannette, Mattia, Blerim, Nastassja, Lucie, Anna, Romana, Michael and Raphael. I have spent great times with all of you, inside and outside of the lab. The solidarity for each other, the unquestioned help given, often carried me through and it will be difficult to find such a team again! My special thanks go to Nastassja, my wonderful master student and to Blerim, our wonderful help in the animal facility and beyond, you both were great support in the work conducted.

An extra hug goes to Laura Bonapace, who was my first lab mate, taught me so many things, gave me a good example and is a great friend.

I am also very grateful to Shai Izraeli for showing me the world of Down-Syndrome ALL and sending us the great exchange students Tali and Ithamar.

Furthermore, I would like to show my gratitude to all the people from the BFM group in Kiel. Petra Breithaupt, Barbara Meissner, Gunnar Cario and Martin Stanulla have been very good partners for this work and wonderful hosts when I visited them.

I would like to thank Beat Schäfer, Joëlle Tchinda, Silvia van Essen and Susanne Kubetzko for their valuable help for the projects regarding the diagnostic methods and for their interest in my work.

Another valuable source of information was the PhD-Program of the Cancer Network Zürich that helped to connect to other PhD students in Zürich.

Best thanks go to each and every one in the Experimental Infectious Diseases and Cancer Research Lab of August-Forel Strasse, for their contribution to the nice atmosphere and to the job-related and non-related discussions.

Besides the science field, I want to express my thanks to my family and to Christoph for their constant support, for trying to understand my work, and for everything else.

Manuscripts

Manuscript 1:
Xenografts of Highly Resistant Leukemia Recapitulate the Clonal Composition of the Leukemogenic Compartment

Own contribution: established xenograft transplantation, performed all mouse experiments, flow cytometry experiments, isolation of DNA for SNP analysis, IgH/TCR analysis by PCR and sequencing, FISH experiments together with N. Scheidegger.

Manuscript 2:
Alternative Technique for Intrafemoral Injection and Bone Marrow Sampling in Mouse Transplantation Models

Own contribution: performed all mouse experiments and flow cytometry.

Manuscript 3:
Induction of Autophagy-Dependent Necroptosis is Required for Childhood Acute Lymphoblastic Leukemia Cells to Overcome Glucocorticoid Resistance

Own contribution: amplification of primary material in mice, helped with mouse treatment experiments.

Manuscript 4:
Down Syndrome Acute Lymphoblastic Leukemia, a Highly Heterogeneous Disease in which Aberrant Expression of CRLF2 is Associated with Mutated JAK2: a Report from the International BFM Study Group

Own contribution: amplification of primary material in mice, determination of CRLF2 and Il7R levels by flow cytometry.

blood

2011 118: 1854-1864
Prepublished online June 13, 2011;
doi:10.1182/blood-2010-11-320309

Xenografts of highly resistant leukemia recapitulate the clonal composition of the leukemogenic compartment

Maike Schmitz, Petra Breithaupt, Nastassja Scheidegger, Gunnar Cario, Laura Bonapace, Barbara Meissner, Paulina Mirkowska, Joelle Tchinda, Felix K. Niggli, Martin Stanulla, Martin Schrappe, Andre Schrauder, Beat C. Bornhauser and Jean-Pierre Bourquin

Blood (print ISSN 0006-4971, online ISSN 1528-0020), is published weekly by the American Society of Hematology, 2021 L St, NW, Suite 900, Washington DC 20036.

Xenografts of highly resistant leukemia recapitulate the clonal composition of the leukemogenic compartment

Maike Schmitz,[1] Petra Breithaupt,[2] Nastassja Scheidegger,[1] Gunnar Cario,[2] Laura Bonapace,[1] Barbara Meissner,[2] Paulina Mirkowska,[1] Joelle Tchinda,[1] Felix K. Niggli,[1] Martin Stanulla,[2] Martin Schrappe,[2] Andre Schrauder,[2] *Beat C. Bornhauser,[1] and *Jean-Pierre Bourquin[1]

[1]Division of Oncology and Children's Research Center, University Children's Hospital, University of Zurich, Zurich, Switzerland; and [2]Department of Pediatrics, University Hospital Schleswig Holstein, Kiel, Germany

Clonal evolution of the leukemogenic compartment may contribute to alter the therapeutic response in acute lymphoblastic leukemia (ALL). Using xenotransplantation of primary leukemia cells, we evaluated the phenotypic and genetic composition of de novo resistant very high risk precursor B-cell ALL, a subgroup defined by the persistence of minimal residual disease despite intensive chemotherapy. Analysis of copy number alterations (CNAs) showed that the xenografted leukemia, even when reconstituted from 100 cells, remained highly related to the diagnostic sample, with minor changes in CNAs, mostly deletions, emerging in most cases in the first passage into mice. At the single-cell level, the pattern of monoallelic and biallelic deletions of the *CDKN2A* locus revealed distinct leukemia subpopulations, which were reproducibly tracked in xenografts. In most very high risk ALL cases, the predominant diagnostic clones were reconstituted in xenografts, as shown by multiplex polymerase chain reaction analysis of immunoglobulin and T-cell receptor loci. In other cases, the pattern in CNAs and immunoglobulin and T-cell receptor rearrangement was less concordant in xenografts, suggesting the outgrowth of subclones. These results unequivocally demonstrate the existence of clonally closely related but distinct subsets of leukemia initiating cells in ALL, which has important implications for drug development and preclinical disease modeling. (*Blood*. 2011;118(7): 1854-1864)

Introduction

For children with precursor B acute lymphoblastic leukemia (ALL) that relapse on current intensive chemotherapy regimens, second-line therapy is challenging.[1] Diagnostic markers that are predictive of poor treatment response are scarce, and modern treatment protocols base risk stratification mostly on in vivo response to treatment by monitoring persistence of minimal residual disease (MRD) after induction chemotherapy.[2] Using xenotransplantation in mice, which provides new opportunities for functional investigation in ALL,[3-7] we established a preclinical model of a subgroup of patients with very high risk for relapse (VHR-ALL),[8] as identified by MRD.[9,10]

The genetic basis of resistant disease is ill defined. Single nucleotide polymorphism (SNP) array analyses revealed that the number of focal copy number alterations (CNAs) is limited to 6 to 8 CNAs per case in ALL.[11] Studies in twins provide insight in the possible sequence of events that are associated with progression to overt disease from a common ancestral clone.[7,12] The most frequent CNAs in ALL involve master transcription factors regulating lymphoid development, such as Ikaros family and tumor suppressor genes of the *INK4A/CDKN2A/B* locus that may represent tumor driving events. Surprisingly, only a limited number of additional changes were detected at relapse, often related to a minor subpopulation in the matched diagnostic sample.[13,14] A candidate gene sequencing approach has identified mutations in several genes in relapsed ALL, mostly detectable in matched diagnosis samples already, sometimes only in minor subpopulations.[15] Thus, leukemia progression does not appear to be associated with a high degree of ongoing genetic instability in ALL but rather with clonal evolution and selection of a limited number of genetic lesions.

Several reports based on xenotransplantation of ALL in NOD/SCID mice have led to the hypothesis that ALL may be maintained from a rare subpopulation of leukemia initiating cells (LICs).[4,16] This concept has been challenged by observations in syngeneic mouse models that indicated a much higher frequency of ALL cells with repopulation capacity[17-19] and by the observation that both sorted leukemia cells from immature ($CD19^-/CD34^+$) and from mature ($CD19^+/CD34^+$) ALL compartments exhibited comparable leukemia repopulating capacity in NOD/scidIL2Rγnull (NSG) mice.[5,18,19] Furthermore, 2 most recent studies provide clear evidence for a dynamic pattern of clonal diversity of the LIC compartment in TEL/AML1-positive ALL[20] and BCR/ABL-positive leukemias.[21] Clonal evolution of the leukemogenic compartment may contribute to disease progression and resistance to therapy.

Here we provide important new functional and genetic data to support the notion that the LIC in ALL consists of highly related subclones that evolve with distinctive additional genetic lesions and that the clonal composition of bulk VHR-ALL samples can be stably propagated by xenotransplantation to constitute a renewable source of leukemia cells, closely related to the original sample. Our

Submitted November 18, 2010; accepted May 23, 2011. Prepublished online as *Blood* First Edition paper, June 13, 2011; DOI 10.1182/blood-2010-11-320309.

*B.C.B. and J.-P.B. contributed equally to this study.

The online version of this article contains a data supplement.

The publication costs of this article were defrayed in part by page charge payment. Therefore, and solely to indicate this fact, this article is hereby marked "advertisement" in accordance with 18 USC section 1734.

results justify the use of unsorted samples to model disease in this system and provide new avenues to investigate the consequences of therapy on the composition of the LIC compartment and disease progression.

Methods

Details can be found in supplemental Methods (available on the *Blood* Web site; see the Supplemental Materials link at the top of the online article).

Patient samples

ALL cells were recovered from cryopreserved anonymized bone marrow aspirates from patients enrolled in the ongoing ALL-BFM 2000 study and had given informed consent in accordance with the Declaration of Helsinki. Approval was obtained from the Institutional Review Board of the Medical School Hannover and the local Institutional Review Board for all participating centers in the trial ALL-BFM 2000. Samples were anonymized with labels that refer to the clinical risk stratification. Depending on the MRD result during induction therapy (MRD1 + 2) and during consolidation therapy (MRD3), patients are defined here as: standard risk (SR) if MRD1 + 2 was negative, high risk (HR) if MRD1 + 2 was positive less than or equal to 10^{-3}, and VHR if HR patients were still positive for MRD3 (supplemental Table 1). Cases are anonymized with a label according to the risk group and with a unique number.

Xenograft model

Primary ALL cells were recovered from cryopreserved presentation samples by scraping the required amount of cells with a sterile scalpel from the cryotube kept on dry ice, washed in phosphate-buffered saline, and transplanted intrafemorally into NSG mice. Unless stated otherwise, 1 million viable cells were transplanted (as assessed by trypan blue exclusion, supplemental Table 2). Engraftment was followed every 3 to 4 weeks (supplemental Table 2) by flow cytometry in the peripheral blood of transplanted animals, using mouse-specific, anti-CD45 combined with human-specific anti-CD45 and anti-CD19 antibodies. Xenografts are labeled with identifiers corresponding to the anonymized patient sample. This labeling system is used consistently for publication. For each xenograft sample, information about the transplantation and identification of the mouse is recorded in our database for later reference.

Flow cytometry

Immunophenotype analyses of primary ALL samples at diagnosis and of xenograft samples were performed as described.[22]

Affymetrix Genome-Wide Human SNP Version 6.0 microarrays

DNA from paired primary leukemic and remission samples as well as matching DNA from xenografts were hybridized on Affymetrix Genome-Wide Human SNP Version 6.0 microarrays according to the manufacturer's protocols (performed by Atlas Biolabs).

Raw intensity data were analyzed using Affymetrix Genotyping Console for quality control and generation of genotype calls. Paired DNA copy number and paired loss of heterozygosity (LOH) were analyzed using the Partek Genomics Suite software (Partek Incorporated).

Fluorescence in situ hybridization

Cryopreserved cells were thawed and fixed with methanol/acetic acid (3:1). A total of 2000 cells were dropped per slide for fluorescence in situ hybridization (FISH) with the LSI CDKN2A Spectrum Orange/CEP9 Spectrum Green FISH Probe Kit (Vysis/Abbott). The LSI CDKN2A probe hybridizes to the 9p21 locus, including *CDKN2A/B*. Slides were hybridized and evaluated as described.[23]

Analysis of clonal Ig/TCR rearrangements

Detection of patient-specific junctional regions of Ig and TCR genes was performed following the protocol established for the clinical follow-up analyses of MRD, which has been established and validated by an international study group and is reported in several publications (supplemental Table 3), summarized by van der Velden et al.[24]

Results

Reconstitution of de novo resistant ALL is faster than SR ALL in NSG mice

To model the relevant risk groups that emerge from in vivo response to treatment,[9] samples from 17 cases with de novo resistant VHR disease (VHR-ALL by MRD) and from 15 cases with SR ALL (SR-ALL, control group) were selected from the repository of the ALL-BFM-2000 study[25] and transplanted into NSG mice (supplemental Table 1), extending our initial series.[8] We also included 4 cases with HR ALL. Using orthotopic intrafemoral transplantation without conditioning, engraftment rates of $> 70\%$ were observed. A total of 1 million viable cells, as determined by trypan blue staining and microscopy, were injected unless stated otherwise at first passage in NSG mice (supplemental Table 2). In 3 cases, less cells were available (0.3-0.7 million). In these cases, engraftment was not delayed compared with the median time of the respective risk group. Subsequent passages were performed consistently with injection of 1 million cells. Reconstitution of the leukemia occurred faster in mice transplanted with VHR-ALL cases (median of $> 75\%$ of patients engrafted at 8 weeks) than in animals transplanted with SR-ALL cells (median of $> 75\%$ of patients engrafted at 20 weeks, $P < .05$; Figure 1A). All leukemias that were retransplanted (24 of 28 samples, supplemental Table 2) repopulated secondary recipient animals with high engraftment levels in bone marrow and spleen, demonstrating conserved NSG repopulating capacity. Strikingly, the time to engraftment was decreased in the second passage in NSG mice for most cases with SR-ALL (median engraftment time, 13.25 weeks for primary transplants vs 6.5 weeks for secondary transplants, $P < .01$), whereas it was unchanged for VHR-ALL cases, suggesting that leukemia cells from de novo drug-resistant cases are more adapted to overcome the xenograft barrier compared with SR-ALL (Figure 1A-B). Xenografted VHR-ALL cells were serially passaged up to 6 times in mice with reconstitution of the full phenotype in mice (Figure 1B; supplemental Table 2). Very high yields of ALL cells were recovered from spleens (Figure 1C). Clinical symptoms of central nervous system disease (eg, palsy or exophthalmoses) were not detected (data not shown). As supported also by others,[3,5,18] these data indicate that xenotransplantation can serve to amplify normally rare primary ALL cells and as model to study resistant disease, provided the consequences of selective pressure from the xenograft barrier are better understood.

ALL xenografts retain phenotypic properties of the diagnostic samples

Alteration of the microenvironment has been shown to influence the leukemia phenotype in a model of MLL rearranged leukemia.[26] Because passage in NSG mice could influence the pattern of leukemia-associated cell surface markers with respect to maturation and differentiation stage, we compared the immunophenotype of xenografts after successive passages in NSG mice to the

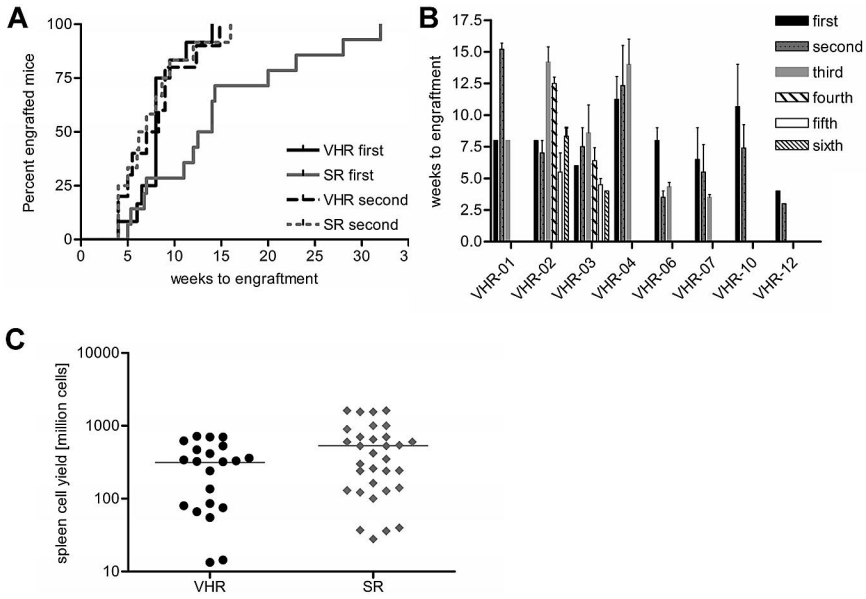

Figure 1. Engraftment characteristics over serial transplantation of primary ALL cells in NSG mice. Cryopreserved diagnostic material was thawed, and 1 million cells were transplanted by intrafemoral injection into NSG mice 6 to 10 weeks of age. Mice were checked every 4 weeks by flow cytometry for human engraftment. Positive engraftment was defined as > 1% human CD19/CD45-positive and mouse CD45-negative cells in the peripheral blood. (A) Analysis of the time to engraftment for 9 VHR-ALL (black) and 13 SR-ALL (gray) patients. The time to engraftment in weeks is plotted for primary (solid lines) and secondary (dashed lines) transplantations. Statistical evaluation was performed with the log-rank test and indicates significant differences for the time to engraftment between VHR-ALL and SR-ALL ($P < .05$) and between primary and secondary transplantation for SR-ALL ($P < .01$). (B) Time to engraftment was analyzed for 7 VHR-ALL patients with up to 6 rounds of serial passages. (C) Number of cells harvested from spleens per mouse at death, when the percentage of human cells in the peripheral blood reached 70%. The mean value was 500 million for VHR-ALL and 650 million cells for SR-ALL xenografts (indicated as horizontal line).

diagnostic sample using the same panel of antibodies for 5 cases for which sufficient material was available (Figure 2; supplemental Table 4A). In addition, we compared the immunophenotypes of 11 additional cases from xenografts to the diagnostic data from the reference laboratory of the BFM study (supplemental Table 4B). In general, the expression of the lineage-associated cell surface markers CD45, CD19, CD10, CD20, CD22, CD38, and CD34, and the pattern of CD7, CD13, CD33, and CD117 coexpression were very similar. Discrepancies were detected in single xenografts in some cases for the markers CD33 (6 of 16), CD20 (3 of 16), CD34 (3 of 16), CD22 (3 of 15), CD13 (2 of 15), CD117 (1 of 14), CD7 (1 of 15), and CD45 (1 of 16). We may slightly overestimate discrepancies in the 11 cases where direct comparison based on the same antibody panel was not available. These changes may reflect minor differences after selection in NSG mice in the context of a xenogenic environment. Based on these observations, it appears justified to continue to immunophenotype xenografts as part of the validation of this preclinical model system.

Because VHR-ALL patients are identified based on persistence of significant MRD loads in vivo and given an earlier study correlating in vitro drug resistance patterns to outcome for ALL,[27] we hypothesized that a major phenotypic feature of VHR-ALL would be resistance to multiple chemotherapeutic agents in vitro. To better reflect the protective bone marrow niche, which contributes to drug resistance in different models,[28,29] we assayed drug response profiles of xenograft cells cocultured on immortalized human mesenchymal stroma cells.[8,30] Xenografts of SR-ALL cells were sensitive to chemotherapeutic agents used for induction chemotherapy (daunorubicine, vincristine and cytarabine), with one exception (SR-02 was not responsive to cytarabine). In contrast, VHR-ALL cells were at least 10-fold less sensitive to these 4 drugs, and resistance to dexamethasone correlated with poor response to prednisone in vivo (Figure 3; supplemental Table 2).[8] Drug response profiles remained mostly unchanged over up to 2 passages in NSG mice for SR-ALL cells and up to 4 passages for VHR-ALL cells (Figure 3; supplemental Table 2). These results extend findings from our earlier study,[8] where some of these samples were used to test for obatoclax-induced steroid resensitization of VHR-ALL samples. In addition, we show that the drug response profiles remain stable over serial transplantation. Our results indicate that an adaptation to the mouse environment rather than a selection of ALL cells that are intrinsically more resistant to chemotherapeutic agents might be responsible for the acceleration of engraftment in cells from SR patients.

LICs are frequent in xenografts of VHR-ALL samples

For many applications of the ALL xenograft model, it will be important to better understand the hierarchy in the malignant hematopoietic tissue with respect to its LIC compartment. Indeed, in analogy to other forms of leukemia,[31] it is conceivable that a restricted compartment of LIC could constitute a reservoir of resistant cells. To functionally evaluate the LIC compartment, we performed serial dilution experiments by intrafemoral injection of ALL cells in NSG mice. In 4 of 6 VHR-ALL cases, 100 xenograft cells were sufficient to fully reconstitute the leukemia without conditioning the mice (Table 1; supplemental Table 5). Flow cytometry analyses of the leukemia-associated cell surface markers revealed complete conservation of the immunophenotype of the leukemia cells resulting from transplantation with 100 cells (supplemental Figure 1). Our results are in line with similar observations by others for precursor B-ALL[32] and T-ALL.[33] We included samples from SR-ALL patients and cryopreserved primary ALL cells whenever available. Overall, 10 000 xenograft VHR-ALL cells were enough to repopulate leukemia in all cases, despite the xenograft barrier (Table 1; supplemental Table 5). Together with other reports,[32-34] our data suggest that the LIC frequency could be higher than initially anticipated in ALL.

Xenografted ALL cells are clonally highly related to the corresponding diagnostic sample

Given the occurrence of multiple genetic aberrations in ALL and the evidence for a prenatal origin for certain genetic subtypes of ALL with the acquisition of additional CNAs, even before the leukemia becomes clinically apparent,[7] it is possible that leukemia samples will be constituted by a pool of related subclones. Extensive studies have established that in most ALL cases a limited number of in part recurrent CNAs can be identified.[11,14] Concordance of genetic aberrations detected by SNP analysis in xenograft samples compared with diagnostic samples was suggested to

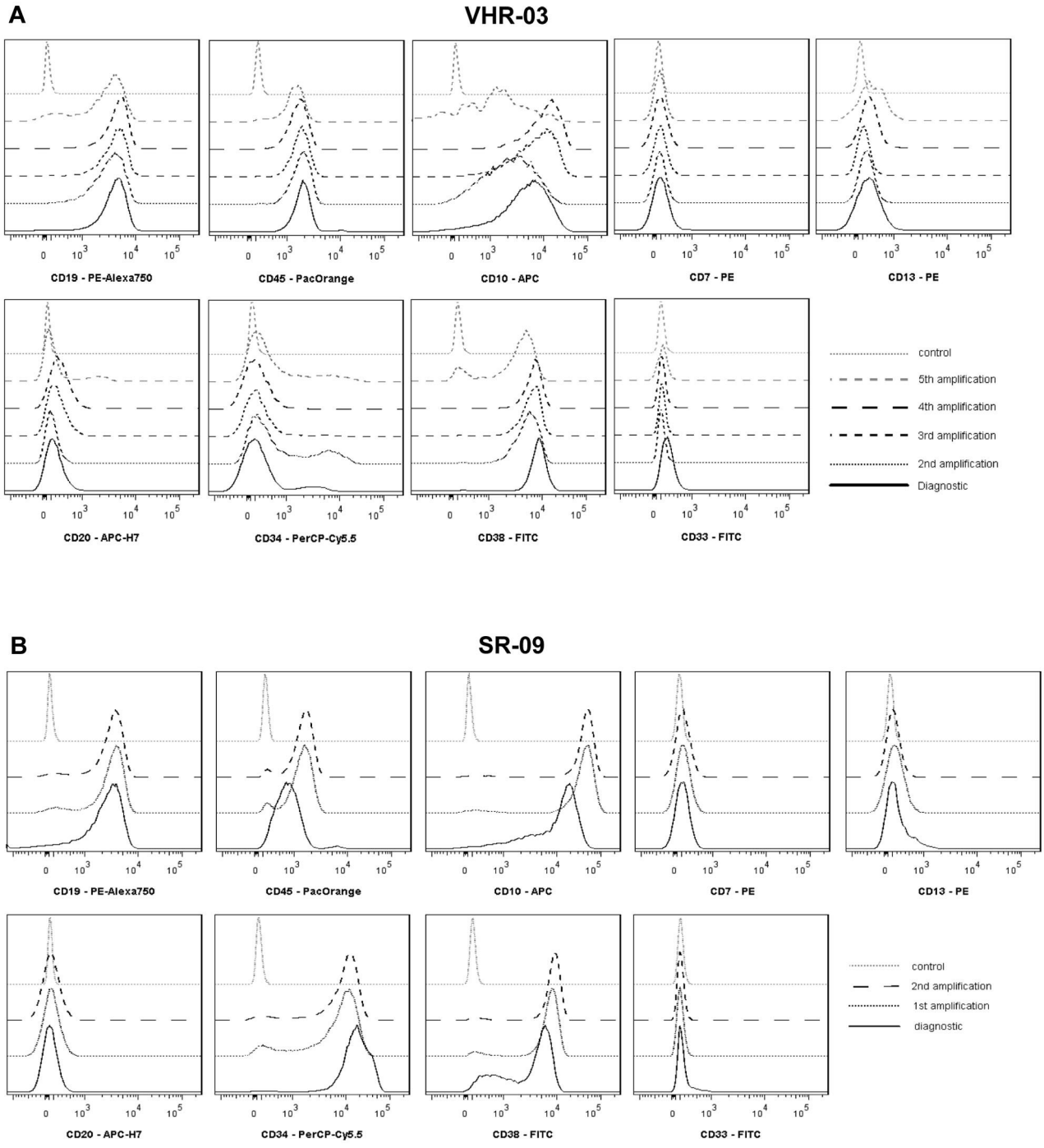

Figure 2. Primary human ALL cells are phenotypically stable in serial xenotransplantation. The immunophenotype of 2 representative cases was determined in the same experiment on cryopreserved diagnostic cells and cells from multiple serial passage in NSG mice. Xenografts from 5 passages were analyzed for case VHR-03 (A) and 2 passages for case SR-09 (B). At least 10 000 viable cells were gated based on forward-side scatter properties, and histograms representing number of events versus signal intensity are shown.

correlate to some extent with poor survival in BCR/ABL-positive ALL.[21] To get insight into the genetic stability of xenografts on serial passage in NSG mice, we performed genome-wide copy number and LOH analysis using Affymetrix SNP Version 6.0 arrays. We compared diagnostic and remission samples of 6 ALL patients with the corresponding samples after serial transplantation in NSG mice (Figure 4; supplemental Table 6). As expected, a low number of focal CNAs ($> 100 < 1000$ kb) and whole arm or total chromosome abnormalities were detected in the diagnostic samples, most of them previously reported in larger studies. In all cases, CNAs corresponding to expected Ig and TCR gene rearrangements were stably detectable over serial transplantation. Only in one case (VHR-04), an additional CNA corresponding to an incomplete rearrangement of the Ig λ (IgL) occurred (Table 2; supplemental Table 6).

We found up to 8 CNAs (deletions and amplifications) and copy neutral LOHs (cnLOH) ranging in size from single gene aberrations to chromosome whole arm deletions/amplifications at diagnosis, with the exception of one high-hyperdiploid patient who had 30 whole chromosome amplifications. On passage into

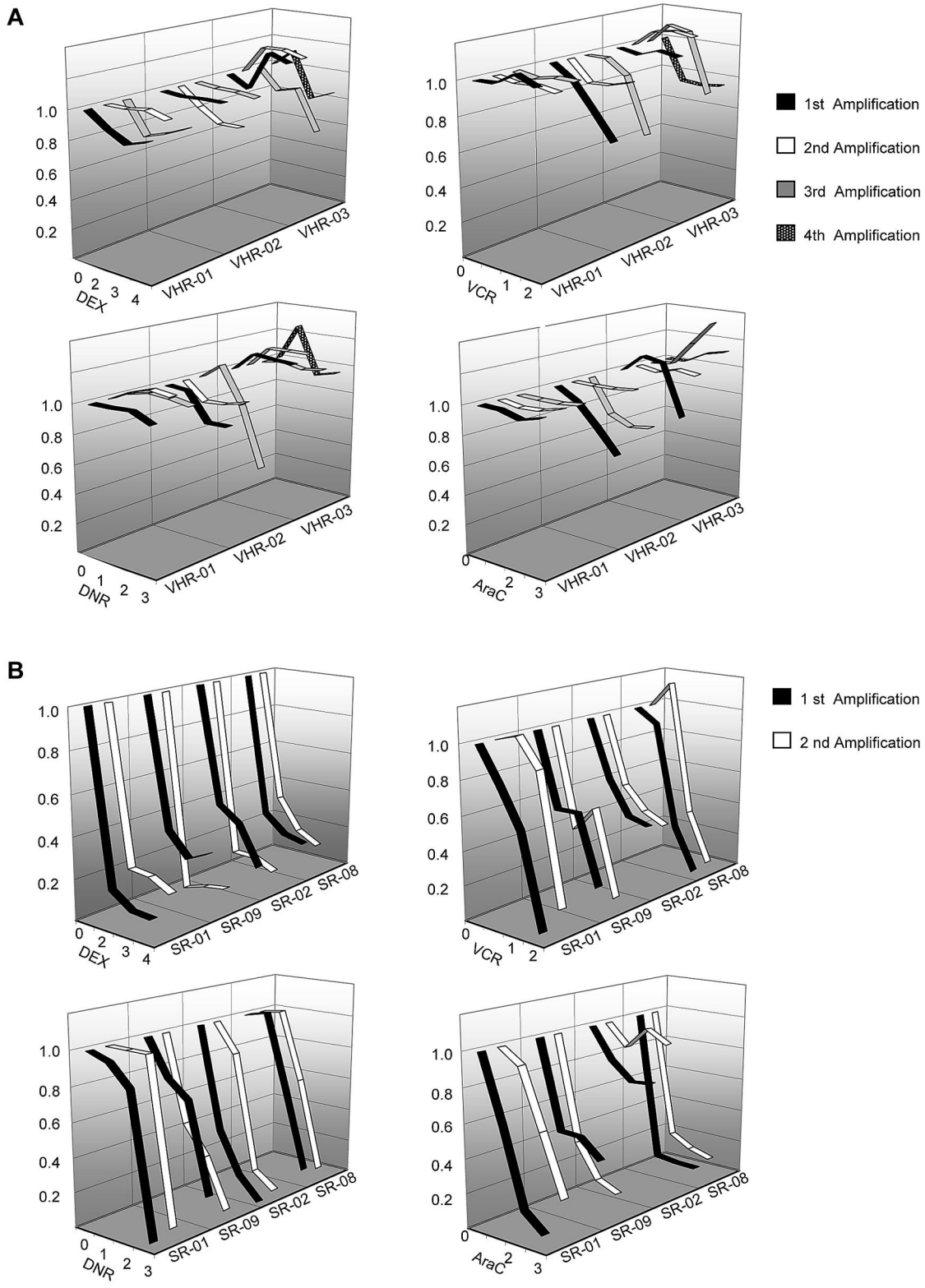

Figure 3. Drug response profiles of xenografts remain stable. Xenograft cells from up to 4 passages from 3 VHR-ALL (A) and 4 SR-ALL (B) were cocultured on hTERT-immortalized mesenchymal stroma cells and treated for 3 days with increasing concentrations of chemotherapeutic agents. Drug concentrations (in nanomolar) are given on the x-axis in a log scale. Measurement of ALL cell survival using 7-AAD and flow cytometry and compared with vehicle-treated controls revealed conserved resistance profiles. DEX indicates dexamethasone; VCR, vincristine; DNR, daunorubicin; and AraC, cytarabine. Experiments were performed twice, and one representative example is shown.

NSG mice, all but 6 lesions found in the diagnostic samples were maintained (Table 2). In one case (VHR-02), a deletion of the *FBXW7* gene at 4q31.3 was lost after transplantation; whereas in VHR-03, deletions at 1q42, the whole 9p arm, and 14q12, which were detected in the diagnostic sample, were not found in corresponding xenografts. Analysis of copy number

Table 1. Serial dilution of 4 VHR-ALL xenografts by intrafemoral and intravenous transplantation

Patient	Round of transplantation	Cell dilution	Intrafemoral engrafted/ total	Intravenous engrafted/ total	Mean engraftment in bone marrow, %
VHR-01	Second	1 000 000	2/4	3/3	88
		10 000	3/3	3/3*	86
		100*	2/3*	0/3	96
VHR-02	Third	1 000 000	1/2	2/3	94
		10 000	3/3	1/3*	97
		100*	2/3*	0/3	90
VHR-03	Third	1 000 000	2/2	2/2	94
		10 000	2/2	2/2*	97
		100*	1/2*	0/2	77
VHR-04	Second	1 000 000	2/2	2/3	99
		10 000	1/3	2/3*	99
		100*	1/3*	0/3	99

Four VHR-ALL patients from different amplification rounds were transplanted intrafemorally and intravenously. Engraftment was considered positive when 1% of human CD19/CD45$^+$ mouse CD45$^-$ cells were detected in peripheral blood by flow cytometry, and spleens and bone marrows were engrafted at harvest.

*Lowest dilution that resulted in engraftment.

ratios indicated that subclones were present in the diagnostic samples harboring these deletions, which were lost in the first round of transplantation. Two amplifications, one in sample SR-02 that involves 7p21 with no known gene detected in the diagnostic sample and one in sample HR-03 at 9p, present in a subclone at diagnosis, were not detected in xenografts.

In addition to that, only few lesions occurred in xenograft samples that were not detected in the corresponding diagnostic sample, namely, up to 2 deletions and up to 2 amplifications per sample (Table 2; Figure 4; supplemental Table 6). Deletions at 9p loci are frequent in childhood ALL[11,35,36] and proposed to be associated with poor risk. In 3 of the 4 analyzed VHR cases, additional deletions detected in xenograft but not in diagnostic samples occurred at 9p, involving genes that control B-cell development, such as *CDKN2A* and *CDKN2B*. Xenografts of VHR-01 had a deletion of the whole 9p chromosome arm; whereas in VHR-02, 2 focal deletions only deleted *CDKN2A* and *B*, along with the *C9orf53*-gene at 9p21.3, and the *ZCCHC7* gene at 9p13.2, respectively. Last, a homozygous deletion at 9p21 and LOH over the whole 9p arm was present in xenografts of VHR-03 also present

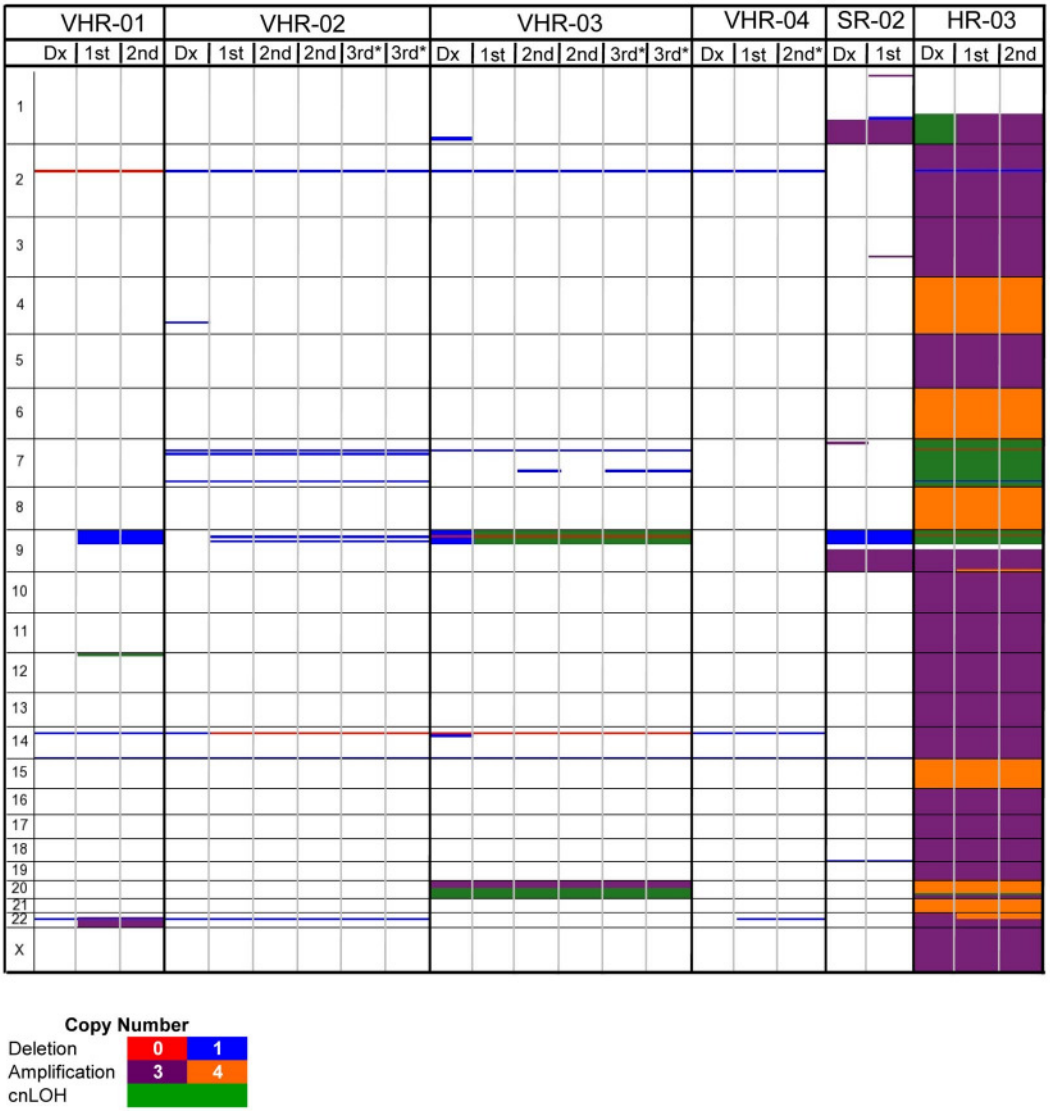

Figure 4. Genetic lesions remain stable in xenograft cells. A copy number heat map was produced from $\log_2$ ratio Affymetrix SNP Version 6.0 analyses of 6 ALL patients and their corresponding xenografts of up to 3 subsequent amplification rounds. All CNAs of > 100 kb in size were included, also showing Ig/TCR gene rearrangements. Dx indicates diagnostic sample; and 1st, 2nd, and 3rd indicates first, second, and third amplification round, respectively. *The xenografts were obtained from transplantations with 100 cells.

Table 2. Changes in CNA between diagnosis and xenograft

Sample	Gain or loss of CNA	Cytoband	Copy number	Overlapping genes	Overlapping miRNAs
Lesions detected only in xenografts, not in matched diagnostic samples					
VHR-01	Gain	9p	Deletion	Many	7
	Gain	12p13	cnLOH	Many, including *ETV6*	4
	Gain	22q	Amplification	Many	26
VHR-02	Gain	9p21.3	Deletion	*C9orf53*, *CDKN2A*,	None
	Gain	9p13.2	Deletion	*CDKN2BAS*, *CDKN2B* Intron of *ZCCHC7*	None
VHR-03	Gain	7q22.3	Deletion	*PIK3CG*	None
VHR-04	Gain	22q11.22	Deletion	*VPREB1*, *IgL*	hsa-miR649
SR-02	Gain	1p36.13	Amplification	*CROCCL1*, *ESPNP*, *MST1P2*,	None
	Gain	1q23.3	Deletion	*MST1P9*, *NBPF1*	None
	Gain	3q22.1	Amplification	*F11R*, *ITLN2* *ALG1L2*, *LOC729375*	None
HR-03	Gain	9q34.11; 22q11.23	Amplification	*BCR-ABL1*, many	13
	Gain	1q	Amplification	Many	45
Lesions not detected in xenografts, only in matched diagnostic samples					
VHR-02	Loss	4q31.3	Deletion	20.34% of *FBXW7*	hsa-miR3140
VHR-03	Loss of CNA in subclone	1q42.11-1q42.13	Deletion	Many	3
	Loss of CNA in subclone	9p	Deletion	Many	7
	Loss of CNA in subclone	14q12	Deletion	*AP4S1*, *C14orf126*, *COCH*, *HEATR5A*, *HECTD1*, *MIR624*, *STRN3*	None
SR-02	Loss	7p21.3	Amplification	None	None
HR-03	Loss of CNA in subclone	9p	Amplification	Many	7

CNAs that changed from diagnosis to xenograft material (additional/lost deletions, amplifications, and cnLOH) are presented. If > 10 genes or 3 miRNAs were in one CNA, it was noted as many or the number was listed.

as subclone in the diagnostic sample. However, a complete deletion of the whole 9p arm was detected in a fraction of the cells at diagnosis as suggested by the analysis of copy number ratios (Table 2; Figure 4; supplemental Table 6).

Other CNAs emerging in xenografts were detected for VHR-01 at 12p13 (cnLOH, including *ETV6*) and at 22q (whole arm amplification), for VHR-03 at 7q22 deleting the gene for *PIK3CG*, for VHR-04 at 22q11 the locus of the IgL rearrangement including *VPREB1*, and for SR-02 at 1q23 (genes for *F11R* and *ITLN2*). In xenografts of SR-02, amplifications at 3q22 (*ALG1L2*) and 1p36 (genes for *CROCCL1, ESPNP, MST1P2, MST1P9*, and *NBPF*1) were also found. Interestingly, xenografts that were derived from an HR patient with BCR-ABL positive and high-hyperdiploid leukemia were remarkably stable but showed an additional amplification of the BCR-ABL fusion gene. With the exception of the abnormalities at 20p and 14q12, these have been described[11,14] to occur in ALL samples, suggesting that these abnormalities are not selected for randomly in NSG mice (Table 2; Figure 4; supplemental Table 6).

To evaluate the genetic stability from passage to passage in the mice, we looked at cells from 2 passages in duplicates and transplanted at limiting dilution with only 100 cells. Interestingly, we observed that differences between diagnostic and xenografted material were present in all mice of all passages and in serial dilution cases with the exception of 2 mice from VHR-03 where the deletion at 7q22 was not detectable (Figure 4; supplemental Table 6). Taken together, these observations suggested that clonal selection may occur to some degree, mostly during the first xenotransplantation already, but that overall the xenograft samples are highly related to the original diagnostic samples.

Persistence of dominant subclones with deletions at the CDKN2A/B locus in xenografts

Given the frequent occurrence of CNAs on chromosome 9p and evidence for the acquisition of additional lesions in this region in xenografts, we performed FISH to assess the clonal heterogeneity with respect to deletions in 9p21 (including the gene for *CDKN2A* and *CDKN2B*) at the single-cell level. We detected 9p21 deletions in subclones in most of the xenograft cases, and these subclones were predominant in 10 of 24 cases (supplemental Table 7). To assess differences between primary samples and xenograft cells, we included matched diagnostic samples from 9 ALL cases, including those from which SNP data were available (Figure 5; supplemental Table 7) and those that showed 9p21 deletions in the xenograft sample. As expected, we detected the existence of subpopulations with respect to their heterozygous or homozygous 9p21 deletion status. In all but one case, the major subclone was maintained in xenografts, although with relative changes in the distribution of respective subclones in some instances. As exception, xenografts of VHR-01 selected for heterozygous deletion of 9p, which was present as minor subclone at diagnosis. In 3 samples (VHR-01, SR-09, and SR-11) clones with heterozygous 9p21 deletions became predominant, indicating selection for heterozygous events. In addition, SR-11 xenografts further showed a gradual shift toward heterozygous and homozygous clones on serial transplantation (Figure 5). The existence of subclones with differences at the 9p21 locus have been described in cytogenetic reports but, to our knowledge, has not been evaluated carefully with respect to its importance in the evaluation of the clonal compartment in ALL.[23,37] Our data show that xenotransplantation results in only

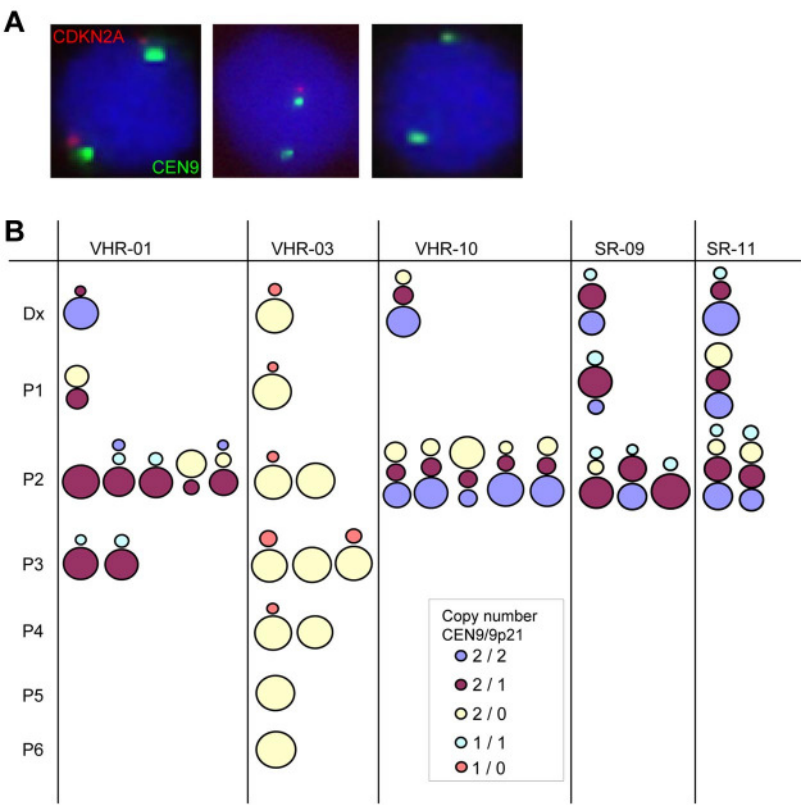

Figure 5. Interphase FISH analysis of 9p21 (*CDKN2A*) lesions reveals the existence of genetically distinct subclones. The clonal composition of ALL samples was analyzed using dual-color FISH probes against 9p21 (*CDKN2A*, red) and the centromer of chromosome 9 (CEN9, green) as control in samples from diagnosis and corresponding xenografts. (A) Representative images are shown, indicating wild-type cells with no deletion in the 9p21 locus (left), a heterozygous deletion (middle), and a homozygous deletion (right). (B) The clonal distribution was analyzed in samples from up to 6 rounds of serial transplantation. A total of 200 cells were counted in each sample. The original data are reported in supplemental Table 7. ALL cells with germline, heterozygous deletion, and homozygous deletions are represented by colored dots of size proportional to the percentage of cells in each category in relation to the total cell number as indicated in the legend. One case, VHR-01, shows clonal selection toward additional deletions at this locus, whereas the 4 other cases analyzed are more stable with respect to the clonal composition based on this genetic feature. Original magnifications ×40 (Leica LX Widefield Microscope DMI6000B with the DFC 350 FX R2 camera).

limited changes overall; however, shifts in the distribution of subclones with respect to particular lesions do occur, indicating that selection of preexisting subclones does occur.

A dominant pattern of Ig/TCR rearrangements is propagated in VHR-ALL xenografts

To detect significant changes in the clonal distribution in ALL, we took advantage of the standardized polymerase chain reaction (PCR)-based methodology to detect clonal specific rearrangements of the Ig and TCR genes in ALL xenografts.[25] In 10 of 14 patient samples analyzed, composing primary up to quaternary xenografts of VHR- and SR-ALL samples, the 2 markers that were used for MRD follow-up in the patients remained stable in the xenografted samples (supplemental Table 8). In 4 cases, one or both of these MRD markers could not be detected after transplantation. This is reminiscent of a large clinical study that reported the loss of both diagnostic MRD markers at relapse in 11% of patients.[38] We then screened 10 cases (5 VHR-ALL and 5 SR-ALL) systematically for the presence of 23 clonal specific Ig/TCR rearrangements in the diagnostic and corresponding xenografts, looking at replica from the same passage number and at serially passaged xenografts (Figure 6). We sequenced all detected bands of the expected size to verify accuracy of the PCR on xenograft material at least once. Two representative examples are shown in Figure 6A, and a summary of all data is represented in a schematic form (Figure 6B; supplemental Figure 2). Overall, the pattern of expected Ig/TCR rearrangements was remarkably stable. In a representative VHR-ALL sample (Figure 6A), 5 markers were stably detected in both the diagnostic and in xenograft samples (boxed in orange in Figure 6A), whereas 4 markers were lost in at least one of the xenograft samples (boxed in red in Figure 6A). In general, a similar pattern of dominant markers could be detected in all xenograft passages, whereas additional markers were lost to a variable degree in xenografts (Figure 6B). Interestingly, in 3 of 5 SR-ALL samples, 1 or 2 new Ig/TCR rearrangements emerged in xenograft samples (Figure 6B). For instance, in SR-9, one new rearrangement was detected as a strong PCR fragment in primary and secondary xenografts, but not in the diagnostic sample (Figure 6A). Interestingly, samples with the appearance of new Ig/TCR rearrangements (SR-9, SR-12, and SR-13) showed the greatest acceleration in engraftment from primary to secondary passage (11 vs 4 weeks, 14 vs 3 weeks, and 28 vs 5 weeks; supplemental Table 2). Whether these rearrangements preexisted in minor subclones at diagnosis or occurred during propagation of the disease in mice cannot be determined based on these data. The Ig/TCR patterns detected in leukemia reconstituted from 100 unsorted cells (VHR01-04) were comparable to the patterns obtained from bulk transplanted samples (Figure 6B). This analysis reinforces the notion that the LIC compartment contains related but distinct clonal subpopulations with a dominant pattern selected in NSG mice.

Taken together, our results indicate that the LIC compartment in ALL is large and consists of a mixed population of related subclones. Expansion in NSG mice is associated with clonal evolution to some extent, as there were corresponding subclones present in the diagnostic samples from which xenografts were derived. In many instances, selection appears to occur with the first passage and the patterns of genetic markers remain sufficiently stable to use the xenograft system to model disease.

Discussion

Understanding the nature of the leukemia propagating cell compartment in resistant ALL will greatly impact on the design and

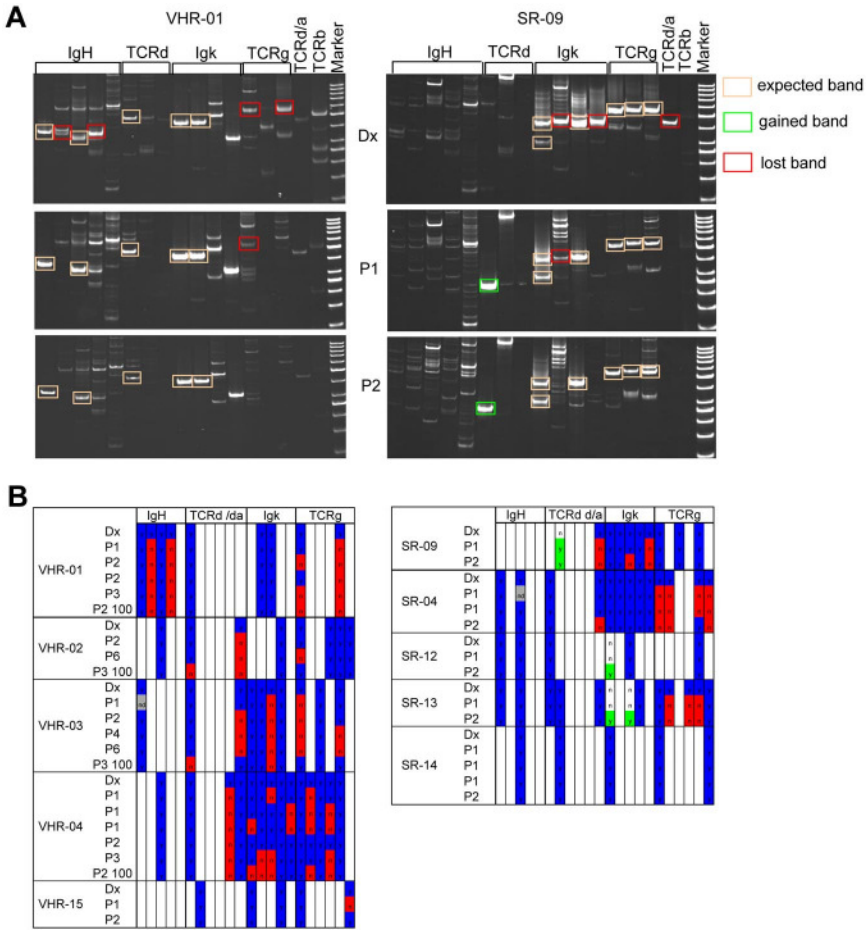

Figure 6. Analysis of Ig/TCR rearrangements reflects the evolution of the clonal compartment in xenografts. The Ig/TCR rearrangement pattern of diagnostic samples and matched xenografts was determined in 5 VHR- and in 5 SR-ALL samples by PCR using standardized sets of primers that are validated for MRD analysis. (A) Representative examples for a VHR-ALL (left panel) and an SR-ALL (right panel) sample, which showed a marked acceleration from primary to secondary passage. All positive bands of the correct size were sequenced once for verification. Stable rearrangements are framed with an orange line; and bands framed in red represent markers that disappeared in xenografts. In this SR sample, one new Ig/TCR rearrangement appeared (framed in green). (B) Overview of Ig/TCR rearrangements detected. Detected Ig/TCR rearrangements are highlighted in blue. Loss of such a marker in a given xenograft is highlighted in red. Newly detected markers in xenografts are highlighted in green.

experimental evaluation of new treatment rationales. We established a xenograft model with diagnostic samples from patients with highly resistant disease based on in vivo response to treatment, which remains the strongest predictor of poor outcome in ALL.[9] Here we provide compelling evidence to propose that both chemoresistant and chemosensitive ALL consist of highly related, albeit genetically diverse, clonal subpopulations. These results corroborate with contemporary studies of ETV6-RUNX1–positive ALL[20] and BCR-ABL–positive ALL[21] and imply that ALL can be propagated as dynamic multiclonal populations of LICs. Functionally, the analysis of both serial and replica xenografts from several independent diagnostic samples reveals that genetically distinct subclones have different NSG repopulation capacity, suggesting selection of properties conferring selective advantages in NSG mice. In many instances, a pattern reflecting the propagation of highly related clonal populations was detected. Only minimal changes in CNAs occurred, mostly in chromosomal regions that were previously reported in ALL, which indicates that these change are neither the result of increased genetic instability, nor specifically the result of selective pressure from the xenogenic environment. The analysis of clonal Ig/TCR rearrangements revealed loss of less predominant markers, suggesting that most changes may be inferred to the loss of minor ALL subclones.

Some differences emerge between highly resistant VHR-ALL and chemosensitive SR-ALL cases. Most notable is the acceleration of the engraftment kinetics with the second passage into mice, which correlates in 3 of 5 cases with the emergence of readily detectable new Ig/TCR rearrangements. It is tempting to speculate that, in VHR-ALL patients with a very unfavorable leukemia biology, ALL clones have been selected with genetic or epigenetic features that favor engraftment and proliferation in a xenogenic environment. This could explain the propagation of dominant subclones of leukemia cells for VHR-ALL in NSG mice. Similarly, in selected cases of BCR-ABL ALL xenografts, the pattern of genetic lesions was more concordant in cases that engrafted mice readily, which was associated with a trend toward shorter survival times in patients.[21] Strikingly, this was strictly associated with additional deletions in the *CDKN2A/B* locus in BCR-ABL ALL xenografts. In our series, the occurrence of additional deletions at this locus was also observed but occurred both in SR-ALL and VHR-ALL cases. Although genome-wide association studies clearly implicate the *CDKN2A/B* locus in the pathogenesis of ALL,[39] the prognostic value of deletions of this locus in ALL is less clear, as the association with relapse is inconsistent.[40] Given that the number of cases included in such xenograft studies is necessarily small and the ALL subgroups compared heterogeneous with respect to their underlying genetic features, we remain cautious with the interpretation of these results. Moreover, the relevant mechanisms to escape the selective pressure of chemotherapy may not necessarily overlap with factors that favor engraftment in a xenogenic environment. Indeed, knowing that in many cases the pattern of clonal-specific genetic markers are dominant over several passage in NSG mice, it will be possible to study the consequences of selective pressure by therapeutic agents or interference with microenvironmental factors with the xenograft system in vivo. As such, this model may be useful to functionally identify driving events that lead to disease progression and resistance to treatment. In particular, the xenograft model may provide the means to evaluate the effect of recurrent

mutations that are more frequently detected at relapse in ALL with respect to clonal selection and drug resistance.[15]

Our data, together with recently published evidence[20,21] showing that the leukemogenic compartment is composed of genetically distinct albeit related clones, challenge the hierarchic model, which proposed that the leukemia is maintained from a subset of immature stem cells.[16] Our findings that 100 VHR-ALL cells are sufficient to reconstitute leukemia in NSG mice, a strain that is more permissive for lymphoid cells,[41] suggests that leukemia propagating cells are not restricted to a rare subset of cells. Similar LIC frequencies were reported for other ALL subtypes.[20,21,33] Likewise, the fact that sorted ALL cells reconstitute immunodeficient mice efficiently independent of their immuno-differentiation status[5,20] supports this notion. In the absence of markers to enrich for NSG repopulating capacity, definitive conclusions with respect to the hierarchy of LIC in ALL have to be deferred. Our limiting dilution experiments indicate that primary diagnostic samples engraft at a lower frequency than samples that were previously established in NSG. These results may be influenced by differences in cell viability in the stored primary patient samples. However, the trend to accelerated engraftment that we observed with samples from chemosensitive patients on the second passage in NSG suggests that selection for better NSG repopulating capacity occurs in some cases. But the xenograft assay is a reflection of combined functions, which include self-renewal capacity, but also homing and protective interactions with the recipient microenvironment. Further improvements of humanized immunodeficient mouse strains may contribute to clarifying this issue.[42] Given 2 other reports that imply an association between NSG repopulation kinetics and adverse outcome,[21,43] prospective and detailed investigation is warranted to understand whether leukemia with a more favorable biology is associated with lower frequencies of LIC and to dissect the nature of the selective advantages in HR leukemias. Studies of relapses cases from patients that were classified in the SR group at initial presentation using the xenograft system will be needed to understand whether outgrowth of minor subclones may be clinically relevant in this setting.

Taken together, our results demonstrate that the clonal composition of leukemia samples from patients with highly resistant disease remains remarkably stable on serial passage in NSG mice. Based on available data, it is probable that a larger proportion of ALL cells are leukemogenic. The oligoclonal or even polyclonal nature of ALL may confer the ground for clonal selection/progression to escape chemotherapy. The mouse xenograft system will enable to investigate the consequences of different types of interventions on the clonal composition of the disease. Clearly, development of new therapeutic approaches will have to take into account that the whole leukemia population has to be eradicated for successful treatment. These considerations also reinforce the importance of combination therapy, which is supported by decades of clinical research in oncology. The development of xenograft models of distinct clinical and genetic entities will greatly improve our capability to evaluate new treatment rationales. With this renewable source of relevant samples, combinatorial studies can be performed taking the clonal complexity of the disease into consideration.

Acknowledgments

The authors thank Beat Schäfer, Silvia van Essen, and Susanne Kubetzko for instructions and reagents to perform the Ig/TCR experiments and Martina Kähler for performing some of the sequence analysis of Ig/TCR rearrangements.

This work was supported by the Swiss National Science Foundation (grant 310030-118392). J.-P.B. was supported by Claus Cramer Stiftung, Empiris Foundation, Fondation pour la recherche cancer de l'enfant, Hanne-Liebermann Stiftung, Oncosuisse, Novartis Foundation for Biomedical Research, Vontobel-Stiftung, Stiftung zur Krebsbekämpfung, Zurich, and Werner und Hedy Berger-Janser Stiftung zur Erforschung der Krebskrankheiten. This work was also supported in part by the Madeleine Schickedanz-Kinderkrebs-Stiftung and the National Genome Research Net (M. Stanulla and M. Schrappe).

Authorship

Contribution: M. Schmitz, P.B., N.S., L.B., P.M., and B.C.B. performed experiments; M. Stanulla and M. Schrappe provided samples and anonymized clinical information; M. Schmitz contributed to writing the manuscript; B.C.B. and J.-P.B. designed research, analyzed data, and wrote the manuscript; and all authors analyzed data.

Conflict-of-interest disclosure: The authors declare no competing financial interests.

Correspondence: Jean-Pierre Bourquin, Division of Oncology and Children's Research Center, University Children's Hospital, University of Zurich, 8032 Zurich, Switzerland; e-mail: jean-pierre.bourquin@kispi.uzh.ch.

References

1. Pui CH, Evans WE. Treatment of acute lymphoblastic leukemia. *N Engl J Med.* 2006;354(2):166-178.
2. Schrappe M. Evolution of BFM trials for childhood ALL. *Ann Hematol.* 2004;83(suppl 1):121-123.
3. Liem NL, Papa RA, Milross CG, et al. Characterization of childhood acute lymphoblastic leukemia xenograft models for the preclinical evaluation of new therapies. *Blood.* 2004;103(10):3905-3914.
4. Castor A, Nilsson L, Astrand-Grundstrom I, et al. Distinct patterns of hematopoietic stem cell involvement in acute lymphoblastic leukemia. *Nat Med.* 2005;11(6):630-637.
5. le Viseur C, Hotfilder M, Bomken S, et al. In childhood acute lymphoblastic leukemia, blasts at different stages of immunophenotypic maturation have stem cell properties. *Cancer Cell.* 2008;14(1):47-58.
6. Teachey DT, Obzut DA, Cooperman J, et al. The mTOR inhibitor CCI-779 induces apoptosis and inhibits growth in preclinical models of primary adult human ALL. *Blood.* 2006;107(3):1149-1155.
7. Hong D, Gupta R, Ancliff P, et al. Initiating and cancer-propagating cells in TEL-AML1-associated childhood leukemia. *Science.* 2008;319(5861):336-339.
8. Bonapace L, Bornhauser BC, Schmitz M, et al. Induction of autophagy-dependent necroptosis is required for childhood acute lymphoblastic leukemia cells to overcome glucocorticoid resistance. *J Clin Invest.* 2010;120(4):1310-1323.
9. Schrauder A, Stanulla M, Flohr T, et al. Prospective evaluation of MRD-kinetics in 274 children with high-risk ALL treated in Trial ALL-BFM 2000: insights into development of resistance and impact on further refinement of treatment stratification strategies. *Blood.* 2007;110(11):585.
10. Flohr T, Schrauder A, Cazzaniga G, et al. Minimal residual disease-directed risk stratification using real-time quantitative PCR analysis of immunoglobulin and T-cell receptor gene rearrangements in the international multicenter trial AIEOP-BFM ALL 2000 for childhood acute lymphoblastic leukemia. *Leukemia.* 2008;22(4):771-782.
11. Mullighan CG, Goorha S, Radtke I, et al. Genome-wide analysis of genetic alterations in acute lymphoblastic leukaemia. *Nature.* 2007;446(7137):758-764.
12. Bateman CM, Colman SM, Chaplin T, et al. Acquisition of genome-wide copy number alterations in monozygotic twins with acute lymphoblastic leukaemia. *Blood.* 2010;115(17):3553-3558.
13. Kuster L, Grausenburger R, Fuka G, et al. ETV6/RUNX1-positive relapses evolve from an ancestral clone and frequently acquire deletions of

genes implicated in glucocorticoid signaling. *Blood.* 2011;117(9):2658-2667.

14. Mullighan CG, Phillips LA, Su X, et al. Genomic analysis of the clonal origins of relapsed acute lymphoblastic leukemia. *Science.* 2008; 322(5906):1377-1380.
15. Mullighan CG, Zhang J, Kasper LH, et al. CREBBP mutations in relapsed acute lymphoblastic leukaemia. *Nature.* 2011;471(7337):235-239.
16. Cox CV, Diamanti P, Evely RS, Kearns PR, Blair A. Expression of CD133 on leukemia-initiating cells in childhood ALL. *Blood.* 2009;113(14): 3287-3296.
17. Kelly PN, Dakic A, Adams JM, Nutt SL, Strasser A. Tumor growth need not be driven by rare cancer stem cells. *Science.* 2007;317(5836): 337.
18. Kong Y, Yoshida S, Saito Y, et al. CD34+CD38+CD19+ as well as CD34+CD38-CD19+ cells are leukemia-initiating cells with self-renewal capacity in human B-precursor ALL. *Leukemia.* 2008;22(6):1207-1213.
19. Vormoor HJ. Malignant stem cells in childhood acute lymphoblastic leukemia: the stem cell concept revisited. *Cell Cycle.* 2009;8(7):996-999.
20. Anderson K, Lutz C, van Delft FW, et al. Genetic variegation of clonal architecture and propagating cells in leukaemia. *Nature.* 2010;469(7330):356-361.
21. Notta F, Mullighan CG, Wang JC, et al. Evolution of human BCR-ABL1 lymphoblastic leukaemia-initiating cells. *Nature.* 2011;469(7330):362-367.
22. Ratei R, Basso G, Dworzak M, et al. Monitoring treatment response of childhood precursor B-cell acute lymphoblastic leukemia in the AIEOP-BFM-ALL 2000 protocol with multiparameter flow cytometry: predictive impact of early blast reduction on the remission status after induction. *Leukemia.* 2009;23(3):528-534.
23. Wehrli LA, Braun J, Buetti LN, et al. Non-classical karyotypic features in relapsed childhood B-cell precursor acute lymphoblastic leukemia. *Cancer Genet Cytogenet.* 2009;189(1):29-36.
24. van der Velden VH, van Dongen JJ. MRD detection in acute lymphoblastic leukemia patients using Ig/TCR gene rearrangements as targets for real-time quantitative PCR. *Methods Mol Biol.* 2009;538:115-150.
25. Conter V, Bartram CR, Valsecchi MG, et al. Molecular response to treatment redefines all prognostic factors in children and adolescents with B-cell precursor acute lymphoblastic leukemia: results in 3184 patients of the AIEOP-BFM ALL 2000 study. *Blood.* 2010;115(16):3206-3214.
26. Wei J, Wunderlich M, Fox C, et al. Microenvironment determines lineage fate in a human model of MLL-AF9 leukemia. *Cancer Cell.* 2008;13(6): 483-495.
27. Den Boer ML, Harms DO, Pieters R, et al. Patient stratification based on prednisolone-vincristine-asparaginase resistance profiles in children with acute lymphoblastic leukemia. *J Clin Oncol.* 2003;21(17):3262-3268.
28. Iwamoto S, Mihara K, Downing JR, Pui CH, Campana D. Mesenchymal cells regulate the response of acute lymphoblastic leukemia cells to asparaginase. *J Clin Invest.* 2007;117(4):1049-1057.
29. Tabe Y, Jin L, Tsutsumi-Ishii Y, et al. Activation of integrin-linked kinase is a critical prosurvival pathway induced in leukemic cells by bone marrow-derived stromal cells. *Cancer Res.* 2007;67(2): 684-694.
30. Mihara K, Imai C, Coustan-Smith E, et al. Development and functional characterization of human bone marrow mesenchymal cells immortalized by enforced expression of telomerase. *Br J Haematol.* 2003;120(5):846-849.
31. Jorgensen HG, Holyoake TL. Characterization of cancer stem cells in chronic myeloid leukaemia. *Biochem Soc Trans.* 2007;35(5):1347-1351.
32. Morisot S, Wayne AS, Bohana-Kashtan O, et al. High frequencies of leukemia stem cells in poor-outcome childhood precursor-B acute lymphoblastic leukemias. *Leukemia.* 2010;24(11):1859-1866.
33. Chiu PP, Jiang H, Dick JE. Leukemia-initiating cells in human T-lymphoblastic leukemia exhibit glucocorticoid resistance. *Blood.* 2010;116(24): 5268-5279.
34. Rehe K, Wilson K, McNeill H, Schrappe M, Irving J, Vormoor J. Disease propagating blasts in standard and high risk acute lymphoblastic leukemia are frequent and of diverse immunophenotype. *Blood.* 2009;114:1421.
35. Novara F, Beri S, Bernardo ME, et al. Different molecular mechanisms causing 9p21 deletions in acute lymphoblastic leukemia of childhood. *Hum Genet.* 2009;126(4):511-520.
36. Heerema NA, Harbott J, Galimberti S, et al. Secondary cytogenetic aberrations in childhood Philadelphia chromosome positive acute lymphoblastic leukemia are nonrandom and may be associated with outcome. *Leukemia.* 2004;18(4): 693-702.
37. van Zutven LJ, van Drunen E, de Bont JM, et al. CDKN2 deletions have no prognostic value in childhood precursor-B acute lymphoblastic leukaemia. *Leukemia.* 2005;19(7):1281-1284.
38. Eckert C, Koehler R, Flohr T, et al. Very early/early relapses of ALL show unexpected changes of clonal markers and high heterogeneity in initial and relapse treatment response: ALL-BFM 2000 and ALL-REZ BFM 96/2002. *Blood.* 2009;114: 2612.
39. Sherborne AL, Hosking FJ, Prasad RB, et al. Variation in CDKN2A at 9p21.3 influences childhood acute lymphoblastic leukemia risk. *Nat Genet.* 2010;42(6):492-494.
40. Sulong S, Moorman AV, Irving JA, et al. A comprehensive analysis of the CDKN2A gene in childhood acute lymphoblastic leukemia reveals genomic deletion, copy number neutral loss of heterozygosity, and association with specific cytogenetic subgroups. *Blood.* 2009;113(1):100-107.
41. Ishikawa F, Yasukawa M, Lyons B, et al. Development of functional human blood and immune systems in NOD/SCID/IL2 receptor γ chain(null) mice. *Blood.* 2005;106(5):1565-1573.
42. Willinger T, Rongvaux A, Takizawa H, et al. Human IL-3/GM-CSF knock-in mice support human alveolar macrophage development and human immune responses in the lung. *Proc Natl Acad Sci U S A.* 2011;108(6):2390-2395.
43. Meyer LH, Eckhoff SM, Queudeville M, et al. Early relapse in ALL is identified by time to leukemia in NOD/SCID mice and is characterized by a gene signature involving survival pathways. *Cancer Cell.* 2011;19(2):206-217.

Supplementary methods

Reagents

FITC-labeled anti-human CD7, FITC-labeled anti-human CD20, FITC-labeled anti-human CD34, PE and PE-AlexaFluor750-labeled anti-human CD19, Alexa 647-labelled anti-mouse CD45, and RPE-Alexa 750-labelled anti-human CD45 antibodies were from AbD Serotec. APC-labeled anti-human CD22, APC-labeled anti-human CD38, PerCP-Cy5.5-labeled anti-human CD34, APC-H7-labeled anti-human CD20, FITC-labeled anti-human CD33 and PE-labeled anti-human CD13 were from BD Biosciences. FITC-labeled anti-human CD45, PE-labeled anti-human CD7 and 7- Amino-actinomycin D (7-AAD) were from eBioscience. FITC-labeled anti-human CD117 was from Abcam. FITC-labeled anti-human CD38 and APC-labeled anti-human CD10 were from Biolegend. Pacific orange-labeled anti-human CD45 was from Invitrogen.

Flow cytometry

Immunophenotype analysis of xenograft material was performed from cryopreserved material. 1 million of cells were thawed and stained in phosphate buffered saline (PBS) containing 0.5% fetal calf serum (FCS). Either 4 or 7 antibodies per tube were combined. 7-AAD was used for discriminating live and dead cells. Fluorescence-minus-one-controls were used for determining background signals. Measurements were carried out on a BD Bioscience FACS Canto II flow cytometer and analyzed using FlowJo software (TreeStar Inc.).

Xenograft model

Xenografted ALL cells were recovered from the spleen by mechanical disruption and filtering (45 µM cell strainer, BD Biosciences) and from bone marrow by flushing dissected femurs and tibias with PBS using a 25 gauge needle, yielding more than 95% human CD45 and CD19 positive cells per harvest as verified by flow cytometry.

For serial dilution experiments 10^2, 10^4 and 10^6 ALL cells recovered from a first or second xenotransplantation in NSG mice were injected intrafemorally or intravenously into cohorts of NSG mice. Leukemia progression was assessed by flow cytometry of the mouse peripheral blood. 1%

human cells detectable in peripheral blood was scored as engrafted leukemia. At more than 75% of human cells in the peripheral blood or if signs of sickness were apparent, animals were euthanized and cells harvested as described. Time to engraftment was calculated as time from transplantation until >1 % of human leukemia cells were detected in the peripheral blood of transplanted animals; statistical evaluation was performed using the log rank test (GraphPad prism).

Cell culture – Coculture

Primary patient samples were co-cultured on hTERT-immortalized human mesenchymal stroma cells (MSC), and drug response curves were generated after incubation with indicated drugs. The following concentrations were used: Dexamethasone was used at 100, 1000 and 7600 nM, vincristine at 3, 10 and 100 nM, daunorubicine at 10, 100 and 1000 nM and cytarabine at 10, 100 and 1000 nM. Cell viability was analyzed with flow cytometry using 7-AAD[8]. Human *hTERT*-immortalized primary bone marrow MSCs[21] were provided by D. Campana (St Jude Children's Research Hospital).

Affymetrix Genome-Wide Human SNP 6.0 microarrays

Copy number aberrations were scored with the segmentation approach available within the Partek software package. Deleted and amplified segments were filtered to be at least 100 kbp long. Segments of sizes between 100kbp and 1000kbp were regarded as focal deletions. Regions of special interest, for example 9p21 and regions of Immunoglobulin rearrangements and T-cell receptors, were investigated separately and exceptions from the >100 kbp-rule were made in these cases. All segments were visually inspected and aberrations that were already present in the matched remission samples were excluded from further analysis.

Fluorescence in situ hybridization

A Leica LX Widefield Microscope DMI6000B with the DFC 350 FX R2 camera was used for the analysis. The A4 filter cube was used for detection of DAPI (UV, Exc: BP 360/40), a L5 filter cube for spectrum green (blue, Exc: BP 480/40) and a TX2 filter cube for spectrum orange. (green, Exc:

BP 515/40). 200 intact single cells were scored at 40x original magnification. Peripheral blood mononuclear cells of healthy donors were used to determine cut off values, which were set to 15 of 200 scored cells for all subsets.

Analysis of clonal Ig/TCR rearrangements.

The following immunoglobuline and T cell receptor genes were analyzed: (IGVH[1-5])-JH), κ-deleting element (IGVκI-IV-Kde), T-cell receptor γ (TCRVγI-IV-Jγ), and T-cell receptor δ (TCRVδ[1-3]-Jδ1; Vδ2-Dδ3; Dδ2-Dδ3; Dδ2-Jδ1). Each positive marker was sequenced using standard methodology.

Supplemental Table 1. Patient characteristics

Part A: Very High Risk patients

Patient	Risk	MRD TP3	additional Information	Relapse	Survival	Age	Sex	Immunology	Leukocyte count	Blasts periph %
VHR-01	VHR	positive	Early, relapse, T(17;19)	yes 2x	no	14.1	m	Common-ALL	6300	13
VHR-02	VHR	positive		yes	yes	12.8	f	Common-ALL	79600	68
VHR-03	VHR	positive	TRM	no	no	17.1	m	Common-ALL	20100	78
VHR-04	VHR	positive		no	yes	5.7	f	Common-ALL	45700	97
VHR-06	VHR	positive	E2A-PBX1, TEL-AML, complex karyotype	yes	no	17.6	m	Pre-B-ALL	8000	73
VHR-07	VHR	positive	MLL-AF4	no	yes	11.6	m	Pro-B-ALL	100000	99
VHR-10	VHR	positive		no	yes	14.4	f	Common-ALL	150000	89
VHR-11	VHR	positive	DS	yes	no	3.1	m	Pre-B-ALL	16000	na
VHR-12	VHR	positive		no	yes	15.3	f	Pre-B-ALL	7410	92
VHR-15	VHR	positive	Deletion 9p	no	yes	13.2	m	Pre-B-ALL	2900	60
VHR-16	VHR	positive		no	yes	10.4	m	Common-ALL	151800	93
VHR-17	VHR	positive	DS	yes	no	16.1	m	Common-ALL	220000	95
VHR-18	VHR	positive	T(17;19), MLL-AF9+ENL	yes	no	3.4	m	Common-ALL	36000	na
VHR-19	VHR	positive		no	yes	16.1	m	Common-ALL	31700	65
VHR-20	VHR	positive		yes	yes	8.2	m	Common-ALL	27400	42
VHR-21	VHR	nd	Early relapse	yes	no	8.8	f	Pre-B-ALL	197200	na
VHR-22	VHR	positive		yes	no	11	m	Common-ALL	16700	23

Part B: Standard and High Risk patients

Patient	Risk	MRD TP3	additional Information	Relapse	Survival	Age	Sex	Immunology	Leukocyte count	Blasts periph %
SR-01	SR	negative		no	yes	10.5	m	Pre-B-ALL	18300	39
SR-02	SR	negative	Amplification AML1	no	yes	12.1	m	Pre-B-ALL	447000	94
SR-03	SR	negative		no	yes	3.4	f	Pre-B-ALL	10600	42
SR-04	SR	negative	E2A-PBX1	no	yes	3.6	f	Common-ALL	19000	55
SR-05	SR	negative	HHD	no	yes	1.7	m	Common-ALL	21600	79
SR-06	SR	negative	HHD	yes	no	3.3	f	Common-ALL	4400	43
SR-07	SR	negative	CNS	no	yes	6.8	m	Pre-B-ALL	46230	72
SR-08	SR	negative	E2A-PBX1	no	yes	12.8	f	Pre-B-ALL	14600	66
SR-09	SR	negative		yes	yes	5.5	f	Common-ALL	317400	na
SR-10	SR	negative		no	yes	7.3	m	Common-ALL	17050	65
SR-11	SR	negative	CNS	yes	yes	6.1	m	Common-ALL	66600	87
SR-12	SR	negative	E2A-PBX1	no	yes	10.4	m	Common-ALL	88500	na
SR-13	SR	negative		no	yes	4.1	f	Common-ALL	21000	na
SR-14	SR	negative	ETV6-RUNX1	no	yes	5.8	m	Pre-B-ALL	124000	44
SR-16	SR	negative	CNS	yes	yes	9.2	f	Common-ALL	92900	14
HR-13	HR	negative	BCR-ABL	no	yes	9.8	m	Common-ALL	3500	3
HR-03	HR	negative	CNS, BCR-ABL, HHD	no	yes	16.9	f	Common-ALL	13300	78
HR-08*	HR	negative	MLL	no	yes	0.3	f	Infant-ALL	446000	na
HR-10*	HR	nd	Early relapse, MLL	yes	no	0.1	m	Infant-ALL	250000	66

MRD-TP3, time point 3 of minimal residual disease measurements by qPCR (according to the ESG-MRD-ALL study group), positive, detectable above threshold of 10^{-8}, negative, not detectable; * denotes patients with infant-ALL that were treated according to the “interfant-ALL” protocol; CNS, disease spread into central nervous system; HHD, high hyperdiploid; DS, Down-Syndrome; na, not available; nd, not determined.

Supplemental Table 2. Xenograft samples characteristics

successful engraftment

Patient	Pred response	Risk group	Passages in NSG	Mean yield (spleen)	Mean spleen%	Mean bone marrow%	Mean blood%	Weeks to engraftment 1/2/3/4/5/6 passages	EC 50 obatoclax	EC 50 ABT-737	DEX	DNR	VCR	araC	% CD34	# of viable cells injected passage 1 (millions)
VHR-01	PPR	VHR	3	4.64E+08	91-99	74-99	10-55	8 / 14 / 8	700nM	6nM	PPR	R	R	R	0	1
VHR-02	PPR	VHR	6	6.82E+08	98-99	75-99	14-91	8 / 7 / 14 / 12 / 8 / 8	2uM	7nM	PPR	R	R	R	69	5
VHR-03	PPR	VHR	6	7.18E+08	93-99	63-99	11-91	6 / 9 / 8 / 7 / 5 / 4	600nM	50nM	PPR	R	R	R	11	1
VHR-04	PGR	VHR	3	7.02E+08	97-99	98-99	14-50	11 / 12 / 14	350nM	6nM	PGR	R	R	R	79	5
VHR-06	PGR	VHR	3	3.33E+08	85-99	84-98	5-87	8 / 4 / 4	800nM	80nM	PGR	R	R	R	1	1.3
VHR-07	PPR	VHR	3	2.22E+08	90-99	97-99	36-75	7 / 6 / 4	1.3uM	50nM	PPR	R	R	R	16	1
VHR-10	PPR	VHR	2	3.08E+08	87-99	74-99	25-76	11 / 8	900nM	200nM	PPR	R	R	R	81	1
VHR-11	PGR	VHR	2	2.12E+08	45-94	95-98	10-40	8 / 5	nd	nd	nd	nd	nd	nd	38	1
VHR-12	PPR	VHR	2	7.08E+08	70-99	96-99	44-82	4 / <4	80nM	95nM	PPR	R	S	R	nd	1
VHR-15	PPR	VHR	2	6.08E+08	95-99	85-99	15-50	6 / 4	500nM	50nM	PPR	R	R	R	92	0.7
SR-01	PGR	SR	1	1.16E+09	98-99	98-99	64-76	7	200nM	10nM	PGR	S	S	S	0	1
SR-02	PGR	SR	3	7.50E+08	96-99	89-99	41-87	5 / 7 / 6	550nM	60nM	PGR	S	S	R	0	1
SR-03	PGR	SR	2	5.89E+08	99	nd	54-73	14 / 7	800nM	10nM	PGR	S	S	S	77	1
SR-04	PGR	SR	2	4.94E+08	97-99	97-99	7-75	18 / 5	nd	nd	nd	nd	nd	nd	0	1
SR-05	PGR	SR	3	4.34E+08	95-99	97-99	23-74	30 / 12 / 17	nd	nd	nd	nd	nd	nd	79	1
SR-06	PGR	SR	1	9.50E+08	96-99	99	65-75	13	nd	nd	nd	nd	nd	nd	44	1
SR-07	PGR	SR	2	7.53E+08	95 - 99	74-92	12-51	28 / 16	nd	nd	nd	nd	nd	nd	7	1
SR-08	PGR	SR	2	3.67E+08	96-99	86-99	14-88	7 / <4	nd	nd	PGR	S	S	S	0	2
SR-09	PGR	SR	2	2.06E+08	94-99	98-99	70-83	11 / 4	150nM	50nM	PGR	M	S	S	96	1
SR-10	PGR	SR	2	1.34E+09	99	99	20-96	32 / 10	90nM	10nM	PGR	S	S	S	57	1
SR-11	PGR	SR	2	1.11E+09	98-99	91-99	53-66	12 / 9	100nM	20nM	PPR	S	S	S	3	0.6
SR-12	PGR	SR	2	4.67E+08	98-99	96-99	53-84	14 / <4	nd	nd	nd	nd	nd	nd	57	1.3
SR-13	PGR	SR	2	1.30E+09	99	99	19-78	28 / 5	nd	nd	nd	nd	nd	nd	14	3.5
SR-14	PPR	SR	2	7.85E+08	94-100	55-93	31-84	10 / 8	300nM	10nM	PPR	M	M	R	61	1
HR-13	PGR	HR	2	4.99E+08	90-99	80-99	52-76	5 / <4	nd	nd	nd	nd	nd	nd	55	1
HR-10	PPR	HR	1	1.85E+08	98	96	57-92	<4	nd	nd	nd	nd	nd	nd	89	1
HR-03	PGR	HR	5	3.82E+08	86-99	70-99	11-95	8 / 9 / 6 / 4 / 4	560nM	nd	PGR	R	R	R	22	1
HR-08	PPR	HR	1	3.08E+08	99	98	30-34	<4	80nM	60nM	PPR	S	S	M	96	0.3

not engrafted

Patient	Pred response	Risk group	# of viable cells injected passage 1 (millions)
VHR-16	PPR	VHR	1
VHR-17	PPR	VHR	1
VHR-18	PGR	VHR	1
VHR-19	PGR	VHR	1
VHR-20	PPR	VHR	1
VHR-21	PPR	VHR	1
VHR-22	PGR	VHR	1
SR-16	PGR	SR	1

Characteristics of all engrafted and not-engrafted SR-, HR- and VHR-patients are shown. Clinical parameters at diagnosis and engraftment characteristics are given (yield, time to engraftment, percentage of human cells, % of CD34 positive cells, drug response). PPR, Prednisone poor response; PGR, Prednisone good response; DEX, dexamethasone; DNR, daunorubicine; VCR, vincristine; araC, Cytarabine; R, resistant; M, intermediate response; S, sensitive; nd, not determined.

Supplemental Table 3. Layout and primers for Ig and TCR gene rearrangement PCR

	Forward	Reverse	Rearrangement
lane 1	VH1/7	JH	
lane 2	VH2	JH	
lane 3	VH3	JH	*IgH* V_H-J_H
lane 4	VH4/6	JH	
lane 5	VH5	JH	
lane 6	Vd2 and Dd2	Dd3	
lane 7	Vd2 and Dd2	Jd1	*TCRD*
lane 8	Vd1	Jd1	
lane 9	VK1 and RS-3	Kde	
lane 10	VK2	Kde	*IGK*
lane 11	VK3	Kde	
lane 12	VK4	Kde	
lane 13	Vg2 and Vg3	$Jg_{1.3/2.3}$	
lane 14	Vg4	$Jg_{1.3/2.3}$ and $Jg_{1.1/2.1}$	*TCRG*
lane 15	Vg1	$Jg_{1.1/2.1}$ and $Jg_{1.3/2.3}$	
lane 16	Vd2	Ja29	*TCRD/A*
lane 17	Vb (23x)	$Jb_{1.1}$ and $Jb_{1.2}$	*TCRB* Vb-Jb

For primer sequences see: van der Velden VH, van Dongen JJ. MRD detection in acute lymphoblastic leukemia patients using Ig/TCR gene rearrangements as targets for real-time quantitative PCR. Methods Mol Biol. 2009;538(115-150).

Supplemental Table 4. Stability of immunophenotypes over serial passages.

Part A: Measurements from diagnostic and xenografted samples carried out on the same flow cytometer.

Patient	CD7	CD19	CD20	CD22	CD10	CD34	CD45	CD13	CD33	CD117	CD38
VHR-01	**-**	**++**	**-**	**++**	**++**	**-**	**++**	**+**	**++**	**-**	**++**
1	-	+	-	+	++	-	++	+	++	-	nd
2	-	++	-	++	++	-	++	+	++	-	nd
2*	-	++	-	+	++	-	++	+	++	+	nd
3	-	++	+	nd	++	-	++	+	++	nd	++
VHR-03	**-**	**++**	**-**	**++**	**+**	**+**	**++**	**+**	**+**	**-**	**++**
2	-	++	+	+	+	+	++	+	+	-	nd
2	-	++	-	nd	++	+	++	+	-	nd	++
3	-	++	-	nd	++	+	++	nd	-	nd	++
3*	-	++	-	++	++	+	++	+	-	-	++
3*	-	++	-	++	++	+	++	+	-	-	++
4	-	++	+	++	++	+	++	+	++	-	nd
4	-	++	-	nd	++	+	++	+	-	nd	++
5	-	++	-	nd	+	+	++	+	-	nd	++
6	-	++	-	nd	+	+	++	+	-	nd	++
VHR-10	**nd**	++	**+**	**+**	**++**	**+**	**++**	**-**	**-**	nd	**+**
1	-	++	++	+	++	++	++	-	-	-	nd
1	-	++	+	+	++	+	++	-	-	nd	nd
2	-	++	+	nd	++	+	++	-	-	nd	+
2	-	++	+	nd	++	+	++	-	-	nd	+
SR-09	**-**	**++**	**-**	**++**	**++**	**++**	**++**	**-**	**-**	**-**	**++**
1	-	++	-	nd	++	++	++	-	-	nd	++
1	-	++	-	++	++	++	++	-	-	-	nd
2	-	++	-	nd	++	++	++	-	-	nd	++
SR-11	**-**	**++**	**-**	nd	**++**	**-**	**-**	**+**	**-**	nd	**++**
1	-	++	-	nd	++	++	-	+	-	nd	++
2	-	++	-	nd	++	++	-	+	-	nd	++

Part B: Measurements from diagnostic samples carried out in the ALL-BFM reference laboratories, and xenograft samples analyzed in Zurich laboratories.

Patient	CD7	CD19	CD20	CD22	CD10	CD34	CD45	CD13	CD33	CD117	CD38
VHR-04	**+**	**++**	**+**	**++**	**++**	**++**	**++**	**+**	**+**	**-**	**++**
1	+	++	+	++	++	++	++	-	-	-	nd
1	+	++	+	nd	++	++	++	+	nd	nd	++
2*	+	++	+	nd	++	++	++	+	nd	nd	++
2	+	++	+	nd	++	++	++	+	nd	nd	++
3	+	++	+	nd	++	++	++	+	nd	nd	++
VHR-06	**-**	**++**	**-**	**++**	**++**	**-**	**++**	**-**	**+**	**-**	nd
1	-	++	-	++	++	-	++	-	+	-	nd
VHR-07	**-**	**++**	**-**	**+**	**-**	**-**	**++**	**-**	**-**	**-**	nd
1	-	++	-	++	-	-	++	-	-	-	nd
HR-03	**-**	**++**	**+**	**++**	**++**	**+**	**++**	**+**	**-**	**-**	nd
1	-	++	++	-	++	++	++	-	+	-	nd
1	-	++	+	-	+	++	++	-	-	-	nd
SR-01	**-**	**++**	**-**	**-**	**++**	**-**	**++**	**-**	**-**	**-**	nd
1	-	++	-	-	++	-	++	-	-	-	nd
1	-	++	-	-	++	-	++	-	-	-	nd
SR-02	**-**	**++**	**+**	**+**	**++**	**-**	**++**	**-**	**-**	**-**	nd
1	-	++	+	+	++	+	++	-	-	-	nd
1	-	++	-	-	+	+	++	-	-	nd	nd
SR-03	**+**	**++**	**++**	**++**	**++**	**++**	**++**	nd	**-**	**-**	nd
1	-	++	+	+	++	++	++	nd	+	-	nd
SR-04	**-**	**++**	**+**	**++**	**++**	**-**	**++**	**-**	**-**	**-**	nd
2	-	++	++	+	++	-	++	-	+	-	nd
SR-08	**-**	**++**	**-**	**++**	**++**	**-**	**++**	**-**	**-**	**-**	nd
1	-	++	-	+	++	+	++	-	-	-	nd
SR-10	**-**	**++**	**++**	**++**	**++**	**++**	**++**	**-**	**-**	**-**	nd
1	-	++	++	-	++	++	++	-	-	-	nd
SR-12	**-**	**++**	**++**	**++**	**++**	**+**	**-**	**-**	**-**	**-**	nd
1	-	++	++	++	++	+	+	-	++	-	nd

Expression of surface markers measured by flow cytometry. First rows show diagnostic measurements (in bold) and following rows show measurements of xenografted material (1-first round, 2-2nd round etc). In part A data are shown with measurements carried out on the same flow cytometer, in part B data from diagnostic measurements carried out at the ALL-BFM reference lab in Berlin are given, together with measurements of xenograft samples performed in Zurich. * depicts sample after 100 cell transplantation; nd, not determined; -, no expression; +, weak expression up to 20%; ++, strong expression in more than 20% of all cells.

Supplemental Table 5. Engraftment of VHR- and SR-ALL in NSG mice after serial dilution.

Patient	Round of amplification	Cell dilution	if engrafted/total	iv engrafted/total	weeks to engraftment
VHR-01	diagnostic	1000000	2/2	nd	8
		10000	**2/2**	nd	20
		100	0/3	nd	-
VHR-01	2nd	1000000	2/4	3/3	14 / 16
		10000	3/3	**3/3**	8 / 14
		100	**2/3**	0/3	14
VHR-02	3rd	1000000	1/2	2/3	10 / 10
		10000	3/3	**1/3**	12 / 12
		100	**2/3**	0/3	26 / -
VHR-03	3rd	1000000	2/2	2/2	9 / 8
		10000	2/2	**2/2**	5 / 12
		100	**1/2**	0/2	14 / -
VHR-04	2nd	1000000	2/2	2/3	12 / 10
		10000	1/3	**2/3**	12 / 10
		100	**1/3**	0/3	18 / -
VHR-06	diagnostic	1000000	2/2	nd	4
		10000	**3/3**	nd	7
		1000	0/3	nd	-
VHR-06	2nd	1000000	2/2	nd	4
		10000	3/3	nd	7
		1000	**1/3**	nd	28
		100	0/5	nd	-
VHR-07	diagnostic	1000000	**2/2**	nd	8
		10000	0/3	nd	-
		100	0/5	nd	-
VHR-07	2nd	1000000	3/3	nd	5
		10000	**3/3**	nd	5
		100	0/5	nd	-
SR-02	diagnostic	80000	**2/2**	nd	8
		10000	0/2	nd	-
		100	0/5	nd	-
SR-02	2nd	1000000	2/2	nd	4
		10000	**2/2**	nd	8
		100	0/5	nd	-
SR-08	diagnostic	500000	**2/2**	nd	10
		10000	0/2	nd	-
		100	0/5	nd	-
SR-08	2nd	1000000	2/2	nd	4
		10000	**1/2**	nd	6
		100	0/5	nd	-
HR-03	3rd	1000000	**2/2**	3/3	9 / 6
		10000	0/3	3/3	0 / 6
		100	0/3	0/3	-

VHR-, SR- and one HR-ALL patients from different amplification rounds were transplanted intrafemoral or intravenous. Engraftment was considered as positive when 1% of humanCD19/CD45 positive mouseCD45 negative cells were detected in peripheral blood by flow cytometry and spleens and bone marrows were engrafted at harvest. if, intra femoral; iv, intra venous; nd, not done.

Supplemental Table 6. Regions of CNAs in diagnostic and xenograft samples.

Sample	Cytoband	CNA	CNA average	Overlapping Genes	Near Genes	Rearrangement
VHR-02: all	2p11.2	Deletion	0.8		FLJ40330	IgK
VHR-02: all	7q34	Deletion	1.1	PRSS1, PRSS2		TCRb
VHR-02: all	7p14.1	Deletion	0.8		TARP	TCRg
VHR-02: 2 mice	14q11.2	Deletion	0.3		DAD1	TCRab
VHR-02: 3 mice	14q11.2	Deletion	0.8		DAD1	TCRab
VHR-02: all	14q32.33	Deletion	1.0	KIAA0125, ADAM6, LOC100133469		IgH
VHR-02: all	22q11.22	Deletion	1.2	VPREB1		IgL
VHR-02: diagnostic	4q31.3	Deletion	1.2	overlaps with 20.34% of FBXW7	FBXW7	
VHR-02: all	7p12.2	Deletion	1.0	parts of IKZF1	IKZF1	
VHR-02: all mice	9p21.3	Deletion	1.0	C9orf53, CDKN2A, CDKN2BAS, CDKN2B		
VHR-02: all mice	9p13.2	Deletion	1.1	intron of ZCCHC7	ZCCHC7	
VHR-03: all	2p11.2	Deletion	0.9		FLJ40330	IgK
VHR-03: all	7p14.1	Deletion	1.1	TARP		TCRg
VHR-03: all	14q11.2	Deletion	0.5		DAD1	TCRab
VHR-03: all	14q32.33	Deletion	1.4	KIAA0125		IgH
VHR-03: diagnostic subclone	1q42.11 - 1q42.13	Deletion	1.6	many		
VHR-03: 3/5 mice	7q22.3	Deletion	1.1	PIK3CG		
VHR-03: all	9p	cnLOH	2.0	many		
VHR-03: all	9p21.3	Deletion	0.4	many, incl. CDKN2A/B		
VHR-03: diagnostic subclone	9p	Deletion	0.6	many		
VHR-03: diagnostic subclone	14q12	Deletion	1.7	AP4S1, C14orf126, COCH, HEATR5A, HECTD1, MIR624, STRN3	NUBPL, SCFD1	
VHR-03: all	20p13 - 20p11.23	Amplification	2.9	many		
VHR-03: all	20q	cnLOH	2.0	many		
VHR-04: all	2p11.2	Deletion	1.0		FLJ40330	IgK
VHR-04: all	14q11.2	Deletion	1.0		DAD1	TCRab
VHR-04: all	14q32.33	Deletion	0.7	KIAA0125, ADAM6, LOC100133146		IgH
VHR-04: all mice	22q11.22	Deletion	1.2	VPREB1		IgL
SR-02: all	14q32.33	Deletion	1.0	KIAA0125, ADAM6		IgH
SR-02: all mice	1p36.13	Amplification	3.4	CROCCL1, ESPNP, MST1P2, MST1P9, NBPF1		
SR-02: all mice	1q23.3	Deletion	1.6	F11R, ITLN2		
SR-02: all	1q	Amplification	3.1	many		
SR-02: all mice	3q22.1	Amplification	3.3	ALG1L2, LOC729375		
SR-02: diagnostic	7p21.3	Amplification	2.5		ARL4A	
SR-02: all	9p	Deletion	1.1	many		
SR-02: all	9q	Amplification	3.1	many		

SR-02: all	19p	Deletion	1.2	many		
VHR-01: all	2p11.2	Deletion	0.5	none		Ig K
VHR-01: all	14q11.2	Deletion	0.9	none		TCRab
VHR-01: all	14q32.33	Deletion	1.2	KIAA0125, ADAM6		IgH
VHR-01: all	22q11.22	Deletion	1.3	VPREB1, LOC96610, ZNF280A,B, PRAME, LOC648691, POM121L1P, GGTLC2,		IgL
VHR-01: all mice	9p	Deletion	1.1	many		
VHR-01: all	12p13	cnLOH	2.0	many		
VHR-01: all mice	22q	Amplification	3.0	many		
HR-03: all	2p11.2	Deletion	1.0	none		IgK
HR-03: all	7p14.1	Deletion	0.3	TARP		TCR g
HR-03: all	7q34	Deletion	0.7	MGAM		TCR b
HR-03: all	14q32.33	Deletion	0.8	KIAA0125, ADAM6, LOC100133146		IgH
HR-03: diagnostic subclone, all mice	1	Amplification	mice 2.89, diagnostic 2.44	many		
HR-03: all	2	Amplification	2.8	many		
HR-03: all	3	Amplification	2.8	many		
HR-03: all	4	Amplification	3.7	many		
HR-03: all	5	Amplification	2.8	many		
HR-03: all	6	Amplification	3.8	many		
HR-03: all	7	cnLOH	2.0	many		
HR-03: all	8	Amplification	3.7	many		
HR-03: all	9p21.3	Deletion	0.5	MTAP, CDKN2A, CDKN2BAS, C9orf53		
HR-03: all	9	cnLOH	2.0	many		
HR-03: diagnostic subclone	9p	Amplification	3.5	many		
HR-03: diagnostic subclone, all mice	9q	Amplification	2.9 to 3.68	ABL1, many		
HR-03: all	10	Amplification	2.9	many		
HR-03: all	11	Amplification	2.9	many		
HR-03: all	12	Amplification	2.9	many		
HR-03: all	13	Amplification	2.9	many		
HR-03: all	14	Amplification	2.9	many		
HR-03: all	15	Amplification	3.8	many		
HR-03: all	16	Amplification	2.9	many		
HR-03: all	17	Amplification	2.9	many		
HR-03: all	18	Amplification	2.9	many		
HR-03: all	19	Amplification	2.9	many		
HR-03: all	20	Amplification	3.7	many		
HR-03: all	20p	Amplification	3.8	many		
HR-03: all	20	cnLOH	2.0	none		
HR-03: all	20q	Amplification	2.8	PTPN1, many		
HR-03: all	21	Amplification	3.7	many		
HR-03: all	22	Amplification	2.9	many		
HR-03: all mice	22q	Amplification	3.8	BCR, many		
HR-03: all	X	Amplification	2.9	many		

Results are shown for six patients and the corresponding xenograft material (between one to five mice) available. CNAs of sizes ranging from at least 100kb to whole chromosomes are shown. CNA average is the mean of the measured copy number over the length of the abnormality. Where no genes were affected by the abnormality the nearest genes are mentioned. Ig or TCR gene rearrangements are mentioned where applicable.

Supplemental Table 7. FISH analysis of chromosome 9p21 abnormalities

	4/4	4/1	4/0	3/5	3/3	3/2	3/1	3/0	2/4	2/3	2/2	2/1	2/0	1/2	1/1	1/0
VHR-01											169	22	1		7	1
P1											13	73	80		14	20
P2											4	184	4		7	1
P2											25	145	3		27	
P2											8	158	5		29	
P2											12	40	128		8	12
P2										1	22	115	41		14	7
P3											3	172	6		19	
P3										1	2	162	6		29	
VHR-02																
P2											31	63	94		6	6
P2											125	56	7		10	2
P3											134	45	11		8	2
P3											174	19			7	
P3											171	19			8	2
P3											136	55	7		2	
P3											156	31	5		8	
VHR-03											5	2	171			22
P1													185			15
P2										1	2	3	175			19
P2			1										187			12
P3											2	4	152		2	39
P3											1	4	185			10
P3			1									2	164			34
P4						3					3	7	167		3	17
P4						8					16	14	157			5
P5								2				1	189			8
P6								1				1	190			8
VHR-04																
P1					1					1	162	20	1		14	
P2										2	163	19	3		13	
P3					6						162	16			16	
VHR-06																
P1										1	28	144	10		14	3
VHR-07																
P1						1	1			2	161	14	9		11	1
VHR-10											110	41	24	13	8	4
P2				1		2		1		25	80	35	45		8	3
P2											111	40	36		4	3
P2									1	4	34	37	119		2	7
P2		1									134	31	21		6	1
P2					1				1	6	113	37	42		6	2
VHR-11																
P1					13	3			1	3	163	3			11	
VHR-12																
P1											153	29	8		9	1

	4/4	4/1	4/0	3/5	3/3	3/2	3/1	3/0	2/4	2/3	2/2	2/1	2/0	1/2	1/1	1/0
SR-01																
P1						1	1				155	14	7		20	1
SR-02											51	123	17		8	1
P1							2	1			21	149	16		9	2
SR-03																
P1					7	1					185				7	
SR-04																
P2										4	179	2			15	
SR-05											56	50	88		4	2
P1											2		177			21
SR-07																
P1										5	49	58	75		6	7
P1					2						155	22	1		20	
SR-08																
P1					5	2					179	8			8	6
SR-09											80	90	5		23	2
P1											8	132	34		23	3
P2							1				29	130	5		34	1
P2											93	86	5		16	
P2						1					4	166	4		25	
SR-10																
P1					1	1					171	9			9	3
SR-11											133	35	13		15	4
P1											74	54	67		4	1
P2											86	66	28		15	5
P2		1								1	57	57	48		21	15
SR-12																
P1					7						151	33	4		5	

	4/4	4/1	4/0	3/5	3/3	3/2	3/1	3/0	2/4	2/3	2/2	2/1	2/0	1/2	1/1	1/0
HR-03																
P1					3	98	21	11			20	33	9		4	
HR-08																
P1						1				1	191	3			3	
P1						2				2	190	6				
HR-09																
P1									1	1	178	11	1		18	
HR-13											22	12	158		2	6
P1					1	1		1			2	3	184			8

9p21 copy abnormalities were measured in 9 VHR-, 11 SR- and 4 HR-ALL samples (diagnostic and/or xenograft material). In the top row, the different configurations with respect to copies detected with the centromer chromosome 9 and the 9p21 (CDKN2A) probe, respectively. 200 cells were counted, and in yellow, the numbers of positive cells for a given configuration above the threshold (15 positive cells per 200 counted) are given.

Supplemental Table 8. Stable detection of diagnostic MRD markers after serial transplantation.

Patient	Round of amplification	Marker detected/total
VHR-01	1st	2/2
	2nd	2/2
VHR-02	2nd	2/2
	3rd	2/2
	after 100 cells	2/2
VHR-03	1st	2/2
	2nd	2/2
	3rd	2/2
	after 100 cells	2/2
	4th	2/2
VHR-04	1st	0/1
	2nd	0/1
HR-03	1st	2/2
	2nd	2/2
	3rd	1/2
	4th	1/2
VHR-06	1st	2/2
VHR-07	1st	0/2
HR-05	1st	2/2
HR-06	1st	2/2
SR-01	1st	2/2
SR-02	1st	2/2
	2nd	2/2
SR-04	1st	2/2
SR-08	1st	1/1
SR-09	1st	1/2

MRD markers of clonal Ig and TCR gene rearrangements were established at diagnosis of each patient and used for detection by qPCR in the amplified material of different rounds of transplantation.

Supplemental Figure 1: Phenotypic stability of ALL cells after serial dilution

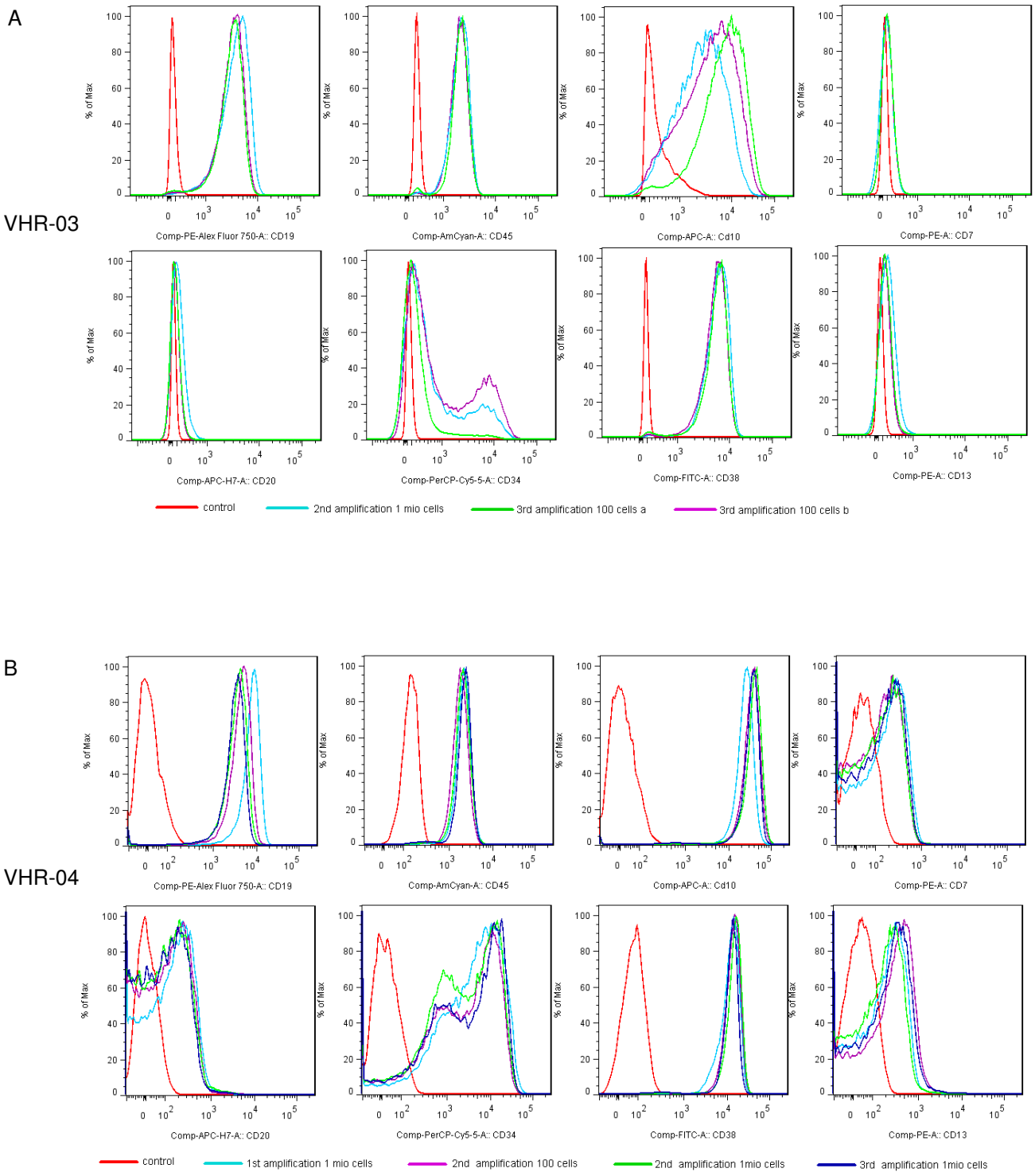

Supplemental Figure 1: Phenotypic stability of ALL cells after serial dilution. Flow cytometry analysis of VHR-03 (A) and VHR-04 (B). Multicolor flow cytometry analyses of primograft cells and secondary transplants thereof performed with 100 cells show preservation of immunophenotype.

Supplemental Figure 2: Analysis of Ig/TCR rearrangements reflects the evolution of the clonal compartment in xenografts.

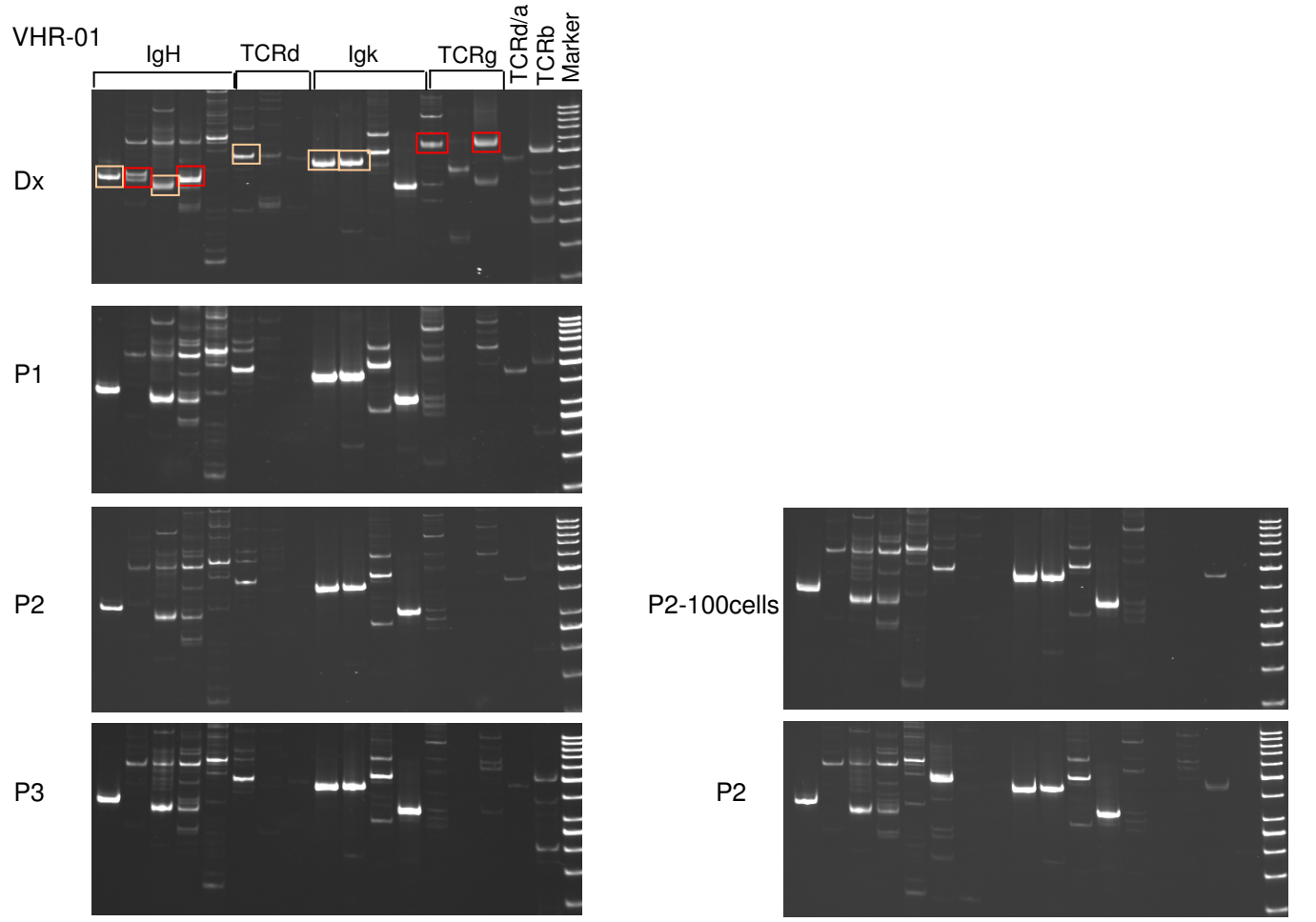

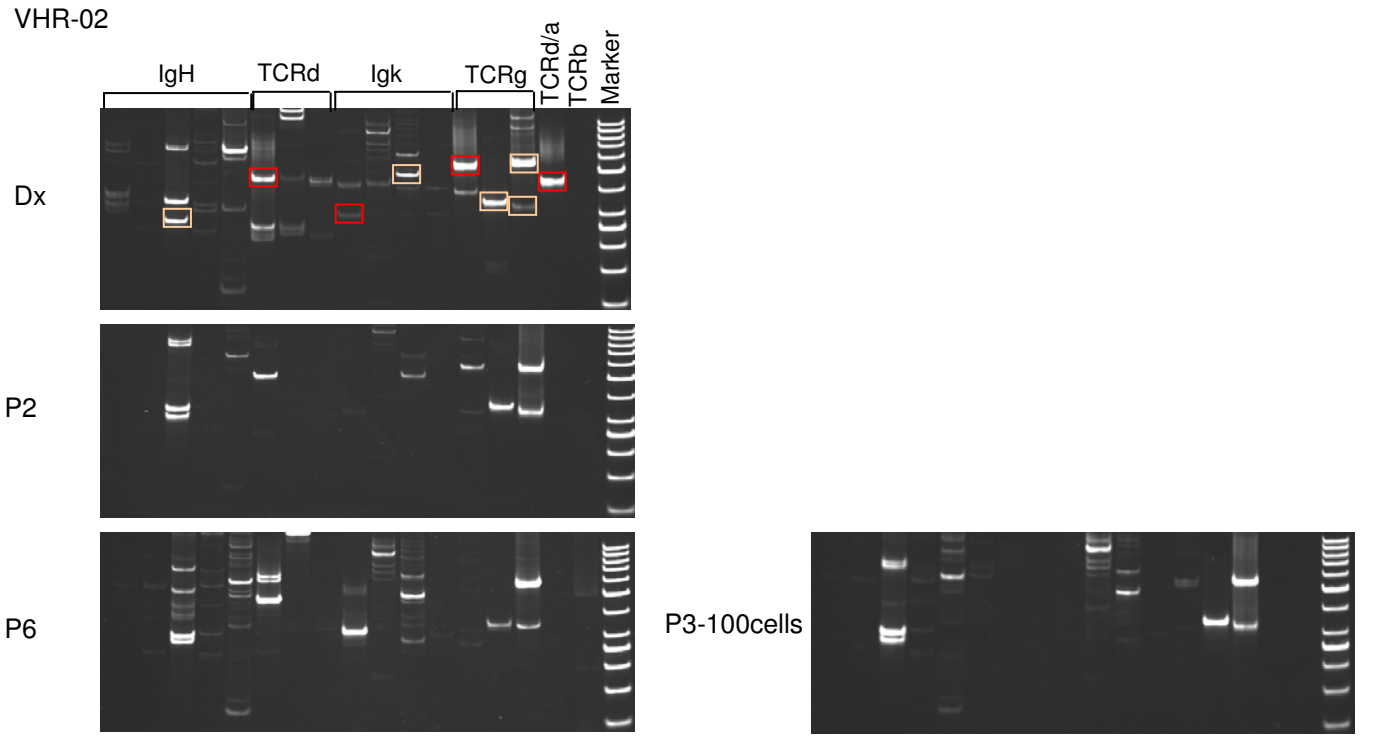

VHR-03

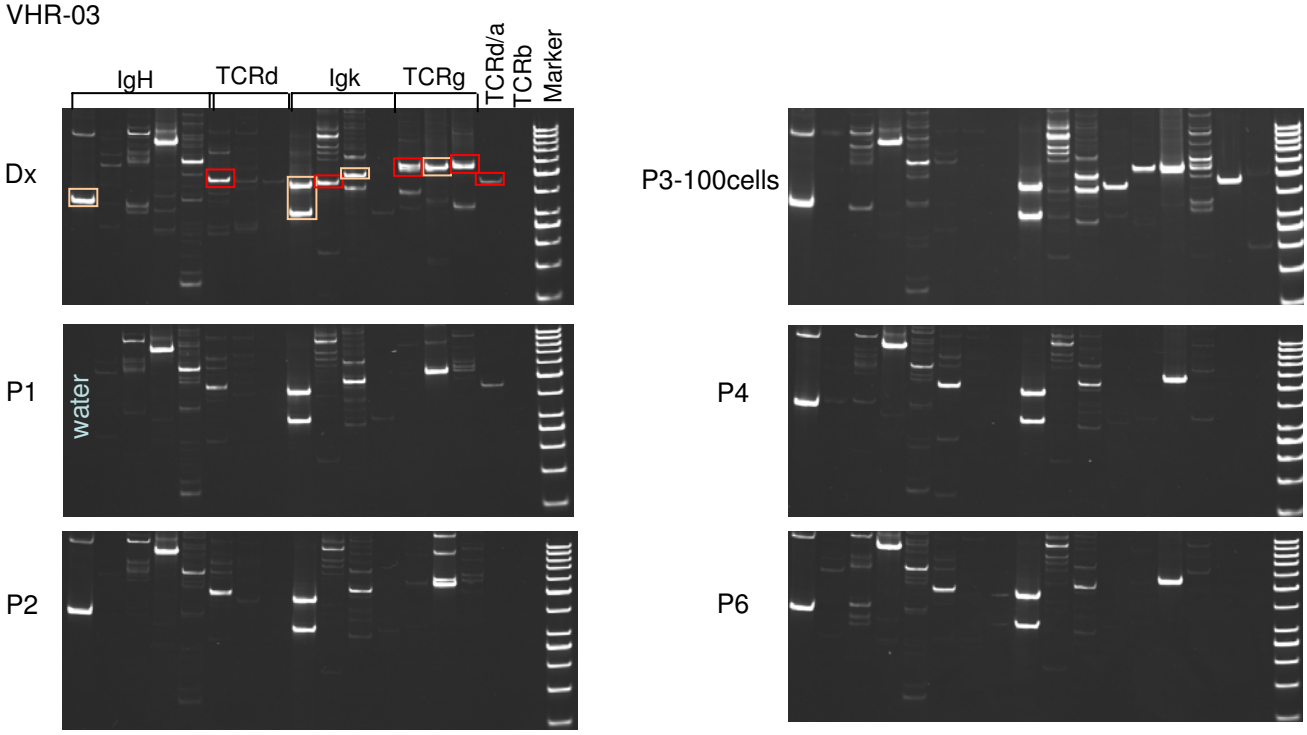
IgH
TCRd
Igk
TCRg
TCRd/a
TCRb
Marker
Dx
P1
water
P2
P3-100cells
P4
P6

VHR-04

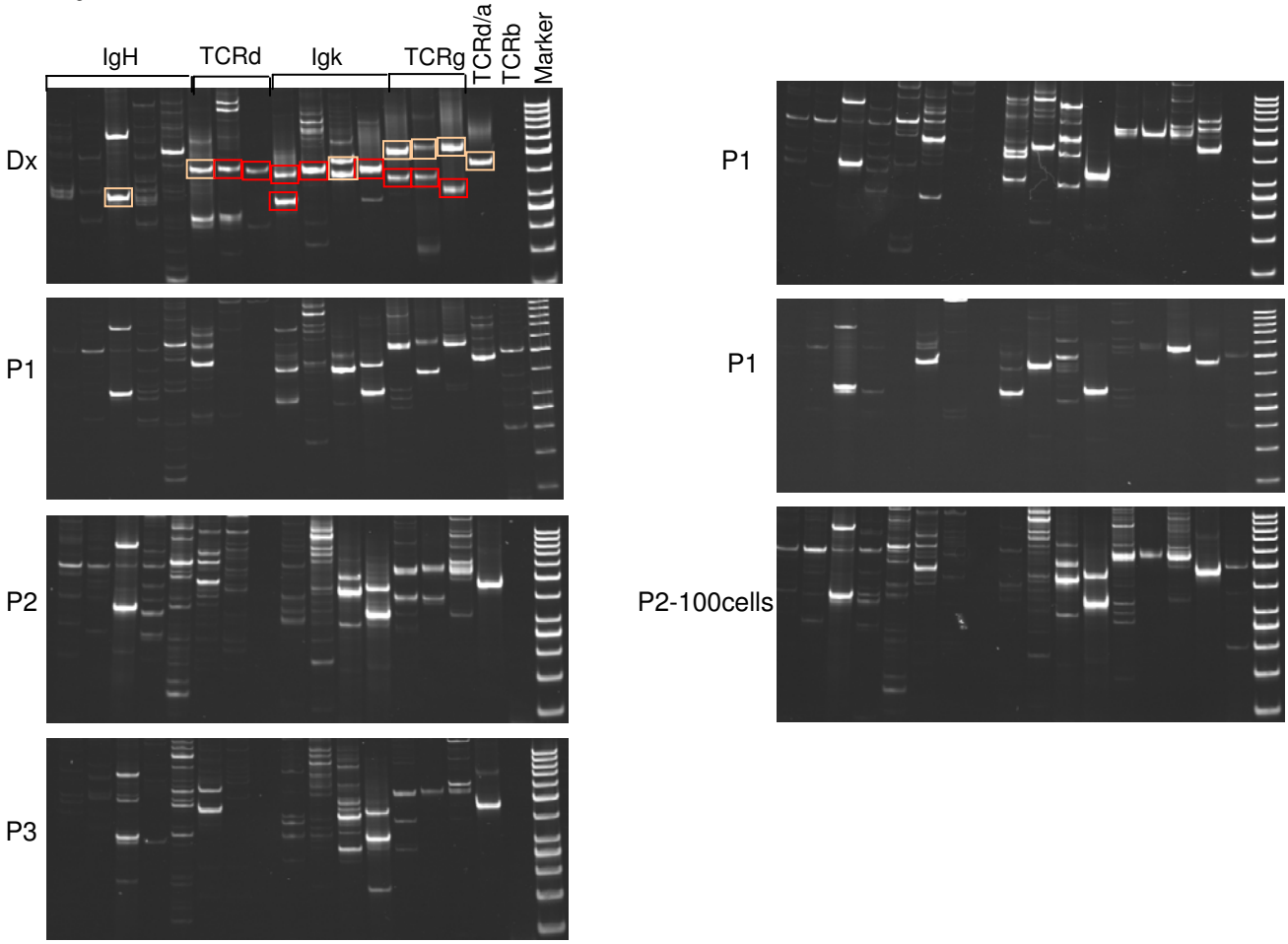
IgH
TCRd
Igk
TCRg
TCRd/a
TCRb
Marker
Dx
P1
P2
P3
P1
P1
P2-100cells

VHR-15

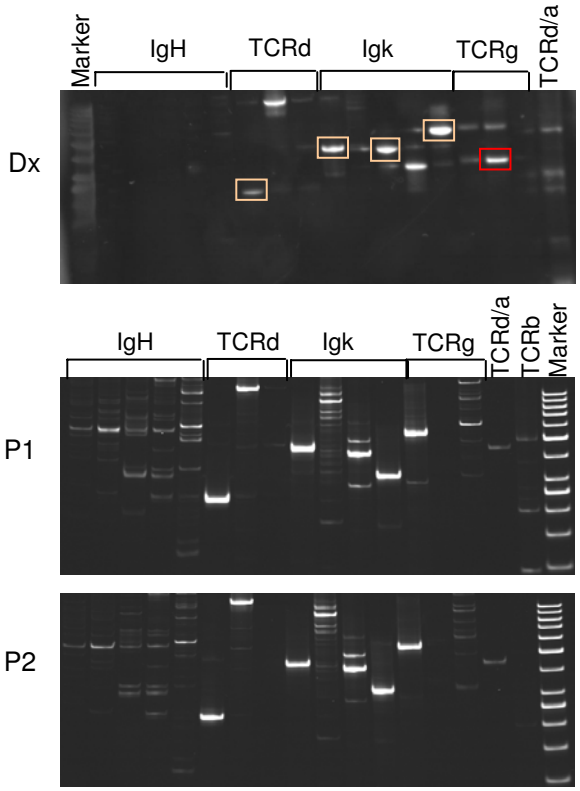
Marker
IgH
TCRd
Igk
TCRg
TCRd/a
Dx
IgH
TCRd
Igk
TCRg
TCRd/a
TCRb
Marker
P1
P2

SR-04

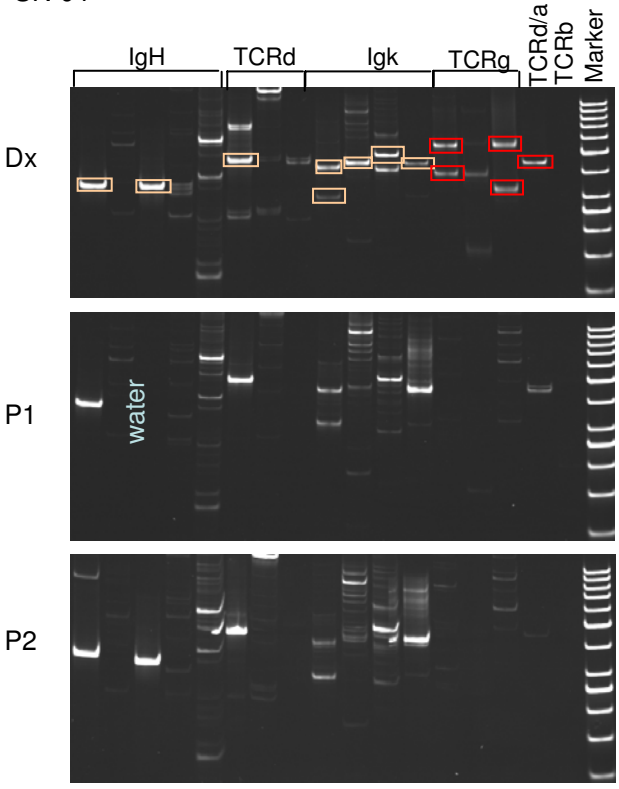
IgH
TCRd
Igk
TCRg
TCRd/a
TCRb
Marker
Dx
P1
water
P2

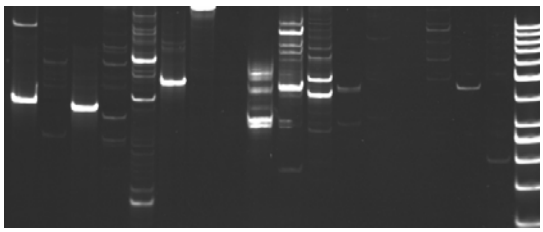
P1

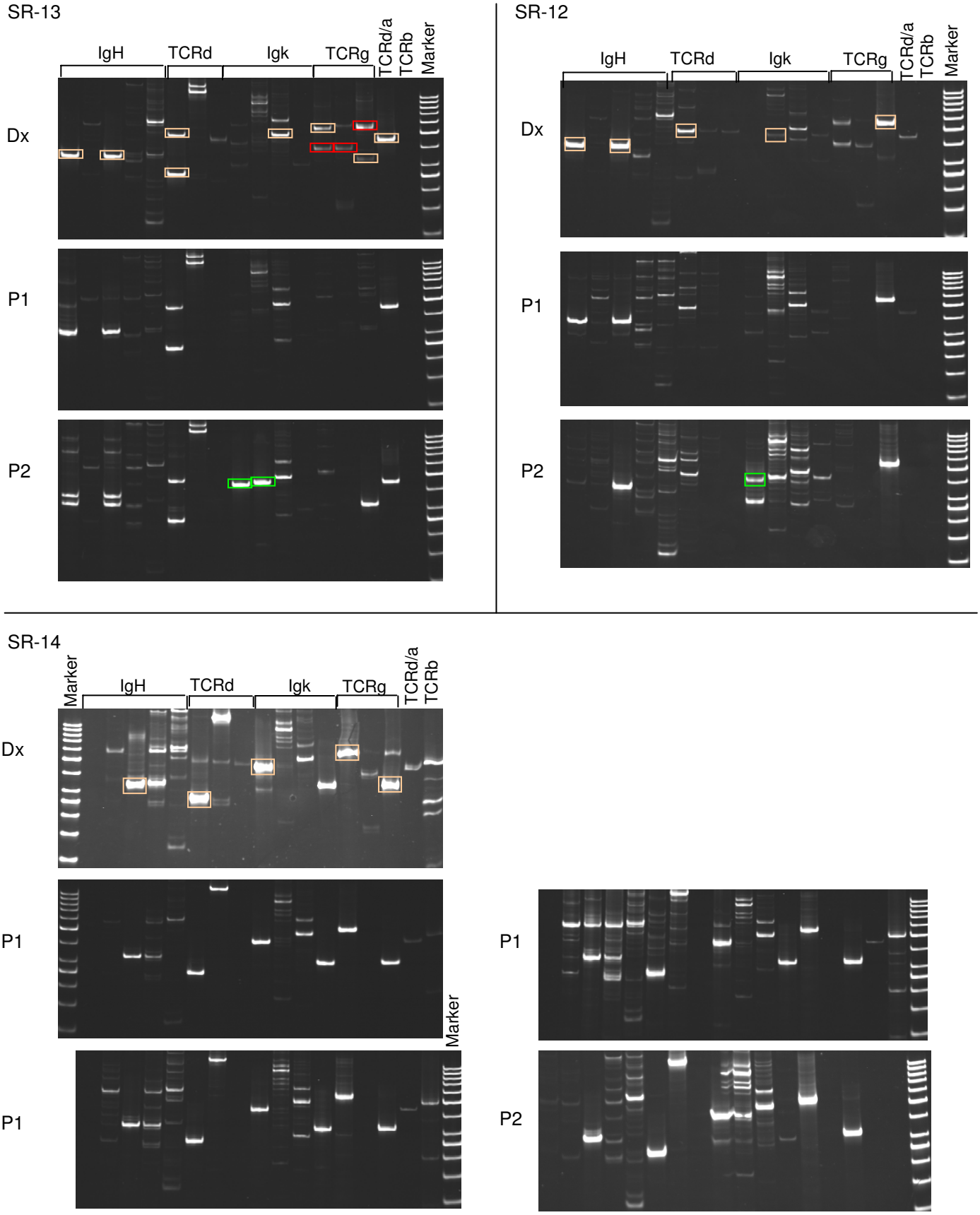

Supplemental Figure S1: Analysis of Ig/TCR rearrangements reflects the evolution of the clonal compartment in xenografts. The Ig/TCR rearrangement pattern of diagnostic samples and matched xenografts was determined in 5 VHR- and in 5 SR-ALL samples by PCR using standardized sets of primers that are validated for MRD analysis. Representative gels for all analyzed VHR-ALL and 4 SR-ALL samples (SR-09 in Figure 6) are provided. All positive bands of the correct size were sequenced once for verification. Stable rearrangements are framed with an orange line, while bands framed in red represent markers that disappeared and green frames represent bands gained in xenografts.

Leukemia & Lymphoma, 2011; Early Online, 1–3

informa
healthcare

LETTER TO THE EDITOR

Alternative technique for intrafemoral injection and bone marrow sampling in mouse transplant models

MAIKE SCHMITZ, JEAN-PIERRE BOURQUIN, & BEAT C. BORNHAUSER

Department of Oncology, University Children's Hospital Zurich, Zurich, Switzerland

(Received 29 January 2011; revised 31 March 2011; accepted 7 April 2011)

Bone marrow punctures are often required when modeling hematologic malignancies in mice. Orthotopic intrabone injection resulted in superior engraftment of human hematopoietic stem cells [1] or of human leukemia cells [2,3] in immunodeficient mice. Similarly, between 10 and 100 cells from patients with acute lymphoblastic leukemia were sufficient to reconstitute leukemia in immunodeficient NOD/scidIL2Rγnull (NSG) mice after intrafemoral injections [4,5]. Current protocols for bone marrow procedures in mice involve a two-step process that requires perforation of the cortical bone with a first needle and retrieval of the orifice subsequently with a needle with a smaller gauge for injection or aspiration of cells. As an alternative, we have used a small needle with a stylet in analogy to bone marrow aspiration needles that are used in the clinic. Here we show that a pediatric spinal tap needle (also called atraucan needle) can be used efficiently and conveniently for bone marrow transplant and sampling procedures in mice. This one-step injection procedure [Figure 1(A)] resulted in highly reproducible engraftment with primary human acute lymphocytic leukemia (ALL) cells (Table I). Forty-four out of 45 xenograft ALL samples repopulated secondary recipients. This technique was used to establish an *in vivo* model of highly resistant leukemia [6]. Furthermore, in serial dilution experiments, 100 ALL cells were sufficient for engraftment in four different cases of ALL [5], demonstrating that the injections can be performed with minimal losses due to dead volume with this needle. Bone marrow aspiration through the atraucan needle did not damage the bone marrow cells, as shown with 7-aminoactinomycin D (7-AAD) stainings for cell viability by flow cytometry [Figure 1(B)]. A homogeneous, viable population of CD19 and CD10 double-positive human leukemia cells was detected in the bone marrow at 8 weeks after transplant. The analysis of engraftment in the peripheral blood showed a lower, although detectable, presence of human leukemia cells. By aspirating the femur contralateral to the injection site we collected up to 15 000 lymphocytes in 10 μL bone marrow aspirate without requirement for subsequent erythrolysis. By tail vein bleeding, we collected 50 μL of blood that was enough to detect at least the same number of lymphocytes.

Taken together, the use of the pediatric atraucan needle very effectively eliminates the need to perform two punctures of the cortical bone in order to inject into or sample cells from the bone marrow cavity. We are convinced that this simple modification will be of great interest to many investigators as xenograft models with human normal or malignant hematopoietic cells are increasingly applied.

Acknowledgements

We thank J. Vormoor and Ch. LeViseur for initial help with intrafemoral transplants. G. Cario, M. Stanulla, and M. Schrappe from the ALL-Berlin–Frankfurt–Münster (BFM) study group provided the patient samples. These originated from patients

Correspondence: Beat C. Bornhauser, Department of Oncology, University Children's Hospital Zurich, 8008 Zurich, Switzerland. Tel: +41-44-634-88-17. Fax: +41-44-634-88-59. E-mail: beat.bornhauser@kispi.uzh.ch

ISSN 1042-8194 print/ISSN 1029-2403 online © 2011 Informa UK, Ltd.
DOI: 10.3109/10428194.2011.580023

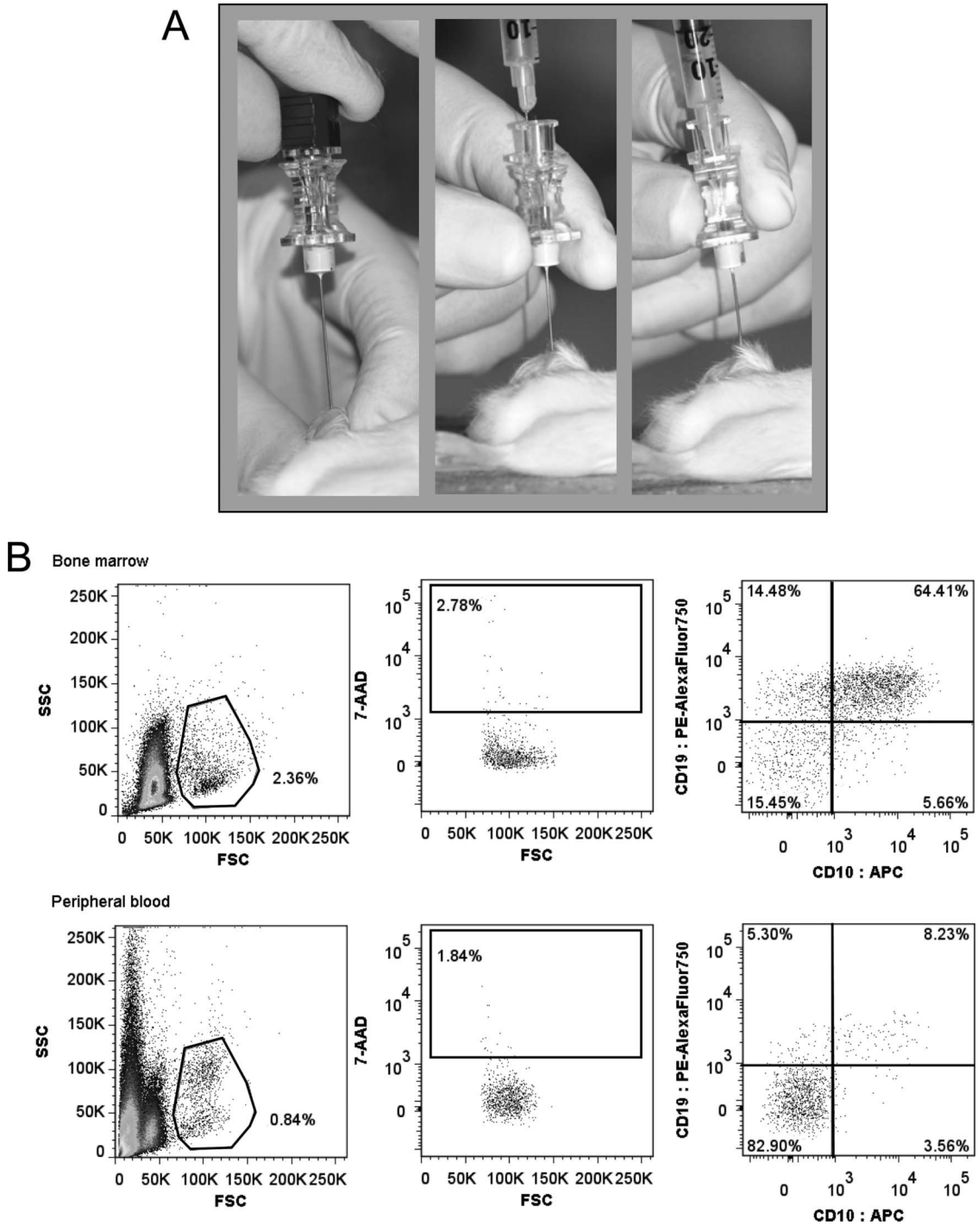

Figure 1. Bone marrow procedures were performed on NSG mice under inhalation anesthesia and analgesia with subcutaneous injections of 0.1 mg/kg temgesic. (A) After removal of the fur, the knee was held in the folded position, with the femur perpendicular to the table surface. The femur head was punctured with a pediatric atraucan 26G needle containing a stylet (B. Braun Medical, Switzerland; left panel). For intrafemoral injections, the stylet of the atraucan needle was removed and the 29G needle of an insulin syringe (BD Micro-fine; BD Biosciences, USA) was inserted directly in the lumen of the atraucan needle (middle and right panels). The use of a needle instead of the direct connection of a syringe to the atraucan needle minimizes the dead volume after injection. Cells, resuspended in a total volume of 30 μL phosphate buffered saline (PBS), were then injected, and the atraucan needle was removed together with the insulin syringe. For bone marrow aspirates, the needle of an insulin syringe containing 30 μL of PBS was inserted into the lumen of the atraucan needle, and bone marrow was sampled by drawing the lever up and down several times. (B) Flow cytometry analysis of bone marrow aspirations and tail vein bleedings of transplanted animals reveals efficient sampling. Bone marrow aspirates (upper panel) and peripheral blood samples from tail vein bleedings (lower panel) were directly used for flow cytometry without erythrolysis. Representative plots of engraftment at 8 weeks after transplant are shown. Cell viability and engraftment of human cells was analyzed by flow cytometry with the following probes and antibodies: 7-AAD for cell viability, PE-Alexa750-labeled anti-human CD19, and APC-labeled anti-human CD10. Gates were set using appropriate control stainings. Numbers refer to respective percentages of cells in the gates. The mean percentage of dead cells was 2.70 $\pm$ 0.54% for bone marrow aspirates and 2.74 $\pm$ 1.32% for tail vein bleedings. Data analysis was performed with FlowJo V7.6 (TreeStar).

Table I. Efficiency of intrafemoral transplant* using the atraucan spinal tap needle.

Patient ID	Patient characteristic	No. of engrafted mice/transplanted mice
VHR-03	Precursor B ALL	6/6
HR-03	Precursor B ALL	4/5
SR-02	Precursor B ALL	5/5
VHR-02	Precursor B ALL	15/15
SR-04	Precursor B ALL	2/2
VHR-06	Precursor B ALL	2/2
VHR-07	Precursor B ALL	2/2
SR13	Precursor B ALL	2/2
SR-05	Precursor B ALL	2/2
VHR-10	Precursor B ALL	2/2
SR-17	Precursor B ALL	2/2

*Primary transplants were done intrafemorally using the herein described method. Engraftment efficiency was 98% with samples that were known to engraft NOD/scidIL2Rγnull (NSG) mice.
ALL, acute lymphocytic leukemia; VHR, very high risk; HR, high risk; SR, standard risk, as described [6].

enrolled in the ALL-BFM 2000 study who had given informed consent in accordance with the Declaration of Helsinki. Approval was obtained from the Institutional Review Board (IRB) of the Medical School Hannover and the local IRB for all participating centers in the trial ALL-BFM 2000. This study was supported by the Swiss National Science foundation (grant no 310030-118392), by the Novartis Foundation for biomedical research, and by the Vontobel-Stiftung.

Potential conflict of interest: Disclosure forms provided by the authors are available with the full text of this article at www.informahealthcare.com/lal.

References

1. Mazurier F, Doedens M, Gan OI, et al. Rapid myeloerythroid repopulation after intrafemoral transplantation of NOD-SCID mice reveals a new class of human stem cells. Nat Med 2003;9: 959–963.
2. le Viseur C, Hotfilder M, Bomken S, et al. In childhood acute lymphoblastic leukemia, blasts at different stages of immunophenotypic maturation have stem cell properties. Cancer Cell 2008;14:47–58.
3. McKenzie JL, Gan OI, Doedens M, et al. Human short-term repopulating stem cells are efficiently detected following intrafemoral transplantation into NOD/SCID recipients depleted of CD122+ cells. Blood 2005;106:1259–1261.
4. Rehe K, Wilson K, McNeill H, et al. Disease propagating blasts in standard and high risk acute lymphoblastic leukemia are frequent and of diverse immunophenotype. Blood 2009; 114(Suppl. 1): Abstract 1421.
5. Schmitz M, Mirkowska P, Breithaupt P, et al. Leukemia-initiating cells are frequent in very high risk childhood acute lymphoblastic leukemia and give rise to relatively Stable phenotypes in immunodeficient mice. Blood 2009;114(Suppl. 1): Abstract 86.
6. Bonapace L, Bornhauser B, Schmitz M, et al. Induction of autophagy-dependent necroptosis is required to overcome glucocorticoid resistance in acute lymphoblastic leukemia. J Clin Invest 2010;120:1310–1323.

Induction of autophagy-dependent necroptosis is required for childhood acute lymphoblastic leukemia cells to overcome glucocorticoid resistance

Laura Bonapace,[1] Beat C. Bornhauser,[1] Maike Schmitz,[1] Gunnar Cario,[2] Urs Ziegler,[3] Felix K. Niggli,[1] Beat W. Schäfer,[1] Martin Schrappe,[2] Martin Stanulla,[2] and Jean-Pierre Bourquin[1]

[1]Department of Oncology, University Children's Hospital, University of Zurich, Switzerland. [2]Department of Pediatrics, University Hospital Schleswig Holstein, Kiel, Germany. [3]Center for Microscopy and Image Analysis, University of Zurich.

In vivo resistance to first-line chemotherapy, including to glucocorticoids, is a strong predictor of poor outcome in children with acute lymphoblastic leukemia (ALL). Modulation of cell death regulators represents an attractive strategy for subverting such drug resistance. Here we report complete resensitization of multidrug-resistant childhood ALL cells to glucocorticoids and other cytotoxic agents with subcytotoxic concentrations of obatoclax, a putative antagonist of BCL-2 family members. The reversal of glucocorticoid resistance occurred through rapid activation of autophagy-dependent necroptosis, which bypassed the block in mitochondrial apoptosis. This effect was associated with dissociation of the autophagy inducer beclin-1 from the antiapoptotic BCL-2 family member myeloid cell leukemia sequence 1 (MCL-1) and with a marked decrease in mammalian target of rapamycin (mTOR) activity. Consistent with a protective role for mTOR in glucocorticoid resistance in childhood ALL, combination of rapamycin with the glucocorticoid dexamethasone triggered autophagy-dependent cell death, with characteristic features of necroptosis. Execution of cell death, but not induction of autophagy, was strictly dependent on expression of receptor-interacting protein (RIP-1) kinase and cylindromatosis (turban tumor syndrome) (CYLD), two key regulators of necroptosis. Accordingly, both inhibition of RIP-1 and interference with CYLD restored glucocorticoid resistance completely. Together with evidence for a chemosensitizing activity of obatoclax in vivo, our data provide a compelling rationale for clinical translation of this pharmacological approach into treatments for patients with refractory ALL.

Introduction

Resistance to the initial phase of chemotherapy, in particular poor response to glucocorticoids (GCs), is a strong predictor of adverse outcome for childhood acute lymphoblastic leukemia (ALL) (1, 2). During the last decade, the cooperative Berlin-Frankfurt-Muenster (BFM) study group has validated an effective risk stratification approach, which is based on the assessment of the in vivo response to chemotherapy by leukemia-specific quantitative PCR. A group of patients at very high risk for relapse (VHR-ALL) can be identified based on persistence of minimal residual disease (MRD) (3). Because this is likely to reflect de novo resistance to multiple conventional antileukemic agents, combination treatment with new agents that modulate regulators of cell death represents an attractive approach to improve treatment response.

In GC-resistant ALL, the mechanisms underlying defective induction of mitochondrial apoptosis are still not understood. Increased expression of antiapoptotic myeloid cell leukemia sequence 1 (MCL-1) was a predominant feature of the gene expression signature of GC resistance (4). A bioinformatic screen of drug-associated signatures identified rapamycin as a sensitizer to GC drugs in GC-resistant ALL. The GC-sensitizing effect of rapamycin was attributed to a decrease in MCL-1 levels, which was proposed to decrease the threshold to apoptotic stimuli by GC drugs (5).

Based on these considerations, we sought to evaluate the potential of the small molecule obatoclax (GX15-070) for combination therapy in refractory childhood ALL. This agent was proposed to act as a BCL-2 family antagonist and to disrupt the interaction between MCL-1 and its proapoptotic counterparts at cytotoxic concentrations (6, 7). Obatoclax was shown to trigger apoptosis at concentrations that resulted in disruption of Bak from MCL-1 and cytochrome *c* release. However, obatoclax was also cytotoxic in cells that are deficient for the apoptosis effectors BAX and BAK, and lower concentrations of compound were sufficient to inhibit clonogenic growth of AML cells, suggesting the existence of additional target mechanisms (8). A recommended phase II dose has been established for adult patients with hematologic malignancies with an acceptable toxicity profile (9, 10), which constitutes the basis for further evaluation of obatoclax in pediatric trials.

In the context of defective apoptosis, an alternative cell death pathway has been identified that is dependent on macroautophagy (11, 12), a major form of autophagy, in which parts of the cytoplasm and intracellular organelles are sequestered within characteristic double-membraned or multi-membraned autophagic vacuoles (hereafter referred to as autophagy) (13). Autophagy is usually triggered to respond to increased metabolic requirements at times of cellular stress. Selected antiapoptotic BCL-2

Authorship note: Laura Bonapace and Beat C. Bornhauser contributed equally to this work.

Conflict of interest: The authors have declared that no conflict of interest exists.

Citation for this article: *J Clin Invest.* 2010;120(4):1310–1323. doi:10.1172/JCI39987.

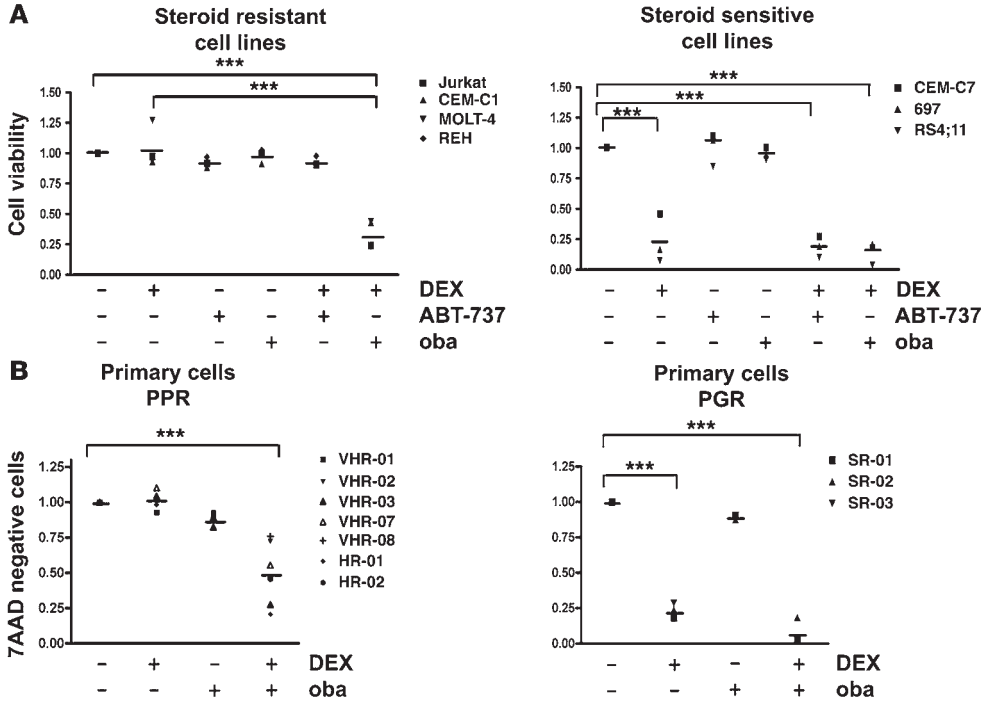

Figure 1

Obatoclax resensitizes GC-resistant ALL cells to dexamethasone. Combination experiments were performed with subcytotoxic concentrations (10% IC_{50}) of obatoclax (oba) or ABT-737 and 1 μM dexamethasone (DEX), and values were normalized to cells treated with vehicle control. (**A**) ALL cell lines were treated for 72 hours as indicated. Cell viability was determined by the MTT assay. (**B**) Primary ALL cells from 7 PPR patients with VHR-ALL and 3 prednisone-good-responder (PGR) patients were treated as indicated for 72 hours. Cell viability was assessed by flow cytometry using 7AAD. ***$P < 0.05$.

family members can engage in cross-talk between the apoptotic and autophagic pathways, as they were show to associate with the autophagy regulator beclin-1 (11, 14, 15). When caspase-dependent apoptosis was blocked, a cell death mechanism that required autophagy was mediated via the receptor-interacting protein 1 (RIP-1) (12). RIP-1 is a central kinase that is associated with death receptor–induced signalling complexes to modulate the switch between survival and death under stress conditions (16). Under defective apoptotic conditions, RIP-1 kinase activity was shown to mediate an alternative cell death pathway that may represent a form of programmed necrosis, also called necroptosis (17, 18). Kinase activity of RIP-1 was shown to be dispensable for induction of cell survival signalling via NF-kB activation or death receptor–mediated apoptosis (17, 19).

Here we show that a subcytotoxic concentration of obatoclax effectively restored the response to dexamethasone in GC-resistant ALL by triggering a nonapoptotic cell death pathway. Subcytotoxic concentrations of obatoclax induced disruption of beclin-1 from MCL-1 and the combination of dexamethasone with obatoclax was associated with inhibition of mammalian target of rapamycin (mTOR) activity, providing a possible mechanism for autophagy induction. Obatoclax also conferred clinically relevant broad chemosensitization in multidrug-resistant primary cells from VHR-ALL patients. We provide genetic and pharmacologic evidence to show that sensitization to dexamethasone occurs via autophagy-dependent necroptotic cell death, while sensitization to other cytotoxic agents was dependent on apoptosis. In a xenograft model, using GC-resistant cells from refractory ALL patients, combination treatment with dexamethasone and obatoclax reduced leukemia progression significantly. Collectively, our data provide a strong rationale for a rapid clinical translation of this approach.

Results

Obatoclax resensitizes GC-resistant ALL to dexamethasone. Because MCL-1 has been proposed to act as a central modulator of steroid resistance in ALL (4, 5), we first compared the effects of 2 small molecules with different selectivity toward MCL-1, ABT-737, and obatoclax in GC-resistant ALL cell lines. ABT-737 is a small molecule BH3 mimetic with selectivity for BCL-2 and BCL-X_L (20). Resistance to ABT-737 has been attributed to its inability to target MCL-1 (21–23). While both compounds displayed strong cytotoxicity across a panel of ALL cell lines (Supplemental Table 1; supplemental material available online with this article; doi:10.1172/JCI39987DS1), subcytotoxic doses of obatoclax but not ABT-737 resensitized GC-resistant cell lines to dexamethasone (Figure 1A and Supplemental Figure 1). We confirmed single-agent activity for obatoclax in VHR-ALL cells (Supplemental Table 2). Low-dose obatoclax restored sensitivity to dexamethasone in cells from all 7 poor-prednisone-responder (PPR) VHR-ALL patients tested (Figure 1B and Supplemental Figure 2). In contrast, no effect on steroid sensitivity using low doses of ABT-737 or obatoclax was evident in steroid-sensitive cells (Figure 1A). Unexpectedly, the pan-caspase inhibitor zVAD.fmk did not interfere with the steroid-sensitizing effect of obatoclax in GC-resistant cells (Figure 2A), whereas zVAD.fmk blocked the cytotoxic effect of dexamethasone with or without obatoclax in GC-sensi-

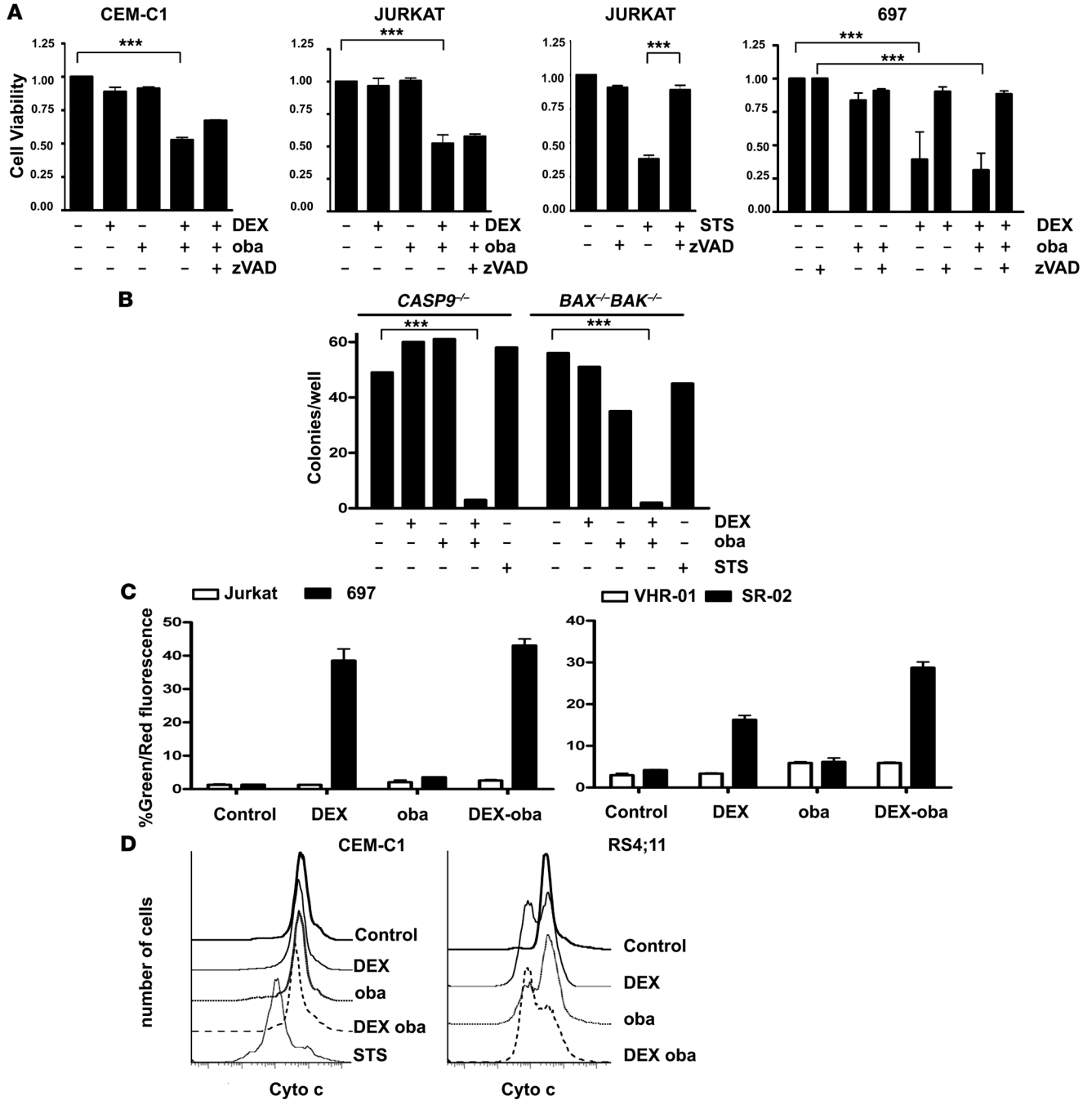

Figure 2

Obatoclax resensitizes GC-resistant ALL cells to dexamethasone without activation of mitochondrial apoptosis. (**A**) ALL cells were treated as indicated for 48 hours, for controls STS or zVAD.fmk (80 nM) was used, and cell viability was assessed with the MTT assay. 697 cells served as GC-sensitive control. (**B**) Jurkat *CASP9*$^{-/-}$ and *BAX*$^{-/-}$*BAK*$^{-/-}$ cells were treated for 72 hours as indicated, and clonogenic survival was assessed after incubation in methylcellulose for 7 days. (**C**) Percentages of cells with JC-1 monomers, corresponding to a loss of the mitochondrial potential, are shown for GC-resistant CEM-C1 and GC-sensitive CEM-C7 cells and in samples from PGR and PPR patients after treatment as indicated for 16 hours. (**D**) Cytochrome *c* release was induced in steroid-sensitive RS4;11 cells but not in the resistant CEM-C1 cell line upon treatment with dexamethasone or dexamethasone and obatoclax. STS was used as positive control. Cytochrome *c* release was detected by flow cytometry. ***$P < 0.05$.

tive cells and in control experiments when cell death was induced by staurosporine (STS). Using clonogenic assays, we confirmed that obatoclax was equally effective in ALL cells that are devoid of caspase-9 or BAX and BAK, when compared with parental cell lines (Figure 2B and Supplemental Figure 3). Furthermore, obatoclax-mediated GC sensitization resulted in neither the restoration of mitochondrial membrane depolarization (Figure 2C) nor an increase in cytochrome *c* release when compared with the effect

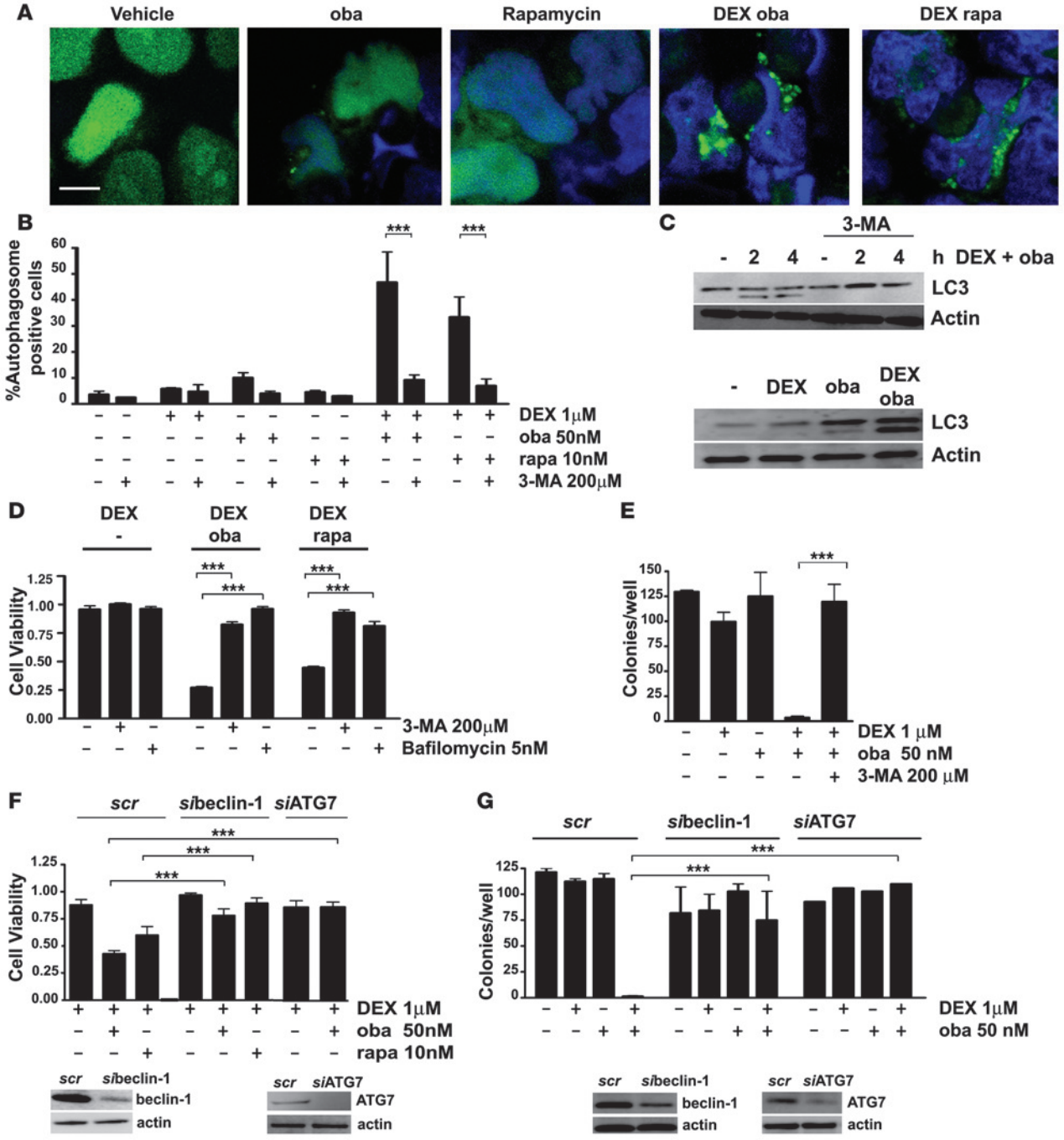

Figure 3

Obatoclax induces autophagy in GC-resistant ALL cells. (**A**) After transient transfection with GFP-LC3, Jurkat cells were treated for 4 hours as indicated. The characteristic punctuate staining pattern indicative of autophagosome formation was detected by confocal microscopy in cells treated with dexamethasone and obatoclax or rapamycin (rapa). Scale bar: 10 μm. (**B**) Quantitation of autophagosome-positive cells. The data represent mean ± SD of 2 independent experiments, counting 200 cells each. (**C**) Detection of endogenous LC3-II by Western blot analysis. Jurkat cells were treated with obatoclax and dexamethasone for the indicated time points in the presence or absence of 3-MA and after 24 hours of treatment as indicated. (**D**) Inhibition of autophagy by 3-MA or bafilomycin impaired sensitization to dexamethasone by 10 nM rapamycin or obatoclax (10% IC_{50}). Cell viability was assessed by MTT. (**E**) Treatment with obatoclax and dexamethasone inhibited clonogenic survival of Jurkat cells. 3-MA rescued GC-resistant cells from cell death induced by combination treatment. Cells were treated for 72 hours with compounds, and clonogenic survival in methylcellulose was assessed after washing and incubation for 7 days. (**F**) Downregulation of beclin-1 or ATG7 using siRNA (si) impaired the resensitization of Jurkat cells to dexamethasone by obatoclax or rapamycin compared with scrambled (scr) controls. Cell viability was assessed by MTT. Efficiency of downregulation at 48 hours was analyzed by Western analysis. (**G**) Downregulation of beclin-1 and ATG7 in Jurkat cells protected cells from obatoclax- and dexamethasone-induced cell death in the clonogenic assay. ***$P < 0.05$.

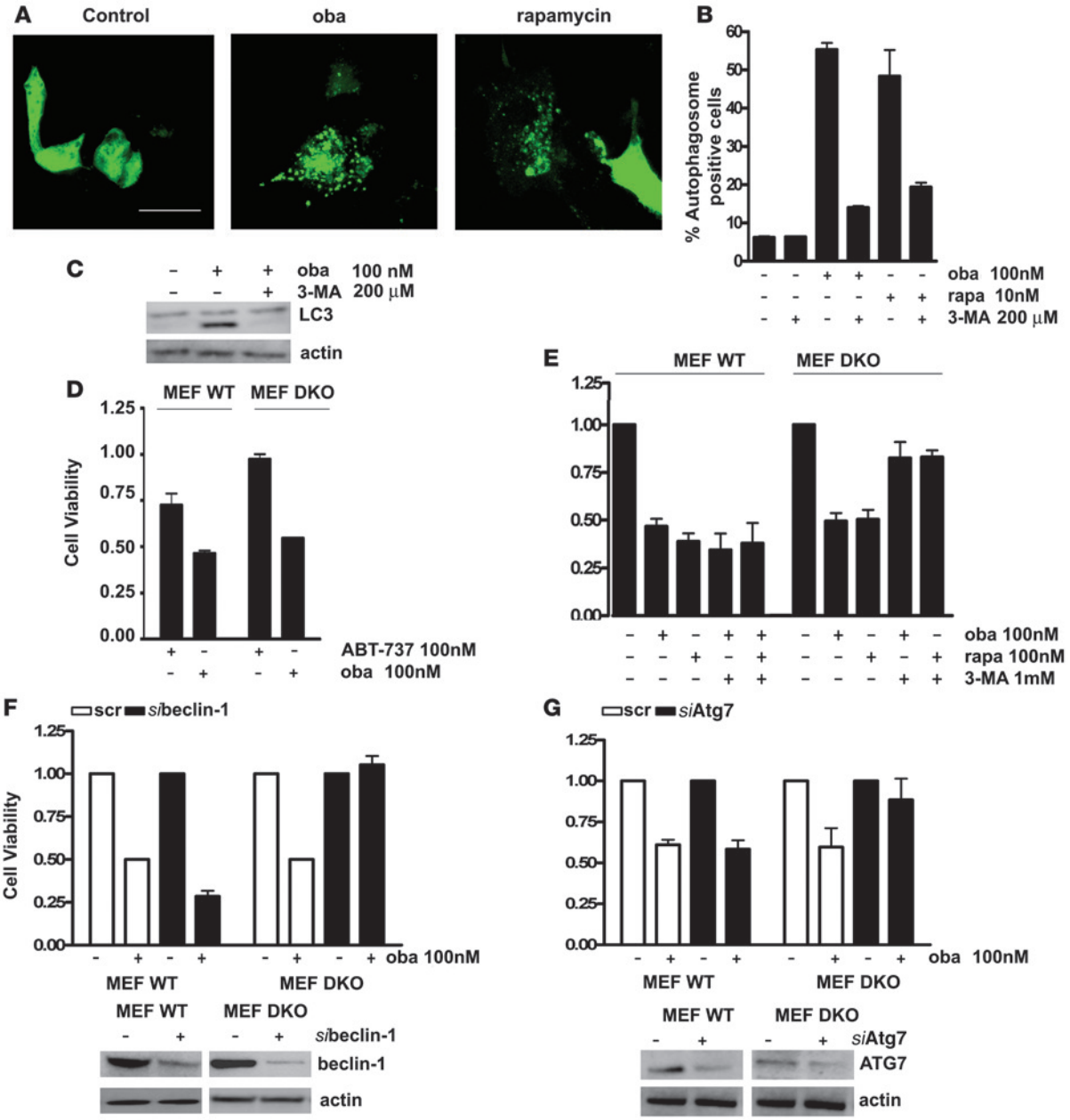

Figure 4

Obatoclax and rapamycin induce autophagic cell death in *Bax*$^{-/-}$*Bak*$^{-/-}$ MEFs. (**A**) *Bax*$^{-/-}$*Bak*$^{-/-}$ MEFs transiently expressing the autophagy marker GFP-LC3 were treated with vehicle, obatoclax (100 nM), or rapamycin (10 nM) for 4 hours. Autophagosome formation was monitored by confocal microscopy. Scale bar: 20 μm. (**B**) Quantitation of autophagosome-positive cells. The data represent mean ± SD of 2 independent experiments, counting 200 cells each. (**C**) Treatment of *Bax*$^{-/-}$*Bak*$^{-/-}$ MEFs with obatoclax induced generation of endogenous LC3-II as detected by Western analysis, an effect which was blocked by 3-MA treatment. (**D**) WT or *Bax*$^{-/-}$*Bak*$^{-/-}$ (DKO) MEFs were incubated for 48 hours with obatoclax or ABT-737, and cell viability assessed by the MTT assay. (**E**) Inhibition of autophagy by 3-MA rescued *Bax*$^{-/-}$*Bak*$^{-/-}$ MEFs but not WT MEFs from cell death induced by 48 hour exposure to obatoclax or rapamycin. (**F**) Downregulation of beclin-1 rescued *Bax*$^{-/-}$*Bak*$^{-/-}$ MEFs but not WT MEFs from cell death induced by obatoclax as evaluated by the MTT assay. Efficiency of downregulation was determined by Western blot analysis. (**G**) Downregulation of ATG7 rendered *Bax*$^{-/-}$*Bak*$^{-/-}$ MEFs but not WT MEFs resistant to obatoclax treatment. Efficiency of downregulation was assessed by Western blotting.

of dexamethasone in GC-sensitive cells (Figure 2D). In line with these findings, caspase-9 was not activated and caspase-3 was only marginally activated in steroid-resistant cells treated with the combination of obatoclax and dexamethasone (Supplemental Figure 4). Collectively, our results indicate that the combination of obatoclax and dexamethasone triggers a cell death mechanism that is independent of the apoptotic function of caspases in steroid-resistant leukemia.

Induction of autophagy is essential for steroid sensitization in ALL cells. Because an autophagy-dependent cell death pathway has been

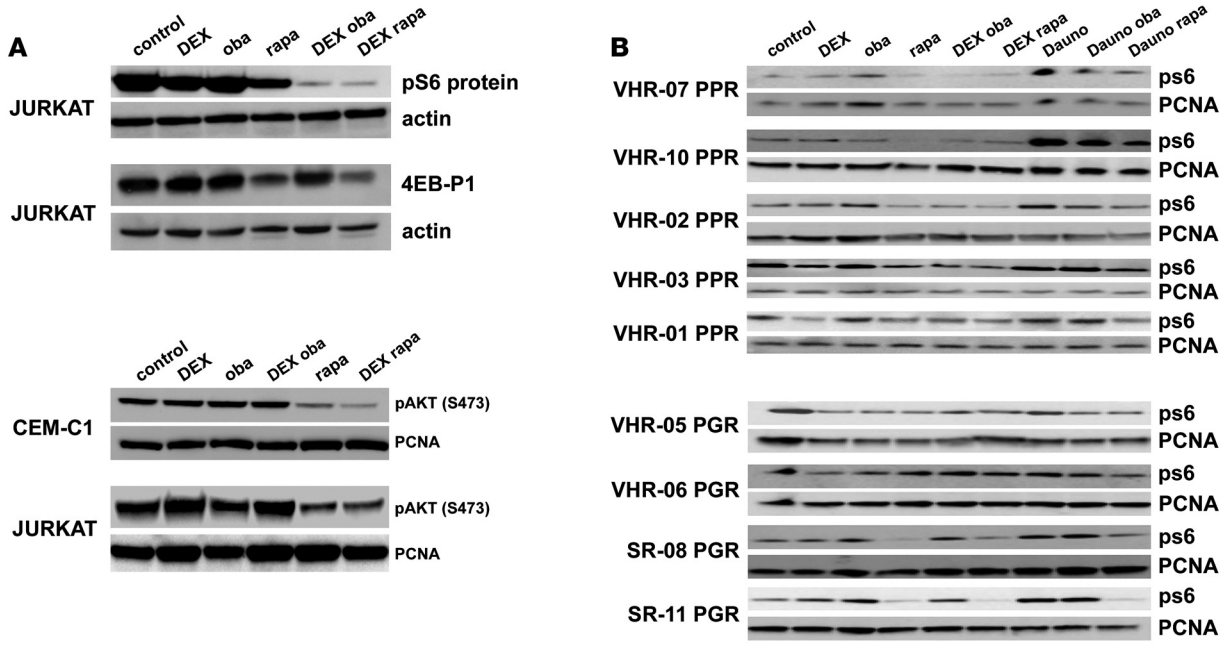

Figure 5

Combination treatment with dexamethasone and obatoclax leads to inhibition of mTOR. (**A**) Jurkat cells were treated for 6 hours as indicated, and phosphorylation of the mTOR targets, S6 protein and 4EB-P1, was assessed. Combination of dexamethasone with either obatoclax or rapamycin resulted in inhibition of mTOR activity (top panel). Rapamycin alone and in combination with dexamethasone, but not obatoclax alone or with dexamethasone, decreased the phosphorylation of AKT at Ser473 in Jurkat and CEM-C1 cells (bottom panel). (**B**) In primary cells from PPR patients with VHR-ALL, treatment with dexamethasone and obatoclax or rapamycin resulted in a decrease of S6 protein phosphorylation. In contrast, in cells from prednisone-good-responder patients, S6 protein was not dephosphorylated after combination treatment.

described in cell line models in which apoptosis is prevented (11, 24), we evaluated next whether autophagy was required for GC sensitization by obatoclax. Indeed, autophagosome formation was evident in GC-resistant cells after 4 hours of exposure to low-dose obatoclax in combination with dexamethasone, which correlated with generation of endogenous LC3-II (Figure 3, A–C). Because rapamycin is known to be an inducer of autophagy (25), we asked whether the GC-sensitizing effect reported recently for rapamycin (5) could also be dependent on autophagy. As we expected, steroid sensitization by rapamycin was associated with hyperautophagic features (Figure 3, A and B). Obatoclax or rapamycin alone only marginally induced autophagosome formation and generation of LC3-II (Figure 3, A–C). Preincubation with the autophagy inhibitor 3-methyladenine (3-MA) abolished autophagosome formation, generation of LC3-II, and GC resensitization by obatoclax and rapamycin (Figure 3, B–D). Both bafilomycin, a late-stage inhibitor of autophagolysosome formation (25), and downregulation of the essential autophagy genes beclin-1 (*BECN1*) and ATG-7 (*ATG7*) by RNA interference blocked GC-resensitization by obatoclax and rapamycin (Figure 3, D–G). These results were confirmed in an independent cell line (Supplemental Figure 5). Clonogenic assays demonstrate that both addition of 3-MA and downregulation of beclin-1 prevented the cytotoxic effect of low-dose obatoclax combined with dexamethasone, since clonogenic growth was comparable to that in untreated controls (Figure 3, F and G). In GC-sensitive ALL cells, inhibition of autophagy by 3-MA only marginally restored GC resistance, despite small amounts of detectable LC3 lipidation (Supplemental Figure 6). These findings implicate autophagy as part of a common mechanism for GC resensitization by obatoclax and rapamycin.

To determine whether obatoclax triggers the autophagy pathway as a general response to blockade of mitochondrial apoptosis, we studied the drug's effects on *Bax*$^{-/-}$*Bak*$^{-/-}$ mouse embryo fibroblasts (MEFs), which exhibit resistance to a broad range of apoptotic stimuli (26). Like rapamycin, obatoclax induced autophagy in *Bax*$^{-/-}$*Bak*$^{-/-}$ MEFs (Figure 4, A–C), as reflected by autophagosome formation (Figure 4, A and B) and generation of LC3-II (Figure 4C). Obatoclax was cytotoxic to WT and *Bax*$^{-/-}$*Bak*$^{-/-}$ MEFs, whereas ABT-737's activity was restricted to WT MEFs (Figure 4D). The death response was blocked by 3-MA (Figure 4E) and downregulation of beclin-1 or ATG-7 (Figure 4, F and G). Taken together, these results indicate that the cytotoxic effects of obatoclax and rapamycin derive from induction of autophagy when mitochondrial apoptosis is blocked.

Modulation of the GC response by obatoclax is associated with inhibition of mTOR. A key regulator of cell fate decisions, including regulation of autophagy, is the kinase mTOR (27). Inhibition of mTOR by rapamycin resensitizes steroid-resistant ALL cells to dexamethasone (5), but the role of autophagy has not been investigated in this study. Since dexamethasone has been shown to inhibit mTOR in other cellular systems (28), we investigated the effect of dexamethasone and obatoclax treatment on mTOR activity. Alone dexamethasone slightly induced a decrease of S6 protein phosphorylation (Figure 5A). Treatment with obatoclax or rapamycin and dexamethasone resulted in a sharp decrease of the phosphorylation of the mTOR targets S6 protein and 4EB-P1 (Figure 5A). Interestingly, rapamycin but not obatoclax, either alone or in combination with dexamethasone, induced dephosphorylation of AKT at Ser473 (Figure 5A). Combination of obatoclax or rapamycin and dexamethasone also resulted in

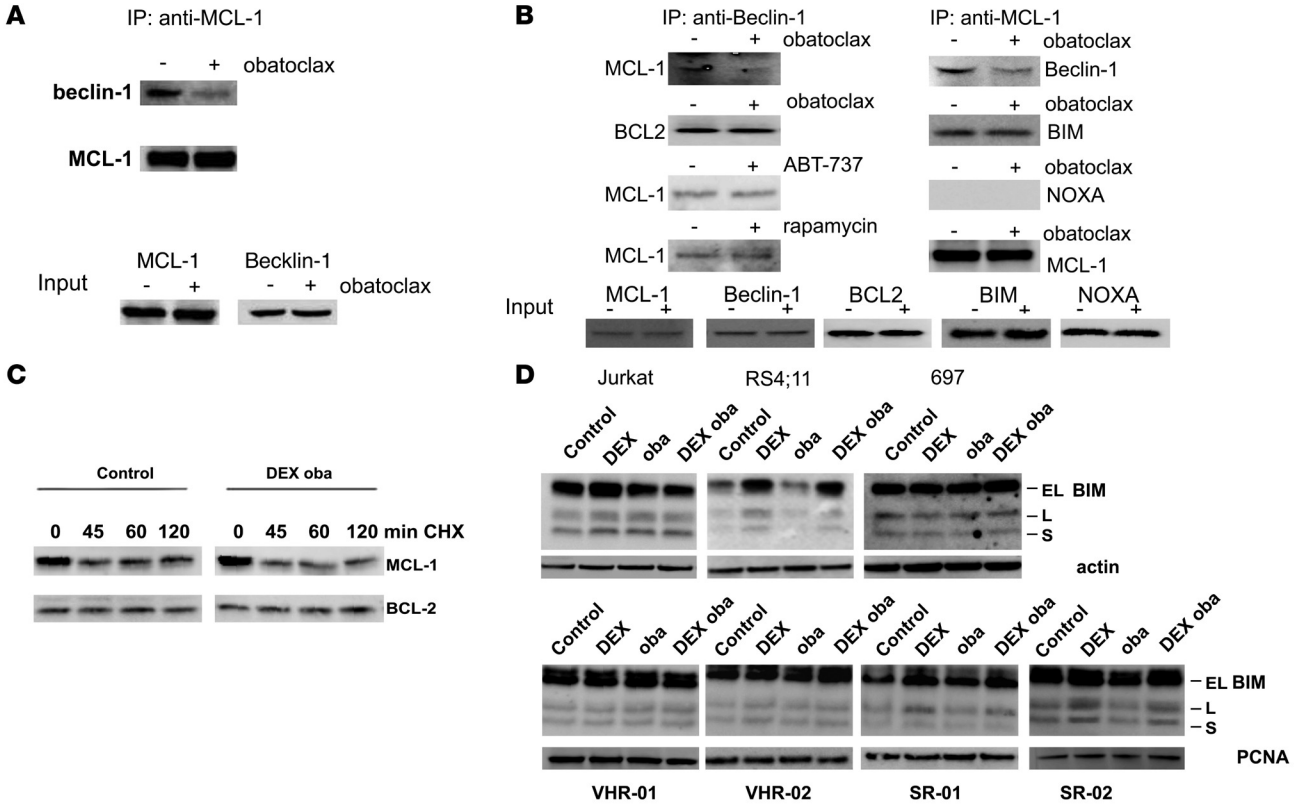

Figure 6

Obatoclax induces disruption of a complex of MCL-1 and beclin-1. (**A**) FLAG-tagged beclin-1 was overexpressed in 293T cells, and MCL-1 immunoprecipitates were analyzed for the presence of beclin-1, with or without obatoclax treatment for 3 hours. (**B**) Jurkat cells were treated with 100 nM obatoclax, 30 nM ABT-737, or 10 nM rapamycin for 3 hours, and MCL-1 or beclin-1 immunoprecipitates were analyzed for the presence of proteins as indicated. Low-dose obatoclax disrupted the interaction between beclin-1 and MCL-1, while interactions between BCL2 and beclin-1 were unaffected. Likewise, ABT-737 or rapamycin did not affect complexes between beclin-1 and MCL-1 or BCL2. (**C**) MCL-1 levels were assessed after treatment with vehicle or the combination of dexamethasone and obatoclax at indicated time points, with or without cycloheximide (CHX). Western blot analyses revealed that MCL-1 levels were unaffected by combination treatment. (**D**) BIM induction was assessed by Western blot in steroid-resistant (Jurkat, VHR-01, and VHR-02) and steroid-sensitive (RS4;11, 697, SR-01, and SR-02) cell lines and primary cells treated with DEX (1 μM), obatoclax (100 nM), or the combination for 24 hours.

dephosphorylation of S6 protein in primary ALL cells from steroid-resistant high risk ALL patients (Figure 5B, left). In contrast, cells from steroid-sensitive patients did not show dephosphorylation of S6 protein after treatment with obatoclax and dexamethasone (Figure 5B, right). Our experiments suggest that in the context of GC resistance, exposure to dexamethasone could cooperate with exposure to obatoclax to decrease mTOR activity. This finding will be exploited to develop correlative markers of biological response to in vivo treatment, for example, using phospho-flow cytometry to monitor the phosphorylation status of S6 protein in leukemia cells.

Obatoclax disrupts a complex between beclin-1 and MCL-1. The antiapoptotic BCL-2 family member MCL-1 was proposed to act as a modulator of GC resistance (5). Because the autophagy regulator beclin-1 was described to interact with antiapoptotic BCL-2 family members, including MCL-1 (11, 14, 15), we next tested the effect of obatoclax on the interaction of beclin-1 with MCL-1. Subcytotoxic concentrations of obatoclax resulted in a markedly decreased detection of MCL-1 that coimmunoprecipitated with overexpressed, epitope-tagged beclin-1 in 293T cells (Figure 6A). We confirmed this result by performing coimmunoprecipitation experiments of endogenously expressed proteins in ALL cells (Figure 6B). Again, in presence of subcytotoxic concentrations of obatoclax, less beclin-1 was shown to coimmunoprecipitate with MCL-1, and inversely, less MCL-1 was pulled down together with beclin-1. Obatoclax did not modify interactions between beclin-1 and BCL-2. Interestingly, incubation with rapamycin or ABT-737 did not affect the complex between beclin-1 and MCL-1. As expected from the reported MCL-1 interaction spectrum (29, 30), BIM was detectable by coimmunoprecipitation from steroid-resistant ALL cells, but binding of BIM to MCL-1 was not altered by treatment with low-dose obatoclax. The BH3-only protein NOXA, which was shown to interact preferentially with MCL-1, did not bind to MCL-1 in this experimental setting (Figure 6B).

Since MCL-1 can be subjected to a high protein turnover (31), we evaluated the effect of combination treatment with obatoclax and dexamethasone on MCL-1 protein levels. In the presence of cycloheximide, MCL-1 levels rapidly decreased after 45 minutes of incubation, independent of the presence of obatoclax and dexamethasone (Figure 6C). Absence of proapoptotic BIM induction by dexamethasone has been described in selected cases of steroid-resistant ALL (32). We did not detect any changes in BIM expression levels to correlate with the restored response to dexamethasone in combination with obatoclax

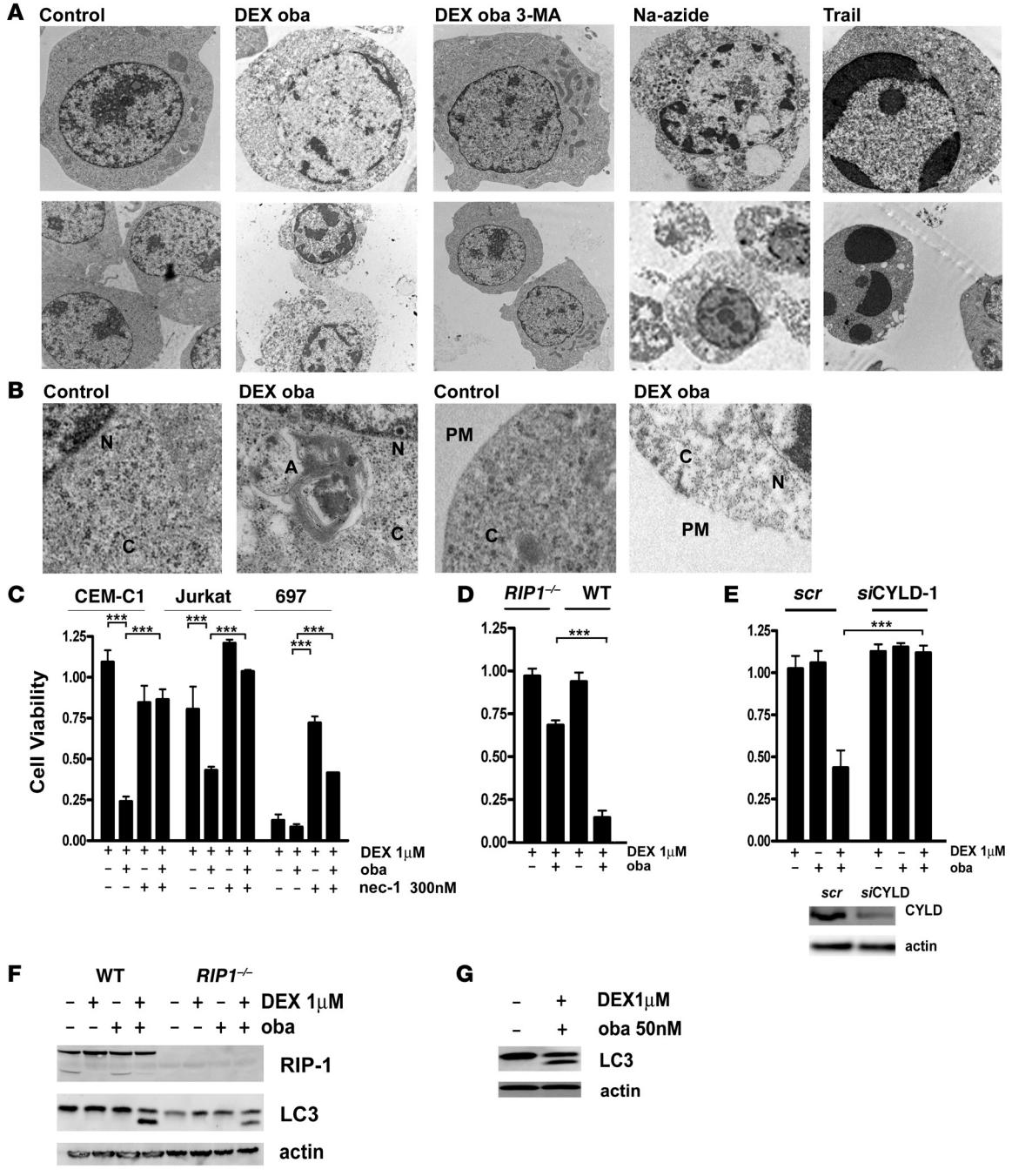

Figure 7

RIP-1 kinase activity is essential for obatoclax-mediated GC sensitization. (**A**) Electron microscopy images reveal features of necroptotic cell death after treatment for 72 hours with obatoclax and dexamethasone. No condensed chromatin was detectable, while Trail treatment induces condensed apoptotic nuclei (top panel) (original magnification, ×7,100). Cells treated with obatoclax and dexamethasone exhibited disintegrated plasma membranes, which was recapitulated by Na-azide. Trail treatment leaved membranes intact (bottom panel) (original magnification, ×5,400). (**B**) A more detailed view of the same experiment. An autophagosome formation with characteristic double membrane structures was detected in the cytoplasm. The plasma membrane was disrupted in cells treated with obatoclax and dexamethasone. N, nucleus; C, cytoplasm; A, autophagosome; PM, plasma membrane (original magnification, ×15,000). (**C**) In steroid-resistant (CEM-C1 and Jurkat) and steroid-sensitive (697) cells treated for 72 hours with dexamethasone (1 μM) and obatoclax (10% IC_{50}), with or without the necroptosis inhibitor nec-1 (300 nM), nec-1 restored steroid resistance as assessed by the MTT assay. (**D**) Jurkat *RIP1*$^{-/-}$ cells were less sensitive to the double treatment for 72 hours with dexamethasone (1 mM) and obatoclax (10% IC_{50}) compared with WT Jurkat cells. Cell viability was assessed by the MTT assay. (**E**) Downregulation of CYLD rescued Jurkat cells from cell death induced by combination treatment for 72 hours with dexamethasone (1 μM) and obatoclax (10% IC_{50}). Efficiency of downregulation was assessed by Western blot analysis after 48 hours. (**F**) LC3-II generation occurred in Jurkat *RIP1*$^{-/-}$ cells and in WT cells after 8 hours of treatment with dexamethasone and obatoclax. (**G**) Treatment with nec-1 did not inhibit LC3-II generation induced by treatment with obatoclax and dexamethasone in Jurkat cells. ***$P < 0.05$.

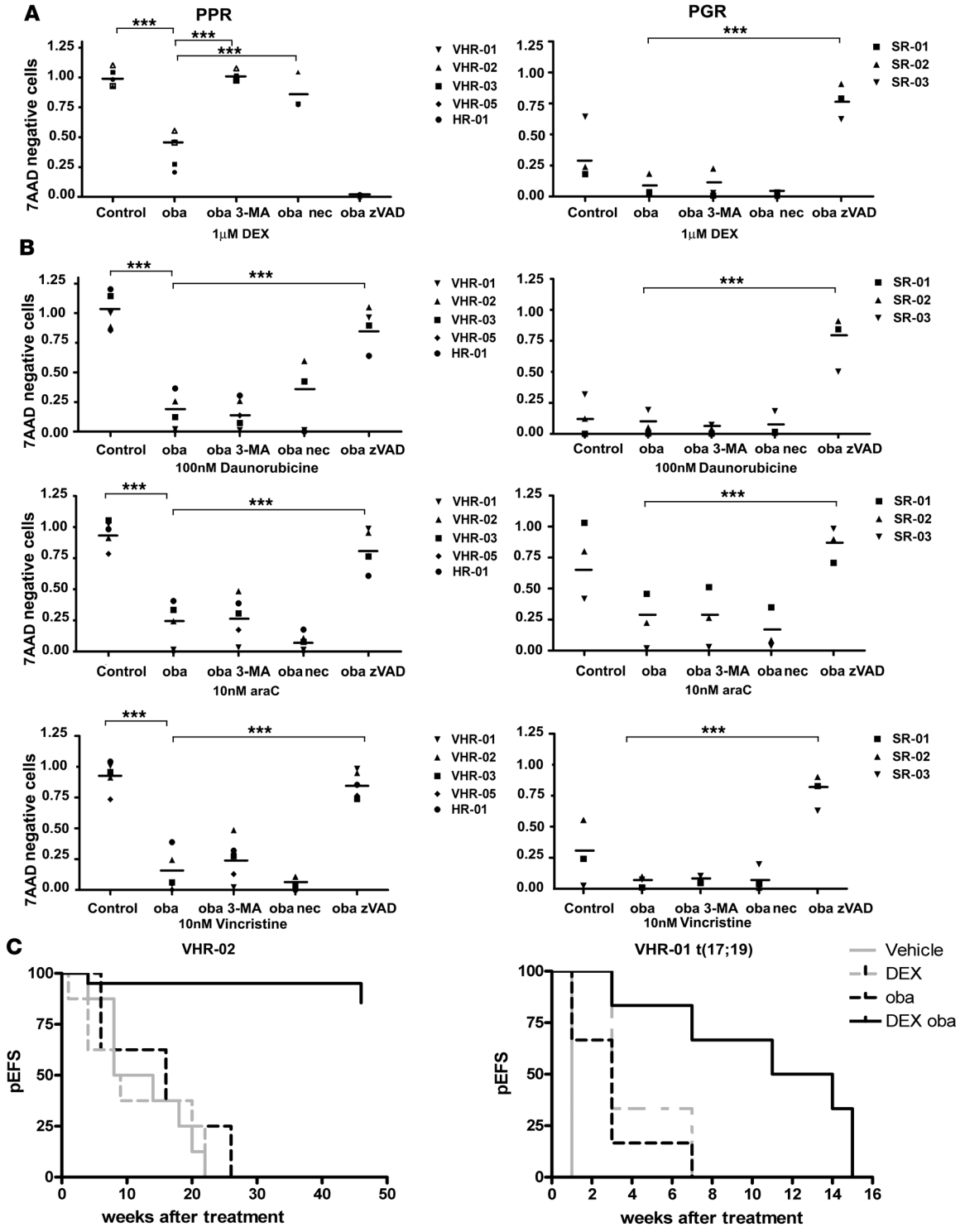
A
PPR
PGR
7AAD negative cells
Control
oba
oba 3-MA
oba nec
oba zVAD
1μM DEX
VHR-01
VHR-02
VHR-03
VHR-05
HR-01
SR-01
SR-02
SR-03
***
B
100nM Daunorubicine
10nM araC
10nM Vincristine
C
VHR-02
VHR-01 t(17;19)
pEFS
weeks after treatment
Vehicle
DEX
oba
DEX oba

Figure 8
Obatoclax displays a strong chemosensitizing activity in multidrug-resistant primary ALL cells from poor risk patients. (**A**) Primary ALL cells from 5 PPR patients and 3 prednisone-good-responder patients were cocultured with hTERT-immortalized bone marrow stroma cells and treated with either dexamethasone (1 μM) alone or in combination with obatoclax (10% IC_{50}) in the presence or absence of 3-MA, nec-1, or zVAD.fmk for 72 hours. Cell viability was assessed by 7AAD staining and flow cytometry. Data are shown as mean ± SD of 2 independent experiments. In combination experiments, values were normalized to cells treated with compounds and/or inhibitors alone at indicated dose. (**B**) Primary ALL cells from 4 VHR, 1 high risk (HR), and 3 standard risk (SR) patients were cocultured with hTERT-immortalized bone marrow stroma cells and treated with either daunorubicin, vincristine, or cytarabine (araC) alone or in combination with obatoclax (10% IC_{50}) in the presence or absence of 3-MA, nec-1, or zVAD.fmk for 72 hours. Cell viability was assessed by 7AAD staining and flow cytometry. Data are shown as mean ± SD of 2 independent experiments. ***$P < 0.05$ (**A** and **B**). (**C**) Percentage of event-free survival (pEFS) of NSG mice after xenotransplantation with primary cells from 2 PPR patients with VHR-ALL (VHR-02, $n = 8$; patient VHR-01, $n = 6$; Supplemental Table 2) and treatment for 3 weeks with either vehicle, dexamethasone, obatoclax, or the combination. $P < 0.02$ for dexamethasone and obatoclax versus vehicle, dexamethasone, or obatoclax alone for both xenograft experiments.

in GC-resistant ALL cells (Figure 6D). Interestingly, induction of BIM was not detectable consistently in steroid-sensitive cells (Figure 6D). While in RS4;11 cells, BIM was readily induced by dexamethasone, neither 697 cells nor primary ALL cell samples from steroid-resistant patients showed induction of this proapoptotic BH3-only protein after dexamethasone treatment (Figure 6D). In cells from steroid sensitive patients, a small increase in the BIM-L and BIM-S but not BIM-EL isoforms was detectable. These data indicate that steroid resensitization by obatoclax is not due to induction of BIM.

To obtain further insight into the role of MCL-1 for the mechanism of action of obatoclax, we modulated MCL-1 expression using RNA interference. A reduction of MCL-1 protein levels resulted in partial resensitization to dexamethasone but, surprisingly, prevented any additional chemosensitization by the combination with obatoclax (Supplemental Results and Supplemental Figure 7). Partial resensitization to dexamethasone was mediated via induction of apoptosis, which was blocked using the pan-caspase inhibitor zVAD.fmk. Inhibition of autophagy with 3-MA did not affect the resensitization effect of MCL-1 knockdown to dexamethasone, even in presence of obatoclax. Instead, caspase-9 activation was detected, which correlated with a caspase-dependent decrease of beclin-1. Thus, it is possible that induction of apoptosis overrides induction of autophagy when MCL-1 is downregulated, which limits the interpretation of these experiments. Taken together, our data indicate that disruption of the beclin–MCL-1 interaction is part of the mechanism triggered by obatoclax and suggest an involvement of MCL-1 in the regulation of an autophagy-dependent cell death pathway, in addition to its role as anti-apoptotic regulator in leukemia cells.

Combination of obatoclax and dexamethasone triggers RIP-1 kinase–dependent necroptosis in GC-resistant ALL. To better assess the nature of cell death occurring with obatoclax and dexamethasone, we proceeded with imaging by transmission electron microscopy. Indeed, autophagosome formation was evident after treatment with obatoclax and dexamethasone, which was completely inhibited by incubation with 3-MA (Figure 7, A and B). Cells displayed features consistent with a nonapoptotic cell death mechanism after exposure to obatoclax and dexamethasone. Condensation of chromatin, a hallmark of classical apoptosis, was incomplete (Figure 7A, top row), which contrasts with the marked chromatin condensation after treatment with TRAIL, which induces death receptor–dependent apoptosis in ALL cells (33). A characteristic feature of dead cells was the disintegration of the plasma membrane (Figure 7B), which is a hallmark of necroptosis (34). Increasing evidence suggests that a programmed necrotic cell death pathway can be triggered in the context of impaired apoptotic effectors, and this is dependent on RIP-1 kinase activity (12, 17). RIP-1 functions at the intersection of cell survival and cell death signalling (35, 36). Therefore, we tested whether inhibition of RIP-1 with necrostatin-1 (nec-1; ref. 17) would interfere with steroid sensitization by obatoclax. Indeed, steroid-resistant ALL cells treated with nec-1 were refractory to obatoclax-induced dexamethasone resensitization (Figure 7C). Nec-1 also reduced the cytotoxic response to dexamethasone, alone or in combination with low-dose obatoclax in steroid-sensitive ALL cells (Figure 7C). Interestingly, nec-1 inhibited induction of BIM in steroid-sensitive cells that showed BIM induction after dexamethasone (Supplemental Figure 8). Consistent with a central role for RIP-1 for the response to GC drugs, RIP-1–deficient ALL cells (37) were resistant to obatoclax-mediated GC resensitization (Figure 7D).

The deubiquitinase cylindromatosis (turban tumor syndrome) (CYLD) is a direct regulator of RIP-1 kinase activity (38). Knocking down CYLD expression showed that CYLD is required for RIP-1–dependent cell death induction by combination of dexamethasone and obatoclax (Figure 7E). Our results are consistent with the current model, which proposes that the deubiquinated form of RIP-1 is mediating cell death signals (35). An important finding is that induction of autophagy could be detected early, within 4 hours of treatment, and that generation of LC3-II was neither inhibited in RIP-1–deficient ALL cells (Figure 7F) nor in nec-1–treated ALL cells (Figure 7G). Taken together, these results demonstrate that the combination of obatoclax and dexamethasone triggers a non-apoptotic cell death pathway, which shares the central features of necroptosis, including the characteristic morphology of cell death shown by electron microscopy, and a strict dependence on RIP-1 kinase activity and RIP-1 deubiquitinase CYLD. Moreover, our data indicate that the autophagic process is triggered upstream of RIP-1 and does not occur as a consequence of necroptosis.

Obatoclax is a broad chemosensitizer in multidrug-resistant primary ALL cells, but activation of autophagy-dependent cell death is specific to the combination with dexamethasone. To validate our results in primary cells, we tested pretreatment samples from PPR patients with precursor B cell ALL, who were further characterized by the molecular persistence of leukemic cells under intensified conventional multiagent chemotherapeutic treatment and predicted to have a very high risk of relapse based on their poor in vivo response to chemotherapy (Supplemental Table 2). Indeed, low-dose obatoclax resensitized GC-resistant ALL cells to dexamethasone in mesenchymal stroma cell (MSC) cocultures, which was completely abolished using 3-MA, implicating autophagy as an essential mechanism in primary refractory ALL cells also (Figure 8A). At this dosage, obatoclax alone induces less than 5% cell death. Importantly, 3-MA did not interfere with the cytotoxic effect of treatment with dexamethasone, alone or combined with obatoclax, on primary ALL cells from GC-sensitive patients (Figure 8A), indicating that autophagy was not required for the death response to GC drugs in GC-sensitive cells. Consistent with our results in ALL cell lines, nec-1 abolished the GC-sensitizing activity of combination treatment in steroid-resistant primary

VHR-ALL cells. In contrast, blocking caspases with zVAD.fmk did not inhibit steroid resensitization in primary GC-resistant ALL cells, while the response to dexamethasone was inhibited by zVAD.fmk treatment in cells from steroid-sensitive ALL patients.

Current treatment protocols include a steroid window followed by multidrug chemotherapy, including cytotoxic agents such as daunorubicin, vincristine, and cytarabine. Low-dose obatoclax resensitized primary refractory ALL cells to all 3 drugs, while the sensitivity of cells from sensitive patients was not increased further. Interestingly, 3-MA did not restore resistance to these cytotoxic agents, indicating that induction of autophagy after treatment with obatoclax is specific for GC resensitization (Figure 8B). In contrast, blocking caspases using zVAD.fmk completely inhibited the resensitizing effect of low-dose obatoclax in combinations with daunorubicin, vincristine, and cytarabine, both in cells from very high risk and from standard risk patients. These results support the notion that autophagy-dependent necroptosis is specifically triggered with GCs in a GC-resistant context. Moreover, obatoclax could serve as a chemosensitizer for established multidrug regimens for ALL treatment, given its broad potential to restore the apoptotic response with non-GC antileukemic drugs.

Combination of obatoclax and dexamethasone is effective in a leukemia xenograft model, using cells from refractory ALL patients. To test the in vivo efficacy of obatoclax in GC resensitization, we transplanted primary ALL cells from 2 VHR-PPR patients into NOD/SCID/IL2rγ^{null} (NSG) mice (39). When 1% human leukemic cells were detected in mouse peripheral blood, we treated mouse cohorts with vehicle, obatoclax (5 mg/kg/d), dexamethasone (5 μg/kg/d), or both for 3 weeks. In vehicle-treated animals, progression to leukemia (>10% peripheral blasts) was observed in a median time of 11 weeks for animals xenografted with cells from patient VHR-02 and 1 week for animals xenografted with cells from patient VHR-01. All mice xenografted with cells from patient VHR-02 and treated with single-agent dexamethasone or obatoclax had to be sacrificed due to leukemia progression, while only 2 out of 8 animals treated with the combination of obatoclax and dexamethasone progressed to leukemia over the 50-week observation period. A significant delay in leukemia progression was achieved by combination treatment with dexamethasone and obatoclax when cells from VHR-01 were used ($P < 0.02$ for combination treatment versus vehicle or single agent treatment). This patient showed the recurrent translocation t(17;19)(q22;p13), which is virtually always associated with early relapse (40) (Figure 8C). This result suggests that GC sensitization of VHR-PPR ALL cells can be achieved in vivo, providing a strong rationale to explore the therapeutic potential of combined dexamethasone and obatoclax clinically.

Discussion

Here we describe a pharmacological approach that we believe to be new to specifically bypass the apoptotic blockade to chemotherapy in multidrug-resistant ALL. Subcytotoxic concentrations of the BCL-2 antagonist obatoclax restored the response to dexamethasone by inducing a nonapoptotic cell death pathway. The activation of autophagy-dependent cell death in cells that are resistant to the apoptotic stimuli by dexamethasone is reminiscent of observations that were reported using experimental systems with defined genetic defects of key regulators of the intrinsic and extrinsic apoptotic response. In *Bax*$^{-/-}$*Bak*$^{-/-}$ MEFs and BCL-2–overexpressing MEFs, cell death triggered by etoposide or STS was dependent on autophagy genes beclin-1 and ATG-5 (11). As also reported by others (6, 8), obatoclax was cytotoxic for *Bax*$^{-/-}$*Bak*$^{-/-}$ cell lines, which we demonstrate to be critically dependent on the autophagy pathway. Similarly, genetic or pharmacologic interference with caspase 8 or death receptor signalling can result in autophagy-dependent cell death with necroptotic features (12, 18, 41). In lymphoid cells, this may constitute an alternative mechanism to control abnormal cellular proliferation in the absence of a normal apoptotic response. In activated T cells from mice with caspase-8 or FADD deficiency, autophagic signalling was required to induce RIP-1–dependent necroptotic cell death (41). We here show that this mechanism of cell death can be activated in GC-resistant leukemia to restore the response to dexamethasone.

Autophagy has been recognized as an important regulatory mechanism of cell fate decisions. While it is clear that autophagy can have a protective function at times of cellular stress, the contribution of autophagy to the execution of programmed cell death is a subject of controversy (13). Our data demonstrate that autophagic signalling is an integral part of the cell death mechanism when the response to dexamethasone is restored with obatoclax or rapamycin. Both inhibitors that interfere early (3-MA) or late (bafilomycin) with the autophagic process and knockdown of genes that are essential for autophagy, *BECN1* and *ATG7*, prevented resensitization to dexamethasone completely. Combination of dexamethasone and obatoclax inhibited clonogenic growth of GC-resistant ALL cells, and electron microscopy imaging unequivocally showed rapid induction of necrotic cell death with autophagic features. There is clear evidence that in cancer, autophagy is not necessarily a protective feature. For example, *BECN1* was shown to act as a haploinsufficient tumor suppressor gene (42, 43), with increased frequency of spontaneous neoplasia, including lymphomas in beclin-1–haploinsufficient mice. The genes that are essential for the autophagic machinery are highly conserved and required in several autophagy-dependent cellular processes (44). Several studies link autophagy genes to programmed cell death. In the central nervous system for example, ATG7 deficiency protected neurons from caspase-dependent and caspase-independent cell death after hypoxic/ischemic brain injury (45). In human glioblastoma, knockdown of the autophagy genes *ATG1* or *ATG5* prevented the cytotoxic effect of cannabinoids, which induce autophagy-dependent cell death via an mTORC1-dependent pathway (46). Autophagy was also shown to regulate programmed cell death during development. The steroid hormone ecdysone triggered autophagy-dependent cell death during morphogenesis of salivary glands from the larval stage to the adult stage in *Drosophila*. This cell death pathway was independent of caspase activity (47), providing compelling evidence for the modulation of an autophagic cell death pathway via steroid hormone signalling in normal development. Similarly, autophagy is required for programmed cell death in the midgut during *Drosophila* metamorphosis, which provides additional evidence for specific regulation of cell death by autophagy, even in presence of an intact apoptotic machinery (48). Combination treatment of obatoclax with GC drugs but not with other cytotoxic agents induced autophagy-dependent cell death in resistant ALL. This raises the question of whether autophagy is also required for the effect of dexamethasone in GC-sensitive ALL. A recent report described increased autophagy after dexamethasone treatment in GC-sensitive ALL cell lines, but cell death was associated with apoptotic features and knockdown of beclin-1 resulted only in partial rescue of this effect (49). We also observed a partial reduction of dexamethasone cytotoxicity using 3-MA (Supplemen-

tal Figure 6) or nec-1 (Figure 7C) in a subset of GC-sensitive cell lines. We could, however, not detect an effect of 3-MA in primary ALL cells, in which caspase-dependent cell death prevailed. Our results identify autophagy as an early and limiting step to steroid sensitization by obatoclax in GC-resistant cells and underscore the importance of understanding the cellular context when designing strategies to target autophagy for cancer treatment.

There is clear evidence for hyperactivation of AKT (50) and mTOR (5) in GC-resistant ALL. Because mTOR is implicated in the control of autophagy in different settings (27), hyperactive AKT-mTOR signalling could prevent induction of autophagy in resistant disease. We hypothesized that GC-resistant ALL cells could therefore be primed for mTOR-controled autophagy. Consistent with this idea, we found that induction of autophagic cell death by the combination of dexamethasone and obatoclax resulted in marked reduction in phosphorylation of the mTOR target S6 protein in resistant cells. The mechanisms by which obatoclax or rapamycin potentiate the effect of dexamethasone on mTOR appear to be different. Indeed combination of dexamethasone with rapamycin, but not with obatoclax, resulted in a marked decrease in phosphorylation of AKT on Ser473, consistent with recent finding showing that mTOR can also act upstream of AKT (51). Modulation of mTOR target phosphorylation was only seen when obatoclax was combined with dexamethasone, but not with other cytotoxic agents, suggesting that dexamethasone exposure contributes to inhibition of mTOR. Indeed, exposure to dexamethasone was reported to be associated with repression of mTOR signalling in myoblast cell lines and lymphoid cells (28, 52). The importance of mTOR for the control of autophagy is also underscored by the results of a comprehensive screen using a chemical compound library in order to identify new pharmacologic inducers of autophagy, in which proautophagic activity of candidate molecules was always associated with decreased phosphorylation of mTOR targets (53). Extensive studies will be required to dissect the primary signalling events triggered by the combination of obatoclax and dexamethasone, as they may provide important clues about the mechanisms of drug resistance in ALL.

GC resistance does not appear to be associated with genetic or functional defects of the GC receptor in ALL (54, 55). Dexamethasone was proposed to induce apoptosis by increasing the levels of the BH3-only proapoptotic protein BIM, which were markedly reduced in selected cases of GC-resistant ALL (32). However, in most cases tested, we could not detect induction of BIM by dexamethasone in GC-sensitive cell lines and primary ALL cells. Furthermore, we did not detect increased levels of BIM, decreased MCL-1 protein levels, or increased MCL-1 protein turnover associated with steroid sensitization. Instead, we found, by immunoprecipitation of endogenous proteins, subcytoxic concentrations of obatoclax to result in the disruption of MCL-1 with beclin-1 in ALL cells. This suggests the possibility that MCL-1 could control induction of autophagy via beclin-1, as it was proposed for other BCL-2 family members recently (14, 15). Interestingly, this effect was not seen in cells treated with rapamycin, again pointing out that the target mechanism of obatoclax is different. We recognize the fact that this effect could also result from indirect mechanisms on the protein complex, including MCL-1 and beclin-1. Furthermore, functional experiments modulating MCL-1 expression levels were not conclusive. Knockdown of MCL-1 resulted in moderate activation of apoptosis and partial sensitization to dexamethasone that was caspase dependent but prevented complete resensitization to dexamethasone by obatoclax and autophagic cell death. Activation of apoptosis is possibly overriding induction of autophagy in this context. In support of this hypothesis, we detected activation of caspase-9 after downregulation of MCL-1, with caspase-9–dependent cleavage of beclin-1. This provides a possible mechanism to prevent autophagy induction when apoptosis is activated. Taken together, steroid modulation with low-dose obatoclax did not involve release of proapoptotic BCL-2 family proteins from MCL-1 but triggered autophagy-dependent cell death by a mechanism that required the presence of MCL-1.

In this context, activation of autophagy is required to induce necroptosis, a form of programmed necrosis that has been described to occur when apoptosis is abortive due to caspase inhibition (16, 56). Execution of necroptosis is dependent on the RIP-1 kinase (17). Our data demonstrate that RIP-1 activity is absolutely required for steroid sensitization by obatoclax and by rapamycin. The cell death morphology that was documented by electron microscopy is consistent with the morphology reported for necroptosis (12, 56). Furthermore, the deubiquitinase cylindromatosis (CYLD), which has been shown to regulate RIP-1 (38), was functionally required for execution of necroptosis. This is consistent with experiments showing that RIP-1 kinase activity was required to trigger cell death and that ubiquitination of RIP-1 prevents cell death signalling (16, 19). RIP-1 and CYLD were included among the core genes that were identified in a functional siRNA screen for genes that were essential for necroptosis (18). To the best of our knowledge, we provide the first clinically relevant model with consistent validation in primary leukemia cells from patients with very high risk disease, in which the necroptotic pathway can be exploited to restore response to therapy. As such, this will constitute a very relevant experimental model to study the mechanisms of necroptosis in depth. Our results clearly imply a direct link between the autophagic pathway and RIP-1–mediated signalling events leading to necroptosis. Autophagy is triggered early and independent of RIP-1 kinase activity, indicating that it acts upstream of necroptotic signals. A number of studies identify RIP functionally as part of a complex with proteins of the death receptor pathway, such as FADD and caspase-8 (35). Experiments using mouse models indicate that autophagy and necroptosis could be linked via recruitment of components of the death receptor pathway to the membrane of autophagosomes (41). It is tempting to speculate that a similar mechanism is triggered in ALL cells upon costimulation with dexamethasone and obatoclax. Our findings warrant extensive biochemical follow-up studies to understand how RIP-1 is activated and how the autophagic machinery is connected to the necroptotic pathway.

Based on promising studies by others (32), we have established a leukemia xenograft model of de novo highly resistant ALL. The power of this approach resides in the possibility to select cases from relevant patient groups, starting from cryopreserved leftover diagnostic samples, from one of the largest cooperative trials for the treatment of childhood ALL. By focusing on cases with VHR-ALL by MRD, we also selected for patients that are most significantly resistant to prednisone in vivo, as defined by the reduction of leukemia cells in the peripheral blood after 1 week of prednisone monotherapy. Accordingly, ALL cells from these patients were completely resistant to dexamethasone and other chemotherapeutic agents in vitro. Low-dose obatoclax restored the response to dexamethasone, both in precursor B cell and T cell ALL cases. The durable remissions observed with 1 year follow-up,

using the leukemia xenograft model, are indicative of strong antileukemic activity. Furthermore, the broad chemosensitizing effect of low-dose obatoclax in combination with daunorubicin, vincristine, and cytarabine in multidrug-resistant primary ALL cells provides a strong basis for further evaluation of obatoclax in combination with a multidrug regimen. The xenograft approach will be essential to validate this approach for heavily pretreated relapse and refractory patients. Our observation that isolated clones can emerge in clonogenic assays after treatment of a cell line with obatoclax and dexamethasone indicates that resistance to this approach may occur. Our established xenograft system will enable us to screen a larger number of ALL cases to verify whether resistance to this approach has to be expected. The identification of resistant cases would provide a model to establish markers that correlate with response or resistance. Based on current data, dynamic changes of mTOR activity with treatment represent a good candidate marker. Such knowledge will serve to optimize patient selection for clinical trials.

Taken together, our data support a model in which the apoptotic blockade in GC-resistant ALL cells can be overcome by activating an autophagy-dependent necroptotic cell death pathway. The characteristic necroptotic features by electron microscopy and the changes in the phosphorylation profile of S6 protein provide tools to assess the biological response to combination treatment with obatoclax and dexamethasone in patients in refractory ALL. Given the acceptable toxicity profile of obatoclax in clinical studies in adults with hematologic malignancies (9, 10), our study provides a compelling rationale for the evaluation of this new pharmacological strategy for the treatment of children with refractory and relapsed ALL.

Methods

Cell culture, reagents, and standard procedures. CEM-C7-14 and CEM-C1-15 cells (referred to CEM-C7 and CEM-C1 in the text) were provided by E.B. Thompson (University of Texas Medical Branch, Galveston, Texas), human *hTERT*-immortalized primary bone marrow MSCs (57) were provided by D. Campana (St Jude Children's Research Hospital, Memphis, Tennessee), caspase-9–deficient and retransfected Jurkat cells (58) as well as *Bax/Bak*-deficient Jurkat cells (59) were provided by K. Schulze-Osthoff (University of Tübingen, Germany), and parental and *Bax/Bak*-deficient MEFs (26) were provided by J.-C. Martinou (University of Geneva, Switzerland). *Rip1*$^{-/-}$ cells were provided by B. Seed (Harvard Medical School, Boston, Massachusetts). Obatoclax was provided by J. Viallet and G. Shore (Gemin X, Malvern, Pennsylvania) and ABT-737 was provided by S. Elmore and S. Rosenberg (Abbott Laboratories, Chicago, Illinois).

Detailed procedures are described in Supplemental Methods. For RNA silencing experiments, 30 nM beclin-1 (sc-29797, Santa Cruz Biotechnology Inc.) was used. pEGFP-LC3 was provided by M. Jäättelä (Danish Cancer Society, Copenhagen) and the FLAG-tagged beclin-1 construct by B. Levine (University of Texas Southwestern Medical School, Dallas). All constructs were transfected by nucleofection (Amaxa) using solution V and Amaxa program T-016 for CEM-C1, A-024 for CEM-C7 cells, and U-020 for MEFs. Transfection efficiency was controlled using the pEGFP plasmid (Clontech).

Patient samples. ALL cells were recovered from cryopreserved anonymized samples from patients who were enrolled in the ongoing ALL-BFM 2000 protocol and had given informed consent in accordance with the Declaration of Helsinki. Approval was obtained from the Institutional Review Board (IRB) of the Medical School Hannover and the local IRB for all participating centers in the trial ALL-BFM 2000. This approval extends to the use of leftover diagnostic material for add-on research projects, including those addressing basic biological questions.

In vitro drug response. In vitro drug response curves in cell lines were established with the MTT assay and were normalized to vehicle control. Primary patient samples were cocultured on hTERT-immortalized human MSCs, and drug response curves were analyzed with flow cytometry using propidium iodide.

Xenograft model. Xenograft experiments were approved by the veterinary office of the Canton of Zurich. In brief, primary ALL cells were recovered from cryopreserved samples and transplanted intrafemorally to NSG mice. Leukemia progression was monitored by flow cytometry with human CD45 and CD19 antibodies (AbD Serotec). ALL cells recovered from spleens of NSG mice after the first xenotransplantation were used for in vivo therapeutic trials. Randomized cohorts were treated with vehicle intramuscularly (i.m.): 3 mg/kg/d obatoclax i.m., 5 mg/g/d dexamethasone i.p., or the combination of dexamethasone i.p. and obatoclax i.m. for 5 days per week for 3 consecutive weeks.

Statistics. All experiments were performed 4 times, unless stated otherwise in the figure legends. Data are represented as mean ± SD. For in vitro experiments, Student's *t* test (2-tailed) was used on triplicates. *P* values of less than 0.05 were considered significant. Event-free survival (EFS) was defined as the time from the start of treatment until 10% of human leukemia cells were detectable in the mouse peripheral blood and was assessed by Kaplan-Meier analysis. Survival curves were analyzed with the log-rank test (GraphPad prism). *P* values of less than 0.05 were considered significant.

Acknowledgments

We thank U. Luethi for assistance with electron microscopy and L. Walensky, I. Maillard, S. Krishnan, and V. Saha for helpful discussions and feedback on the manuscript. This work was supported by grants to J.-P. Bourquin from the Fondation pour la Recherche Cancer de l' Enfant, the Swiss Cancer League, the Swiss National Science Foundation, the Foundation for Research at the Medical Faculty, University of Zurich, the Julius Müller Foundation, and the Huggenberger-Bischoff Foundation.

Received for publication May 26, 2009, and accepted in revised form January 6, 2010.

Address correspondence to: Jean-Pierre Bourquin, Department of Oncology, University Children's Hospital Zurich, Steinwiesstrasse 75, CH-8032 Zurich, Switzerland. Phone: 41.44.266.7304; Fax: 41.44.266.7171; E-mail: jean-pierre.bourquin@kispi.uzh.ch.

1. Pui CH, Evans WE. Treatment of acute lymphoblastic leukemia. *N Engl J Med*. 2006;354(2):166–178.
2. Schrappe M. Evolution of BFM trials for childhood ALL. *Ann Hematol*. 2004;83(Suppl 1):S121–S123.
3. Schrauder A, et al. Prospective evaluation of MRD–Kinetics in 274 children with high-risk ALL treated in trial ALL–BFM 2000: Insights into development of resistance and impact on further refinement of treatment stratification strategies. *Blood*. 2007;110:585.
4. Holleman A, et al. Gene-expression patterns in drug-resistant acute lymphoblastic leukemia cells and response to treatment. *N Engl J Med*. 2004;351(6):533–542.
5. Wei G, et al. Gene expression-based chemical genomics identifies rapamycin as a modulator of MCL1 and glucocorticoid resistance. *Cancer Cell*. 2006;10(4):331–342.
6. Nguyen M, et al. Small molecule obatoclax (GX15-070) antagonizes MCL-1 and overcomes MCL-1-mediated resistance to apoptosis. *Proc Natl Acad Sci U S A*. 2007;104(49):19512–19517.
7. Perez-Galan P, Roue G, Villamor N, Campo E, Colomer D. The BH3-mimetic GX15-070 synergizes with bortezomib in mantle cell lymphoma by enhancing Noxa-mediated activation of Bak. *Blood*. 2007;109(10):4441–4449.
8. Konopleva M, et al. Mechanisms of antileukemic activity of the novel Bcl-2 homology domain-3 mimetic GX15-070 (obatoclax). *Cancer Res*. 2008;

68(9):3413–3420.
9. O'Brien SM, et al. Phase I study of obatoclax mesylate (GX15-070), a small molecule pan-Bcl-2 family antagonist, in patients with advanced chronic lymphocytic leukemia. *Blood*. 2009;113(2):299–305.
10. Schimmer AD, et al. A phase I study of the pan bcl-2 family inhibitor obatoclax mesylate in patients with advanced hematologic malignancies. *Clin Cancer Res*. 2008;14(24):8295–8301.
11. Shimizu S, et al. Role of Bcl-2 family proteins in a non-apoptotic programmed cell death dependent on autophagy genes. *Nat Cell Biol*. 2004;6(12):1221–1228.
12. Yu L, et al. Regulation of an ATG7-beclin 1 program of autophagic cell death by caspase-8. *Science*. 2004;304(5676):1500–1502.
13. Kroemer G, Levine B. Autophagic cell death: the story of a misnomer. *Nat Rev Mol Cell Biol*. 2008;9(12):1004–1010.
14. Maiuri MC, et al. Functional and physical interaction between Bcl-X(L) and a BH3-like domain in Beclin-1. *EMBO J*. 2007;26(10):2527–2539.
15. Pattingre S, et al. Bcl-2 antiapoptotic proteins inhibit Beclin 1-dependent autophagy. *Cell*. 2005;122(6):927–939.
16. Holler N, et al. Fas triggers an alternative, caspase-8-independent cell death pathway using the kinase RIP as effector molecule. *Nat Immunol*. 2000;1(6):489–495.
17. Degterev A, et al. Identification of RIP1 kinase as a specific cellular target of necrostatins. *Nat Chem Biol*. 2008;4(5):313–321.
18. Hitomi J, et al. Identification of a molecular signaling network that regulates a cellular necrotic cell death pathway. *Cell*. 2008;135(7):1311–1323.
19. O'Donnell MA, Legarda-Addison D, Skountzos P, Yeh WC, Ting AT. Ubiquitination of RIP1 regulates an NF-kappaB-independent cell-death switch in TNF signaling. *Curr Biol*. 2007;17(5):418–424.
20. Oltersdorf T, et al. An inhibitor of Bcl-2 family proteins induces regression of solid tumours. *Nature*. 2005;435(7042):677–681.
21. Deng J, Carlson N, Takeyama K, Dal Cin P, Shipp M, Letai A. BH3 profiling identifies three distinct classes of apoptotic blocks to predict response to ABT-737 and conventional chemotherapeutic agents. *Cancer Cell*. 2007;12(2):171–185.
22. Konopleva M, et al. Mechanisms of apoptosis sensitivity and resistance to the BH3 mimetic ABT-737 in acute myeloid leukemia. *Cancer Cell*. 2006;10(5):375–388.
23. van Delft MF, et al. The BH3 mimetic ABT-737 targets selective Bcl-2 proteins and efficiently induces apoptosis via Bak/Bax if Mcl-1 is neutralized. *Cancer Cell*. 2006;10(5):389–399.
24. Shao Y, Gao Z, Marks PA, Jiang X. Apoptotic and autophagic cell death induced by histone deacetylase inhibitors. *Proc Natl Acad Sci U S A*. 2004;101(52):18030–18035.
25. Luo S, Rubinsztein DC. Atg5 and Bcl-2 provide novel insights into the interplay between apoptosis and autophagy. *Cell Death Differ*. 2007;14(7):1247–1250.
26. Lindsten T, et al. The combined functions of proapoptotic Bcl-2 family members bak and bax are essential for normal development of multiple tissues. *Mol Cell*. 2000;6(6):1389–1399.
27. Sarbassov DD, Ali SM, Sabatini DM. Growing roles for the mTOR pathway. *Curr Opin Cell Biol*. 2005;17(6):596–603.
28. Wang H, Kubica N, Ellisen LW, Jefferson LS, Kimball SR. Dexamethasone represses signaling through the mammalian target of rapamycin in muscle cells by enhancing expression of REDD1. *J Biol Chem*. 2006;281(51):39128–39134.
29. Certo M, et al. Mitochondria primed by death signals determine cellular addiction to antiapoptotic BCL-2 family members. *Cancer Cell*. 2006;9(5):351–365.
30. Chen L, et al. Differential targeting of prosurvival Bcl-2 proteins by their BH3-only ligands allows complementary apoptotic function. *Mol Cell*. 2005;17(3):393–403.
31. Maurer U, Charvet C, Wagman AS, Dejardin E, Green DR. Glycogen synthase kinase-3 regulates mitochondrial outer membrane permeabilization and apoptosis by destabilization of MCL-1. *Mol Cell*. 2006;21(6):749–760.
32. Bachmann PS, Gorman R, Mackenzie KL, Lutze-Mann L, Lock RB. Dexamethasone resistance in B-cell precursor childhood acute lymphoblastic leukemia occurs downstream of ligand-induced nuclear translocation of the glucocorticoid receptor. *Blood*. 2005;105(6):2519–2526.
33. Fakler M, et al. Small molecule XIAP inhibitors cooperate with TRAIL to induce apoptosis in childhood acute leukemia cells and overcome Bcl-2-mediated resistance. *Blood*. 2009;113(8):1710–1722.
34. Miao B, Degterev A. Methods to analyze cellular necroptosis. *Methods Mol Biol*. 2009;559:79–93.
35. Declercq W, Vanden Berghe T, Vandenabeele P. RIP kinases at the crossroads of cell death and survival. *Cell*. 2009;138(2):229–232.
36. Galluzzi L, Kroemer G. Necroptosis: a specialized pathway of programmed necrosis. *Cell*. 2008;135(7):1161–1163.
37. Ting AT, Pimentel-Muinos FX, Seed B. RIP mediates tumor necrosis factor receptor 1 activation of NF-kappaB but not Fas/APO-1-initiated apoptosis. *EMBO J*. 1996;15(22):6189–6196.
38. Wright A, et al. Regulation of early wave of germ cell apoptosis and spermatogenesis by deubiquitinating enzyme CYLD. *Dev Cell*. 2007;13(5):705–716.
39. Shultz LD, et al. Human lymphoid and myeloid cell development in NOD/LtSz-scid IL2R gamma null mice engrafted with mobilized human hemopoietic stem cells. *J Immunol*. 2005;174(10):6477–6489.
40. Matsunaga T, et al. Regulation of annexin II by cytokine-initiated signaling pathways and E2A-HLF oncoprotein. *Blood*. 2004;103(8):3185–3191.
41. Bell BD, et al. FADD and caspase-8 control the outcome of autophagic signaling in proliferating T cells. *Proc Natl Acad Sci U S A*. 2008;105(43):16677–16682.
42. Qu X, et al. Promotion of tumorigenesis by heterozygous disruption of the beclin 1 autophagy gene. *J Clin Invest*. 2003;112(12):1809–1820.
43. Yue Z, Jin S, Yang C, Levine AJ, Heintz N. Beclin 1, an autophagy gene essential for early embryonic development, is a haploinsufficient tumor suppressor. *Proc Natl Acad Sci U S A*. 2003;100(25):15077–15082.
44. Levine B, Kroemer G. Autophagy in the pathogenesis of disease. *Cell*. 2008;132(1):27–42.
45. Koike M, et al. Inhibition of autophagy prevents hippocampal pyramidal neuron death after hypoxic-ischemic injury. *Am J Pathol*. 2008;172(2):454–469.
46. Salazar M, et al. Cannabinoid action induces autophagy-mediated cell death through stimulation of ER stress in human glioma cells. *J Clin Invest*. 2009;119(5):1359–1372.
47. Berry DL, Baehrecke EH. Growth arrest and autophagy are required for salivary gland cell degradation in Drosophila. *Cell*. 2007;131(6):1137–1148.
48. Denton D, et al. Autophagy, not apoptosis, is essential for midgut cell death in Drosophila. *Curr Biol*. 2009;19(20):1741–1746.
49. Laane E, et al. Cell death induced by dexamethasone in lymphoid leukemia is mediated through initiation of autophagy. *Cell Death Differ*. 2009;16(7):1018–1029.
50. Bornhauser BC, et al. Low dose arsenic trioxide sensitizes glucocorticoid-resistant acute lymphoblastic leukemia cells to dexamethasone via an Akt-dependent pathway. *Blood*. 2007;110(6):2084–2091.
51. Guertin DA, Sabatini DM. Defining the role of mTOR in cancer. *Cancer Cell*. 2007;12(1):9–22.
52. Wang Z, Malone MH, Thomenius MJ, Zhong F, Xu F, Distelhorst CW. Dexamethasone-induced gene 2 (dig2) is a novel pro-survival stress gene induced rapidly by diverse apoptotic signals. *J Biol Chem*. 2003;278(29):27053–27058.
53. Balgi AD, et al. Screen for chemical modulators of autophagy reveals novel therapeutic inhibitors of mTORC1 signaling. *PLoS ONE*. 2009;4(9):e7124.
54. Bachmann PS, et al. Divergent mechanisms of glucocorticoid resistance in experimental models of pediatric acute lymphoblastic leukemia. *Cancer Res*. 2007;67(9):4482–4490.
55. Tissing WJ, et al. Glucocorticoid-induced glucocorticoid-receptor expression and promoter usage is not linked to glucocorticoid resistance in childhood ALL. *Blood*. 2006;108(3):1045–1049.
56. Degterev A, et al. Chemical inhibitor of nonapoptotic cell death with therapeutic potential for ischemic brain injury. *Nat Chem Biol*. 2005;1(2):112–119.
57. Iwamoto S, Mihara K, Downing JR, Pui CH, Campana D. Mesenchymal cells regulate the response of acute lymphoblastic leukemia cells to asparaginase. *J Clin Invest*. 2007;117(4):1049–1057.
58. Janssen K, Pohlmann S, Janicke RU, Schulze-Osthoff K, Fischer U. Apaf-1 and caspase-9 deficiency prevents apoptosis in a Bax-controlled pathway and promotes clonogenic survival during paclitaxel treatment. *Blood*. 2007;110(10):3662–3672.
59. Samraj AK, Stroh C, Fischer U, Schulze-Osthoff K. The tyrosine kinase Lck is a positive regulator of the mitochondrial apoptosis pathway by controlling Bak expression. *Oncogene*. 2006;25(2):186–197.

blood

2010 115: 1006-1017
Prepublished online Nov 24, 2009;
doi:10.1182/blood-2009-08-235408

Down syndrome acute lymphoblastic leukemia, a highly heterogeneous disease in which aberrant expression of CRLF2 is associated with mutated JAK2: a report from the International BFM Study Group

Libi Hertzberg, Elena Vendramini, Ithamar Ganmore, Gianni Cazzaniga, Maike Schmitz, Jane Chalker, Ruth Shiloh, Ilaria Iacobucci, Chen Shochat, Sharon Zeligson, Gunnar Cario, Martin Stanulla, Sabine Strehl, Lisa J. Russell, Christine J. Harrison, Beat Bornhauser, Akinori Yoda, Gideon Rechavi, Dani Bercovich, Arndt Borkhardt, Helena Kempski, Geertruy te Kronnie, Jean-Pierre Bourquin, Eytan Domany and Shai Izraeli

Blood (print ISSN 0006-4971, online ISSN 1528-0020), is published semimonthly by the American Society of Hematology, 1900 M St, NW, Suite 200, Washington DC 20036.

Down syndrome acute lymphoblastic leukemia, a highly heterogeneous disease in which aberrant expression of *CRLF2* is associated with mutated *JAK2*: a report from the International BFM Study Group

*Libi Hertzberg,[1-3] *Elena Vendramini,[4] *Ithamar Ganmore,[1,2] Gianni Cazzaniga,[5] Maike Schmitz,[6] Jane Chalker,[7] Ruth Shiloh,[1] Ilaria Iacobucci,[8] Chen Shochat,[1,2,9] Sharon Zeligson,[1] Gunnar Cario,[10] Martin Stanulla,[10] Sabine Strehl,[11] Lisa J. Russell,[12] Christine J. Harrison,[12] Beat Bornhauser,[6] Akinori Yoda,[13] Gideon Rechavi,[1,2] Dani Bercovich,[9] Arndt Borkhardt,[14] Helena Kempski,[7] †Geertruy te Kronnie,[4] †Jean-Pierre Bourquin,[6] †Eytan Domany,[3] and †Shai Izraeli[1,2]

[1]Pediatric Hemato-Oncology and the Cancer Research Center, Sheba Medical Center, Tel Hashomer, Ramat-Gan, Israel; [2]Sackler Faculty of Medicine, Tel Aviv University, Tel Aviv, Israel; [3]Department of Physics of Complex Systems, Weizmann Institute of Science, Rehovot, Israel; [4]Hemato-Oncology Laboratory, Department of Pediatrics, University of Padova, Padova, Italy; [5]Centro Ricerca Tettamanti, Clinica Paediatrica Università di Milano-Bicocca, Ospedale San Gerardo, Monza, Italy; [6]Department of Pediatric Oncology, University Children's Hospital, University of Zurich, Zurich, Switzerland; [7]Paediatric Malignancy Cytogenetics Unit, Camelia Botnar Laboratories, Great Ormond Street Hospital & Institute of Child Health, London, United Kingdom; [8]Department of Hematology/Oncology L. and A. Seràgnoli, University of Bologna, Bologna, Italy; [9]Human Molecular Genetics and Pharmacogenetics Laboratory, Migal–Galilee Biotechnology Center, Kiryat Shmona, and Tel-Hai Academic College, Tel Hai, Israel; [10]Department of Pediatrics, University Hospital Schleswig-Holstein, Campus Kiel, Kiel, Germany; [11]Children's Cancer Research Institute, St Anna Kinderkrebsforschung, Vienna, Austria; [12]Leukaemia Research Cytogenetics Group, Northern Institute for Cancer Research, Newcastle University, Newcastle, United Kingdom; [13]Department of Medical Oncology, Dana-Farber Cancer Institute, Harvard Medical School, Boston, MA; and [14]Clinic of Pediatric Oncology, Hematology, and Clinical Immunology, Children's University Hospital, Heinrich Heine University, Düsseldorf, Germany

We report gene expression and other analyses to elucidate the molecular characteristics of acute lymphoblastic leukemia (ALL) in children with Down syndrome (DS). We find that by gene expression DS-ALL is a highly heterogeneous disease not definable as a unique entity. Nevertheless, 62% (33/53) of the DS-ALL samples analyzed were characterized by high expression of the type I cytokine receptor *CRLF2* caused by either immunoglobulin heavy locus (*IgH@*) translocations or by interstitial deletions creating chimeric transcripts *P2RY8-CRLF2*. In 3 of these 33 patients, a novel activating somatic mutation, F232C in *CRLF2,* was identified. Consistent with our previous research, mutations in R683 of *JAK2* were identified in 10 specimens (19% of the patients) and, interestingly, all 10 had high *CRLF2* expression. Cytokine receptor-like factor 2 (CRLF2) and mutated Janus kinase 2 (Jak2) cooperated in conferring cytokine-independent growth to BaF3 pro-B cells. Intriguingly, the gene expression signature of DS-ALL is enriched with DNA damage and *BCL6* responsive genes, suggesting the possibility of B-cell lymphocytic genomic instability. Thus, DS confers increased risk for genetically highly diverse ALLs with frequent overexpression of *CRLF2,* associated with activating mutations in the receptor itself or in *JAK2*. Our data also suggest that the majority of DS children with ALL may benefit from therapy blocking the CRLF2/JAK2 pathways. (Blood. 2010;115:1006-1017)

Introduction

Children with Down syndrome (DS) have a higher rate of acute lymphoblastic leukemia (DS-ALL). DS-ALLs are mostly of B-cell precursor (BCP) origin and similar in the age of diagnosis and immunophenotype to high hyperdiploid (HD) or *TEL-AML*1 ALLs,[1] the 2 most common genetic subtypes of childhood ALL. Given that these cytogenetic abnormalities are less frequent in DS-ALL,[2] the existence of unique collaborating somatic genetic events in DS-ALL, similar to the *GATA1* mutation in DS-acute megakaryoblastic leukemia,[3] has been postulated.

We and others reported the presence of somatic activating mutations in *JAK2* in approximately 20% of DS-ALLs.[4-6] Similar mutations are present in approximately 10% of high-risk ALLs in non-DS children, corresponding to approximately 3% of unselected childhood ALLs.[7] We hypothesized that the mutated Janus kinase 2 (JAK2) may cooperate with a type I cytokine receptor that is aberrantly expressed in DS-ALL.[4]

To characterize additional molecular abnormalities in DS-ALL, we performed genomic analysis of a large group of DS-ALLs. This analysis reveals, next to a striking heterogeneity of these leukemias, an aberrant expression of the cytokine receptor *CRLF2* in 62% of the patients, associated with somatic activating mutations in *JAK2* or in the receptor itself.

Methods

Patient samples

RNA and DNA were derived from diagnostic bone marrow samples of children with DS and BCP-ALL enrolled on treatment protocols with an informed consent and approval of the ethics committees of all participating institutions in accordance with the Declaration of Helsinki. Samples were

Submitted August 5, 2009; accepted November 1, 2009. Prepublished online as *Blood* First Edition paper, November 24, 2009; DOI 10.1182/blood-2009-08-235408.

*L.H., E.V., and I.G. are co–first authors.

†G.t.K., J.-P.B., E.D., and S.I. are co–senior authors.

The online version of this article contains a data supplement.

The publication costs of this article were defrayed in part by page charge payment. Therefore, and solely to indicate this fact, this article is hereby marked "advertisement" in accordance with 18 USC section 1734.

Table 1. Description of the gene expression datasets analyzed

Dataset symbol	No. samples					Platform
	Total	DS-ALL	HD	TEL-AML1	Other	
AIEOP*	97	25	26	29	4 E2A-PBX1, 6 MLL, 7 BCR-ABL	Affymetrix HG-U133 Plus 2.0
ICH	15	6	5	4		Affymetrix HG-U133 Plus 2.0
BFM[8]* + St Jude[10]†	36	7	12	17		Affymetrix HG-U133A
IL†	27	11	10	6		Affymetrix Exon 1.0 ST

AIEOP indicates Associazione Italiana Ematologia Oncologia Pediatrica; ICH, Institute Child Health; BFM, Berlin-Frankfurt-Munster; and IL, Israel.
*IL is partially overlapping with AIEOP (5 DS-ALLs) and BFM (4 different DS-ALLs).
†We used a subgroup of HD and TEL-AML1 samples from St Jude dataset.

anonymized for the study. Patients' clinical data are described in supplemental Tables 1 and 2 (available on the *Blood* website; see the Supplemental Materials link at the top of the online article). Seventy-six of these patients were included in our previous publication describing the *JAK2* mutations in DS-ALL.[4] The study was approved by the Israeli Health Ministry Ethic committee (approval no. 920070771).

Genomic studies

RNA processing and hybridization to Affymetrix arrays were performed according to the manufacturer's instructions and as previously published.[8,9] Only specimens containing more than 70% blasts were included. There were 4 datasets obtained by different teams as summarized in Table 1. Associazione Italiana Ematologia Oncologia Pediatrica (AIEOP) is the main dataset used for gene expression analysis, comprising 97 diagnostic ALL samples: 25 DS-ALL, and 72 non–DS-ALL samples, described in Table 1. The additional 3 datasets were used for validations. The primary gene expression data files have been deposited in National Center for Biotechnology Information's Gene Expression Omnibus (GEO; http://www.ncbi.nlm.nih.gov/geo/)[11] (GEO series accession no. GSE17459).

Genomic DNA from 42 diagnostic bone marrow ALLs and 34 paired remission samples were genotyped with Affymetrix GeneChip Human Mapping 100K set (Affymetrix) according to the manufacturer's directions. See supplemental data for details.

Mutation analysis

Mutation analysis was performed as we previously described.[4,12] *CRLF2* (NM_022148.2) primers are described in supplemental Table 3.

Quantitative real-time PCR

Quantitative real-time polymerase chain reaction (qRT-PCR) was performed using Applied Biosystems TaqMan Gene-Expression Assays (*CRLF2* Hs_00845692, *GAPDH* Hs_99999905) according to the manufacturer's instructions. Each sample was run in triplicate. The endogenous control gene was *GAPDH*.

FISH

Fluorescence in situ hybridization (FISH) for detection of *IGH@-CRLF2* translocation or the presence of a microdeletion upstream to *CRLF2* was performed as described.[13]

Flow cytometric analysis

Flow cytometric analysis (FACSCanto II [Becton Dickinson]; FlowJo software [TreeStar]) was performed on primary cryopreserved ALL cells after the first xenotransplantation in Nod/LtSzScid interleukin-2γ (IL2γ)–null mice. Antibodies used were anti–cytokine receptor-like factor 2 (CRLF2; clone 1D3, ab48482; Abcam), goat anti–mouse Alexa Fluor 488 (Invitrogen), anti-IL7RA Alexa 647 (CD127, clone HIL-7R-M21; BD), anti-CD19 phycoerythrin (clone LT19, MCA1940; AbD Serotec), and 7-amino-actinomycin D (AbD Serotec). All samples were gated on the viable (7-amino-actinomycin D–negative) and leukemic ($CD19^+$) population before analysis of CRLF2 and IL7RA. For the calculation of delta mean fluorescence intensity (MFI), background nonspecific staining was evaluated in populations gated by CD19, comparing tubes with or without anti-CRLF2 antibodies. This background MFI was similar to the MFI of CRLF2-negative populations in normal human blood.

Plasmid construction

The *FLAG-mJak2* wild-type and R683S were cloned into the pHRSINCSGW lentivirus,[12] which carries spleen focus-forming virus (SFFV) promoter and an emerald green fluorescent protein reporter. pMX-Puro-hCRLF2 was used as a template for the generation of *CRLF2* mutations by site-directed mutagenesis (QuikChange-II-XL; Stratagene).

Cell lines

BaF3 cells were cultured in RPMI-1640 containing 10% fetal calf serum and 10% WHEI-3B conditioned media as a source of interleukin-3.

Parental BaF3 cells were transduced with pMX-Puro-hCRLF2,[14] and *hCRLF2*-expressing cells were selected with puromycin (2 μg/mL). Parental BaF3 and BaF3-CRLF2 cells were transduced with the appropriate *Jak2*-expressing vector and green fluorescent protein–positive cells were sorted by flow cytometry 3 to 4 days later.

BaF3 proliferation assays and Western blotting

BaF3 proliferation assays and Western blotting were performed as described before.[4] Antibodies used were anti-JAK2 (C-20; Santa Cruz Biotechnology), anti–signal transducer and activator of transcription 5 (STAT5), anti–phospho-JAK2 Tyr1007 (Cell Signaling Technology), anti–phospho-STAT5 Tyr694 (Epitomics), anti–human thymic stromal lymphopoietin (hTSLPR; AF981; R&D Systems), anti–FLAG-M2, and anti–α-tubulin (Sigma-Aldrich).

Pharmacologic inhibition of JAK2

BaF3 cells expressing Jak2 R683S and BaF3/CRLF2 cells expressing wild-type (wt) or R683S Jak2 were cultured without cytokines in different concentrations of JAK inhibitor I (Calbiochem). Controls were BaF3/EpoR cells expressing BCR-ABL. Viable cells were counted after 72 hours. Data from 3 independent experiments were combined for analysis. We calculated the normalized viability by dividing the cell number at each inhibitor concentration by the cell number with vehicle alone.

Bioinformatics

Gene expression preprocessing is described in supplemental Methods.

Combining probe sets of the same gene. For those genes that were represented by more than one probe set, we used, when needed, a combination procedure to create a single representation of a gene's expression (supplemental Methods).

GSEA. The first ingredient of Gene Set Enrichment Analysis (GSEA)[15] is a list of genes *(L),* ranked by some attribute *(A),* ordered from low to high values of *A*. The second ingredient is a set of genes *(S)* that is a subset of *L*. GSEA aims at answering whether the members of *S* are randomly distributed along the ranked list *L*, or whether they are skewed toward one of the sides. For details see supplemental Methods and Subramanian et al.[15]

Refining DS-ALL profile genes. The preliminary DS-ALL profile gene list, which was constructed using the AIEOP dataset, was narrowed down using GSEA[15] to select genes that show consistent expression pattern in at least 2 of the other 3 datasets (Table 1). We used the up-regulated members

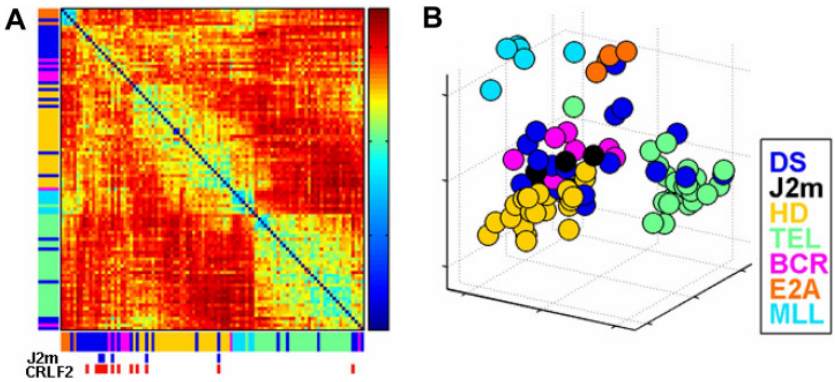

Figure 1. Unsupervised analysis of the AIEOP dataset. (A) Samples' Euclidian distance matrix. The color in each entry (y,x), where x,y = 1, . . . , 97 (the number of samples), represents the Euclidian distance between the expression profiles of samples x and y. It was measured after centering and normalization of each sample's expression, using 1500 probe sets with highest standard deviation. The samples are ordered by SPIN along both the x-axis and y-axis. The color bars next to both axes represent the different ALL subtypes, listed on the right of the figure. The blue marks at bottom specify DS-ALL samples with mutant JAK2 (J2m), and the red marks specify samples with high CRLF2 expression levels (CRLF2) (see "Aberrant expression of the cytokine receptor CRLF2 in DS-ALLs" section on CRLF2). (B) Projection of all samples onto the first 3 principle components of the expression. DS indicates Down syndrome ALL; J2m, Down syndrome ALL with mutated JAK2 R683; HD, high hyperdiploid; TEL, TEL-AML1; BCR, BCR-ABL; E2A, E2A-PBX1; and MLL, MLL-AF4.

of the preliminary DS-ALL genes as our set *S* (see "Bioinformatics") and the genes of 1 of the other 3 experiments constituted *L*. The genes of *L* were ordered according to their differential expression in DS versus the rest of the samples (see Refining DS-ALL profile genes in supplemental Methods). The process was repeated for each of the 3 datasets and for the down-regulated genes, yielding for each case genes that were identified as consistently up-regulated (or down-regulated) in the AIEOP dataset and the other dataset tested (Figure 2A).

Results

Marked heterogeneity of DS-ALLs revealed by unsupervised gene expression analysis

We first explored the extent of similarity between DS-ALLs and other defined BCP-ALL genetic subtypes using in the analysis the 1500 probe sets with the highest standard deviation among the AIEOP samples. Two unsupervised analysis algorithms were used: Sorting Points Into Neighborhoods (SPIN),[16] which places samples with similar expression profiles near each other (Figure 1A), and Principal Component Analysis (PCA; MATLAB 7.4 software [Mathworks]; Figure 1B). Both gave similar results.

In agreement with previous studies,[10] unsupervised analysis of gene expression tends to group the pediatric ALL samples according to their genetic subtypes. As can be seen in the Euclidian distance matrix in Figure 1A, the ALL subgroups that are the most homogenous (exhibiting high similarity of samples of the same subtype) are *E2A-PBX1*–positive ALL and *MLL-AF4*–positive ALL, followed by *TEL-AML1*–positive ALL. HD-ALL samples are also grouped together, but are relatively more distant from each other than the *E2A-PBX1*, *MLL-AF4*, and *TEL-AML1* samples. Although *BCR-ABL* ALLs are clustered together, they are less homogeneous, consistent with previous reports.[10]

In contrast, DS-ALLs are very heterogeneous (Figure 1A-B). Approximately half are grouped together, relatively close to both *BCR-ABL* and HD-ALL. However even here, individual DS samples are further separated from each other than a typical pair of samples within the other ALL subtypes (Figure 1A-B). The other half are grouped with other ALL subtypes: 6 with *TEL-AML1*, 6 with HD, 2 with *BCR-ABL,* and 1 with *E2A-PBX1*. Of these 15 DS-ALLs, only 3 carried the chromosomal translocation of the subtype of ALL to which they are most similar (1 *E2A-PBX1*, 2 *TEL-AML1*) and only 1 DS-ALL sample was found to be also HD. Even the 5 DS-ALL samples with somatic mutations in *JAK2* (blue boxes below Figure 1A and black circles at Figure 1B) are not clustered together.

This unsupervised gene expression analysis reveals that DS-ALLs are markedly less homogenous than the other ALL genetic subtypes. It suggests that DS is a predisposing condition to several genetic subtypes of B-cell precursor ALLs, and that unlike the myeloid leukemia of DS should not be considered as a unique molecular entity.

Genomic analysis of DS-ALL

We performed 100-K single nucleotide polymorphism array analysis of 34 paired diagnosis and remission samples (15 DS-, 9 HD-, and 10 *TEL-AML* ALLs, supplemental Methods). Copy number and loss-of-heterozygosity analyses (supplemental Figure 3; supplemental Table 10) generally confirm previous reports[5,17] that deletions are more common in DS and *TEL-AML1* compared with HD-ALLs. The frequency of deletions in genes regulating normal B-lymphoid development (supplemental Table 9) in DS-ALL was 53%, slightly higher than the 40% reported for of BCP-ALL.[18] Recently, deletions in the *IKZF1* gene were reported in the majority of patients with *BCR/ABL* and "*BCR/ABL*-like" ALL.[19,20] Because most of these deletions involve only a subset of exons (most commonly exons 4-7), the 100-K single nucleotide polymorphism platform is inadequate to detect these abnormalities. Therefore, 38 additional diagnostic DS-ALL specimens were screened for *IKZF1* deletions by PCR analysis as previously reported.[21] Monoallelic *IKZF1* deletions were identified in 9 patients (24%; supplemental Table 8 and supplemental Figure 3). Thus the frequency of deletions in B-cell differentiation genes, including *IKZF1,* in DS-ALL is similar to other non–*BCR-ABL* subtypes of BCP-ALL.

DS-ALL gene expression profile

We hypothesized that, despite their heterogeneity, DS-ALLs share a common gene expression signature. We reasoned that by comparing the gene expression in DS-ALL to the relatively similar groups, HD and *TEL-AML1,* we could potentially isolate the "DS-ALL" characteristics from the other ALL characteristics that might be similar between these groups. In addition, the analysis was done in a way that only genes that differentiate DS from *TEL-AML1* and from HD-ALLs are depicted. The fact that *TEL-AML1* and HD-ALLs have dissimilar expression profiles (denoted by dark red entries in Figure 1A) helps to identify genes that characterize DS-ALL, and not one of the groups to which it is compared.

We first identified probe sets that had significant differential expression in DS-ALL samples, compared with both HD and *TEL-AML1* ALLs in the AIEOP dataset (supplemental Methods).

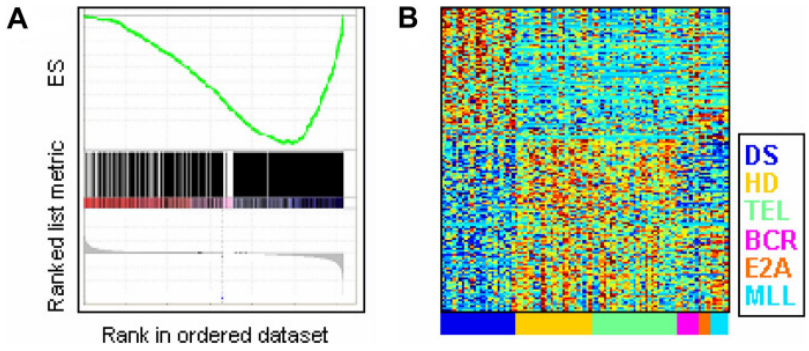

Figure 2. DS-ALL gene expression profile. (A) GSEA analysis on ICH dataset. Genes are ranked (bottom of panel, gray) according to their expression in DS-ALL samples versus the rest of the samples, by GSEA, using the default parameters. The members of a gene set *S* (here, the set of 535 genes down-regulated in DS-ALL, AIEOP data) are tested: are they randomly distributed in the ranked gene list, or primarily found at the top or bottom? Occurrences of members of the gene set *S* in the ranked gene list are shown as vertical black lines above the ranked signature. The green curve and upper y-axis represent the enrichment score (ES) as a function of the number of ranked genes tested for enrichment of gene set *S*. See supplemental Methods for full details. (B) Expression levels of the genes from the refined DS-ALL lists, measured on the AIEOP dataset. Four hundred twenty-three probe sets that belong to the refined DS-ALL profile gene lists are centered and normalized. Values for each individual case are represented by a color, with red representing deviation above the mean and blue representing deviation below the mean. The colors along the x-axis represent the different ALL subtypes, listed on the right of the plot. DS indicates Down syndrome ALL; HD, high hyperdiploid; TEL, TEL-AML1; BCR, BCR-ABL; E2A, E2A-PBX1; and MLL, MLL-AF4.

This "preliminary DS-ALL profile" consisted of 792 genes up-regulated and 535 genes down-regulated in DS-ALL. To check consistency with each of the other 3 gene expression datasets ("BFM," "ICH," and "IL"), we performed GSEA[22] separately on each of the 3. A representative enrichment analysis is shown in Figure 2A; here the genes are ordered according to their DS-ALL differential expression in the ICH dataset (used as the list *L;* "Bioinformatics"), and the 535 genes down-regulated in DS-ALL are used as the set *S,* tested for enrichment. Six such analyses showed significant enrichment of the preliminary gene lists (both up- and down-regulated) obtained from AIEOP, in the other 3 datasets (Table 2). We refined our AIEOP-based lists by including only genes that showed consistent expression patterns in at least 2 of the 3 other datasets. The "refined DS-ALL profile genes" (Figure 2B) consists of 152 up-regulated and 199 down-regulated genes (supplemental Tables 4-5).

Pathway analysis and *BCL6* signature

To identify molecular pathways that showed differential expression in the refined DS-ALL profile, we interrogated the DAVID database[23] of Gene Ontology functional categories.[24] Constituent genes of 8 pathways were significantly (false discovery rate [FDR] $< 10\%$) overrepresented in the DS-ALL expression profile (Table 3 and supplemental Table 6). The most enriched pathway ($P < .001$) is "Response to DNA damage stimulus": 10 of the 341 genes assigned by DAVID to this pathway are down-regulated and 6 are up-regulated in DS-ALL. One of the up-regulated genes is *BCL6,* with a mean fold change of 1.46 in DS-ALL compared with non DS-ALL (supplemental Table 4). BCL6 is a transcription factor expressed primarily in mature B cells at the germinal centers, where it facilitates immunoglobulin (Ig) affinity maturation by repressing the DNA damage response. It is also a known oncogene in diffuse large B-cell lymphomas.[25,26]

To search for evidence for BCL6 activity in the DS-ALL gene expression profile, we used the Oncomine (http://www.oncomine.org)[27,28] database, in which cancer gene expression signatures derived from different expression analyses are stored as molecular concept maps. These are lists of differentially expressed genes between 2 logical groupings of normal or malignant human tissue or cell lines. We tested BCL6 direct targets and each of the 24 Oncomine molecular concept maps that involve BCL6 (supplemental Table 7) for enrichment in DS-ALL up- and down-regulated genes, and 8 of these 25 gene groups passed at false discovery rate (FDR)[29] of 15% (Table 4). These include the target genes of BCL6,[32] genes modified by ectopic expression of BCL6 in lymphoblastoid B cells,[30] and the gene expression signature of B-cell lymphomas with oncogenic activation of BCL6.[31] Hence the targets and pathways downstream to BCL6 in lymphomas and mature B cells are modified in the DS-ALL expression profile.

Aberrant expression of the cytokine receptor *CRLF2* in DS-ALLs

We have previously hypothesized that a cytokine receptor may be aberrantly expressed in DS-ALL and cooperate with JAK2 carrying

Table 2. GSEA for genes of the DS-ALL expression signature, identified from the AIEOP dataset, in 3 other datasets

	Enrichment score	Nominal *P*	FDR q-value
DS-ALL up-regulated genes			
ICH dataset	0.437993	.010	0.008979
IL dataset	0.361621	.035	0.022851
BFM dataset	0.344479	.002	0.009101
DS-ALL down-regulated genes			
ICH dataset	−0.50601554	.006	0.012959
IL dataset	−0.5008136	.012	0.006397
BFM dataset	−0.55240697	.002	0.001131

Table 3. Gene ontology pathways overrepresented in the differential DS-ALL signature

Gene ontology group	Size	*P*	FDR, %
GO:0006974~ response to DNA damage stimulus	16	< .001	0.77
GO:0006397~ mRNA processing	13	.002	2.80
GO:0015031~ protein transport	24	.002	3.30
GO:0008104~ protein localization	26	.002	3.70
GO:0046907~ intracellular transport	24	.003	4.40
GO:0065003~ macromolecular complex assembly	20	.004	5.80
GO:0051649~ establishment of cellular localization	27	.005	7.60
GO:0043067~ regulation of programmed cell death	19	.006	9.10

For details, see supplemental Table 6.

Table 4. Enrichment of BCL6-related gene expression signatures and direct targets in DS-ALL profile genes (FDR < 15%)

	Size	*P*	Q-value
Oncomine "Molecular Concepts" enriched in DS-ALL up-regulated genes			
EREB lymphoblastoid cell line BCL6 transfection top 10% overexpressed[30]	17	.004	0.093
Ramos Burkitt lymphoma cell line BCL6 pest mutant top 5% underexpressed in anti-IgM[30]	11	.011	0.138
Lymphoma BCL6 break top 5% overexpressed[31]	11	.019	0.138
Lymphoma BCL6 break top 10% overexpressed[31]	17	.022	0.138
BCL6 direct targets[32]	11	.030	0.147
Oncomine "Molecular Concepts" enriched in DS-ALL down-regulated genes			
Lymphoma BCL6 break top 10% underexpressed[31]	36	< .001	0.001
EREB lymphoblastoid cell line BCL6 transfection top 10% underexpressed[30]	26	< .001	0.001
Lymphoma BCL6 break top 5% underexpressed[31]	20	.001	0.008

the "lymphoid" mutation in R683.[4] Examination of the DS-ALL expression signature (supplemental Table 4) reveals that the third most differentially expressed gene is *CRLF2* (cytokine receptor-like factor 2, *TSLPR*) located at the pseudoautosomal region of the sex chromosomes. As depicted in Figure 3A, increased expression of *CRLF2* was noted in 23 (62.1%) DS-ALLs of 37 samples that were hybridized to U133 family of arrays (*CRLF2* is not represented on the exon arrays used in the IL dataset), compared with other ALL subtypes (see supplemental Methods). *CRLF2* expression along DS-ALL versus all other ALL subtypes yielded *t* test *P* values less than .001 for AIEOP, BFM, and ICH datasets.

CRLF2 is known to dimerize with IL7RA to form the heterodimeric receptor for thymic stromal lymphopoietin (TSLP).[33] Whereas *CRLF2* is aberrantly expressed in DS-ALLs (Figure 3A), expression of *IL7RA* is similar in the different ALL subtypes (Figure 3B).

To validate the findings of the expression arrays and to analyze additional DS-ALL samples, we measured the expression of *CRLF2* by qRT-PCR in 32 patients (Figure 3C). Microarray data were available for 16 of these cases. The qRT-PCR confirms the *CRLF2* expression levels seen in the arrays (Pearson correlation = 0.85, $P < .001$). In 2 patients' *CRLF2* expression was analyzed in RNA derived from diagnostic and remission bone marrows and was seen only in the diagnostic sample. In one patient, similar *CRLF2* expression levels were seen in bone marrow samples from diagnosis and relapse (supplemental Figure 2). Altogether, 33 (62.3%) of 53 DS-ALL patients analyzed by either qRT-PCR or microarrays overexpressed *CRLF2*. The surface expression of the CRLF2 protein was also verified on 4 samples by flow cytometry (Figure 3D). IL7RA is also expressed on the leukemic blasts independent of CRLF2 expression.

Recently, Russell et al[13] reported aberrant expression of *CRLF2* caused by either chromosomal translocations to the *IGH@* locus or interstitial deletions upstream to *CRLF2* juxtaposing *CRLF2* with the *P2RY8* regulatory elements in approximately 5% of childhood ALLs. To examine whether the increased *CRLF2* expression in our specimens was caused by the same genomic aberrations, 12 available diagnostic DS-ALL samples overexpressing *CRLF2* were analyzed by FISH (Figure 4A). *IGH@* translocations were seen in 4 specimens and interstitial deletions in 7. In the remaining sample (no. DS-32; supplemental Table 2), in which the CRLF2 expression level was just above the threshold, the FISH pattern of CRLF2 appeared normal. Further evidence supporting the presence of the deletions is provided by a statistically significant inverse correlation between *CRLF2* and *P2RY8* expression ($P = .02$, Figure 4B).

To test whether the deletion caused a fusion between the *P2RY8* and *CRLF2,* we performed RT-PCR with primers derived from both genes (supplemental Table 3). A transcript fusing the first noncoding exon of P2RY8 and the first exon of CRLF2 prior to the ATG was detected in the 2 DS patients with the deletion detected by FISH but not in the patient with the IgH@ translocation (Figure 4C). A similar chimeric transcript was described in a single patient with splenic lymphoma, fusing P2RY8 to SOX5 resulting in overexpression of SOX5.[34] We extended the analysis and identified the chimeric transcript in 7 of 10 patients with overexpression of CRLF2 and in none of 8 samples with no expression of CRLF2 (supplemental Table 2). Thus, consistent with the FISH findings,[13] the interstitial deletion is more common than the IgH@ translocation.

To explore the effect of CRLF2 on gene expression, we compared the 30% of DS-ALLs with the highest *CRLF2* expression and the 30% of DS-ALLs with the lowest *CRLF2* expression in the AIEOP database. Only 5 probe sets passed FDR of 30%, with *CRLF2* being 1 of the 5 (Table 5). This is consistent with the finding that samples that overexpress *CRLF2* (red marks in Figure 1A) do not cluster separately from DS-ALLs that do not express *CRLF2*. Interestingly, the *IGJ* gene that differentiates these 2 groups (fold change, 36.4; Table 5) is also the most differentiating gene between DS-ALL and non–DS-ALL in our datasets (supplemental Table 4).

Clinical significance of *CRLF2* expression in DS-ALL

Clinically, children with high/medium expression of *CRLF2* were diagnosed younger (Table 6) than children with no/low expression of *CRLF2* (5.56 vs 9.87 years, $P = .004$).

No significant differences between the 2 groups regarding their sex or white blood cell count at diagnosis were found. Patients expressing *CRLF2* tended to have a lower probability for event-free survival (supplemental Figure 4, $P = .12$ log-rank test).

Cooperation between *JAK2 R683* mutations and *CRLF2* aberrant expression

Among the 53 DS-ALL samples for which *CRLF2* expression was available, 10 had somatic mutations in *JAK2 R683*. We identified chimeric P2RY8-CRLF2 transcripts in 3 additional patients with JAK2 R683 mutations (supplemental Table 2). Thus all mutations occurred in specimens with aberrant expression of *CRLF2,* supporting our initial hypothesis that CRLF2 may act as type I cytokine receptor for mutated JAK2.

To examine whether CRLF2 and mutated JAK2 cooperate, we generated BaF3 cells that express hCRLF2 (BaF3-CRLF2) and transduced both BaF3 and BaF3-CRLF2 cells with wild-type m*Jak2-FLAG*, R683S m*Jak2-FLAG*, and empty vector. As depicted in Figure 5A, there was synergism between CRLF2 and both wt Jak2 and R683S mutated Jak2, with the best cytokine-independent growth observed in cells expressing CRLF2 and the mutated Jak2. These functional effects on cell growth are reflected

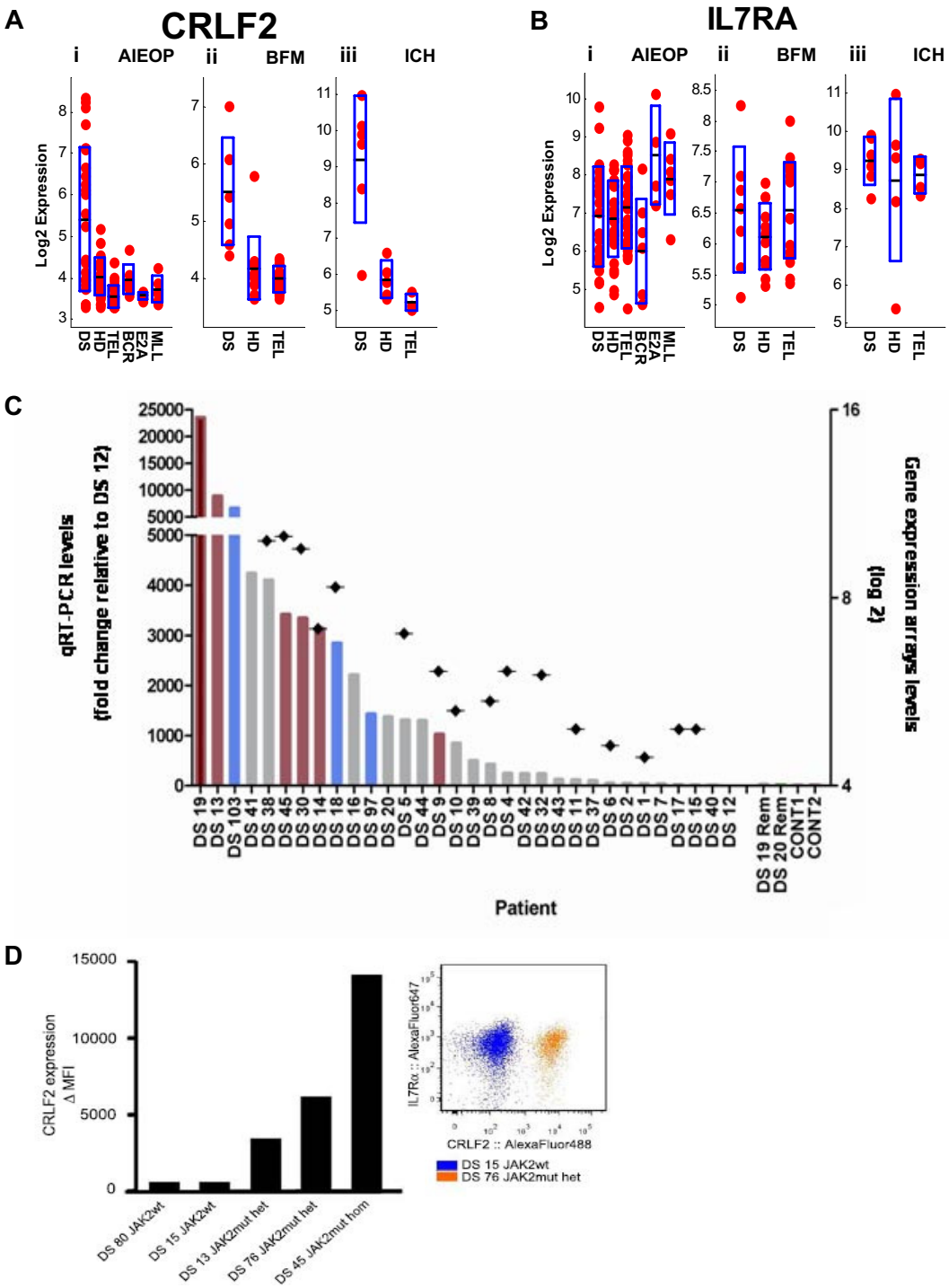

Figure 3. CRLF2 expression in DS-ALL. (A) CRLF2 expression in the AIEOP (i), BFM (ii), and ICH (iii) datasets. The y-axis represents CRLF2 log basis 2 expression. The x-axis represents the different ALL subtypes. Each point corresponds to a sample. The black line in each ALL subtype is the CRLF2 mean (log basis 2) expression in this subtype. The height of the blue rectangle in each ALL subtype is the measured standard deviation of CRLF2 (log basis 2) expression. DS-ALL versus all other ALL yielded *t* test *P* values of less than .001 for AIEOP (i), BFM (ii), and ICH (iii). DS indicates Down syndrome ALL; HD, high hyperdiploid; TEL, TEL-AML1; BCR, BCR-ABL; E2A, E2A-PBX1; and MLL, MLL-AF4. (B) IL7RA expression in the AIEOP (i), BFM (ii), and ICH (iii) datasets. There are no statistically significant differences between DS-ALLs and non–DS-ALLs. (C) Verification of CRLF2 expression levels by qRT-PCR. Bars represent qRT-PCR CRLF2 expression levels (left, y-axis: fold change relative to patient DS-12, the lowest CRLF2 expressor). Rhombuses represent gene expression array CRLF2 expression levels (right, y-axis: log basis 2). Red bars represent patients with JAK2 R683 mutation; blue bars, patients with CRLF2 F232C mutation (Figure 6). Rem indicates CRLF2 levels of available remission samples (patients DS-19 and DS-20); CONT, control CRLF2 expression levels in peripheral white blood cells of healthy donors. (D) CRLF2 and IL7RA protein expression on the surface of DS-ALL leukemic blasts. (Left panel) Delta mean fluorescence intensity of the signal detected by flow cytometry using specific anti-CRLF2 antibodies compared with background unspecific staining ("Flow cytometric analysis"), indicating an apparent association between the JAK2 mutational status and the level of expression of CRLF2 on DS-ALL blasts. (Right panel) Dot plot of 2 representative CRLF2 and IL7RA costainings. IL7RA is highly expressed on leukemic blasts independent of JAK2 mutational status and level of CRLF2 expression in all cases examined. wt indicates wild-type; mut, mutant; het, heterozygous; and hom, homozygous.

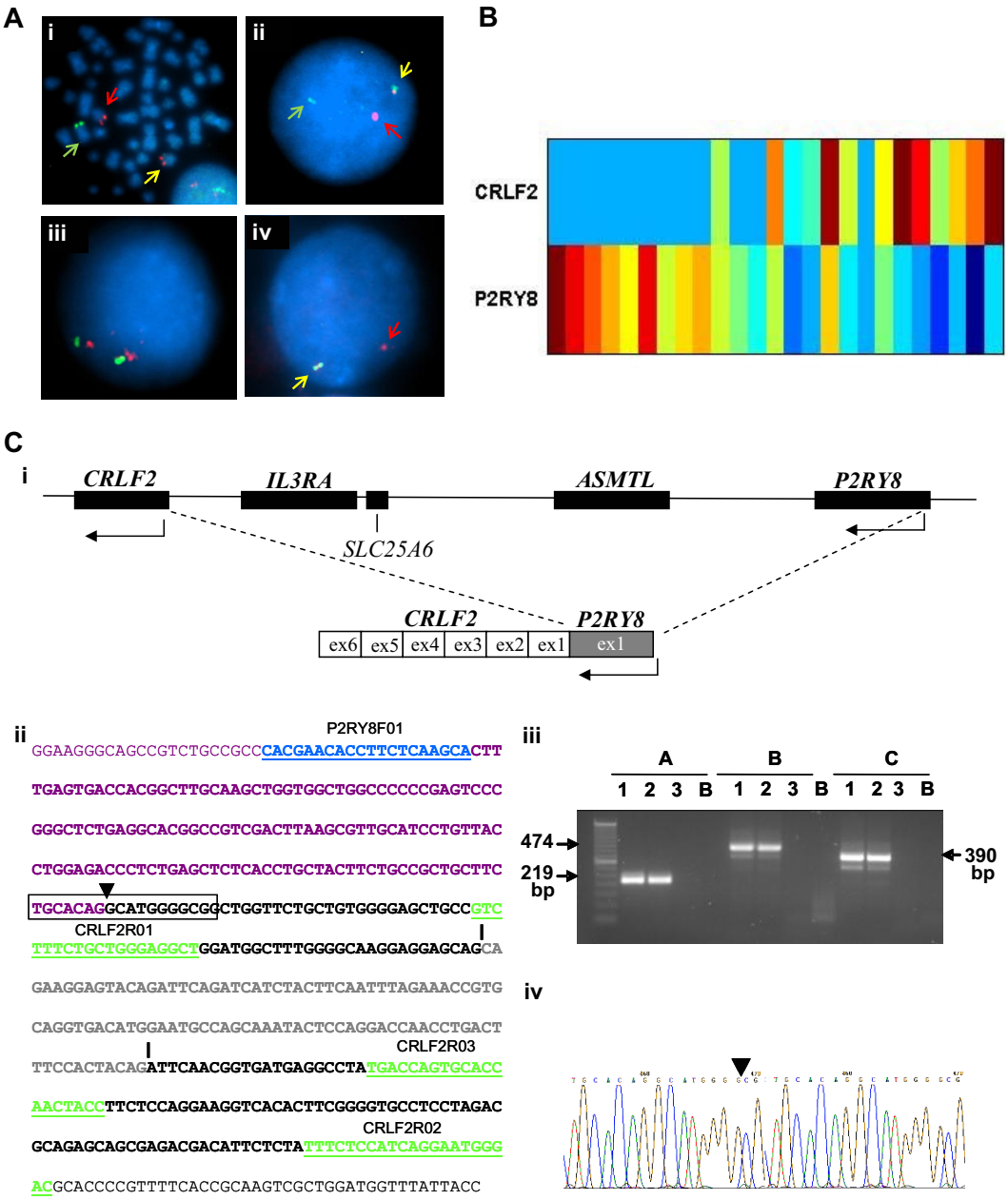

Figure 4. Genomic analysis of CRLF2 aberrations. (A) FISH analysis of DS-ALL expressing CRLF2 (i-ii) *IGH@ CRLF2* translocation, patient DS-85: (i) Metaphase showing a positive result with the LSI *IGH@* break-apart rearrangement probe (Abbott Molecular): normal chromosome 14 (yellow arrow) derived chromosome 14 (red arrow), derived X chromosome (green arrow). (ii) Interphase nucleus from the same patient hybridized with the homegrown *CRLF2* probe showing a split signal pattern, 1R1G1F, confirming its involvement in the translocation (1 fusion signal [yellow arrow], 1 red signal [red arrow], and 1 green signal [green arrow]). (iii-iv) CRLF2 microdeletion, patient DS-82. (iii) Interphase nucleus hybridized with the *IGH@* probe showing the normal 0R0G2F signal pattern confirming the presence of 2 normal copies of *IGH@*. (iv) Interphase nucleus from the same patient hybridized with the homegrown *CRLF2* probe showing the deletion of the green portion of the probe (1 red signal [red arrow] and 1 fusion signal [yellow arrow]) denoting the presence of a centromeric interstitial deletion. (B) CRLF2 and P2RY8 expression in DS-ALL samples. Centered and normalized log basis 2 expression of CRLF2 and P2RY8 along DS-ALL samples in AIEOP dataset. Values for each individual case are represented by a color, with red representing deviation above the mean and blue representing deviation below the mean. The samples are sorted using SPIN. Pearson correlation between CRLF2 and P2RY8: −0.45 ($P = .02$). (C) Detection of the *P2RY8-CRLF2* fusion transcript. (i) Schematic representation of the deletion breakpoint region at the telomeric end of chromosome X/Y with gene locations. The dashed lines represent the genomic deletion leading to the fusion of the first noncoding exon of *P2RY8* and to the first (coding) exon of *CRLF2*. (iii) RT-PCR experiments on cDNA of DS patients. (Lanes 1-3) DS diagnostic ALL samples (DS93 and DS82 with FISH determined deletion and DS92 with FISH determined IgH@ translocation). (Lane 4) Blank. The 3 patient samples were positive for *ABL* amplification (not shown). Primer sets used are (A) *P2RY8* F01/*CRLF2* R01; (B) *P2RY8* F01/*CRLF2* R02; (C) *P2RY8* F01/*CRLF2* R03 shown on the sequence on the left (ii). Chimeric transcripts are present in the first 2 lanes of each set. (ii) Nucleotide sequencing of the largest PCR fragment confirming the fusion transcript; vertical lines indicate exon boundaries; the arrowhead indicates the *P2RY8*/*CRLF2* transcript junction. As seen, the fusion is just upstream to the ATG of CRLF2. Reference sequences are P2RY8-001 (ENST00000381297) and CRLF2-001 (ENST00000400841). Boxed sequence around the transcript junction is represented in the electropherogram on the right lower side (iv).

in protein analysis of the JAK/STAT pathway (Figure 5B). Interestingly, despite identical levels of CRLF2 at the time of transduction, the levels of CRLF2 were consistently higher in cells transduced with Jak2 compared with empty vector or parental cells. Examination of Stat5 and Jak2 phosphorylation 5 hours after cytokine withdrawal reveals that when CRLF2 was expressed, phosphorylation levels in cells transduced with wt Jak2 were increased, whereas no change was observed in the already high

Table 5. CRLF2 differentiating genes

Probe set ID	Gene symbol	Description	Band	Fold change
212592_at	*IGJ*	Immunoglobulin J chain	4q13.3	36.4
208303_s_at	*CRLF2*	Cytokine receptor-like factor 2 isoform 1	Xp22.33	8.47
244871_s_at	*USP32*	Ubiquitin specific protease 32	17q23.2	2.77
221523_s_at	*RRAGD*	Ras-related GTP binding D	6q15	0.551
208765_s_at	*HNRNPR*		1p36.12	0.716

List of statistically significant differentiating genes (FDR 30%) between 8 DS-ALL samples with highest CRLF2 expression and 8 DS-ALL samples with lowest CRLF2 expression in AIEOP dataset. The fold change value is between the mean expression in the 2 groups.

phosphorylation levels in cells expressing the mutated Jak2. The marked advantage in cytokine-independent growth rate of cells coexpressing CRLF2 and R683S Jak2 despite similar Stat5 phosphorylation may indicate the involvement of additional signaling pathways.

To test whether the cells expressing CRLF2 and/or either wt or R683 mutated Jak2 depend on activated JAK signaling, we incubated BaF3 cells transduced with the different vectors cultured without IL3 in the presence of different concentrations of JAK inhibitor 1 (Figure 5C). Although BaF3 cells transduced with CRLF2/Jak were more sensitive to the inhibitor compared with the control cells expressing BCR-ABL ($P = .04$, analysis of variance), the cells expressing CRLF2 and mutated Jak2 were the least sensitive.

Activating mutations of *CRLF2* in DS-ALL

To identify additional events leading to *CRLF2* activation, we screened 87 diagnostic DS-ALL samples for mutations in *CRLF2* (Figure 6). In addition to polymorphisms V136M and V244M that were present also in remission samples and in healthy controls, we identified in 3 patients a somatic mutation replacing phenylalanine 232, located at the juxtamembranous domain, with cysteine (F232C). Genomic data were available for one of the patients (DS-97) who displayed the *P2YR8-CRLF2* transcript. Although F232C induced constitutive Stat5 phosphorylation in cytokine-deprived BaF3 cells (Figure 6E), it did not provide a consistent survival advantage. Whereas during the first few days after cytokine withdrawal more cells expressing F232C CRLF2 were alive compared with cells expressing wt CRLF2, at day 7 almost all BaF3 cells were dead (not shown). To examine the collaboration with wt Jak2, BaF3 cells stably expressing wt Jak2 were transduced with retroviral vectors expressing either wt CRLF or F232C CRLF2 (Figure 6D-E). In the presence of exogenous wt Jak2, there was an approximately 15-fold increase in the growth rate of cells expressing the mutant CRLF2 compared with those expressing wt CRLF2 ($P = .02$, paired t test). Together these observations demonstrate that the F232C CRLF2 activates Jak/Stat signaling and cooperates with Jak2 to provide significant growth advantage in a cytokine-deprived environment.

Discussion

Here we report the results of a genome-wide study of DS-ALL based on a dataset of unprecedented size. Unexpectedly, the molecular phenotype obtained by gene expression profiling is strikingly less homogeneous in DS-ALL than any of the common genetic subtypes of childhood BCP-ALLs. However, despite this heterogeneity, we describe a major feature that is shared by up to two-thirds of the patients—the aberrant expression of the wt or mutated cytokine receptor *CRLF2* and its association with mutations in *JAK2*.

That DS-ALL is less uniform than the specific DS-associated myeloid leukemia has been suggested by a large cytogenetic study performed by the International BFM Study Group.[2] However, neither that study nor the genomic analysis reported here or previously[5,17] explains the level of inhomogeneity in gene expression. Even those DS-ALLs that clustered together were not similar to each other. Such heterogeneity suggests that unlike the common aberrations of childhood ALL (*TEL-AML1,* hyperdiploidy, *E2A-PBX1,* etc), constitutional trisomy 21 is not a typical initiating event. Rather, DS is a predisposing condition to multiple genetic subtypes of BCP-ALLs.

To identify genes and pathways common to DS-ALLs, we have generated a DS-ALL gene expression signature, exploiting the

Table 6. Clinical and diagnostic characteristics of patients with DS-ALL with high/medium expression of CRLF2 versus low/no expression of CRLF2

	No/low CRLF2 expression (n = 20)	High/medium CRLF2 expression (n = 33)	*P*
Sex			> .999*
Male	11	17	
Female	9	16	
Age, y			.004†
Mean (SE)	9.87 (1.21)	5.56 (0.67)	
Median (range)	11.62 (1.74-18.7)	4.06 (1.99-20.22)	
White blood cell count at diagnosis, cells/L			.392†
Mean (SE)	$41.6 * 10^9$ ($8.7 * 10^9$)	$39.8 * (9.7 * 10^9)$	
Median (range)	$23.9 * 10^9$ ($2.4\text{-}130 * 10^9$)	18 930 ($1.5\text{-}259 * 10^9$)	
JAK2 R683 mutations			.008*
Yes	0	10	
No	20	22	

*According to Fisher exact test.
†According to Mann-Whitney *U* test.

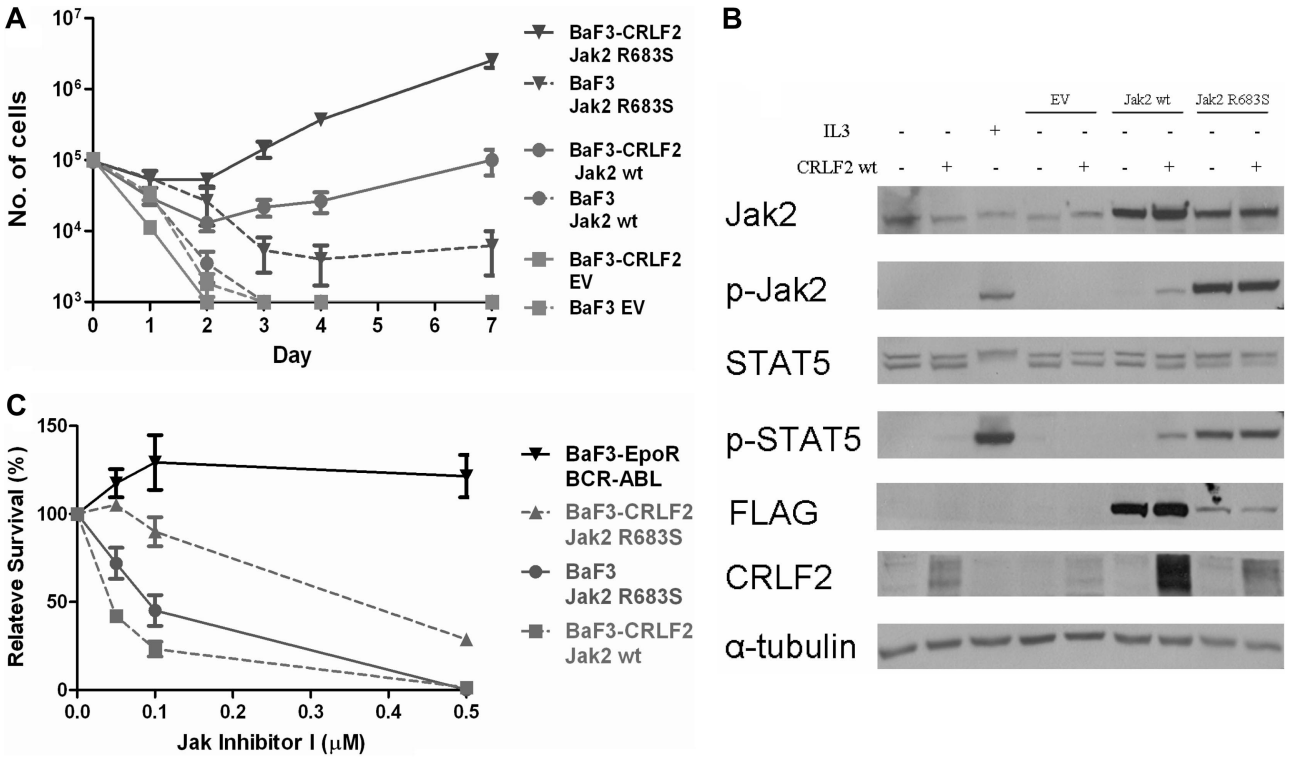

Figure 5. Functional significance of CRLF2 expression. (A) Cytokine withdrawal assay of BaF3 and BaF3-CRLF2 cells infected with either empty vector (EV), mouse FLAG-Jak2 wild-type (wt), or mouse FLAG-Jak2 R683S. Error bars represent SE. (B) Constitutive activation of the Jak/Stat5 pathway in BaF3 and BaF3-CRLF2 cells expressing mouse FLAG-Jak2 wild-type (wt) or R683S, after 5 hours of cytokine deprivation. IL3+ indicates cells harvested after 5 hours of interleukin-3 deprivation followed by 15 minutes of interleukin-3 stimulation. (C) Effect of JAK inhibitor I on growth of BaF3 cells expressing Jak2 R683S and BaF3-CRLF2 cells expressing either wt Jak2 or Jak2 R683S.

advantage of having several datasets. *CRLF2* is 1 of the 3 genes that most differentiates between DS-ALLs and non–DS-ALLs. Confirming the expression of *CRLF2* RNA and protein in DS-ALLs and extending these observations to patients for whom array data were not available, we observed increased expression of *CRLF2* in 62% of 53 patients with DS-ALL. These data are corroborated by the recent report describing IGH@ translocations or interstitial deletions upstream of *CRLF2* in 5% of nonselected childhood ALL, and in 35 (52%) of 68 DS-ALLs consecutively enrolled in United Kingdom treatment protocols.[13]

We report that the interstitial deletion results in fusion transcript in which the first noncoding exon of *P2YR8* fuses to the coding region of *CRLF2,* thereby driving *CRLF2* expression by the *P2YR8* promoter. A similar mechanism was reported in a single patient with splenic lymphoma and *P2YR8-SOX5* fusion[34] and is reminiscent of the common *SIL-SCL (STIL-TAL1)* rearrangement in T-ALL.[35] Cloning of the genomic breakpoints is required to determine whether, like *SIL-SCL,* the deletion is caused by aberrant V(D)J activity.

Although we do not have genomic data for all *CRLF2*-expressing samples, the FISH and RT-PCR results of 17 of 33 specimens overexpressing *CRLF2,* the inverse correlation between *CRLF2* and *P2YRY8* expression, and the similar frequency of *CRLF2* overexpression in our and Russell et al's[13] 2 independent cohorts suggest that most, if not all, aberrant *CRLF2* expression is caused by genomic rearrangements.

CRLF2 dimerizes with IL7RA to form the receptor to thymic stromal-derived lymphopoietin (TSLP), an epithelial-derived cytokine that plays a role in inflammation and lymphoid development.[14,36-38] The expression of *IL7RA* on the leukemic blasts suggests that some of the aberrantly expressed CRLF2 may interact with IL7RA and form a TSLP receptor on the leukemic cells. However, we also demonstrate that CRLF2 cooperates with Jak2 to transform BaF3 cells lacking expression of IL7RA (Figure 5A and supplemental Figure 5). This suggests that CRLF2 may act independently of IL7RA, possibly through homodimerization similar to other type I cytokine receptors.

We report an unusual cooperation between CRLF2 and ectopically expressed wt Jak2 in BaF3 cells, a phenomenon not observed with other type I cytokine receptors such as erythropoietin receptor (EPOR) or thrombopoietin receptor (TPOR). CRLF2 is an atypical type I cytokine receptor that contains only one of the 2 "boxes" that mediate binding of JAK enzymes and only one tyrosine in its C-terminal domain. Hence it is a weak activator of JAK2.[39] This may explain the requirements for higher levels of Jak2 for activation of the Jak/Stat pathway. Interestingly, the levels of CRLF2 were higher in the presence of ectopically expressed wt or mutated Jak2. Positive regulation of the expression of a type I cytokine receptor by JAK2 and Tyk2 was previously reported.[40-42] Thus one mechanism by which Jak2 may cooperate with CRLF2 is by increasing the expression of the latter.

We observed 2 acquired events associated with the increased expression of *CRLF2.* The most common event is activating "lymphoid" somatic mutation in *JAK2*. All DS-ALLs specimens with *JAK2* mutations in our series and in the cohort reported by Russell et al[13] had aberrant expression of *CRLF2,* strongly implying that CRLF2 is the cytokine receptor cooperating with R683 mutated JAK2. Indeed, in BaF3 cytokine weaning assays, only the combination of CRLF2 and mutated Jak2 led to a robust cytokine-independent growth, demonstrating for the first time that these 2 proteins cooperate in providing growth and survival advantage.

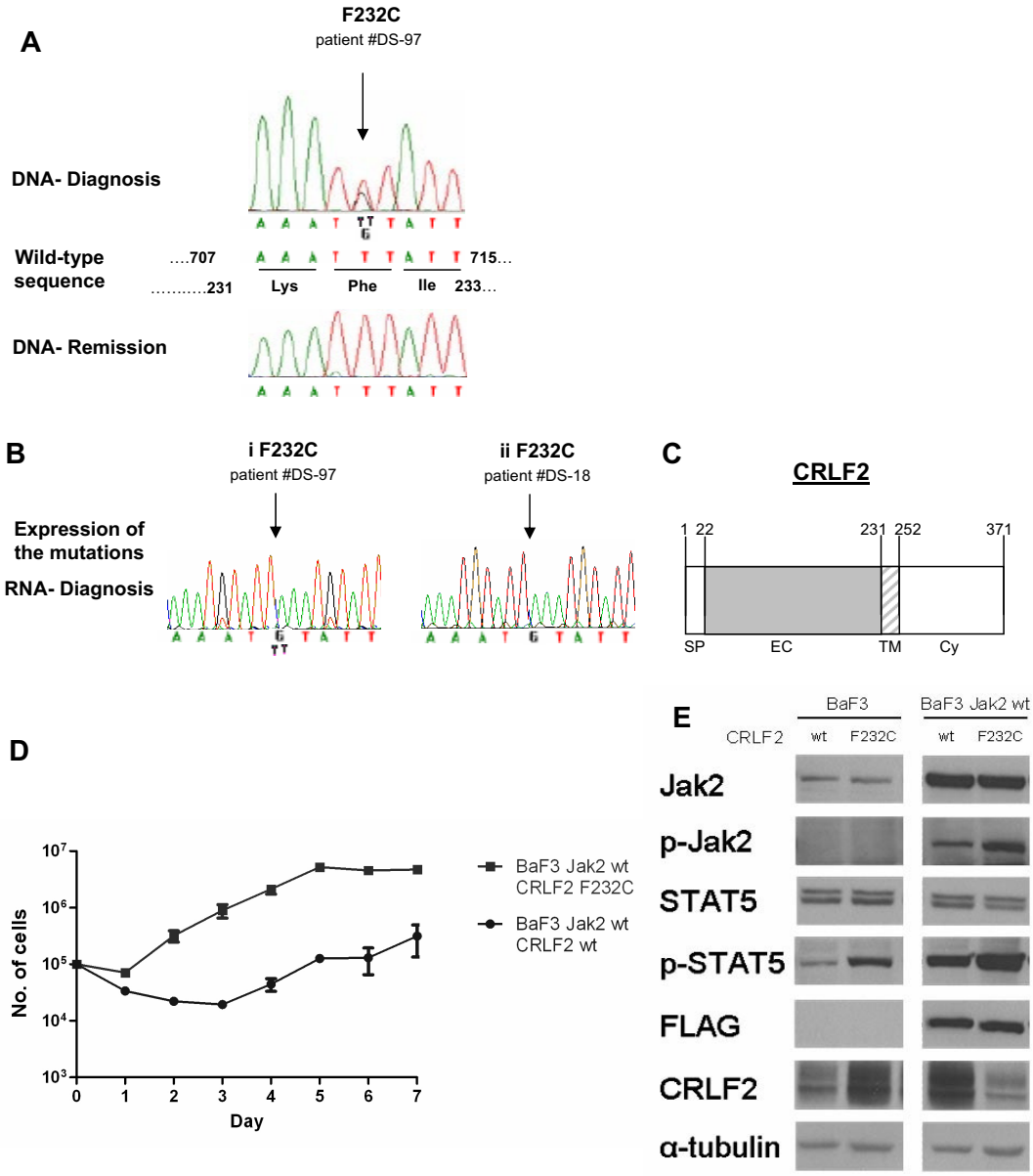

Figure 6. Mutations of CRLF2 in patients with Down syndrome–associated acute lymphoblastic leukemia. (A) Example of sequences depicting the F232C in CRLF2. The F232C (arrowed) is present at diagnosis but not in remission. The wild-type sequence denotes positions of both nucleotides and amino acids. (B) Expression of CRLF2 F232C mutation. Examples of 2 patients: in one (i) both alleles, wild-type and mutated, are expressed, whereas in the other (ii) only the mutated allele is expressed. (C) Schematic presentation of CRLF2. SP indicates signal peptide; EC, extracellular region; TM, transmembrane region; and Cy, cytoplasmic region. Numbers indicate amino acid position. (D) Cytokine withdrawal assay of BaF3 cells stably expressing wild-type mouse FLAG-Jak2 that were transduced with either wild-type human CRLF2 or human CRLF2 F232C. Error bars represent SE. (E) Constitutive activation of the Jak/Stat5 pathway in BaF3 cells expressing wild-type mouse FLAG-Jak2 and either wild-type human CRLF2 (wt) or human CRLF2 F232C (F232C), after 5 hours of cytokine deprivation.

The second less common event is an activating mutation in *CRLF2*. Yoda et al[43] reported an E40G activating somatic mutation in *CRLF2* in a single patient with adult BCP-ALL. We now found that 3 of the 33 patients with DS-ALL overexpressing *CRLF2* have a somatic mutation replacing phenylalanine in the juxtamembrane position 232 by cysteine. This mutation caused constitutive phosphorylation of Stat5 associated with robust cytokine-independent growth of BaF3 cells ectopically transduced with wt Jak2. Introduction of cysteines in this region in the erythropoietin receptor, another type I cytokine receptor signaling through JAK2, caused its constitutive activation by enhancing ligand-independent dimerization.[44]

Although several scenarios may be possible, a reasonable model (Figure 7) is that the overexpression of *CRLF2* is the first event occurring in approximately 60% of DS-ALL patients. The expanded preleukemic clone then acquires additional genetic aberrations, among them an activating mutation in *JAK2* or *CRLF2* or thus far unidentified events that may involve the JAK/STAT pathway. This model explains 3 key observations: (1) All samples with mutated *JAK2* and the only evaluable patient with mutated *CRLF2* also had aberrant CRLF2 expression. (2) Many *CRLF2*-overexpressing samples do not have mutation in *JAK2*. (3) In one reported patient,[13] an aberrant *CRLF2* genomic rearrangement was present at diagnosis whereas mutant JAK2 was present only in the relapse sample.

The most intriguing question is why there is a dramatic 10-fold increase in genomic lesions causing *CRLF2* overexpression in DS (60% in DS-ALL compared with 5% in sporadic ALL) and how this relates to trisomy 21. Only a single Hsa21 gene, *SON,* was

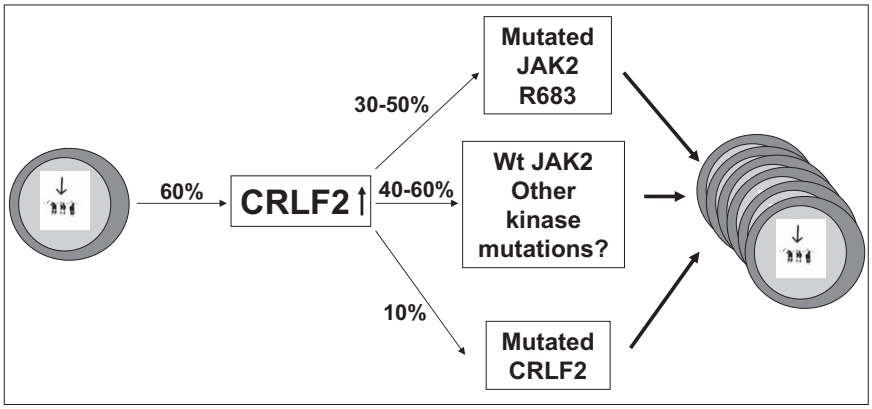

Figure 7. CRLF2 in DS-ALL: a model. Increased CRLF2 expression caused by genomic aberration is followed by progression event consisting of activating mutations in CRLF2, in JAK2, or other alterations in yet unidentified kinases. The percentages in the figure are approximations based on combination of the data in our paper and in the paper by Russell et al.[13]

included in the DS-ALL signature and it was only slightly (1.3) up-regulated (supplemental Table 4). Indeed, we found no major difference in the gene expression from the trisomic chromosome 21 between DS-ALL and HD-ALL (data not shown). Yet our data suggest that DS-ALL and HD-ALL are to a great extent different leukemias. There are obvious fundamental differences between constitutional and acquired trisomy,[45] such as the developmental stage in which the trisomy occurs and the fact that a constitutional trisomy is present both in the leukemia cells and in their microenvironment.

Regardless of the role of the constitutional trisomy, our data generate an intriguing hypothesis. We observe a significant enrichment in DNA damage and repair genes in DS-ALL and identify increased expression and clear "footprint" of BCL6 in these leukemias. BCL6 regulates the germinal center B-cell maturation, through its effects on the DNA damage response. Recent studies by Duy et al[46] suggest for the first time a role for BCL6 in BCP-ALL. We speculate that DS may predispose to ALL through B-cell lymphocytic specific genomic instability involving *BCL6*. The signatures of BCL6 and the DNA damage response pathway may be related to previous reports on impaired cellular response to DNA damage in DS[47] and to the increased prevalence of *IgH@* chromosomal translocation in DS-ALL.[13,48] At present, however, it is impossible to determine whether the *BCL6* signature precedes or follows the *CRLF2* rearrangements. As high expression of *CRLF2* blocks B-cell differentiation,[13] one cannot exclude the possibility that it causes a developmental arrest of the preleukemic cell in a stage in which *BCL6* is active. Distinguishing between these 2 hypotheses will require the identification and study of preleukemic cells in children with DS.

Finally, our data imply that therapeutics targeting JAK/STAT signaling may be of potential benefit to the majority of DS-ALLs not limited only to those with mutated JAK2. Although we demonstrate that BaF3 cells coexpressing CRLF2 and mutated Jak2 are more susceptible to JAK inhibitor l than cells transformed with BCR-ABL, they were relatively resistant in comparison with cells transformed only with mutated Jak2. This preliminary observation requires further testing in primary leukemic cells. It may indicate that targeting other pathways activated by CRLF2 or the use of anti–CRLF2-specific antibodies will synergize with JAK2 inhibitors in treatment of DS-ALL and non–DS-ALL with aberrant *CRLF2* expression.

Acknowledgments

We thank Dr T. Enver for supplying the pHRSINCSGW lentivirus plasmid and Dr Kitamura for providing the CRLF2 expression construct. We thank N. Amariglio, G. Basso, V. Binder, A. Biondi, S. Bresolin, O. Haas, J. Harbott, M. Grazia, G. Martinelli, M. Schrappe, S. Orkin, D. Weinstock, A. Yitzhaky, Y. Shinar, A. Ovadia, and the members of E. Domany's and S. Izraeli's groups, in particular Y. Birger and E. Ben-Meir, for their important contributions to the study.

Funding for this study was provided by the Israel Ministry of Science (E.D. and S.I.), Israeli Ministry of trade (D.B. and S.I.), Israeli Ministry of Health (S.I.), German Israeli Foundation (S.I. and A.B.), Israeli Science Foundation and Morasha program (S.I.), US Israel Binational Science Foundation (S.I.), Children with Leukemia UK (S.I.), Curtis Katz (S.I.), Wolfson Foundation (E.D. and S.I.), Foulkes Foundation (L.H. and I.G.), The Ridgefield Foundation (E.D.), Converging Technologies Program (L.H.), Constantiner Institute for Molecular Genetics (I.G.), Hans Altschüler-Stiftung (S.I. and J.P.B.), Swiss National Science Foundation (J.P.B.), Leukemia Research Fund, UK (C.H. and L.J.R.), PRIN/Programmi di ricerca di Relevante Interesse Nazionale, Rome (GteK), European LeukemiaNet, AIRC, AIL, Fondazione Del Monte di Bologna e Ravenna, FIRB 2006 (II). Reagents for the AIEOP GEP study were supplied by Roche Molecular Diagnostics in the framework of the MILE study.[49]

This study has been performed as partial fulfillment of the requirement for a PhD degree from the Tel Aviv University Faculty of Medicine to L.H., I.G., and C.S.

Authorship

Contribution: S.I., E.D., J.-P.B., H.K., G. Cazzaniga, G.K., G.R., and M. Stanulla conceived and planned the study; G. Cazzaniga, G. Cario, M. Stanulla, S.S., A.Y., and A.B. provided reagents and/or important data; E.V., I.G., G. Cazzaniga, M. Schmitz, J.C., R.S., I.I., C.S., S.Z., L.J.R., C.J.H., B.B., D.B., J.-P.B., G.K., and S.I. performed and/or analyzed experiments; L.H. and E.D. performed all the bioinformatics analysis; L.H., I.G., S.I., and E.D. wrote the paper with contributions by M. Schmitz, I.I., R.S., C.S., S.Z., G. Cazzaniga, S.S., and L.J.R. S.I. assumes full responsibility for the content of the paper including supplemental files.

Conflict-of-interest disclosure: The authors declare no competing financial interests.

Correspondence: Shai Izraeli, Pediatric Hematology Oncology Dept, Sheba Medical Center, Tel Hashomer Ramat Gan 52621 Israel; e-mail: sizraeli@sheba.health.gov.il.

References

1. Malinge S, Izraeli S, Crispino JD. Insights into the manifestations, outcomes, and mechanisms of leukemogenesis in Down syndrome. *Blood.* 2009; 113(12):2619-2628.
2. Forestier E, Izraeli S, Beverloo B, et al. Cytogenetic features of acute lymphoblastic and myeloid leukemias in pediatric patients with Down syndrome: an iBFM-SG study. *Blood.* 2008;111(3): 1575-1583.
3. Rainis L, Bercovich D, Strehl S, et al. Mutations in exon 2 of GATA1 are early events in megakaryocytic malignancies associated with trisomy 21. *Blood.* 2003;102(3):981-986.
4. Bercovich D, Ganmore I, Scott LM, et al. Mutations of JAK2 in acute lymphoblastic leukaemias associated with Down's syndrome. *Lancet.* 2008; 372(9648):1484-1492.
5. Kearney L, Gonzalez De Castro D, Yeung J, et al. Specific JAK2 mutation (JAK2R683) and multiple gene deletions in Down syndrome acute lymphoblastic leukemia. *Blood.* 2009;113(3):646-648.
6. Gaikwad A, Rye CL, Devidas M, et al. Prevalence and clinical correlates of JAK2 mutations in Down syndrome acute lymphoblastic leukaemia. *Br J Haematol.* 2009;144(6):930-932.
7. Mullighan CG, Zhang J, Harvey RC, et al. JAK mutations in high-risk childhood acute lymphoblastic leukemia. *Proc Natl Acad Sci U S A.* 2009; 106(23):9414-9418.
8. Bourquin JP, Subramanian A, Langebrake C, et al. Identification of distinct molecular phenotypes in acute megakaryoblastic leukemia by gene expression profiling. *Proc Natl Acad Sci U S A.* 2006;103(9):3339-3344.
9. Bungaro S, Dell'Orto MC, Zangrando A, et al. Integration of genomic and gene expression data of childhood ALL without known aberrations identifies subgroups with specific genetic hallmarks. *Genes Chromosomes Cancer.* 2009;48(1):22-38.
10. Ross ME, Zhou X, Song G, et al. Classification of pediatric acute lymphoblastic leukemia by gene expression profiling. *Blood.* 2003;102(8):2951-2959.
11. National Center for Biotechnology Information. Gene Expression Omnibus (GEO). http://www.ncbi.nlm.nih.gov/geo. Accessed August 2009.
12. Hong D, Gupta R, Ancliff P, et al. Initiating and cancer-propagating cells in TEL-AML1-associated childhood leukemia. *Science.* 2008; 319(5861):336-339.
13. Russell LJ, Capasso M, Vater I, et al. Deregulated expression of cytokine receptor gene, CRLF2, is involved in lymphoid transformation in B-cell precursor acute lymphoblastic leukemia. *Blood.* 2009;114(13):2688-2698.
14. Fujio K, Nosaka T, Kojima T, et al. Molecular cloning of a novel type 1 cytokine receptor similar to the common gamma chain. *Blood.* 2000;95(7): 2204-2210.
15. Subramanian A, Tamayo P, Mootha VK, et al. Gene set enrichment analysis: a knowledge-based approach for interpreting genome-wide expression profiles. *Proc Natl Acad Sci U S A.* 2005;102(43):15545-15550.
16. Tsafrir D, Tsafrir I, Ein-Dor L, Zuk O, Notterman DA, Domany E. Sorting points into neighborhoods (SPIN): data analysis and visualization by ordering distance matrices. *Bioinformatics.* 2005; 21(10):2301-2308.
17. Lo KC, Chalker J, Strehl S, et al. Array comparative genome hybridization analysis of acute lymphoblastic leukaemia and acute megakaryoblastic leukaemia in patients with Down syndrome. *Br J Haematol.* 2008;142(6):934-945.
18. Mullighan CG, Goorha S, Radtke I, et al. Genome-wide analysis of genetic alterations in acute lymphoblastic leukaemia. *Nature.* 2007; 446(7137):758-764.
19. Den Boer ML, van Slegtenhorst M, De Menezes RX, et al. A subtype of childhood acute lymphoblastic leukaemia with poor treatment outcome: a genome-wide classification study. *Lancet Oncol.* 2009;10(2):125-134.
20. Mullighan CG, Miller CB, Radtke I, et al. BCR-ABL1 lymphoblastic leukaemia is characterized by the deletion of Ikaros. *Nature.* 2008;453(7191): 110-114.
21. Iacobucci I, Storlazzi CT, Cilloni D, et al. Identification and molecular characterization of recurrent genomic deletions on 7p12 in the IKZF1 gene in a large cohort of BCR-ABL1-positive acute lymphoblastic leukemia patients: on behalf of Gruppo Italiano Malattie Ematologiche dell'Adulto Acute Leukemia Working Party (GIMEMA AL WP). *Blood.* 2009;114(10):2159-2167.
22. Subramanian A, Tamayo P, Mootha VK, et al. From the Cover: gene set enrichment analysis: a knowledge-based approach for interpreting genome-wide expression profiles. *Proc Natl Acad Sci U S A.* 2005;102(43):15545-15550.
23. National Institute of Allergy and Infectious Diseases. Database for Annotation, Visualization and Integrated Discovery (DAVID). http://david.abcc.ncifcrf.gov. Accessed March 2009.
24. Dennis G Jr, Sherman BT, Hosack DA, et al. DAVID: Database for Annotation, Visualization, and Integrated Discovery. *Genome Biol.* 2003; 4(5):P3.
25. Lossos IS, Czerwinski DK, Alizadeh AA, et al. Prediction of survival in diffuse large-B-cell lymphoma based on the expression of six genes. *N Engl J Med.* 2004;350(18):1828-1837.
26. Parekh S, Polo JM, Shaknovich R, et al. BCL6 programs lymphoma cells for survival and differentiation through distinct biochemical mechanisms. *Blood.* 2007;110(6):2067-2074.
27. Rhodes DR, Yu J, Shanker K, et al. ONCOMINE: a cancer microarray database and integrated data-mining platform. *Neoplasia.* 2004;6(1):1-6.
28. Compendia Bioscience, Inc. Oncomine. http://www.oncomine.org. Accessed January 2009.
29. Benjamini Y, Hochberg Y. Controlling the false discovery rate: a practical and powerful approach to multiple testing. *J Roy Stat Soc.* 1995;57(Ser B):289-300.
30. Basso K, Margolin AA, Stolovitzky G, Klein U, Dalla-Favera R, Califano A. Reverse engineering of regulatory networks in human B cells. *Nat Genet.* 2005;37(4):382-390.
31. Hummel M, Bentink S, Berger H, et al. A biologic definition of Burkitt's lymphoma from transcriptional and genomic profiling. *N Engl J Med.* 2006; 354(23):2419-2430.
32. Polo JM, Juszczynski P, Monti S, et al. Transcriptional signature with differential expression of BCL6 target genes accurately identifies BCL6-dependent diffuse large B cell lymphomas. *Proc Natl Acad Sci U S A.* 2007;104(9):3207-3212.
33. Liu YJ, Soumelis V, Watanabe N, et al. TSLP: an epithelial cell cytokine that regulates T cell differentiation by conditioning dendritic cell maturation. *Annu Rev Immunol.* 2007;25:193-219.
34. Storlazzi CT, Albano F, Lo Cunsolo C, et al. Up-regulation of the SOX5 by promoter swapping with the P2RY8 gene in primary splenic follicular lymphoma. *Leukemia.* 2007;21(10):2221-2225.
35. Aplan PD, Lombardi DP, Ginsberg AM, Cossman J, Bertness VL, Kirsch IR. Disruption of the human SCL locus by "illegitimate" V-(D)-J recombinase activity. *Science.* 1990;250(4986):1426-1429.
36. Rochman Y, Leonard WJ. The role of thymic stromal lymphopoietin in CD8+ T cell homeostasis. *J Immunol.* 2008;181(11):7699-7705.
37. Ziegler SF, Liu YJ. Thymic stromal lymphopoietin in normal and pathogenic T cell development and function. *Nat Immunol.* 2006;7(7):709-714.
38. Pandey A, Ozaki K, Baumann H, et al. Cloning of a receptor subunit required for signaling by thymic stromal lymphopoietin. *Nat Immunol.* 2000; 1(1):59-64.
39. Carpino N, Thierfelder WE, Chang MS, et al. Absence of an essential role for thymic stromal lymphopoietin receptor in murine B-cell development. *Mol Cell Biol.* 2004;24(6):2584-2592.
40. Ragimbeau J, Dondi E, Alcover A, Eid P, Uze G, Pellegrini S. The tyrosine kinase Tyk2 controls IFNAR1 cell surface expression. *EMBO J.* 2003; 22(3):537-547.
41. Huang LJ, Constantinescu SN, Lodish HF. The N-terminal domain of Janus kinase 2 is required for Golgi processing and cell surface expression of erythropoietin receptor. *Mol Cell.* 2001;8(6): 1327-1338.
42. Royer Y, Staerk J, Costuleanu M, Courtoy PJ, Constantinescu SN. Janus kinases affect thrombopoietin receptor cell surface localization and stability. *J Biol Chem.* 2005;280(29):27251-27261.
43. Yoda A, Yoda Y, Chiaretti S, et al. Functional screening identifies CRLF2 in precursor B-cell acute lymphoblastic leukemia. *Proc Natl Acad Sci U S A.* 2010;107(1):252-257.
44. Lu X, Gross AW, Lodish HF. Active conformation of the erythropoietin receptor: random and cysteine-scanning mutagenesis of the extracellular juxtamembrane and transmembrane domains. *J Biol Chem.* 2006;281(11):7002-7011.
45. Ganmore I, Smooha G, Izraeli S. Constitutional aneuploidy and cancer predisposition. *Hum Mol Genet.* 2009;18(R1):R84-R93.
46. Duy C, Yu j, J, Cerchietti L, et al. BCL6-mediated survival signaling promotes drug-resistance in BCR-ABL1-driven acute lymphoblastic leukemia [abstract]. *Proc 50th Ann Meet Am Soc Hematol.* 2008:Abstract 295.
47. Morawiec Z, Janik K, Kowalski M, et al. DNA damage and repair in children with Down's syndrome. *Mutat Res.* 2008;637(1-2):118-123.
48. Lundin C, Heldrup J, Ahlgren T, Olofsson T, Johansson B. B-cell precursor t(8;14)(q11;q32)-positive acute lymphoblastic leukemia in children is strongly associated with Down syndrome or with a concomitant Philadelphia chromosome. *Eur J Haematol.* 2009;82(1):46-53.
49. Haferlach T, Kohlmann A, Wieczorek L, et al. The clinical utility of microarray-based gene expression profiling in the diagnosis and subclassification of leukemia: report on 3334 cases from the International MILE Study Group. *J Clin Oncol.* In press.